The Institution of Engineering and Technology

Energy Generation and Efficiency Technologies for Green Residential Buildings

Edited by
David S-K Ting and Rupp Carriveau

IET ENERGY ENGINEERING 155

Energy Generation and Efficiency Technologies for Green Residential Buildings

Other volumes in this series:

Volume 1 **Power Circuit Breaker Theory and Design** C.H. Flurscheim (Editor)
Volume 4 **Industrial Microwave Heating** A.C. Metaxas and R.J. Meredith
Volume 7 **Insulators for High Voltages** J.S.T. Looms
Volume 8 **Variable Frequency AC Motor Drive Systems** D. Finney
Volume 10 **SF_6 Switchgear** H.M. Ryan and G.R. Jones
Volume 11 **Conduction and Induction Heating** E.J. Davies
Volume 13 **Statistical Techniques for High Voltage Engineering** W. Hauschild and W. Mosch
Volume 14 **Uninterruptible Power Supplies** J. Platts and J.D. St Aubyn (Editors)
Volume 15 **Digital Protection for Power Systems** A.T. Johns and S.K. Salman
Volume 16 **Electricity Economics and Planning** T.W. Berrie
Volume 18 **Vacuum Switchgear** A. Greenwood
Volume 19 **Electrical Safety: A guide to causes and prevention of hazards** J. Maxwell Adams
Volume 21 **Electricity Distribution Network Design, 2nd Edition** E. Lakervi and E.J. Holmes
Volume 22 **Artificial Intelligence Techniques in Power Systems** K. Warwick, A.O. Ekwue and R. Aggarwal (Editors)
Volume 24 **Power System Commissioning and Maintenance Practice** K. Harker
Volume 25 **Engineers' Handbook of Industrial Microwave Heating** R.J. Meredith
Volume 26 **Small Electric Motors** H. Moczala *et al.*
Volume 27 **AC–DC Power System Analysis** J. Arrillaga and B.C. Smith
Volume 29 **High Voltage Direct Current Transmission, 2nd Edition** J. Arrillaga
Volume 30 **Flexible AC Transmission Systems (FACTS)** Y.-H. Song (Editor)
Volume 31 **Embedded Generation** N. Jenkins *et al.*
Volume 32 **High Voltage Engineering and Testing, 2nd Edition** H.M. Ryan (Editor)
Volume 33 **Overvoltage Protection of Low-Voltage Systems, Revised Edition** P. Hasse
Volume 36 **Voltage Quality in Electrical Power Systems** J. Schlabbach *et al.*
Volume 37 **Electrical Steels for Rotating Machines** P. Beckley
Volume 38 **The Electric Car: Development and future of battery, hybrid and fuel-cell cars** M. Westbrook
Volume 39 **Power Systems Electromagnetic Transients Simulation** J. Arrillaga and N. Watson
Volume 40 **Advances in High Voltage Engineering** M. Haddad and D. Warne
Volume 41 **Electrical Operation of Electrostatic Precipitators** K. Parker
Volume 43 **Thermal Power Plant Simulation and Control** D. Flynn
Volume 44 **Economic Evaluation of Projects in the Electricity Supply Industry** H. Khatib
Volume 45 **Propulsion Systems for Hybrid Vehicles** J. Miller
Volume 46 **Distribution Switchgear** S. Stewart
Volume 47 **Protection of Electricity Distribution Networks, 2nd Edition** J. Gers and E. Holmes
Volume 48 **Wood Pole Overhead Lines** B. Wareing
Volume 49 **Electric Fuses, 3rd Edition** A. Wright and G. Newbery
Volume 50 **Wind Power Integration: Connection and system operational aspects** B. Fox *et al.*
Volume 51 **Short Circuit Currents** J. Schlabbach
Volume 52 **Nuclear Power** J. Wood
Volume 53 **Condition Assessment of High Voltage Insulation in Power System Equipment** R.E. James and Q. Su
Volume 55 **Local Energy: Distributed generation of heat and power** J. Wood
Volume 56 **Condition Monitoring of Rotating Electrical Machines** P. Tavner, L. Ran, J. Penman and H. Sedding
Volume 57 **The Control Techniques Drives and Controls Handbook, 2nd Edition** B. Drury
Volume 58 **Lightning Protection** V. Cooray (Editor)
Volume 59 **Ultracapacitor Applications** J.M. Miller

Volume 62 **Lightning Electromagnetics** V. Cooray
Volume 63 **Energy Storage for Power Systems, 2nd Edition** A. Ter-Gazarian
Volume 65 **Protection of Electricity Distribution Networks, 3rd Edition** J. Gers
Volume 66 **High Voltage Engineering Testing, 3rd Edition** H. Ryan (Editor)
Volume 67 **Multicore Simulation of Power System Transients** F.M. Uriate
Volume 68 **Distribution System Analysis and Automation** J. Gers
Volume 69 **The Lightening Flash, 2nd Edition** V. Cooray (Editor)
Volume 70 **Economic Evaluation of Projects in the Electricity Supply Industry, 3rd Edition** H. Khatib
Volume 72 **Control Circuits in Power Electronics: Practical issues in design and implementation** M. Castilla (Editor)
Volume 73 **Wide Area Monitoring, Protection and Control Systems: The enabler for smarter grids** A. Vaccaro and A. Zobaa (Editors)
Volume 74 **Power Electronic Converters and Systems: Frontiers and applications** A. M. Trzynadlowski (Editor)
Volume 75 **Power Distribution Automation** B. Das (Editor)
Volume 76 **Power System Stability: Modelling, analysis and control** B. Om P. Malik
Volume 78 **Numerical Analysis of Power System Transients and Dynamics** A. Ametani (Editor)
Volume 79 **Vehicle-to-Grid: Linking electric vehicles to the smart grid** J. Lu and J. Hossain (Editors)
Volume 81 **Cyber-Physical-Social Systems and Constructs in Electric Power Engineering** S. Suryanarayanan, R. Roche and T.M. Hansen (Editors)
Volume 82 **Periodic Control of Power Electronic Converters** F. Blaabjerg, K. Zhou, D. Wang and Y. Yang
Volume 86 **Advances in Power System Modelling, Control and Stability Analysis** F. Milano (Editor)
Volume 87 **Cogeneration: Technologies, optimisation and implentation** C.A. Frangopoulos (Editor)
Volume 88 **Smarter Energy: From smart metering to the smart grid** H. Sun, N. Hatziargyriou, H.V. Poor, L. Carpanini and M.A. Sánchez Fornié (Editors)
Volume 89 **Hydrogen Production, Separation and Purification for Energy** A. Basile, F. Dalena, J. Tong and T.N. Veziroğlu (Editors)
Volume 90 **Clean Energy Microgrids** S. Obara and J. Morel (Editors)
Volume 91 **Fuzzy Logic Control in Energy Systems with Design Applications in MATLAB®/Simulink®** İ.H. Altaş
Volume 92 **Power Quality in Future Electrical Power Systems** A.F. Zobaa and S.H. E.A. Aleem (Editors)
Volume 93 **Cogeneration and District Energy Systems: Modelling, analysis and optimization** M.A. Rosen and S. Koohi-Fayegh
Volume 94 **Introduction to the Smart Grid: Concepts, technologies and evolution** S.K. Salman
Volume 95 **Communication, Control and Security Challenges for the Smart Grid** S.M. Muyeen and S. Rahman (Editors)
Volume 96 **Industrial Power Systems with Distributed and Embedded Generation** R. Belu
Volume 97 **Synchronized Phasor Measurements for Smart Grids** M.J.B. Reddy and D.K. Mohanta (Editors)
Volume 98 **Large Scale Grid Integration of Renewable Energy Sources** A. Moreno-Munoz (Editor)
Volume 100 **Modeling and Dynamic Behaviour of Hydropower Plants** N. Kishor and J. Fraile-Ardanuy (Editors)
Volume 101 **Methane and Hydrogen for Energy Storage** R. Carriveau and D.S.-K. Ting
Volume 104 **Power Transformer Condition Monitoring and Diagnosis** A. Abu-Siada (Editor)
Volume 106 **Surface Passivation of Industrial Crystalline Silicon Solar Cells** J. John (Editor)
Volume 107 **Bifacial Photovoltaics: Technology, applications and economics** J. Libal and R. Kopecek (Editors)

Volume 108 **Fault Diagnosis of Induction Motors** J. Faiz, V. Ghorbanian and G. Joksimović
Volume 110 **High Voltage Power Network Construction** K. Harker
Volume 111 **Energy Storage at Different Voltage Levels: Technology, integration, and market aspects** A.F. Zobaa, P.F. Ribeiro, S.H.A. Aleem and S.N. Afifi (Editors)
Volume 112 **Wireless Power Transfer: Theory, technology and application** N. Shinohara
Volume 115 **DC Distribution Systems and Microgrids** T. Dragičević, F. Blaabjerg and P. Wheeler
Volume 117 **Structural Control and Fault Detection of Wind Turbine Systems** H.R. Karimi
Volume 119 **Thermal Power Plant Control and Instrumentation: The control of boilers and HRSGs, 2nd Edition** D. Lindsley, J. Grist and D. Parker
Volume 120 **Fault Diagnosis for Robust Inverter Power Drives** A. Ginart (Editor)
Volume 123 **Power Systems Electromagnetic Transients Simulation, 2nd Edition** N. Watson and J. Arrillaga
Volume 124 **Power Market Transformation** B. Murray
Volume 126 **Diagnosis and Fault Tolerance of Electrical Machines, Power Electronics and Drives** A.J.M. Cardoso
Volume 128 **Characterization of Wide Bandgap Power Semiconductor Devices** F. Wang, Z. Zhang and E.A. Jones
Volume 130 **Wind and Solar Based Energy Systems for Communities** R. Carriveau and D.S.-K. Ting (Editors)
Volume 131 **Metaheuristic Optimization in Power Engineering** J. Radosavljević
Volume 132 **Power Line Communication Systems for Smart Grids** I.R.S Casella and A. Anpalagan
Volume 157 **Electrical Steels, 2 Volumes** A. Moses, K. Jenkins, Philip Anderson and H. Stanbury
Volume 905 **Power System Protection, 4 Volumes**

Energy Generation and Efficiency Technologies for Green Residential Buildings

Edited by
David S-K Ting and Rupp Carriveau

The Institution of Engineering and Technology

Published by The Institution of Engineering and Technology, London, United Kingdom

The Institution of Engineering and Technology is registered as a Charity in England & Wales (no. 211014) and Scotland (no. SC038698).

First published 2019

The Institution of Engineering and Technology
Michael Faraday House
Six Hills Way, Stevenage
Herts, SG1 2AY, United Kingdom

www.theiet.org

British Library Cataloguing in Publication Data
A catalogue record for this product is available from the British Library

ISBN 978-1-78561-947-2 (hardback)
ISBN 978-1-78561-948-9 (PDF)

Typeset in India by MPS Limited
Printed in the UK by CPI Group (UK) Ltd, Croydon

Contents

About the editors

David S-K Ting is a professor in Mechanical, Automotive and Materials Engineering and the founder of the Turbulence & Energy Laboratory at the University of Windsor, Canada. He has co/supervised over 70 graduate students primarily in the Energy and Turbulence areas and co-authored more than 120 related journal papers.

Rupp Carriveau is a professor with the Turbulence & Energy Laboratory, University of Windsor, Canada. His research focuses on the smart optimization of energy systems. He collaborates with energy and water utilities, agricultural, and automotive industries. He serves on the boards of several related journals, and is Co-Chair of the IEEE Ocean Energy Technology Committee.

This page intentionally left blank

Chapter 1

Introduction and motivation

Zahra Naghibi[1,2], Jacqueline A. Stagner[1,3], David S.-K. Ting[1,4], and Rupp Carriveau[1,2]

The residential building sector is one of the key consumers of energy [1], with the trend predicted to increase over the coming years [2]. According to the International Energy Agency (IEA) statistics (2014), energy consumption in the residential sector (19%), after the transportation (34%) and manufacturing industries (27%), is one of the highest shares of energy consumption across IEA countries (Figure 1.1) [3]. Totally, worldwide residential sector energy consumption ranges from 16% to 50% of the total amount of energy consumed [4]. Therefore, the residential sector has a significant contribution to global warming, due to its high greenhouse gas emissions over the last few decades [5]. End-use energy consumption in the residential building sector could be for heating and cooling, electric appliances, and lighting. The increasing number of buildings, the general increase in the size of dwellings, growing quality of life, and increasing home electrification are reasons for this upcoming trend in the energy consumption by this sector [2,6,7]. Thus, moving forward, it is critical to employ more efficient energy systems based on renewable energy resources, to reduce the energy demand in this sector, and to reduce the environmental impacts of this sector.

To achieve reduced environmental impacts throughout a building's life cycle, the theory of green buildings has been introduced [8], and many countries have been trying to upgrade their existing buildings to green buildings [9]. There are many definitions of green buildings. For example, Cassidy quoted the Office of the Federal Environmental Executive definition of green buildings as "the practice of (1) increasing the efficiency with which buildings and their sites use energy, water, and materials and (2) reducing building impacts on human health and the environment through better siting, design, construction operation, maintenance, and removal—the complete building life cycle" [10]. What is common in almost all definitions of green buildings is a focus on the buildings' energy consumption. Reducing energy consumption and using replenishable energies are the two most

[1]Turbulence & Energy Lab, University of Windsor, Canada
[2]Civil & Environmental Engineering, University of Windsor, Canada
[3]Faculty of Engineering, University of Windsor, Canada
[4]MAME, University of Windsor, Canada

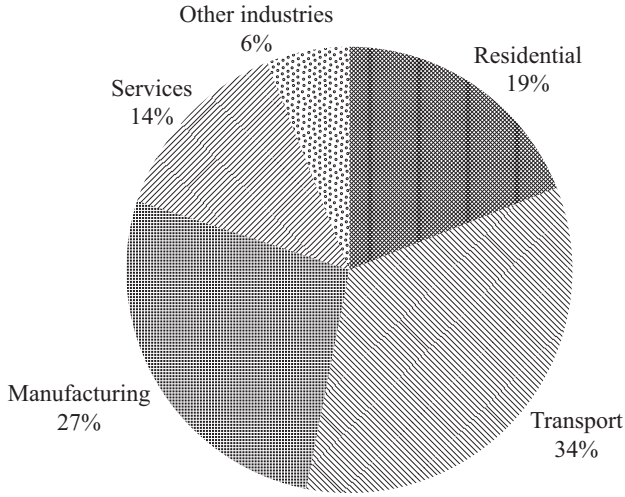

Figure 1.1 Largest energy end-uses in IEA countries, 2014 (other industries include agriculture, mining, and construction) (based on data from Ref. [3])

important aspects that make green buildings sustainable [8,9]. As such, we may define a green building as a building which uses replenishable energies while minimizing energy resources consumption.

Among all renewable energies, solar energy attracts attention because of its abundance and cleanliness. The amount of annual solar energy which strikes the earth is equal to 1.5×10^{18} kWh [11]. Only a very small fraction of this energy (~0.01%) would be sufficient to supply the total world energy demand [11]. This amount of energy is 10,000 times more than the total annual energy consumption in the world [12]. The proportion of the annual solar energy available and the annual world energy demand is illustrated in Figure 1.2. Humans need to design equipment to collect this huge amount of energy to supply their energy demands. Photovoltaic (PV) systems for supplying electricity and solar thermal systems for supplying the thermal energy for hot water and space heating are quite well known in the residential building sector. The utilization of solar energy is an important step toward sustainability in this sector.

It is of great importance to study the energy performance of green buildings to assess their sustainability. The sustainability rating of green buildings is a topic discussed in Chapter 2. One of the challenges in the application of PV panels is that there is not enough performance data available to compare them with design predictions. In Chapter 3, monitoring data of a PV system for a year is used to compare with a simulation. This comparison is necessary to provide confidence that the designed system will perform as predicted. The evaluation of the effective parameters on the solar systems' efficiency helps to make the most advantage of solar radiation in both electricity and heat energy generation. The effects of parameters

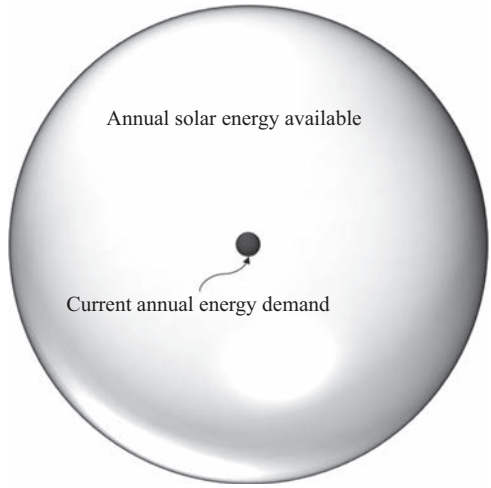

Figure 1.2 Annual solar energy available versus current annual energy demand

such as building orientation, shading effect, roof angle, and roof size on solar PV system efficiencies are studied in Chapter 4. In Chapter 10, solar panel efficiency is optimized by utilizing real solar radiation values. Solar thermal harvesting and storage systems are discussed in Chapter 5.

In addition to focusing on using renewable resources in producing buildings' required energy, it is crucial to concentrate on reducing the energy demand in the buildings to achieve energy conservation. In order to reduce energy demand in buildings, special attention should be given to the building components and the construction cost. Thermophysical properties of envelopes, as one of the main components of buildings, can greatly affect the thermal energy consumption of buildings. Improving the envelope thermal performance of a building helps to reduce the building's energy demand. It can be in the form of energy storage in the envelope or cutting heating energy demand as the result of proper insulation. Nowadays, integration of phase change materials (PCMs) as a latent heat storage unit in building walls has become a very popular option because of PCMs' high heat of fusion at an almost constant temperature. PCM utilization in building walls has several advantages; it can be effective in shifting peak-hour energy loads [13] and, with consideration of the adequate melting temperature of the PCM in the design phase, it can be effective in the reduction of indoor air temperature fluctuations while improving the comfort of occupants [13]. How much the employment of PCM in a brick wall can be more efficient over a simple brick wall is numerically studied in Chapter 6. Chapter 7 pays close attention to the importance of building insulation materials in buildings' energy performance. In addition to evaluating the importance of building envelopes in the energy consumption prediction of buildings, consideration of the construction costs can be helpful to accurately predict this value. Recently, machine-learning analytics have been employed by many researchers to model the correlation

between building costs in the construction phase and the energy consumption during the operational stage. Chapter 8 allows developers to properly adjust their investment strategies to improve the energy efficiency of green building technologies.

In order to remove the barrier of the misalignment between solar energy generation and the energy demand in buildings, solar energy storage has been employed. The excess power generated by PV systems can be stored in electrical energy storage (EES) units. There are two configurations for PV systems: off-grid systems (also called stand-alone systems) and grid-connected systems. Off-grid PV systems are independent of the grid and excess energy can be stored in an EES unit. Although an EES unit is not essential in the grid-connected PV systems, using EES systems can be a solution to reduce the impact of PV systems on the instability of the networks [14]. Among all methods of electrical storage units, electrochemical storage, such as batteries, can be efficient and suitable in terms of scalability, lifespan, discharge time, and the weight of the system [15]. Choosing the right battery for PV systems can change the project lifetime, maintenance operations, and energy performance of the system. As well, having a reliable battery recycling program can ensure the overall sustainability of battery technologies [16]. In Chapter 10, there are comparisons among different battery options that can be used as a guideline to choose a proper option for a special project. In addition, the importance of electrochemical battery recycling is discussed in this chapter.

Solar energy can also be used to provide food in the urban context. It can be the main source of power for nature-based solutions to rapidly growing urbanization problems and their reported consequences. Integration of these nature-based solutions into buildings leads to having more sustainable cities. What can be better than learning from the intelligent design of nature? In Chapter 11, a system consisting of three main nature-based elements is proposed; green roofs that filter water, photobioreactors that cultivate microalgae, and aquaponics that combine aquaculture with hydroponics to grow both fish and vegetables.

References

[1] M. A. R. Biswas, M. D. Robinson, and N. Fumo, "Prediction of residential building energy consumption: A neural network approach," *Energy*, vol. 117, pp. 84–92, 2016.

[2] M. Calero, E. Alameda-Hernandez, M. Fernández-Serrano, A. Ronda, and M. Á. Martín-Lara, "Energy consumption reduction proposals for thermal systems in residential buildings," *Energy Build.*, vol. 175, pp. 121–130, 2018.

[3] International Energy Agency, "The IEA Energy Efficiency Indicators Database," 2017. [Online]. Available: https://www.iea.org/newsroom/news/2017/december/the-iea-energy-efficiency-indicators-database.html. [Accessed: 20-Nov-2018].

[4] J. U. Ahamed, R. Saidur, H. H. Masjuki, S. Mekhilef, M. B. Ali, and M. H. Furqon, "An application of energy and exergy analysis in residential sector of Malaysia," *Energy Policy*, vol. 35, pp. 1050–1063, 2007.

[5] Y. Geng, W. Chen, Z. Liu *et al.*, "A bibliometric review: Energy consumption and greenhouse gas emissions in the residential sector," *J. Clean. Prod.*, vol. 159, pp. 301–316, 2017.
[6] C. Chang, N. Zhu, K. Yang, and F. Yang, "Data and analytics for heating energy consumption of residential buildings: The case of a severe cold climate region of China," *Energy Build.*, vol. 172, pp. 104–115, 2018.
[7] M. Gray and J. Zarnikau, "Getting to Zero: Green Building and Net Zero Energy Homes," in *Energy*, *Sustainability and the Environment*, F. P. Sioshansi, Ed. Oxford: Butterworth-Heinemann, 2011, pp. 231–271.
[8] C. Xia, Y. Zhu, and B. Lin, "Renewable energy utilization evaluation method in green buildings," *Renew*. *Energy*, vol. 33, no. 5, pp. 883–886, 2008.
[9] Y. Jeong, M. Lee, and J. Kim, "Scenario-based design and symposium assessment of renewable energy supply systems for green building applications," *Energy Procedia*, vol. 136, pp. 27–33, 2017.
[10] R. Cassidy, "White paper on sustainability," *Build. Des. Constr*., vol. 10, no. November, 2003.
[11] I. Rey-stolle, "Fundamentals of photovoltaic cells and systems," in *Solar Energy*, G. M. Crawley, Ed. Singapore: World Scientific, 2016, pp. 31–67.
[12] L. Yang, B. He, and M. Ye, "The application of solar technologies in building energy efficiency: BISE design in solar-powered residential buildings," *Technol. Soc.*, vol. 38, pp. 111–118, 2014.
[13] E. Meng, H. Yu, C. Liu, Z. Sun, and B. Zhou, "Design of phase change material wall based on the heat transfer characteristics in summer," *Procedia Eng.*, vol. 121, pp. 2201–2208, 2015.
[14] T. T. D. Tran and A. D. Smith, "Thermoeconomic analysis of residential rooftop photovoltaic systems with integrated energy storage and resulting impacts on electrical distribution networks," *Sustain. Energy Technol. Assessments*, vol. 29, pp. 92–105, 2018.
[15] J. Cho, S. Jeong, and Y. Kim, "Commercial and research battery technologies for electrical energy storage applications," *Prog. Energy Combust. Sci.*, vol. 48, pp. 84–101, 2015.
[16] D. Larcher and J. M. Tarascon, "Towards greener and more sustainable batteries for electrical energy storage," *Nat. Chem.*, vol. 7, no. 1, pp. 19–29, 2015.

This page intentionally left blank

Chapter 2

Clean energy generation in residential green buildings

Ekin Özgirgin Yapıcı[1] *and Ece Ayli*[1]

Due to the recent investigations, buildings consume a considerable amount of the electricity, drinking water, global final energy use and as a result are responsible for one third of the global carbon emissions. Therefore, building sector has a key role to reach global energy targets. In this sight, this study draws attention to the sustainable energy performances of green buildings (GBs) and aims towards the GBs concept which includes renewable sources in the construction and lifetime utilization. The remainder of the chapter is subjected as follows: Section 2.1 gives a brief information about residential GBs, and in Section 2.2, certification systems for sustainability ratings of residential GBs are given. This is followed by case studies related to the certification systems in Section 2.3 part. In Section 2.4, GBs incentives are summarized. Section 2.5 provides information about energy demand modelling for residential GBs, and in Section 2.6, clean energy generation systems in residential GBs are described in detail. Finally, outlook for the works that is performed up to now and the outlook for the future is given.

2.1 Introduction to residential green buildings

Due to the recent investigations, buildings consume about 60, 15 and 35 per cent of the consumed electricity, drinking water, global final energy use, respectively (Figure 2.1), and as a result, they are responsible from one-third of the global carbon emissions [1]. Therefore, building sector has a key role to reach global energy targets. The uncontrollable increase in the global warming and environmental pollution, the natural products that nature serves us rapidly decreases and the living area of the living things get restricted. In order to be able to overcome those troubles, the idea of green buildings (GBs) become a popular title in last decades.

While interest in the construction of environmentally friendly buildings is increasing, GBs have emerged. The houses that are named as 'Green' or 'Sustainable' use key resources such as energy, water, materials and land more efficiently

[1]Department of Mechanical Engineering, Çankaya University, Turkey

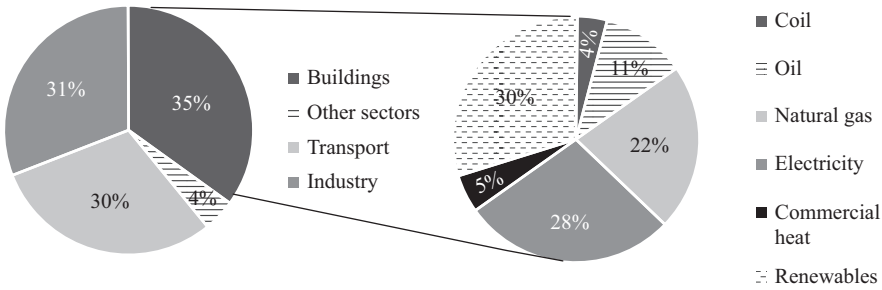

Figure 2.1 (a) Final energy consumption by sectors and (b) energy distribution for buildings (Adapted from [1])

than traditional buildings. There are many factors that distinguish the green houses from other buildings. In these houses, to fulfil the needs of electricity, heating, cooling and conditioning renewable energy solutions are utilized. Designs are performed with maximizing the usage of natural light. In garden watering, domestic waste water is used after the purification process. Even this situation plays an important role in saving water. Energy saving bulbs, taps, showers and smart toilets are used. With using heat pumps, soil heat is transported into the building. Construction wastes are recovered by various methods and environmental pollution is minimized. Environmentalist approaches are applied in the selection and construction of the buildings. Materials are supplied which has no danger of depletion and as close as possible to the construction area. Also in the selection of the building construction materials, it is noteworthy that materials should be chosen that has no danger to the human health. In particular, the exhaust gas-free paints are used in order to increase air quality [2].

GBs that are certificated with various certification systems are ecological, comfortable, reduce the energy consumption and what is more they are respectful to nature. Energy efficient buildings reduce the energy demand by 40 per cent by using more natural light and saving water, and they are beneficial for developers, tenants and owners [3,4]. Robichaud and Anantamula [5] state four critical pillars of GBs such as minimization of environmental impacts, increasing the health conditions of users, economical returns and the life cycle. Kibert [6,7] defines GBs as buildings that are designed, built, operated, renovated and disposed by using ecologic principles with promoting health and efficient resource usage. Some benefits of GBs are

- adding value to urban living spaces;
- improving the economic value of the construction;
- minimizing the ecocide that occurs in the construction phase;
- providing clean energy usage;
- assessing waste material that originates from the excavation;
- purifying rainwater by green roof application;
- using of rain water, thus decreasing the load of the sewer system;

- taking the advantage of solar and wind energy;
- taking the advantage of natural light;
- producing oxygen with green layers;
- decreasing the heating and cooling costs and carbon dioxide emission with isolation systems and
- using of recyclable wastes.

2.2 Certification systems for sustainability ratings of residential green buildings

Insight of such amazing benefits, many countries developed GB label programs to measure the buildings' sustainability level. With rating systems, solving the existing building problems, limiting the environmental impacts, minimizing the health-threating situations and reducing building costs become easier. In the building sector, two main rating tools are given as criteria-based credit system and Life Cycle Assessment (LCA) (Table 2.1) [8]. In the criteria-based system, a specified credit in a prescribed range is given to each topic for all of the categories that describe the assessment tools which has an impact on GB efficiency and sustainability. The certification methods that are classified as criteria based includes the Leadership in Energy and Environmental Design (LEED) in the United States, Building Research Establishment (BRE) Environmental Assessment Method (BREEAM) in the United Kingdom, GBTool in Canada, EcoProfile in Norway and Environmental Status in Sweden [6–9]. All of these methodologies analyse the buildings energy consumptions, characteristics of the buildings and the effects on health [8,9].

The second methodology, LCA, is based on the selection of all of parameters like construction materials, building design criteria and waste management during

Table 2.1 Classification of green-building-assessment methods

Assessment tool	Tool type	Developer	International recognition
BREEAM	Multi-criteria based	Building Research Establishment (BRE) [11]	More than 60 countries
LEED	Multi-criteria based	US Green Building Council [12,13]	USA and other 30 countries
Green Star	Multi-criteria based	Australian Green Building Council [14]	Australia, New Zealand and South Africa
CASBEE	Multi-criteria based	Japan Sustainable Building Consortium [15]	–
BEES	LCA	US National Institute of Standards and Technology (NIST) [16]	–
BEAT	LCA	Danish Building Research Institute (SBI) [17]	–
EcoQuantum	LCA	IVAM, the Netherlands [18]	–

the design phase. Within LCA, different weighting methods are used to assess the environmental impacts of buildings. Some of the LCA-based criterion systems are Bees in USA, Beat in Denmark and EcoQuantum in the Netherlands [8,9,10]. Mattoni *et al.* [9] compared two rating systems and they believed that LCA methodology is more complex and onerous than the criteria-based credit system.

Libovich [19] stated that only considering environmental performance is not affordable in the developing world, also social and economic perspectives should be considered since they are important topics. Therefore, assessment methods are crucial for developing countries. The main difference between the rating systems are their calculation methodologies, credits and weights which has a dominant effect on the final score. Due to the local climatic and geographic conditions, green labelling systems vary between the counties [20,21]. The rating systems enables comparability between the projects and ranges the projects as not acceptable as GB to an excellent GB system. As it can be also seen in Figure 2.2, several rating tools have been developed in the world wide. However, this study focuses on the most popular rating tools such as BREEAM (1990), LEED (1998), ITACA (2002) and Comprehensive Assessment System for Built Environment Efficiency (BEE) (CASBEE) (2001) rating systems.

2.2.1 Building Research Establishment Environmental Assessment Method

BREEAM which is launched in 1990, is the first sustainability assessment method for buildings owned by the United Kingdom, BRE [22]. The main aim of the BREEAM is classifying the buildings with respect to their environmental benefits and to reveal the impacts of building on the environment. The categories that BREEAM give credits are management, energy, transport, health and wellbeing, water consumption, materials, land use and ecology and pollution. Even BREEAM is developed by the United Kingdom and is supported by some other national organizations; thus, for the United Kingdom, Germany, the Netherlands, Norway, Spain, Sweden and Austria, country-specific schemes are developed. The weighting procedure of the BREEAM is given in Table 2.2. All of the categories are divided to the subcategories. Once the number of credits are achieved after reaching the target, the final point is determined by the sum of the weighted category scores.

2.2.2 Leadership in Energy and Environmental Design (LEED) system

The United States Green Building Council (USGBC) [13] has developed the LEED system, which is the most widely used point-based rating system in the world. LEED [23] methodology is composed of five main parts as sustainable sites, water efficiency, energy and atmosphere, materials and resources and indoor environmental quality. For all categories, there are sub-categories, each having a specific credit. Total point is calculated as the credits are summed up. Increase in the earned point means increase in the certification level. LEED scoring criteria and criteria weights are given in Table 2.3 [20].

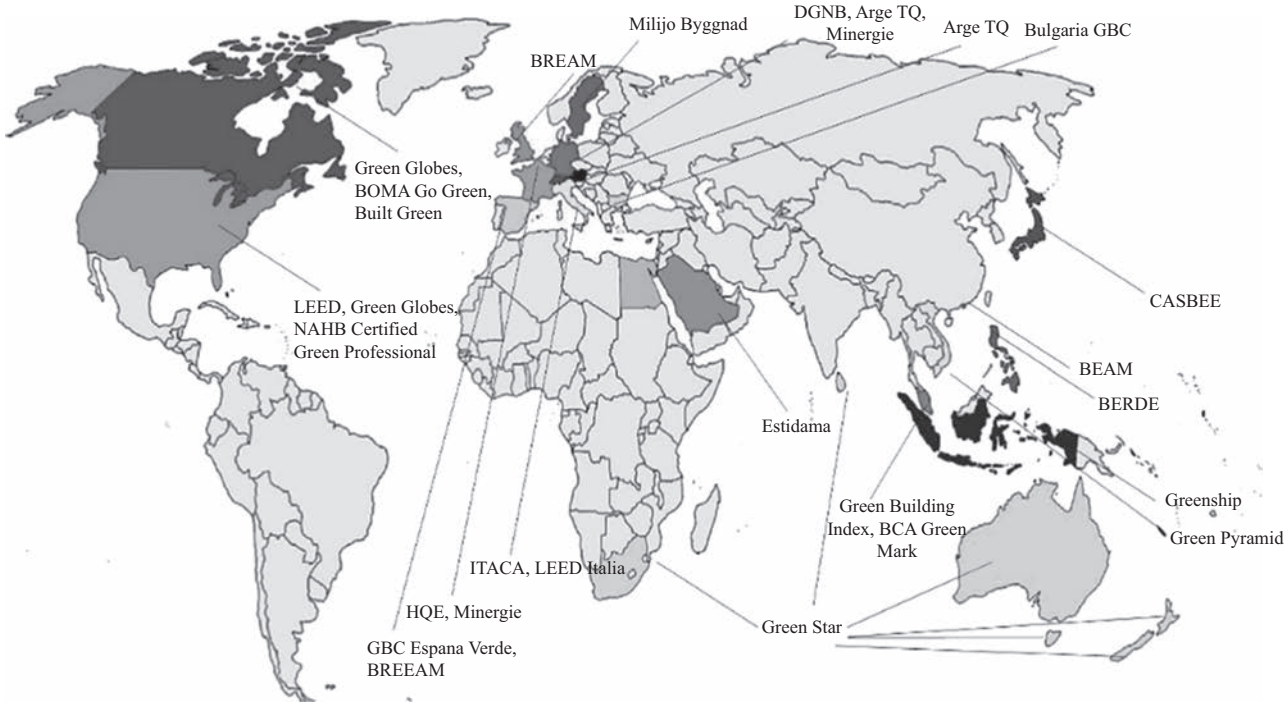

Figure 2.2 A global map for Green Building Ranking System (Adapted from [9])

Table 2.2 BREEAM categories and scores [22]

Categories	Category weights (points)
Management	12
Health and wellbeing	15
Energy	19
Transport	8
Water	6
Materials	12.5
Waste	7.5
Land use and ecology	10
Pollution	10
Total	100
Innovation	10

Table 2.3 LEED v.3 categories and scores [20]

LEED v.3, categories	Category weights (points)
Sustainable sites	26
Water efficiency	10
Energy and atmosphere	35
Materials and resources	14
Indoor environmental quality	15
Innovation	6
Regional priority	4
Total	110

The certification levels are described by USGBC [20] such as

- *Total point*<39: *Not Certified*
- *40<Total point<49: Certified*
- *50<Total point<59: Silver*
- *60<Total point<79: Gold*
- *Total point>80: Platinum*

Some categories and their relative importance are given in Figure 2.3. When all of the parameters are compared with each other, it is obvious that, primary concern is energy consumption and Green House Gas emissions [15]. As LEED is described for the United States, some of the input parameters among these 13 parameters are consistent with the United States locations and does not reflect global scales. Therefore, in 2011, LEED introduced a new database for international projects. LEED international roundtable presents the impact and application of LEED worldwide [20,24].

Lippiatt [16] analysed the regional priority (RP) credits for four countries which are Canada, Turkey, China and Egypt. In Table 2.4, for Canada, Egypt,

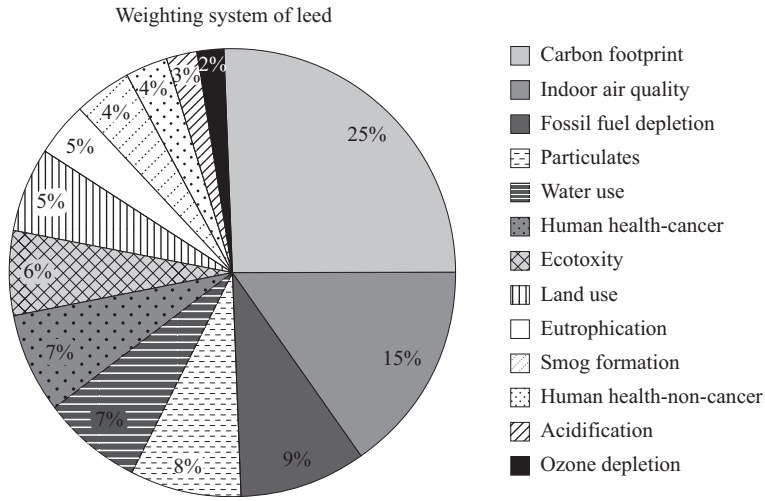

Figure 2.3 Assessment of the relative importance of concerns for LEED (Adapted from [20])

Table 2.4 LEED v.3., regional priority credits for several countries [16]

	Regional priority credits	**Explanation**
Canada	EAc1 (up to 19 points)	Optimize energy performance
	MRc2 (up to 2 points)	Construction waste management
	MRc5 (up to 2 points)	Regional materials
	SSc2 (5 points)	Development density and community connectivity
	SSc6.1 (1 point)	Storm water design – quantity control
	WEc3 (up to 4 points)	Water use reduction
Turkey	EAc1 (up to 19 points)	Optimize energy performance
	EAc2 (up to 7 points)	On-site renewable energy
	EAc7.2 (1 point)	Thermal comfort verification
	MRc1.2 (1 point)	Building reuse – maintain interior nonstructural elements
	SSc6.1 (1 point)	Storm water design – quantity control
	SSc7.2 (1 point)	Heat island effect roof
China	EAc1 (up to 19 points)	Optimize energy performance
	EAc2 (up to 2 points)	Enhanced commissioning
	EAc5 (up to 3 points)	Measurement and verification
	SSc6.1 (1 point)	Stormwater design – quantity control
	WEc1 (up to 4 points)	Water efficient landscaping
	WEc2 (up to 2 points)	Innovative wastewater technologies
Other countries	EAc1 (up to 19 points)	Optimize energy performance
	EAc2 (up to 2 points)	Enhanced commissioning
	EAc5 (up to 3 points)	Measurement and verification
	WEc1 (up to 4 points)	Water efficient landscaping
	WEc2 (up to 2 points)	Innovative wastewater technologies
	WEc3 (up to 4 points)	Water use reduction

Turkey and for several countries, LEED RP credits set by USGBC [13] is given. Canada LEED RP credits and Canada Green Building Council (CAGBC) credits are different from each other, Suzer [20] claims that CAGBC seems to reflect the local conditions of a project more realistically. As it is shown in Table 2.4, for Turkey, two parameters that gained credits for the system are thermal comfort verification, recycling, quantity control of storm water and minimizing heat island effect. Due to the author, as Turkey has limited energy resources and its economy depends on foreign supply, credits are canalizing the designer to use renewable energy sources for minimization of the energy consumption. As China is the most crowded country, credits that encourage the usage of carbon-free transportation, rehabilitation of damaged sites destroying virgin land and increasing ratio of green area is important.

In the Egyptian GB rating system (Green Pyramid), the flagship is water efficiency category while energy efficiency is the second one. On the other hand, in the LEED energy conservation is considered to be the primary global concern (the RP credits for EGYPT is given in Table 2.4, in the other country part). Therefore, LEED and Green Pyramid differs from each other for Egypt in this important point. Suzer believed that for each country as climatic, geographic, social, economic and cultural aspects differ from each other, each region may have different priorities in the ranking system.

2.2.3 ITACA system

ITACA system is the national protocol of the Italy Institute for Innovation and Transparency of Contracts and Environmental Compatibility which is a multi-criteria ranking tool. As it is given in Table 2.5, ITACA ranking system is classified in five macro categories: quality of the site, resource consumption, environmental tools, indoor comfort and quality of the service. The certification levels are A+, A, B, C, D. If the total score is lower than 40, level of certification is D which is insufficient to get the certificate of environmental sustainability. If score is between 40 and 55, building gets a C, if score is between 55 and 70, building gets a B and if score is between 70 and 85, grade is A. If the score is higher than 85, A+ is given to the GB. Asdrubali [25] makes a comparison between LEED and ITACA systems as the macro-areas of the certification systems differ from each other. Especially,

Table 2.5 ITACA categories and scores [25]

Categories	**Category weights (points)**
Site quality	4
Resource consumption	53.6
Environmental loads	17.5
Indoor environmental quality	18.2
Service quality	6.7
Total	100

overall energy performance criterias vary. While in the LEED protocol the orientation of the building, the envelope, the materials and the construction processes are significant, in the ITACA, environmental loads and the resulting CO_2 emissions are also important. Pagliaro *et al.* [26] compare the weighting procedures of BREEAM, ITACA and LEED. ITACA gives the highest importance to the building management, indoor environmental quality, water and environmental loads.

2.2.4 Comprehensive Assessment System for Built Environment Efficiency

CASBEE is developed in Japan in 2001. Various CASBEE schemes are developed whole over the Japan with the help of the academia, industry, national and local governments [15]. According to Doan *et al.* [27], although the CASBEE-certified buildings are still modest, it is the rating tool that evaluates the broadest context (Figure 2.4).

CASBEE ranking process is divided into three phases. First phase evaluates the effects on the building interior and occupants. The second phase is the evaluation of environmental impacts which is originated from buildings. In the last phase, both negative and positive sides of the buildings are evaluated. The CASBEE system provides four categories of assessment, which are energy efficiency, resource efficiency, local environment and indoor environment [20]. Under CASBEE, there are two main assessment categories such as built environment quality (Q) and built environment load (L). To find the BEE Q is divided by L. The use of BEE enables simpler and clearer presentation of building environmental performance assessment results. Due to this formula, increasing Q and decreasing L means increasing the sustainability level of the building. Ranking diagram for CASBEE is shown in Figure 2.5. In this figure, horizontal axis denotes built environment quality (Q) and

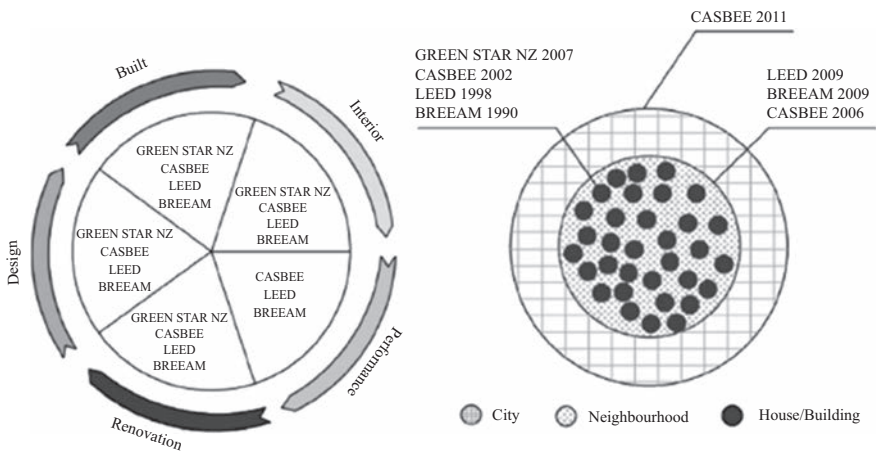

Figure 2.4 Overview of Green Rating Tools (Permission from the Elsevier, Reference [27])

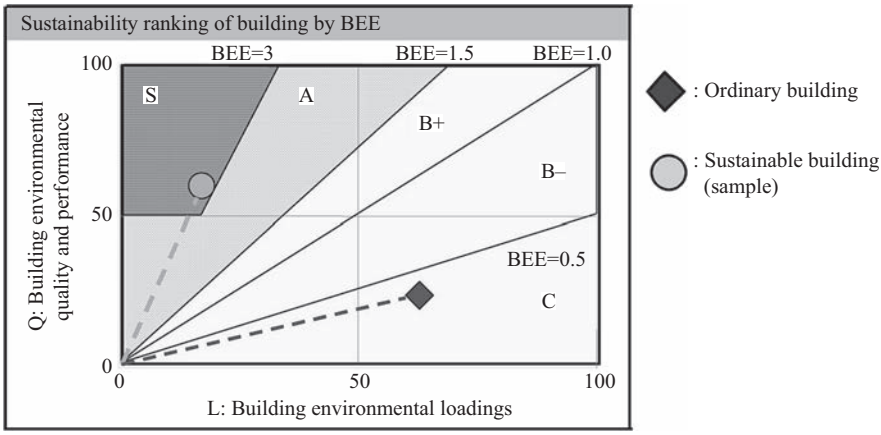

Figure 2.5 Ranking based on the BEE [15]

vertical axis denotes built environment load (L) and BEE value will show the sustainability level of the building which is classified as by classes C, B−, B+, A and S (excellent) [15].

2.3 Case studies related to certification systems and their comparison

Azhar *et al.* [28] conducted a case study on Salisbury University's Perdue School of Business Building to demonstrate the use of BIM (Building Information Model) for sustainable design and the LEED certification process. First of all, researchers developed a conceptual framework to establish the relationship between BIM and LEED rating processes. After developing their own methodology, they validated it with a case study. For sustainability analyses, virtual environment software is used as Azhar and Brown [29] revealed that this software is the most powerful tool in the sustainability analyses. As a conclusion, they showed that their analysis results has a good agreement with the calculations. Slight differences between the results are originated from inaccuracy of the BIM developed for this project.

In 2008, new graduate student housing in Harvard Campus with 151 living units and 101,659 sq ft total size was constructed. In this place, LEED for new construction rating system is used. The project obtained 13 out of 14 credits from LEED program including protecting open space, public transportation and bicycling, campus zip car, storm water, heat island effect, erosion and sedimentation. For energy savings, variable speed pump is used when full load is not necessary, pumps slow down to reduce the energy consumption. Also as the building has so many windows, good insulation and light visibility is important. In this sight, high-quality efficient windows were installed. In addition, high velocity stream shower heads are used in the baths to reduce water flow. In the building, 21 per cent of the used materials contains recycled content and 91 per cent of whole material waste

was diverted from landfills to be either reused or recycled. In Table 2.6, Harvard Real Estate Services LEED rating is given [30].

Aqtake *et al.* [31] examined building-assessment results for Kobe Branch Office Building which suffered damage in the Hanshin-Awaji Earthquake in 1995 and rebuilt in 2000. In this study, CASBEE, BREEAM and LEED systems are compared for the chosen building. Due to CASBEE tool, as energy consumption of this building is smaller when compared with the others in the Japan, 'energy' score is very high (4.5). On the other hand, as building is not constructed with eco-friendly materials, 'resource and material' score is low (3.2). In addition, as there are roads around the building, 'outdoor environment on site' point is low. Due to BREEAM98, building gets similar rankings with CASBEE tool. According to LEED certification, buildings were ranked as silver. By comparison of three ranking tools, researches claimed that, trend of each assessment result are similar among three different tools.

Asdrubali *et al.* [32] compared the LEED and ITACA rating systems in sight of the buildings in Italy. One of the building that is used for comparison is 'Molino Albergo la Nona' which has three above-ground levels directly connected to the underground garage by a common staircase. The building has a solar greenhouse capable of storing heat during the winter period, natural ventilation system, and shielded by trees to prevent overheating in the summer [33,34]. Solar panels are placed in the roof of the building which is insulated by wooden panels. As a water recycling method, underground tank for recovery of the rainwater is used as well as reusing of grey water by phytodepuration. In Figure 2.5, comparison between LEED and ITACA certification systems for the building is shown. For ITACA, building is 'Class B' certified with 61.94 per cent and for LEED, it is 'certified' with 43 per cent. As ITACA is a local ranking tool for Italy and the examined building is in Italy, building gets a higher ranking from this system. Due to their results, it is obvious that LEED gives higher attention to quality of site, while ITACA gives higher attention to materials, energy and indoor environmental quality.

Politi and Antonini [35] developed a methodology to compare the rating systems for residential buildings. The developed methodology enables the designers to see the common criteria of the rating tools while proposing a mutual platform for all the users.

Table 2.6 Harvard Real Estate Services LEED rating (Adapted from [30])

Gold	**41***
Sustainable sites	13/14
Water efficiency	3/5
Energy and atmosphere	2/17
Material and resources	6/13
Indoor environmental quality	12/15
Innovation and design	5/5

*Out of possible 69 points.

In Oakland, multifamily residential is constructed with Green Point rating of 79 points, which is a high mark in the energy-efficiency category. As a resource conservation, 50 per cent of the construction waste is recycled. Drainage system is used. In the energy efficiency part, Energy Star cool roof membrane and Aluminium windows are used, HVAC system is designed, ductwork is installed within conditioned space [36].

2.4 Green buildings incentives

GB investments are usually high, and pay back times are not so satisfying which are between 7 and 20 years; so to overcome these barriers, incentives act as a way to minimize or eliminate costs or issues related to their adoption. Incentives are important for motivating and influencing developers and investors to decide on investing in green properties [36].

GB incentives are categorized into two: external incentives and internal incentives. For the external incentives, beneficiaries are required to carry out specified conditions or requirements to get the incentive, while by the internal incentives, beneficiaries are incentivised out of their will for having the benefits of GBs. The external incentives are mostly provided by the government and these are divided into two: financial and non-financial, later being widely used. Both external and internal incentives are very important means for promoting GBs, and they should be attractive and easy to use, which are explained in detail in the following sections [37].

2.4.1 External incentives

External incentives are incentives provided by the government. In other words, the beneficiaries are obligated to meet a specified GB-related condition or requirement to get government incentives.

The government has a very significant role in motivating GB development [38], also recently, construction sector is positively affecting the society through GB construction [39], and as the largest owner in construction as well, government has an important influence to make people realise the advantages of GBs. As already explained before, external incentives are categorized into two as: financial and non-financial, in other word, cost free [40].

2.4.1.1 Financial incentives

Since it is usually difficult to convince private clients to invest on extra necessities for green and sustainable building construction, which makes the total initial cost higher and pay pack time of the investment increase considerably, financial incentives provided by the government make the investment pretty much attractive.

The most common financial incentives provided by the government include direct grants, rebates and discounted development application fees and also tax incentives [37,39]. These provide very effective financial gains for the beneficiaries. For instance, as a result of such incentives, there has been an increasing number of GBs and related certification in Malaysia between years 2009 and 2013,

since owners of GBs are offered great tax deductions by the government if they have these green certificates (known as GBs label programmes or renewable documents) [41]. Exemption of tax payment for GBs is also very popular in America, in most of the Asian countries and in some European countries [42–44].

2.4.1.2 Non-financial incentives

The non-financial incentives include the government granting the owners the right or additional rights that are beyond the normally allowable ones when certain conditions are fulfilled. These include zoning/floor area ratios (floor-to-area density (FAR)) [45], accelerated permitting, business planning assistance, technical assistance, marketing assistance, regulatory relief, guarantee programmes and dedicated green management teams in building and planning departments [46].

The FAR incentive allows the owners to construct more building area than permitted by the usual zoning. Accelerated permitting enable owners who incorporate GBs to get their plans and permits more quickly from government or municipalities. Technical or administrative assistance provided by governmental teams may help the beneficiaries proceed more quickly and secure with the processes.

2.4.2 Internal incentives

There are some mostly self-motivated incentives other than the governmental sourced ones, which can be classified under the heading 'internal incentives'. These include such unique benefits as opportunity to efficiently use resources, increased marketability and increased communal reputation [38], which appeal to the benefit of project owners and encourage their interest in construction of GBs. Despite the forced nature of external incentives, internal incentives arise from a person's feelings or connection about the activity, and they are not forced.

2.4.2.1 Human well-being-related incentives

Humans staying in buildings for a long time expect that they prefer a high level of comfort which makes comfort an internal incentive for building occupants. Also the benefits of GB in terms of human well-being turn them into attractions for project owners [37,38].

2.4.2.2 Market-demand-related incentives

The fact that the GBs have a greater market demand, willingness to pay [38,44,47] and higher rental values than conventional buildings become an internal incentive which encourages project owners to provide GBs [37,38,44].

2.4.2.3 Human self-motivation sourced incentives

The human self-motivation sourced incentives are as follows:

Gratifying incentives: Gratifying incentives are those that come with recognition of the awards and green certification to the owners of GBs. The achievements led to a feeling of gratification, increase of reputation and image [39]. For example, in the United States, the LEED certification level

becomes a competition in the real estate industry. LEED platinum projects are differentiated and prided by the owners extensively.

Altruistic incentives: Another incentive are the altruistic of personal moral norms and values on environmental beliefs. Aliahga explained that, one of the concerns of the GB owners is that green technology can reduce the effects of climate on humans and environment [48,49].

Persuasion-related incentives: Very high-energy costs and other unfavourable circumstances persuaded people towards construction of GBs.

2.4.3 Concluding remarks

GB incentives which are very important for motivating the construction and ownership of GBs are divided into two categories as external and internal, based on their manner of motivation as explained clearly earlier in this section. External incentives, promoted by government, can be a benefit for the developers' or investors' expected financial returns and so directly influence and affect the kind, nature and degree of GB supply. Internal incentives on the other hand are self-motivated and intrinsic in nature, but they also influence the owner's willingness towards GB construction [49].

GBs are getting more and more especially in the United States, largely due to the incentives [50], which clearly prove the effectiveness of incentives. Recent studies show that, even the governments are more involved in providing incentives; private sector's role is getting bigger and bigger every day. For increasing the awareness of GBs, increasing awareness of knowledge on incentives is very important as the way, quality and quantity of the promoting incentives distinguishes the GBs.

2.5 Energy demand modelling for residential green buildings

The energy demand of a building represents the energy used by all energy systems to provide the energy needs in the building. For that, energy systems' efficiency and behaviour should be taken into account. The energy consumption refers to the total energy demand over a period. Power demand on the other hand represents the instantaneous energy demand [51].

For residential or commercial buildings, energy demand modelling or so-called building energy consumption determination is very important since a close match between the demand and the supply is always advantageous in terms of efficiency, better utilization of resources and protecting the environment.

In buildings, most of the energy goes towards space heating, space cooling, water heating and lighting, followed by electronics use, cooling, ventilation, cleaning, cooking and computers [52].

Different parameters affecting overall energy consumption are occupancy and occupant behaviour, building characteristics and building systems, climate and meteorological conditions. Also, depending on the building site, the source of

energy may be electricity, natural gas, oil, and it may include poly-generation renewable energy sources and passive solar gains [53].

Modelling of energy demand and efficiency in buildings is a useful tool, which allows the quantification of building energy consumption and distribution of end uses [53]. It may provide a good prediction of consumed energy on a regional or national scale, it can determine the requirements for energy supply, it can provide useful feedback on decision for different types of applications of energy-generation methods, related new technologies, new materials and help to predict the amount of investment and pay back periods.

A general approach for the development of a tool for the estimation of the building energy consumption and the supply costs is given as a case study at the end of this section, after all relevant information is given about demand modelling.

2.5.1 Classification of modelling approaches

In literature, there are different modelling approaches which use the input data to simulate the energy consumption of buildings or more over, regions. These vary on the availability and details of the data, details of the required information and the data acquisition approach. First of all, two approaches for urban energy issues are defined as top-down and bottom-up models [51,53]. Bottom-up models calculate the energy consumption of individual or groups of buildings and then extrapolate these results to represent the region or national scale. Since they separately estimate the energy consumption for each building, different approaches can be used such as statistical or engineering approaches. According to the approach, relevant models can be applied to predict the behaviour of the energy consumption of the building. Usually historical information is used to establish the relation between the energy consumption of the building and the end use of energy [53,54].

On the other hand, top-down models utilize the estimation of total building sector energy consumption and some other variables to find the energy consumption of the entire building sector. Top-down includes econometrics and technological models and a massive data which in some cases is difficult to obtain. Another important classification is according to the details of the required information. As already mentioned, modelling or so-called building energy simulation can be done by a physical approach, a statistical approach or a combination of both [53,54]. The classification of models and information on techniques can be found in Figure 2.6. Later in this section, all methods are explained in order.

2.5.1.1 Physical approaches

Physical approaches use sets of equations to solve the phenomena like energy conservation, heat transfer and require many details about building such as consumption related to the people in the building, hot water supply, electric devices in workplace and architectural information. Numerical software is usually used and mainly computational fluid dynamics (CFD) methods, zonal (2-D) methods or multizone/nodal (1-D) methods are employed.

The most complete physical approach is the CFD method, which is a microscopic approach of the thermal energy modelling which gives a detailed description

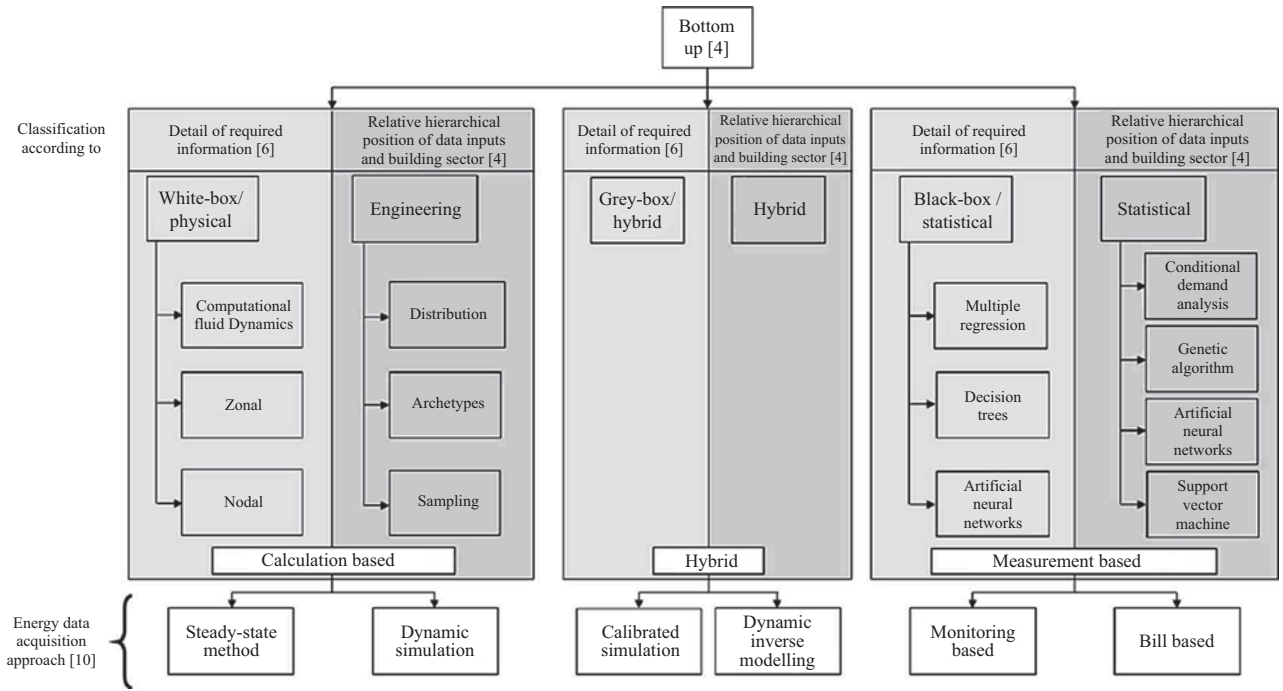

Figure 2.6 Building modelling approaches classification (Permission from Elsevier, Reference [53])

of airflow, pollutant flow, heat flow, etc. in the building. By this method, complex geometries can be studied. Each building zone is divided in a large number of volumes with global mesh. This method is called three-dimensional approach, but on the other hand, CFD methods require a huge computing time, and when the models are complex, implementation of the programs may be difficult without previous knowledge on fluid dynamics and the specific software [55]. Examples of most common software programs are FLUENT, COMSOL Multiphysics for CFD methods.

As an example to this approach, Wang and Wong [56] used FLUENT and ESP-r to simulate the natural ventilation in a double zone residential building. The ESP-r building simulation contained the geometrical information, thermal properties of the construction and the airflow system for the whole building. To reduce the computation time, the authors chose to apply the CFD simulation only in one zone. The ESP-r simulation results provided boundary conditions to the CFD simulation.

Second method; the zonal method is simplification of the CFD technique. Bouia and Dalicieux have introduced this method [57] in the beginning of 1990s. This approach is advantageous to find details of the indoor environment and it estimates a zone thermal comfort. Each building zone is divided into several cells. One cell corresponds to a small part of a room. The zonal method is considered to be a two-dimensional approach. Examples of most common software programs are Haghighat with POMA and SimSPARK for such models. The down side is that, this technique requires knowledge of the flow profiles, and the user may not be able to find accurate detailed results of the flow field [55].

This method was used by Brun *et al.* [58] where they proposed experimental and numerical studies to model heat transfers in a naturally ventilated roof cavity in buildings in Grenoble, France. They used SPARK to estimate the heat gain.

The multizone or nodal approach, which is usually the simplest physical approach, considers the assumption of treating each building zone as an homogeneous volume defined by uniform variables of state (temperature, pressure and concentration). One zone is approximated to a node. The energy equations are solved for each node of the system [55]. TrnSys (Transient Simulation Program), EnergyPlus, IDA-ICE, Clim2000, BSim are the most well-known software for building simulations which use the nodal approach.

As an example of multi-zone approach, Kalogirou [59] used TrnSys to determine the energy consumption in a building in Nicosia, Cyprus. He compared a hybrid photovoltaic (PV)-thermal solar system with a standard PV panel in terms of energy-demand behaviours.

Zhai *et al.* [60] used EnergyPlus software to study effects of ventilation in summer on simulated data of indoor temperature. They compared experimental and simulation results in three different building offices with distinct properties; one in Belgium, one in Denmark and another one in the United Kingdom.

2.5.1.2 Statistical approaches

Statistical methods are mainly multiple linear regression [61] or conditional demand analysis (CDA), artificial neural networks (ANNs), genetic algorithm (GA)

and decision trees which rely on training data to extract system function and do not require physical information. These do not require heat-transfer equations, thermal or geometrical parameters, but they require a large amount of training data collected over a long period of time. Statistical models are based on the implementation of a function concluded from training data samples which describe the behaviour of a specific system and it may be difficult to interpret results in physical terms [55].

Linear regression methods (CDA techniques) can be used both for prediction or forecasting and for data mining. These methods have an advantage which is the simplicity of use by beginners since no specific expertise of the method is required. Such a model was successfully used to calculate the residential end use energy consumption by Aydinalp-Koksal *et al.* [62], but it has some disadvantages such that, it cannot be used for nonlinear problems [61,62].

The GA which is an artificial intelligence method is a stochastic optimization technique. It has been introduced by Holland in 1975 [63], but its use in the area of building simulation as an optimization tool started in the 1990s [55]. GA deals with a powerful optimization method and is able to resolve every problem provided the convexity of the describing function.

Caldas *et al.* [64] used GAs for optimization of building envelopes and they designed a HVAC system and study the control of the system. Another advantage of the GA is its ability to give several final solutions to a complex problem even if there is a large number of inputs. It allows the user to choose the most probable solution. Most important disadvantage of this approach is, sometimes a large computation time may be required.

Ozturk *et al.* [65] used a stochastic optimization technique in developing Turkey's electric energy estimation. Electricity consumption estimation is determined for the industrial sector and for the total electricity demand in Turkey. They developed two different nonlinear estimation models and validated these models with actual data. They also estimated future electricity demand projected between 2002 and 2025.

The last statistical approach is based on ANN which is a nonlinear statistical technique used for prediction. This artificial intelligence method was inspired by the biological neural networks (including neurons, dendrites, axons and synapses) that constitute animal brains. The original aim of the method is to solve problems in the same way that a human brain would solve. In 1943, Lettvin *et al*. has studied this method in mathematical form [66]. There are numerous advantages of the ANN. First, information can be stored on the entire network, and even with some missing information, network can still perform. Also, it has a higher error tolerance and it overcomes the discretization problem. ANNs can learn events and make decisions by commenting on similar events, and they have parallel processing ability. However, the ANNs are limited by the fact that it implies to have a relevant database. Indeed, it may be challenging to train an ANN with a huge learning data with representative and complete samples.

In the building simulation, ANN are usually used to predict the energy consumption or the forecasting of energy use (as cooling or heating demand) without knowing the thermal properties or the specific geometry of the building. Kalogirou

[67] has studied various ANN-based building energy simulation but particularly, in 2000, he presented a review in the scope of applications of the ANN in the field of energy systems.

2.5.1.3 Hybrid methods

Hybrid methods combine physical and statistical approaches where an undetailed description of building geometry and a smaller amount of training data are adequate. In this method, results can be interpreted in terms of physical parameters [53]. The main advantage of the hybrid method is that it allows considering only a limited number of data and computational times are relatively short compared with physical methods.

There are three strategies for this method which are [55] as follows:

- Using machine learning as physical parameters estimator.
- Using statistics in order to implement a learning model built from a physical approach to describe building behaviour.
- Using statistical method in fields where physical models are not effective enough (e.g. in order to implement the whole system, both physical and statistical methods can be combined).
- Determining the heat behaviour in a multiple zone building where the thermal properties of some rooms would be unknown. (Some zones can be physically studied while others can be statistically described.)

Disadvantage, on the other hand, is that computation time for both physical and statistical codes may be long, since this method couples two distinct scientific domains. This approach can be said to be of a great scientific interest.

Philippe *et al.* [68] combined finite difference method via the CODYRUN which is a multizone software with a GA. They implemented a model and solved the energy and mass transfer equations in a building which has a simple geometry. Aim of the study is to optimize the value of the dry air temperature inside the building and the study is based on experimental data.

As another example, Essia *et al.* [69] studied energy consumption in a building in which it is located in Tunisia. They optimized the architectural parameters to improve the energy efficiency in this Mediterranean building. They also considered the economic point of view. They used a simplified tool for building energy evaluation used by the Mediterranean countries to a GA for identification of the architectural parameters. They studied the problem both for summer and for winter. They showed that the optimal solutions are different considering either energy saving or economics.

2.5.2 Case study about building energy-consumption determination

As one complete example, the general procedure for energy demand modelling considering physical methods will be explained later in this section as adopted from Grubera *et al.* [70]. They proposed a computer tool that combines architectural characteristics and user interactions with a building to estimate its energy

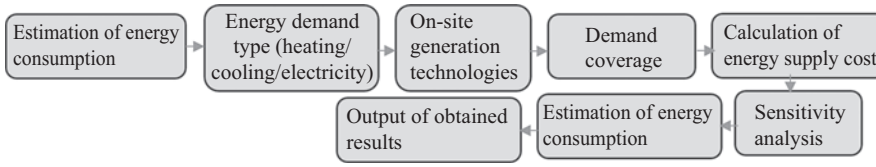

Figure 2.7 General structure for estimation of building energy consumption and supply cost (Adapted from [70])

consumption and costs of energy supply. The tool also determines the sensitivity of the energy consumption and the related costs for changes applied in the building model or in the energy tariffs. They then applied the developed tool to a building located in Madrid (Spain).

Generally, the building energy assessment tool which is developed by using MATLAB® R2013b has two main functions: it helps to estimate the energy consumption and supply costs and to analyse sensitivity with respect to changes in the building configuration. Steps for such a procedure are seen in Figure 2.7.

The tool estimates the energy demand for a whole year on an hourly basis. The building model considers both the building architecture and the presence of occupants of the building. The model developed is based on steady-state condition. When the demand is estimated, it is divided in heating, cooling and electricity loads. Afterwards, the demands which are to be supplied are distributed on different generation technologies (heat pump, chiller, etc.) and energy sources (electricity, gas, renewable, etc.). Finally, to define the building's overall energy system, the total cost for the energy supply are calculated on basis of the demands. The tool also determines the critical building parameters and use them to reduce energy consumption for an improved energy efficiency [70].

A wide range of different building types can be modelled by the proposed tool; the authors has conducted an energy analysis of an office building located in Madrid. They observed that, the heat demand decreases from 60 kW to approximately 10 kW during the months of June and July. In the same period, the cooling demand increases from 80 to 180 kW. Maximum electrical demand is 60 kW. Heating demand is covered by a gas-fired boiler and for cooling purposes, a chiller is used in the building. The resulting total annual energy costs for the considered building is found to be precisely 73,592 Euro (21,639.5 Euro for the gas supply and 51,952.5 Euro for electricity).

2.6 Clean energy generation in residential green buildings

2.6.1 Evaluation of building towards clean energy generation

In the last few decades, building design towards clean energy generation become a popular title in all over the world. Building transformation starts first with

minimizing the energy demand with passive solutions, which is known as passive buildings. Then, it goes with nearly zero energy buildings (nZEB). The main objective of nZEB buildings is to increase the energy performance while decreasing the energy, which comes from non-fossil resources. With the last evolution, new approach is having smart buildings with lowest cost and environmental impact over the building lifecycle. Historical development of building transformation is shown in Figure 2.8 [71,72]. There are a lot of researches on passive, nZeb and smart buildings, examined in the respected order, in the previous paragraphs.

Passive houses which provide high quality of indoor conditions with lower energy demands were first described in Darmstadt, Germany. Schneiders revealed that [73] nearly 22 per cent of the total energy is used in space heating in the buildings in Germany. The space heat demand is approximately 150, 100, 70 kW h per square metre in 1982, 1995 and 2002, respectively. With introducing the passive houses, this demand reduces to nearly 15 kW h/m^2 a, where 'a' denotes per annum (year), without a conventional distribution system. To be a passive building, building heating load should not exceed 10 W/m^2. To design such a system, building envelope, windows and automatic ventilation system should be optimized in order to minimize the heat losses. This type of houses are known as 'passive' because of the 'passive' use of incidental heat gains – delivered externally by solar irradiation through the windows. In the passive house concept, the major criteria are superinsulation, heat recovery and passive solar gain.

Taleb [74] suggested several passive cooling strategies to reduce energy consumption in a building. Solar shading performance is calculated by using Sun Can Analysis which is the part of IES software. Also, DesignBuilder software is used for validation. Temperatures are recorded for 24 months and average values are taken for each month. With using the measured temperature values, thermal analysis are performed. Due to the results, shading devices block the solar heat, optimizing the proper window openings to increase the indoor fresh air. Due to the

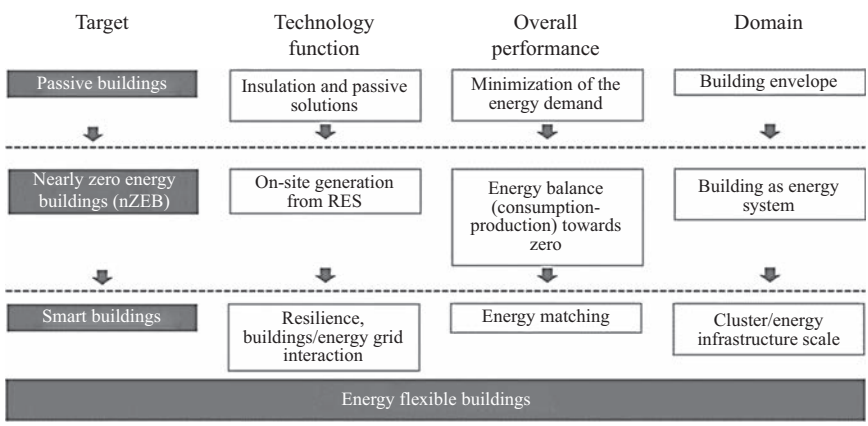

Figure 2.8 Historical development of building transformation (Permission from the Elsevier, Reference [71])

results that is obtained from the IEC software, it is seen that with appropriate cooling strategies, cooling load can be decreased by 9 per cent.

Badescu *et al.* [75] described the cooling requirements for passive buildings with making a case study in Romania. The investigated building is both an office building and a residential. For this building, steady state analysis of the cooling load is performed by using Passive House Planning Package (PHPP) software [76]. The results obtained with the PHPP are compared with the traditional building. Due to their results, the standard building requires heating mainly during October to April, while the passive building must be heated just from December to February.

Dan *et al.* [77] studied the indoor parameters that has a direct effect on energy consumption. They monitored the indoor temperature values, energy consumption, carbon dioxide level and humidity of the building for 2 years. They used PHPP and DOSET software to calculate the energy demand by using the input parameters.

Gou *et al.* [78] optimize the passive design of newly built residential buildings in hot summer and cold winter period of China. In sight of these objective, researchers set their model for multi-objective optimization, and second-stage sensitivity analysis is performed to reduce the dimensions of input variables. They performed multi-objective optimization by using non-dominated sorting GA-II (NSGA-II) coupled with the ANN. According to their proposed methodology for optimizing passive design of buildings, researchers investigate the impact of 37 passive design parameters.

Germany, which is a country that gives high importance to energy saving, sets a CO_2 emission reduction target for 2020. Especially for buildings, it is suggested that heat-demand reduction should be in the level of 20 per cent by 2020 when compared to 2010. Other European countries also aim to reduce the greenhouse emissions in the building sector, and in this context, directive of the European Parliament and of the Council on the energy performance of buildings announced that, by the end of 2020, EU states should assure that all new buildings must consume nearly zero energy. In the nearly zero buildings, energy demand should be met almost wholly from the renewable sources. nZEB are defined as energy saving buildings with little or no CO_2 emission and increased indoor thermal comfort. Energy saving and minimum emission production are achieved by reducing the energy demand and using renewable energy sources such as wind, solar, geothermal and water. The basic principles of sustainability such as recycling and reusing are also the basis of the nZEB [79,80].

Schimschar *et al.* [81] examine the German energy performance buildings in German building sector. Researchers claimed that Germany will reach their energy end emission reduction targets by 2020. In Finland, the first house that is designed with the objective of minimum energy consumption is monitored for 3 years. With using the input data that is collected from monitoring, it is estimated that the cost of additional investments for energy efficiency usage pays itself back in 5–6 years [82]. Pylsy and Kalema [83] found that for reducing the space-heating energy, the most important parameter is thermal insulation. Due to Saari *et al.* [84], repay time of the heating systems depend on the interest rate and building construction. Hamdy and Siren [85] developed a multistage simulation-based optimization

methodology to find the cost-optimal and nearly zero energy-building solutions. The methodology is applied to a single-family house in Finland, and several combinations of building-envelopes, heat-recovery units, cooling and heating options, as well as solar-thermal and PV solar systems are explored with a suitable number of iterations. Cakmanus [86] argued that the construction of nZEB does not require huge investments. The first costs do not exceed 10 per cent. In this context, increasing the performance of the building envelope (to minimize heating, cooling and ventilation loads), free cooling for residual loads, heat recovery, thermal storage, natural ventilation, use of renewable energy sources, use of high efficiency HVAC systems, etc. need to be considered.

After evolution of nZEB, new discussion began in 2007 about smart buildings with lowest cost and environmental impact over the building lifecycle. The use of zero energy in buildings has become even more important because of the increase in fuel prices which led to 'fuel poverty', and it has attracted the attention of a wider international audience. The United Kingdom was the first country to provide an original definition of zero carbon homes in late 2006s [87,88]. At the same time, a new definition came from the USA initiated by Torcellini *et al.* [89]. Torcellini defined ZEB as

> A net zero-energy building (ZEB) is a residential or commercial building with greatly reduced energy needs through efficiency gains such that the balance of energy needs can be supplied with renewable technologies.

For zero energy buildings, significant technological developments have been attracting attention in the last few decades especially for insulation materials in building technology, renewable energy utilization equipment and stricter building regulations on energy efficiency [90]. Thormark [91] points out the importance of the building material to decrease the life cycle energy use of the buildings. Day by day, ZEB demonstration projects increases. Kristjansdottir *et al*. [92] redesign the previous concept for a single-family Zero Greenhouse Gas Emission Building (ZEB). The new model that researchers proposed has 78 m^2 PV area which is 19 m^2 larger than the previous design. The insulation material is changed to glass wool insulation with low carbon concrete. However, their new design does not meet the new ZEB model. Panagiotidou and Fuller [93] compare the four ZEBs with each other. Each of them settled in different countries with having different climatic conditions, legislative context and building technologies. The buildings are 'Home for Life' EnergyPlus Building in Norway, the 'Solar House' Autonomous ZEB in Germany, the 'EcoTerra House' Net-ZEB in Canada and the 'CarbonLight Homes' Near-ZEB in the United Kingdom. Due to their study, it is informed that, ZEBs are still in demonstration in 2013 and there is an absence of a mass implementation for the concept. Nowadays, renovation towards nZEB is an important goal in many European countries. From 2013 to the present day, several researches design nZEB and ZEB [94–96].

2.6.2 Classification of clean energy generation systems

Clean energy or so-called renewable energy generation systems, varying from solar to geothermal, hydrogen to wind power must be located where the natural energy

flux occurs, like inside or around the buildings, unlike conventional fossil-fuel generation systems. Renewable energy generation technologies have the largest percentage of the cost as the construction cost unlike fossil fuel energy generation techniques since they do not have fuel costs.

Renewable energy generation systems can be classified into three titles such as: active systems, passive systems and hybrid systems which are formed by coupling different clean energy generation systems with each other or with conventional fossil fuel energy generation systems.

2.6.2.1 Active systems

Active clean energy generation systems cover wind turbines, solar energy collectors, solar chimney and fuel cells, which are explained in this section shortly.

Small wind systems

The wind energy comes from the pressure differences in the atmosphere in the form of air currents. Electricity generation by wind energy is achieved by converting the kinetic energy of the wind (motion) into first mechanical energy, then to electrical energy. No harmful gases are released to the atmosphere during the energy recovery from the wind, and there is no cost of transporting raw materials as well.

For harvesting wind energy, wind turbines are used, which are relatively simple machines operated very simply and for a long time with a little maintenance cost. Also, the investment cost of wind system is less than the solar system of the same size [97].

Wind turbines are modular, can be manufactured in any size (capacity) and can be utilized alone or in groups. If desired, they can be disassembled in a short time and moved to another place as they can be transported in fragments without problems. Their life span is about 25–30 years and pay pack times of such investments are about 5–6 years. In the simplest sense, a wind turbine shown in Figure 2.9

Figure 2.9 Şamlı wind power plant-Balıkesir-Türkiye [99]

consists of three parts: first and most important part is the propeller which rotates when the wind blows, so that kinetic (motion) energy is obtained by wind energy. Second, there is the shaft connected to the propeller, which transmits the rotation to the generator and the generator where electrical energy is produced by electromagnetic induction [98].

Capacity of a wind turbine varies between 20 kW and 1.5 MW depending on the size of the turbine (blades). These can be coupled to an energy production system of a building or a cluster of buildings according to the required electrical energy.

Fuel cell systems

Hydrogen, which is one of the most abundant elements in nature, has an important place in alternative energy sources. The systems that uses hydrogen energy to obtain direct current electrical energy are known as fuel cell systems. Fuel cells have become one of the most important clean energy production methods due to their high efficiency, reliability, quietness, robustness, ability to generate high power and environmental friendliness because of their low emissions. On the other side, usage of fuel cell requires a lot of information and advanced technology, also system costs are a little more when it is compared to other clean power generation systems.

Fuel cells can be used in portable devices mostly in transportation and services sectors and mobile devices (mobile phones or computer-based mobile applications), as well as in modular buildings and domestic power generation and cogeneration applications as it is given in Figure 2.10 [100,101].

Hydrogen–oxygen or hydrogen–air is required to operate the fuel cell. The fuel cell is formed by an electrolyte that is placed between two electrodes. Air passes over the anode surface. While the electrons are transported through the cathode by the external circuit, hydrogen ions move through the electrolyte to the oxygen electrode. Water is produced by the reaction of electrons with oxygen and hydrogen ions in the cathode. Electricity is generated by the flow of electrons through the

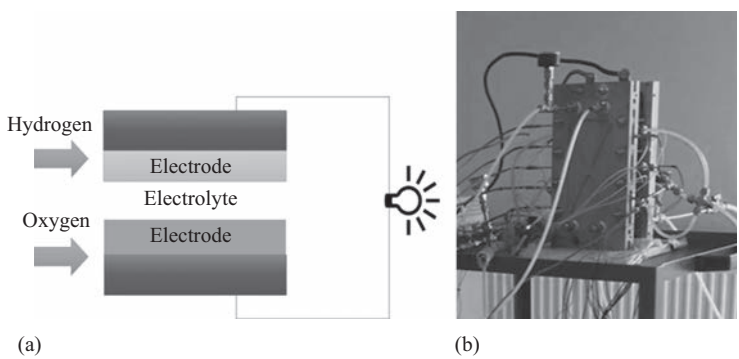

Figure 2.10 (a) Schematic representation of a fuel cell and (b) a proton exchange membrane fuel cell (PEMFC) fuel cell (Courtesy of Özgirgin, Reference [100])

external circuit. As a by-product in the fuel system, water is obtained in the form of heat and steam and can be used on-site if required.

Fuel cells are classified accordingly due to the electrolyte usage types [102]:

- alkaline fuel cells,
- polymer electrolyte membrane or PEMFCs,
- phosphoric acid fuel cells,
- molten carbonate fuel cells and
- solid oxide fuel cells.

The choice of the type of fuel cell to be employed in the system depends on the application area, air/oxygen feeding method and energy demand. Commercially available fuel cell capacities vary from 5 kW to almost up to 1,000 kW. Used in modules (stacks), higher power can be utilized for necessary applications.

Some of the active solar energy systems are as follows:

1. *Flat plate/Heat pipe solar collectors for water heating or space*
   Solar energy is the most important and popular source of renewable and clean energy which is provided by the sun in the form of solar radiation. Solar energy technologies do not produce any emissions, are relatively cheap, maintenance costs are low, do not require highly qualified staff and easy to implement. These technologies are classified into two such as active and passive solar-energy technologies. Active technologies cover water or air heating (using collectors), space heating and cooling, boiling or superheating water for expanding in steam turbine (mechanical energy generation). The first two applications are suitable for utilization in buildings [103].

   There are some disadvantages though: solar energy is very low in winter and it is not available during night-time. Also, since solar energy is not continuous, it should be stored using batteries, heat storage tanks, etc. which increase the investment cost. While implementing, it is important that, there should be no obstacles around the solar systems, which can shade. Another problem is that, for maximum efficiency, sun rays should strike the solar systems vertically, for that sun-tracking systems are sometimes used which also increases investment and maintenance costs [103].

   Useful energy in forms of heat or hot water can be utilized with the help of solar energy collectors. Solar energy collectors are special heat exchangers that transform solar radiation energy of the sun into internal energy in the form of hot water or hot air using active mechanical systems such as pumps or fans as seen in Figure 2.11. Energy is carried to the demand point with the help of heat transfer fluid [104].

   There are two types of solar collectors:

   (i) Non-concentrating or stationary collectors have the same area for intercepting and absorbing solar radiation. Examples of these types are flat plate collectors and evacuated (vacuum) tube collectors [103]. These have a simple geometry, they are easy to utilize and cheap, but they have lower efficiencies. These are suitable for low temperature applications, and usually used in single or multiple buildings thermal systems.

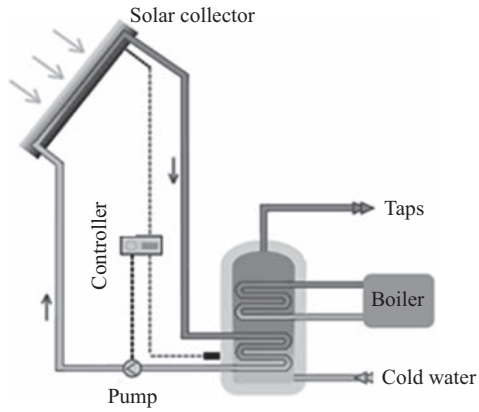

Figure 2.11 Schematic view of solar collector system (Adapted by [104])

(ii) Concentrating collectors usually have sun-tracking mechanism, concave reflecting surfaces to intercept and focus the sun's beam radiation to a smaller receiving area. They have higher efficiencies compared to non-concentrating collectors since they increase the radiation flux, but they are expensive and complex structures. Examples are compound parabolic collector, parabolic trough collector, linear Fresnel reflector, parabolic dish and central receiver. Concentrating collectors are suitable for high-temperature applications but most of the time they are used for centralized electricity or heat production.

Home size thermal collector applications utilizing flat plate or evacuated tube type collectors are easily coupled with district heating systems; they increase the systems thermal efficiency and decrease the costs for heating water or space heating applications [103].

2. *Solar chimney:*

The solar chimney power plant (SCPP) is one of the most beneficial applications of solar power. Is a device, which produces electricity with the help of the wind turbine, placed in the centre of the chimney, driven by airflow generated by buoyancy resulting from greenhouse effect inside the collector. SCPP system contains various components; the solar collector, chimney, wind turbine auxiliary connecting equipment and sometimes heat exchangers. The collector heats up ambient air entering the system by buoyancy force [105]. The hot air leads to a flow through the turbine and drives the pressure-staged turbine in the chimney base to generate electricity [106]. A simple schematic of the chimney can be seen in Figure 2.12 [107].

When compared with the conventional power-production methods, SCPP has a lot of advantages which can be summarized in the next few lines. Their design procedure is easier, power generation cost is lower, have higher operational reliability and few running components, maintenance costs are cheaper,

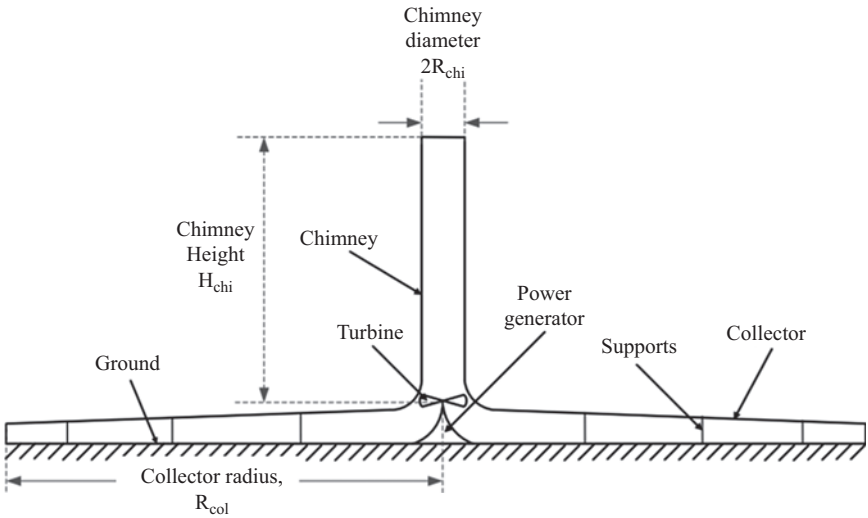

Figure 2.12 Schematics of a transformation (Permission from the Elsevier, Reference [107])

environmentally friendly and the turbines can be ran continuously in a stable manner [108]. In addition, it can partly or wholly meet electricity demand in regions where conventional fossil fuel resources are limited, and they can be coupled to interconnected line to cover a buildings or group of buildings electricity demand.

2.6.2.2 Passive systems

Passive systems include solar PV power and thermal storage wall, which are described in this section.

1. *Solar PV systems*
   PV refers to the direct generation of electricity by solar irradiation by PV effect. PV cells or so-called solar cells are often made of silicon material, which is manufactured on the forms of plates of different sizes and shapes, including square, rectangle and concave.

   PV equipment has no moving parts and, as a result, do not require massive maintenance. PV systems have a long life and they generate electricity without producing harmful emissions, in a very silent way. They can be built in almost any size and they are highly reliable. On the other hand, their efficiencies are relatively low and for high powers, a lot of space may be required [103].

   A solar cell, which is a solid-state electrical device (*p–n* junction) that operates as a semiconductor diode, absorbs the solar energy (photon) and then raises an electron to a higher energy state, and then the flow of this high-energy electron to an external circuit produces electricity [109].

   During the day, the energy produced in large batteries can be stored for use in the absence of the sun. So storing electrical energy in batteries is one of the

most important aspect of PV systems which increases the investment costs relatively. A typical home size PV application can be seen in Figure 2.13.

2. *Solar wall (thermal storage wall)*

A thermal storage wall is a large panel, which has a high-capacitance directly coupled to the inside of a building. Absorbed solar radiation reaches the room by conduction through the wall from which it is convected and radiated into the room or by the hot air flowing through the air gap between the room and the wall as it is given in Figure 2.14 [103].

Solar heated fresh air is distributed to the building through the existing HVAC system or with separate air-conditioning fans or sometimes flow directly into the

Figure 2.13 A typical PV application [110]

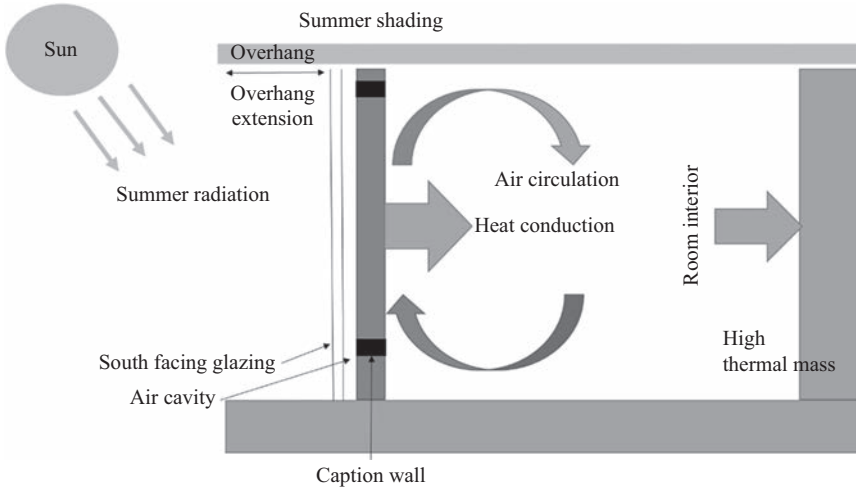

Figure 2.14 Thermal storage wall

room by thermophonic effect. There are different constructions of the Solar Wall technology based on an energy requirements of a building or according to the requirements of the costumers; however, one of the most common application of thermal storage wall can be seen in Figure 2.14. The most important component of the system is the exterior part which is the solar cladding which is heated by the solar radiation from the sun [111].

2.7 Conclusion

Building sector is the largest end use energy consumer; therefore, minimizing the energy consumption in buildings has a key role in order to reduce emissions and fuel energy consumption. In the whole world, new specific policies are still developing aimed to reduce energy consumptions, green gas emissions, pollution and increase quality of the indoor comfort level, productivity, usage of recycling material by using renewable energy sources. In the light of above, this study draws attention on the use of renewable energy applications, the evaluation of building performance and clean energy use, certification systems for sustainability ratings of residential GBs. Due to the current investigation, following observations can be made:

- In sight of the reviewed papers, authors suggest that for each country as climatic, geographic, social, economic and cultural aspects are differ from each other; each region may have different priorities in the raking system. Therefore, for each country, it is important and crucial to develop their own ranking systems or they should use international GB rating tools.
- There are different modelling approaches, which use the data of the buildings to simulate the energy consumption or more over to construct, classify and rank the buildings. In this aspect of energy demand, modelling has a key role. When the demand is estimated, it is divided in several loads and the demands, which are to be supplied, are distributed on different generation technologies (heat pump, chiller, etc.) and energy sources (electricity, gas, renewable, etc.). In this aspect, the authors explained the variety of clean energy sources, which can be utilized in buildings.
- GB incentives are very important for motivating the construction and ownership of GBs. Recent studies show that, even the governments are more involved in providing incentives, private sector's role is getting bigger and bigger every day. For increasing the awareness of GBs, increasing awareness of knowledge on incentives is very important as the way, quality and quantity of the promoting incentives distinguishes the GBs.
- In the last few decades, building design towards clean energy generation becomes a popular title in all over the world. Building transformation starts first with minimizing the energy demand with passive solutions, which is known as passive buildings. Then, it goes with nZEBs. Authors suggest that, as nZEB are the most efficient way to conserve natural resources and minimize greenhouse emissions, it has a pioneer role for planning the future.

References

[1] *Transition to Sustainable Buildings: Strategies and Opportunities to 2050* [Internet] 2018 [cited 10 September 2018]. Available from: https://www.iea.org/publications/freepublications/publication/Building2013_free.pdf, ISBN: 978-92-64-20241-2.

[2] Erten, D., *Sustainable Production and Technology Publications V*, Green Buildings, Available from: https://recturkey.files.wordpress.com/2017/02/yesil-binalar.pdf, 2017, (in Turkish) [Accessed 10 September 2018].

[3] Kats, G.H., Green Building Costs *and Financial Benefits*, Barr Foundation, Environmental Business Council of New England, Inc., Equity Office Properties, Massachusetts Technology Collaborative, Massport, 2003.

[4] Sharma, M., 'Development of a "Green Building sustainability model" for Green buildings in India', *Journal of Cleaner Production*, 2018;**190**:538–551.

[5] Robichaud, L.B., and Anantamula, V.S., 'Greening project management practices for sustainable construction', *Journal of Management in Engineering*, 2011;**27**:48–57.

[6] Kibert, C.J., 'Green buildings: an overview of progress', *Journal of Land Use & Environmental Law*, 2018;**19**:491–502.

[7] Liu, Y., Hong, Z., Yan, J., Qi, J., and Liu, P., 'Promoting green residential buildings: residents environmental attitude, subjective knowledge, and social trust matter', *Energy Policy*, 2018;**112**:152–161.

[8] Ali, H.H., and Nsairat, S.A., 'Developing a green building assessment tool for developing countries – case of Jordan', *Building and Environment*, 2009;**44**:1053–1064.

[9] Mattoni, B., Guattari, C., Evangelisti, L., Bisegna, F., Gori, P., and Asdrubali, F., 'Critical review and methodological approach to evaluate the differences among international green building rating tools', *Renewable and Sustainable Energy Review*, 2018;**82**:950–960.

[10] Assefa, G., Glaumann, M., Malmqvist, T., *et al.*, Environmental assessment of real estates – where natural and social sciences meet: the case of Eco-effect. *In: Proceedings of the 2005 world sustainable building conference* (SB05Tokyo), 27–29 September 2005; Tokyo.

[11] Lee, W.L., and Burnett, J., 'Benchmarking energy use assessment of HK-BEAM, BREEAM and LEED', *Build Environment*, 2008;**43**:1882–1891.

[12] Scofield, J.H., 'Do LEED-certified buildings save energy? Not really', *Energy and Buildings*, 2009;**41**(12):1386–1390.

[13] United States Green Building Council (USA), Available from: https://new.usgbc.org/, 2018, [Accessed 10 September 2018].

[14] Green Star. *Homepage of Green Star*. Available from: https://www.gbca.org.au/green-star/rating-tools/, https://new.usgbc.org/, 2018, [Accessed 10 September 2018].

[15] CASBEE. *Homepage of CASBEE*. Available from: http://www.ibec.or.jp/CASBEE, 2018.

[16] Lippiatt, B., Building for environment and economical sustainability. Technical manual and user guide (BEES 2.0). Report NISTIR 6220. National Institute of Standards and Technology (NIST); June 2000.
[17] Forsberg, A., and von Malmborg, F., 'Tools for environmental assessment of the built environment'. *Build Environment*, 2004;**39**:223e8.
[18] Kortman, J., van Ejwik, H., Mak, J., Anink, D., and Knapen, M., Presentation of tests by architects of the LCA-based computer tool EcoQuantum domestic. *In: Proceedings of green building challenge*, 1998; Vancouver, Canada.
[19] Libovich, A., Assessing green building for sustainable cities. *In: Proceedings of the world sustainable building conference*, 2005; Tokyo. pp. 1968–1971.
[20] Suzer, O., 'A comparative review of environmental concern prioritization: LEED vs other major certification systems', *Journal of Environmental Management*, 2015;**154**:266–283.
[21] Bahaudin, A.Y., Elias, E.M., and Saifudin, A.M., A comparison of the green building's Criteria. *In: Web of Conferences*, 2014.
[22] Homepage of BREEAM, Available from: https://www.breeam.com/, 2018, [Accessed 10 September 2018].
[23] *LEED for Homes Green Building Rating System – U.S. Green Building Council, Version,* Available from: https://new.usgbc.org/leed, 2018, [Accessed 10 September 2018].
[24] Muenz, J., 2012. *Ask Jeremy, 'How Do Regional Priority (RP) Credits Work?'*, Available from: http://www.usgbc.org/articles/ask-jeremy-how-doregional-priority-rp-credits-work (Posted by LEED), [Accessed 10 September 2018].
[25] Asdrubali, F., Baldinelli, G., Bianchi, F., and Sambucao, S., 'A comparison between environmental sustainability rating systems LEED and ITACA for residential buildings', *Building and Environment*, 2015;**86**:98–108.
[26] Pagliaro, F., Cellucci, L., Burattini, C., *et al.*, 'A methodological comparison between energy and environmental performance evaluation', *Sustainability*, 2015;**7**:10324–10342.
[27] Doan, D.T., Ghaffarianhoseini, A., Naismith, N., Zhang, T., Ghaffarianhoseini, A., and Tookey, J., 'A critical comparison of green building rating systems', *Building and Environment*, 2017;**123**:243–230.
[28] Azhar, S., Carlton, W.A., Olsen, D., and Ahmad, I., 'Building information modelling for sustainable design and LEED rating analysis', *Automation in Construction*, **201**;**20**:217–224.
[29] Azhar, S., and Brown, J., 'BIM for sustainability analyses', *International Journal of Construction Education and Research*, 2005;**5**:276–292.
[30] *The Green Building Resource*, Harvard Energy & Facilities [Internet] 2018 [cited 10 September 2018]. Available from: http://www.energyandfacilities.harvard.edu/green-building-resource.
[31] Aqtake, N., Ofuji, N., Mıura, M., Shımada, N., and Nıwa, H., Comparison among results of various comprehensive assessment systems – case study for a model building using CASBEE, BREEAM and LEED. *In: The 2005 World Sustainable Building Conference*, 27–29 September 2005; Tokyo.
[32] Asdrubali, F., Baldinelli, G., Bianchi, F., and Sambuco, S., 'A comparison between environmental sustainability rating systems LEED and ITACA for residential building', *Building and Environment*, 2015;**86**:98–108.

[33] Asdrubali, F., and Baldinelli, G., 'Theoretical modelling and experimental evaluation of the optical properties of glazing systems with selective films', *Building Simulation*, 2009;**2**:75–84.
[34] Baldinelli, G., 'Double skin façades for warm climate regions: analysis of a solution with an integrated movable shading system', *Building and Environment*, 2009;**44**:1107–1118.
[35] Politi, S., and Antonini, E., An expeditious method for comparing sustainable rating systems for residential buildings. *In*: *8th International Conference on Sustainability in Energy and Buildings*, 11–13 September 2016; Turin, Italy.
[36] *Green Building Case Study*, City of Oakland [Internet] 2018 [cited 10 September 2018]. Available from: http://www2.oaklandnet.com/oakca1/groups/ceda/documents/report/oak023102.pdf.
[37] Li, Y., and Yang, Y., 'Green building in China: needs great promotion', *Sustain Cities*, 2014;**11**:1–6.
[38] Olubunmi, O.A., Xia, P.B., and Skitmore, M., 'Green building incentives: a review', *Renewable and Sustainable Energy Reviews*, 2016;**59**:1611–1621.
[39] Diyana, N.A., and Zainul, A.N., 'Motivation and expectation of developers on green construction: a conceptual view', *World Academy of Science, Engineering and Technology*, 2013;**7**:914–918.
[40] Robichaud, L.B., and Anantatmula, V.S., 'Greening project management practices for sustainable construction'. *Journal of Management in Engineering*, 2010;**27**:48–57.
[41] Taylor, J.M., Sustainable building practices: legislative and economic incentives. *In: Management and Innovation for a Sustainable Built Environment,* June 2011; Amsterdam, The Netherlands.
[42] Rainwater, B., and Martin, C., *Local Leaders in Sustainability: Green Counties*. *American Institute of Architects*; 2008.
[43] Simsek, H.A., and Simsek, N., 'Recent incentives for renewable energy in Turkey', *Energy Policy*, 2013;**63**:521–530.
[44] Gou, Z., Lau, S.S.-Y., and Prasad, D., 'Market readiness and policy implications for green buildings: case study from Hong Kong', *Journal of Green Building*, 2012;**8**(2):162–173.
[45] Sentman, S.D., Del Percio, S.T., and Koerner, P., 'A climate for change: green building policies, programs, and incentives', *Journal of Green Building*, 2008;**3**(2):46–63.
[46] Choi, C., 'Removing market barriers to green development: principles and action projects to promote widespread adoption of green development practices', *Journal of Sustainable Real Estate*, 2009;**1**(1):107–138.
[47] Sundbom, D., 'Green Building Incentives: a strategic outlook', *Ms. Thesis*, Division of Building and Real Estate Economics, STH, Stockholm; 2011.
[48] Aliagha, G.U., Hashim, M., Sanni, A.O., and Ali, K.N., 'Review of green building demand factors for Malaysia', *Journal of Energy Technology and Policy*, 2013;**3**:471–478.
[49] Onuoha, I.J., Aliagha, G.U., and Rahman, M.S.R. 'Modelling the effects of green building incentives and green building skills on supply factors affecting green commercial property investment', *Renewable and Sustainable Energy Reviews*, 2018;**90**:814–823.

[50] Marker, A.W., Mason, S.G., and Morrow, P., 'Change factors influencing the diffusion and adoption of green building practices', *Performance Improvement Quarterly*, 2014;**26**(4):5–24.
[51] Frayssinet, L., Merlier, L., Kuznik, F., Hubert, J.L., Milliez, M., and Rou, J.J., 'Modeling the heating and cooling energy demand of urban buildings at city scale', *Renewable and Sustainable Energy Reviews*, 2018; **81**:2318–2327.
[52] US Department of Energy, Energy Efficiency Trends in Residential and Commercial *Buildings*, 2008.
[53] Koulamas, C., Kalogeras, A.P., Pacheco-Torres, R., Casillas, J., and Ferrarini, L., 'Suitability analysis of modeling and assessment approaches in energy efficiency in buildings', *Energy and Buildings*, 2018;**158**: 1662–1682.
[54] Christoph, F., Reinhart, C., and Davila, C., 'Urban building energy modeling – a review of a nascent field', *Building and Environment*, 2016;**97**:196–202.
[55] Foucquier, A., Robert, S., Suard, F., Stephan, L., and Arnaud, J, 'State of the art in building modelling and energy performances prediction: a review', *Renewable and Sustainable Energy Reviews*, 2013;**23**:272–288.
[56] Wang, L., and Wong, N.H., 'Coupled simulations for naturally ventilated residential buildings', *Automation in Construction*, 2008;**17**:386–398,
[57] Bouia, H., and Dalicieux, P., Simplified modelling of air movements inside dwelling room. *In: Proceedings of Building Simulation 91 Conference*, 1991; Nice, France, IBPSA (The International Building Performance Simulation Association). pp. 106–110.
[58] Brun, A., Wurtz, E., and Quenard, D., Experimental and numerical comparison of heat transfer in a naturally ventilated roof cavity. *In: Building Simulation Fourth National Conference of* IBPSA-USA; 2010. p. 160–169.
[59] Kalogirou, S.A., 'Use of TRNSYS for modelling and simulation of a hybrid PV–thermal solar system for Cyprus', *Renewable Energy*, 2011;**23**:247–260.
[60] Zhai, Z., Johnson, M.H., and Moncef, K., 'Assessment of natural and hybrid ventilation models in whole-building energy simulations', *Energy and Buildings*, 2011;**43**:2251–2261.
[61] Kruger, E., and Givoni, B., 'Predicting thermal performance in occupied dwellings', *Energy and Buildings*, 2004;**36**(3):301–307.
[62] Aydinalp-Koksal, M., and Ugursal, V.I., 'Comparison of neural network, conditional demand analysis, and engineering approaches for modeling end-use energy consumption in the residential sector', *Applied Energy*, 2008; **85**(4):271–296.
[63] Holland, J.H., *Adaptation in Natural and Artificial Systems*, Ann Arbor: The MIT Press; 1975.
[64] Caldas, L.G., and Norford, L.K., 'Genetic algorithms for optimization of building envelopes and the design and control of HVAC systems', *Journal of Solar Energy Engineering*, 2003;**51**:125–343.
[65] Ozturk, H.K., Ceylan, H., Canyurt, O.E., and Hepbasli, A., 'Electricity estimation using genetic algorithm approach: a case study of Turkey'. *Energy*, 2005;**30**:1003–1012.

[66] Lettvin, J., Maturana, H.R., McCulloch, W.S., and Pitts, W.H., What the frog's eye tells the frog's brain. *In: Proceedings of the Institute of Radio Engineers*, 1959. pp. 47–51.

[67] Kalogirou, S.A., 'Applications of artificial neural-networks for energy systems', *Applied Energy*, 2000;**67**:17–35.

[68] Philippe, L., Harry, B., Carine, R., and Alain, B., 'A genetic algorithm applied to the validation of building thermal models', *Energy and Buildings*, 2005;**37**:858–866.

[69] Essia, Z., Nadia, G.M., and Atidel, H.A., 'Optimization of Mediterranean building design using genetic algorithms', *Energy and Buildings*, 2007;**39**: 148–153.

[70] Grubera, J.K., Prodanovica, M., and Alonso, R., 'Estimation and analysis of building energy demand and supply costs', *Energy Procedia*, 2015;**83**:216–225.

[71] Vigna, I., Pernetti, R., Pasut, W., and Lollini, R., 'New domain for promoting energy efficiency: energy flexible building cluster', *Sustainable Cities and Society*, 2018;**38**:526–533.

[72] Dracou, M.K., Santamouris, M., and Papanicolas, C.N., 'Achieving nearly zero buildings in Cyprus, through building performance simulations, based on the use of innovative energy technologies', *Procedia Engineering*, 2017; **134**:636–644.

[73] Schnieders, J., and Hermelink, A., 'CEPHEUS results: measurements and occupants satisfaction provide evidence for passive houses being an option for sustainable building', *Energy Policy*, 2006;**34**:151–171.

[74] Taleb, H.M., 'Using passive cooling strategies to improve thermal performance and reduce energy consumption of residential buildings in U.A.E. buildings', *Frontiers of Architectural Research*, 2014;**3**:154–165.

[75] Badescu, V., Laaser, N., and Crutescu, R., 'Warm season cooling requirements for passive buildings in South-Eastern Europe (Romania)', *Energy*, 2010;**35**:3284–3300.

[76] Feist, W., Puger, R., Kaufmann, B., Schnieders, J., and Kah, O., 'Passive house planning package 2007', *Specification for Quality Approved Passive Houses, Passive House Institute*, Darmstadt, Germany.

[77] Dan, D., Tanasa, C., Stoian, S., Brata, D., Gyorgy, S.C., and Florut, S.C., 'Passive house design- an efficient solution of residential buildings in Romania', *Energy for Sustainable Development*, 2016;**32**:99–109.

[78] Gou, S., Nİk, V.M., Scartezzini, J.L., Zhao, Q., and Li, Z., 'Passive design optimization of newly-built residential buildings in Shanghai for improving indoor thermal comfort while reducing building energy demand', *Energy & Buildings*, 2018;**169**:484–506.

[79] *Towards Nearly Zero Energy Buildings Definition of Common Principles under the EPBD* [Internet] 2018 [cited 10 September 2018]. Available from: https://ec.europa.eu/energy/en/topics/energy-efficiency/buildings/nearly-zero-energy-buildings.

[80] Ferrara, M., Fabrizio, E., Virgone, J., and Filippi, M., 'A simulation-based optimization method for cost-optimal analysis of nearly zero energy buildings', *Energy and Buildings*, 2014;**84**:442–457.

[81] Schimschar, S., Blok, K., Boermans, T., and Hermelink, A., 'Germany's path towards nearly zero-energy buildings—enabling the greenhouse gas mitigation potential in the building stock', *Energy Policy*, 2011;**39**:3346–3360.
[82] Rakennuslehti Magazine, Helsinki, Finland [Internet] 2016 [cited 10 September 2018]. Available from: https://www. nytimes.com/interactive/2016/07/07/travel/what-to-do-36-hours-helsinkifinland.html.
[83] Pylsy, P., and Kalema, T., *Concepts for Low-Energy Single-Family Houses*, Tampere University of Technology, Department of Mechanics and Design, *Research Report* **1**; 2008.
[84] Saari, A., Kalamees, T., Jokisalo, J., Michelsson, R., Alanne, K., and Kurnutski, J., 'Financial viability of energy-efficiency measures in a new detached house design in Finland', *Applied Energy*, 2012;**92**:76–83.
[85] Hamdy, M., Hasan, A., and Siren, K., 'A multi-stage optimization method for cost-optimal and nearly-zero-energy building solutions in line with the EPBD-recast 2010', *Energy and Buildings*, 2013;**56**:189–203.
[86] Cakmanus, I., 'Almost net zero buildings (nZEB)', *Yeşil Bina Dergisi*, 2011; (7), Available from: http://www.yesilbinadergisi.com/yayin/701/yaklasik-sifir-enerjili-binalar-nnzeb-21118.html#.Wyt9l1UzZaQ, accessed in: 21/06/2018 (in Turkish) [Accessed 10 September 2018].
[87] Panagiotidou, M., and Fuller, R.J., 'Progress in ZEBs – a review of definitions, policies and construction activity', *Energy Policy*, 2013;**62**:196–206.
[88] Marszal, A., Bourelle, J., Nieminen, J, Gustavsen, A., and Heiselberg, P., North European understanding of zero energy/emission buildings. *In: Renewable Energy Conference*, 2010; Trondheim, Norway.
[89] Torcellini, P., Pless, S., Deru, M., and Crawley, D., *Zero Energy Buildings: A Critical Look at the Definition*. National Renewable Energy Laboratory and Department of Energy, US; 2006.
[90] Chee, L., Akçakaya, A., and Erdoğan, C., 'Net zero energy utilization in buildings', *Bina Elektrik, Elektronik, Mekanik ve Kontrol Sistemleri Dergisi*; 2018. (in Turkish).
[91] Thormark, C., 'The effect of material choice on the total energy need and recycling potential of a building', *Building and Environment*, 2006;**41**:1019–1026.
[92] Kristjansdottir, T.F., Houlihan-Wiberg, A., Andresen, I., *et al.*, 'Is a net life cycle balance for energy and materials achievable for a zero emission single-family building in Norway?', *Energy & Buildings*, 2018;**168**:457–469.
[93] Panagiotidou, M., and Fuller, R.J., 'Progress in ZEBs – a review of definitions, policies and construction activity', *Energy Policy*, 2013;**62**:196–206.
[94] Silva, S.M., Mateus, R., Marques, L., Ramos, M., and Almeida, M., 'Contribution of the solar systems to the nZEB and ZEB design concept in Portugal – energy, economics and environmental life cycle analysis', *Solar Energy Materials & Solar Cells*, 2016;**156**:59–74.
[95] Lamnatou, C., Notton, G., Chemisana, D., and Cristofari, C., 'The environmental performance of a building-integrated solar thermal collector, based on multiple approaches and life-cycle impact assessment methodologies', *Building and Environment*, 2015;**87**:45–58.

[96] Birgisdottir, H., Houlihan-Wiberg, A.A.M., Malmqvist, T., Moncaster, A., and Nygaard Rasmussen, F., *Evaluation of Embodied Energy and CO_2eq for Building Construction (Annex 57) Subtask 4: Case Studies and Recommendations for* the *Reduction* of Embodied Energy and Embodied Greenhouse Gas Emissions from Buildings, International Energy Agency, Institute for Building Environment and Energy Conservation, ISBN 978-4-909107-08-4, Japan; 2017.

[97] Rüzgar Enerjisi Sistemleri [Internet] 2018 [cited 28 June 2018]. Available from: http://www.cn.com.tr/ruzgar-enerjisi-sistemleri.

[98] Turkish Wind Energy Association [Internet] 2018 [cited 28 June 2018]. Available from: https://www.tureb.com.tr/.

[99] Enerji Atlası [Internet] 2018 [cited 28 June 2018]. Available from: http://www.enerjiatlasi.com/ruzgar/samli-ruzgar-santrali.html.

[100] Ozgirgin, E., Devrim, Y., and Albostan, A., 'Modelling and simulation of a hybrid photovoltaic (PV) module-electrolyzer-PEM fuel cell system for micro-cogeneration applications', *International Journal of Hydrogen Energy*, 2015;**40**:15336–15342.

[101] Cetinkaya, M., and Karaosmanoğlu, F., 'Fuel Cells', *In: Presented at Tesisat Mühendisliği*, 2003 May, pp. 18–30 (In Turkish).

[102] Barbir, F., *PEM Fuel Cells: Theory and Practice*. Academic Press, USA; 2013.

[103] Kalogirou, S., *Solar Energy Engineering (Process and Systems)*, Academic Press, USA; 2009.

[104] UK Weather Energy [Internet] 2018 [cited 28 June 2018]. Available from: http://www.weatherenergy.co.uk/solar-thermal/how-it-works.

[105] Mirhosseini, M., Rezania, A., and Rosendahl, L., 'View factor of solar chimneys by Monte Carlo method', *Energy Procedia*, 2017;**142**:513–518.

[106] Zou, Z., Guan, Z., and Gurgenci, H., Numerical modelling on solar enhanced natural draft dry cooling tower. *In: 18th Australasian Fluid Mechanics Conference*, 2012; Australia.

[107] Cao, F., Li, H., Zhao, L., Bao, T., and Guo, L., 'Design and simulation of the solar chimney power plants with TRNSYS', *Solar Energy*, 2013;**98**:23–33.

[108] Tingzhen M., *Solar Chimney Power Plant Generating Technology*, Elsevier; 2016.

[109] The Florida Solar Energy Center (FSEC) [Internet] 2018 [cited 28 June 2018]. Available from: http://www.fsec.ucf.edu/en/consumer/solar_electricity/basics/how_pv_system_works.htm.

[110] Conversation [Internet] 2018 [cited 28 June 2018]. Available from: http://theconversation.com/explainer-what-is-phototaic-solar-energy-12924.

[111] Solar Wall [Internet] 2018 [cited 28 June 2018]. Available from: http://solarwall.com/en/products/solarwall-air-heating/how-solarwall-works.php.

This page intentionally left blank

Chapter 3

Performance monitoring of a 60 kW photovoltaic array in Alberta

Oksana Treacy[1] and David Wood[2]

Solar photovoltaic (PV) systems are relatively new and there is not a large amount of performance data available for them with which to compare design calculations. This comparison is also necessary to provide confidence that newer systems will perform as predicted. This chapter describes a year's monitoring of a 60 kW PV system near Strathmore, Alberta, latitude 51°, installed in November 2016. The modules were flush mounted to a roof with 8° of pitch. There was no shading and the installation was near an Alberta Department of Agriculture meteorological station which provided the weather data. The measured capacity factor was 13.8%, and there was a loss of 11%–12% of the yearly production to snow. We demonstrate that satellite-based production forecasts of the array irradiance underestimated the solar resource at this location. The predictions of actual energy production from two different modeling tools showed that the more detailed System Advisor Model software was more accurate than RETScreen.

3.1 Introduction

It is well known that solar photovoltaic (PV) systems are declining in cost and increasing dramatically in numbers [1]. Many of these systems are small and fall in the category of distributed generation, whereby they feed into the local electricity grid. In the fall of 2016, Wheatland County installed a 60 kW power plant on the roof of its administration building about 50 km east of Calgary and were then keen to analyze its energy and financial performance. The research described in this chapter concentrates on performance to answer the following key questions:

- Is the system performing as designed?
- What features of the operation are important for future PV system designs?

The Wheatland County PV project is part of a province-wide effort to develop renewable energy, which is key to Alberta's strategy for reducing carbon

[1]Skyfire Energy, Canada
[2]Department of Mechanical and Manufacturing Engineering, University of Calgary, Canada

emissions. Southern Alberta has excellent solar resources as documented by Environment Canada (http://www.nrcan.gc.ca/18366) but also has very cheap electricity, mostly produced by fossil fuels [2]. At present, the payback period for unsubsidized PV systems in Alberta is over 15 years, but this is expected to fall with the continually decreasing cost of PV modules and rising electricity prices.

The installation is located ~270 m from the Alberta Department of Agriculture meteorological station which provided the weather data. The following section describes the PV system, followed by the weather monitoring methodology. The simulations of system performance using RETscreen and System Advisor Model (SAM) are detailed next and compared to the 1-year actual performance data. The subsequent section describes the minor malfunctions and failures. Next, we consider the effects on electricity production of the weather in terms of irradiance, wind speed, and ambient temperature. We then revisit the prediction of system performance, now using the measured irradiance. The final section has the conclusions.

3.2 Description of the PV system

The system consists of 215 Canadian Solar 280-Watt Mono-crystalline modules [3] flush-mounted facing south at the roof angle of approximately 8° to the horizontal position. This is less than the optimal angle for a fixed array, which is around 40° for this latitude (51°), but the advantages of flush mounting were viewed as justifying the slight loss in performance. These include ease of installation and minimization of shading. There was no shading of the system at any time of the year from any source. This considerably simplifies the analysis of the performance as models for the effects of shading tend to be either simplistic and uncertain or complex and difficult to implement, e.g., [4]. The 60.2 kW system rating refers to direct current (DC) generated by the modules. Figure 3.1 shows the layout of the plant which takes advantage of the maximum available roof area.

Four 14.4 kW SolarEdge inverters convert DC electricity to alternating current (AC), with a total output of 57.6 kW. Each of the four inverters is connected to three strings of modules, a string being a sequence of modules connected in series. There are 18 modules in each string, except for the first string which has only 17 modules. The modules in each string are set up in pairs, with a power optimizer and monitor provided per pair. The exception is one module in the first string that is individually optimized and monitored. Optimizers implement maximum power point tracking (MPPT) for each pair but do not convert DC to AC. MPPT aims to achieve the highest possible power output even when modules are partially shaded and when the insolation and cell temperature changes [5].

Electricity production data was collected directly at the administration building from December 2016 to the end of December 2017. The system performance data is available on-line in real time via SolarEdge monitoring software, which records electric output variables at 15-minute time intervals. Figure 3.2 shows a sample screenshot of the SolarEdge monitoring software. In December 2016, the system

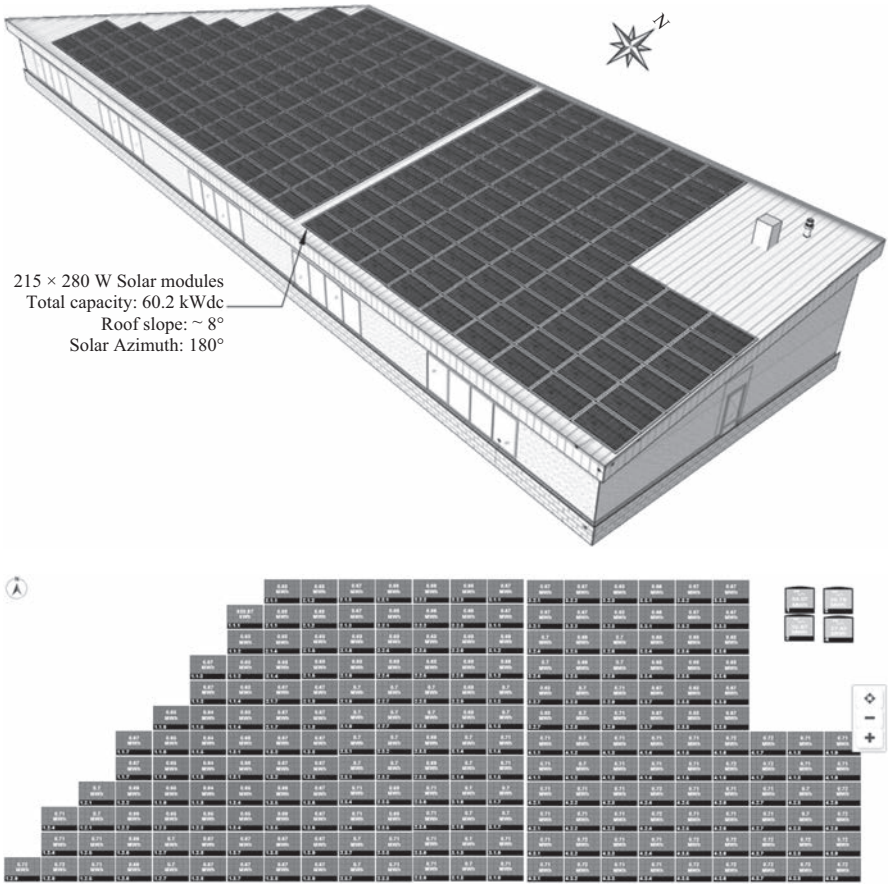

Figure 3.1 Schematic of the 60 kW system (top) and partial screenshot of the web monitoring system (bottom)

operated for only a part of the month. Therefore, data for that month was excluded from the analysis. This chapter considers one year's data from January 1 to December 31, 2017.

3.3 Weather monitoring

Strathmore IMCN weather station, managed by Alberta Agriculture and Forestry, is situated near the administration building, as shown in Figure 3.3, making it possible to obtain accurate solar irradiance, wind speed, temperature, and precipitation measurements for the site. The station provides hourly averaged and daily weather data for download (https://agriculture.alberta.ca/acis/alberta-weather-data-viewer.jsp). Ten years of historical weather data is also available and was analyzed to obtain a 10-year average solar insolation shown in Figure 3.4.

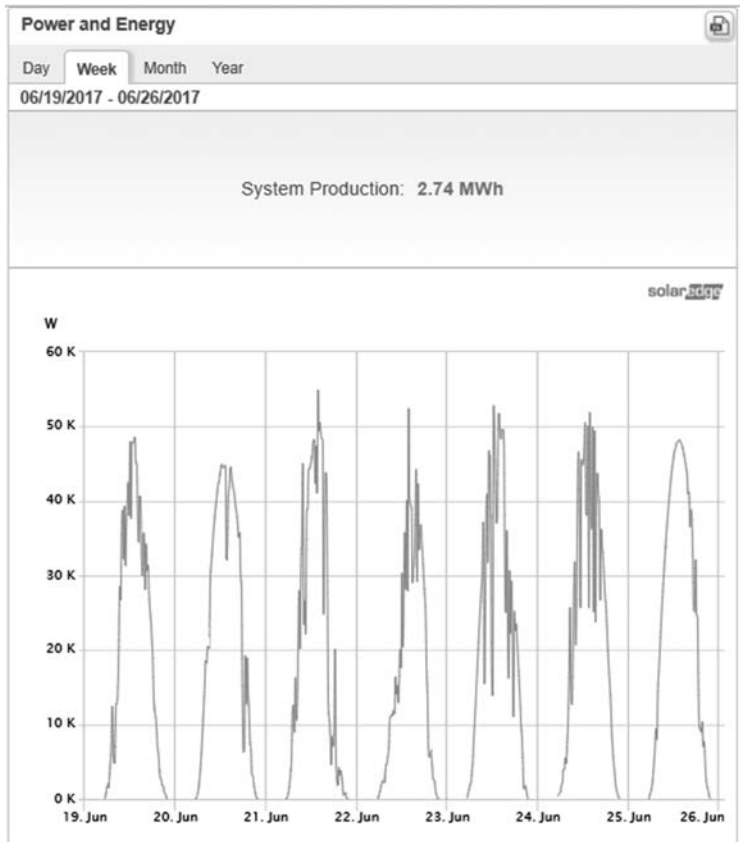

Figure 3.2 Screenshot of the data shown on the web monitoring system

Figure 3.3 Photograph of the meteorological station (https://agriculture.alberta.ca/acis/alberta-weather-data-viewer.jsp)

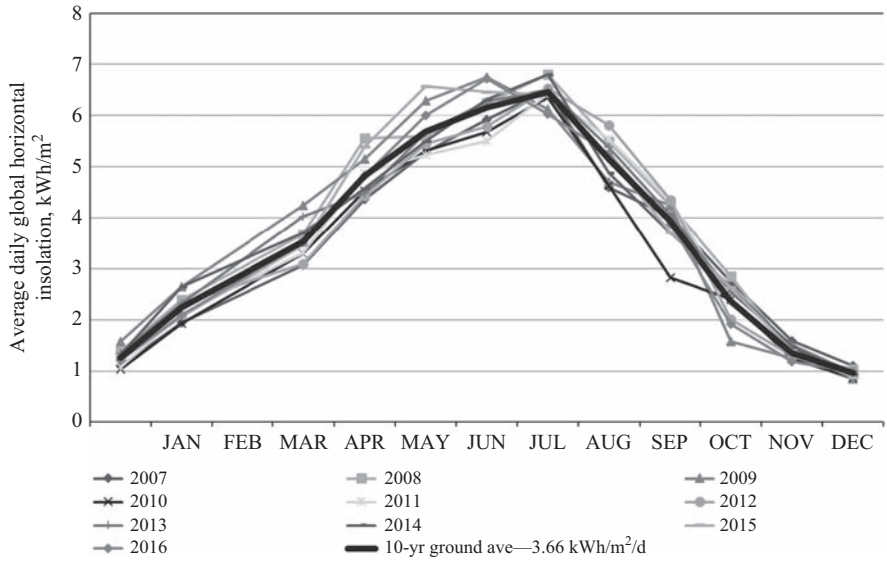

Figure 3.4 Ten years of solar insolation from the meteorological station

3.4 Electricity production modeling

The first-year energy production was forecast by the installer to be 65,186 kWh using RETScreen from Natural Resources Canada; the monthly breakdown of electricity production is given in Table 3.1. RETScreen models the installation angle and the module and inverter characteristics and estimated losses from the solar PV system, http://www.nrcan.gc.ca/energy/software-tools/7465. Note that energy production degrades over time as all module efficiencies monotonically decrease—by about 10% over the 20+-year lifetime of well-made modules—so it is important to specify the year for which the production is modeled. RETScreen is freely available, but a license fee must be paid to allow the saving of the output files. It utilizes satellite data from NASA to approximate local weather conditions. RETScreen has some modeling limitations. For example, loss estimates are all user-defined and can only be entered on an annual basis. Thus, a miscellaneous loss of 13.5% accounts for snow in the winter, differences between modules and other losses. This loss factor was derived from the installer's experience in the area. However, this approach can result in overestimating winter and underestimating summer energy production for the system.

An alternative modeling software, the open-source SAM provided by National Renewable Energy Laboratory (NREL), was also used, https://sam.nrel.gov/. SAM provides a more detailed PV performance model and allows a more extensive set of input parameters, such as different weather files, inverter characteristics, and various loss factor. SAM predicted a production of 62,238 kWh in year one, 4.5% lower than the RETScreen forecast.

Table 3.1 RETscreen predictions and measured monthly energy production

Month	Predicted insolation-tilted (kWh/m^2/day)	Actual insolation-tilted (kWh/m^2/day)	Predicted energy (MWh)	Actual energy (MWh)	Difference in energy (%)	Monthly capacity factor (%)
January	1.35	1.76	2.211	1.888	−14.6	4.23
February	2.30	2.67	3.336	1.999	−40.1	4.96
March	3.60	4.07	5.617	4.858	−13.5	10.9
April	4.95	4.60	7.167	7.236	0.96	16.8
May	5.60	6.35	8.169	10.556	29.2	23.7
June	5.87	6.83	8.148	10.902	33.8	25.2
July	6.22	7.02	8.795	11.24	27.8	25.2
August	5.29	5.81	7.541	9.32	23.58	20.81
September	3.95	4.39	5.621	6.852	21.91	15.81
October	2.71	2.72	4.141	4.419	6.70	9.87
November	1.61	1.84	2.484	1.854	−25.38	4.28
December	1.2	1.43	1.956	1.419	−27.44	3.17
2017 Totals	44.65	49.53	65.186	72.54	11.28	13.76

Part of the difference in predicted energy arises from the different methods used by RETscreen and SAM to generate satellite-based solar irradiance forecasts. The former uses NASA's automated database of satellite-derived daily values of surface meteorological parameters for a 30+-year period and in near real time [6]. SAM employs the Physical Solar Model to estimate solar irradiance in Canadian locations [7]. The two satellite-based estimates for Wheatland County are plotted in Figure 3.5 and compared to Strathmore weather station's 10-year average ground data from Figure 3.4.

Both sets of satellite data predict lower annual average values for solar irradiance than the ground weather station data. NASA annual average is 5.5% lower than ground data, while NREL is 6.5% lower, with the difference especially pronounced for irradiance during the winter months.

It is not uncommon for satellite-derived data to vary significantly from ground measurements. The uncertainty associated with satellite-derived data is estimated to range from 5% to 17% [8]. Uncertainty of satellite-derived solar data arises from many sources: errors and gaps in imagery; terrain, albedo, snow, and spatial resolution; influence of clouds; presence of aerosols, to name a few. Improving the accuracy of solar resource estimation is an important topic for researchers worldwide.

Thus, in the case of Wheatland County administration building, the PV installation can be expected to perform better than originally projected, because the satellite data used to predict its performance tends to underestimate the actual solar resource.

Of major concern for Canada, RETScreen does not have the capability to estimate snow losses. The estimated snow impact is lumped into the annual miscellaneous loss factor. SAM, on the other hand, can forecast snow impact using snow depth data. The closest source of local snow depth data is the Calgary Airport weather station (~50 km away). To generate the SAM forecast, an average of all available measurements of snow depth since 2010 was calculated after discarding

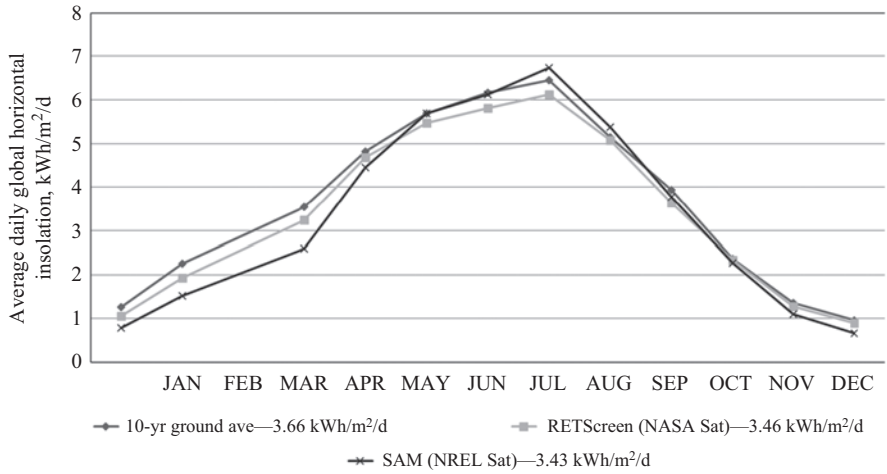

Figure 3.5 Comparison of satellite estimates of insolation compared to the 10-year average from the weather station

the obviously erroneous data, such as the negative values and the large positive ones in the summer months. Once the snow depth data is imported into the program, SAM models snow impact based on this data and other parameters, such as the tilt angle and temperature. SAM calculated a snow loss of 8.36% for the Wheatland County system. The accuracy of this estimate may be affected by the low quality of snow depth data and the low tilt angle (8°), which is slightly outside the range of 10–45° for which the SAM method was developed. For comparison, an empirical 5-year study of snow impact in Alberta measured the average annual snow loss of ~4% for low tilt angles [9].

The total energy produced in 2017 (72.54 MWh), exceeded the RETscreen forecast by 11.3% and the SAM one by 11.7%. The actual production corresponds to a yearly capacity factor of 13.76% and an energy yield of 1,205 kWh/kWdc (1,259 kWh/kWac). During winter, the electricity generation was significantly below expectations, while exceeding predictions in the spring/summer, see Table 3.1. Solar insolation was also above forecast by 10.93%.

3.5 Malfunctions and performance issues

Between February 15 and March 22, one string of 18 PV modules was not operational due to a hardware issue, resulting in an estimated loss of 0.3–0.4 MWh in electricity generation, as shown in Figure 3.6, which compares energy production between it and the adjacent strings. Production loss was estimated by calculating the difference in energy generation between the failed string and the adjacent strings during that period.

From early September to early December, the module pair numbered P3.1.4 continuously underperformed, compared with all the surrounding modules (see Figure 3.7).

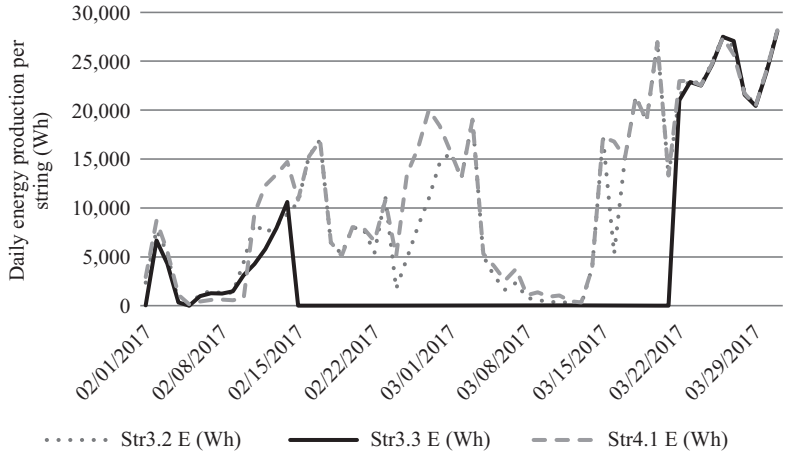

Figure 3.6 Malfunction of string 3.3 during February–March

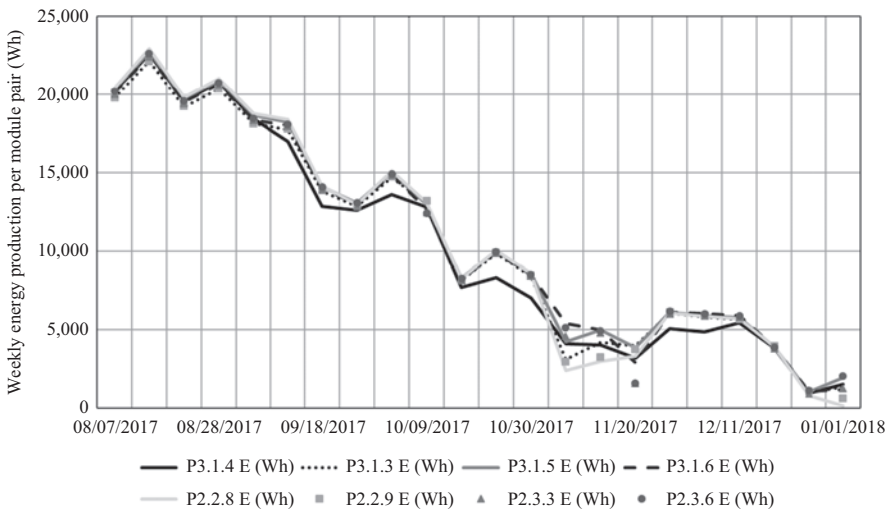

Figure 3.7 Malfunction of module pair P3.1.4

One of the modules in the pair was replaced on December 7. It was found to have a faulty bypass diode. The total energy loss due to this issue is 10 kWh, which was estimated by comparing electricity production with the adjacent module pairs.

Overall, losses due to operational issues described above total between 0.3 and 0.4 MWh, which represents ~0.5% of the annual production. Therefore, the 2017 solar PV electricity generation was not significantly affected by these malfunctions.

In a PV system, differences between PV modules are unavoidable. They are mainly caused by manufacturing tolerance mismatch, soiling and shading of the

modules, uneven module aging, and different orientations, although the last two are not applicable to the current study. A major advantage of controlling individual module performance via micro-inverters or power optimizers is the ability to quantify any mismatch between the modules. A system or a string inverter cannot do this. A high mismatch between modules may indicate underperforming modules. On the other hand, a high mismatch may also be attributed to specific site characteristics, such as partial shading of some modules, so it is important to consider these characteristics when analyzing a site's mismatch.

The SolarEdge monitoring system provides mismatch analysis for detecting modules that may be underperforming, by comparing each module's peak power and energy production to the average of all modules in the system. In the absence of malfunctions and shading, energy and power produced by modules of the same orientation and tilt angle are not expected to deviate from the average by more than 6% [10]. Figure 3.8 presents the results of module energy mismatch analysis at the inverter level. Module energy mismatch exceeds tolerances throughout the winter months. Energy mismatch is indicative of the effect of snow throughout the winter which is likely to be unevenly distributed over the modules. It also points toward the string malfunction at Inverter 3 in February–March, which saw much higher mismatch percentages than the other three inverters during that time. From March to October, module mismatch was well within tolerance, indicating uniformity in system performance. Then in November, snow impact is seen again. In general, module mismatch analysis results are in good agreement with the findings of system performance evaluation in the previous sections. However, the mismatch analysis is only available monthly and did not detect the faulty bypass diode in P3.1.4. If the mismatch analysis could be executed on just one clear sunny day, it should be more effective in detecting such operational issues.

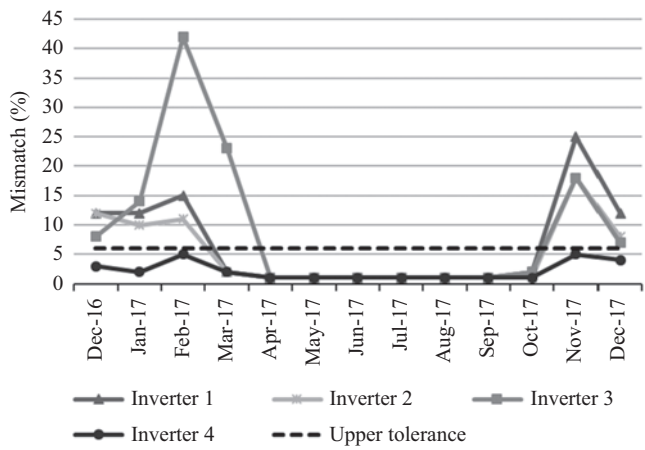

Figure 3.8 Mismatch in inverter energy production over the year

3.6 Effect of weather on performance

Figure 3.9 shows the relationship between irradiance and power output over the year. As solar irradiance increases, so do the current and power generated by the PV modules. The measurements that fall significantly below the trend line were recorded during or immediately after snow events or malfunctions.

The operating temperature of the PV cells has a significant impact on the voltage, and subsequently on the power generated, with hotter temperatures decreasing efficiency. While cell temperatures are rarely measured directly, they correlate with ambient air temperature. PV cells produce heat and thus operate at temperatures that are significantly higher than ambient. PV manufacturers provide temperature coefficients for voltage and power on the module datasheet. For the Canadian Solar modules in Wheatland County, the power and voltage decrease by 0.41% and 0.3%, respectively, for each °C increase in cell temperature [3]. Figure 3.10 demonstrates the relationship between ambient temperature and array efficiency in Wheatland County, where the efficiency is calculated as the ratio of daily AC electricity generated by the array to the solar insolation. This data was analyzed from May to September 2017, so as not to include any values affected by snow accumulation. As can be expected, there is a decrease in array efficiency with increasing ambient temperatures.

Wind has a secondary effect on PV electricity production, as it helps to cool the cells, thus increasing their efficiency. However, since the cell temperature is rarely measured directly, the relationship between wind speed and efficiency is a complex one. This is illustrated in Figure 3.11, created with data recorded during snow-free months of 2017. It shows a slight increase in array efficiency with

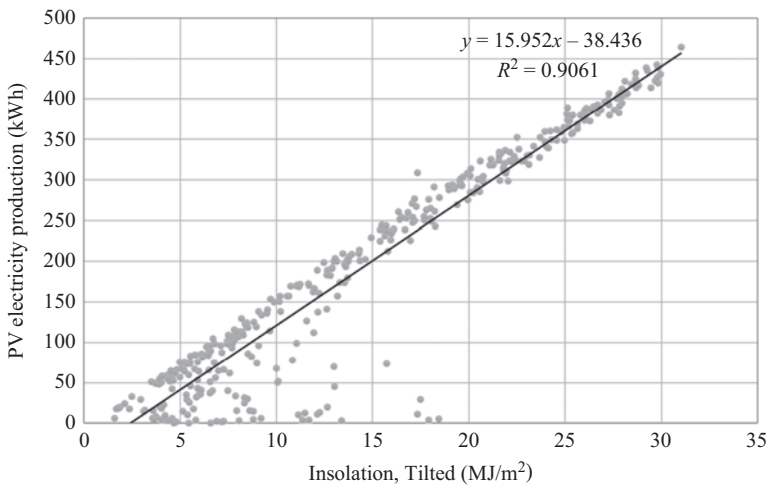

Figure 3.9 Power production as a function of irradiance for the year

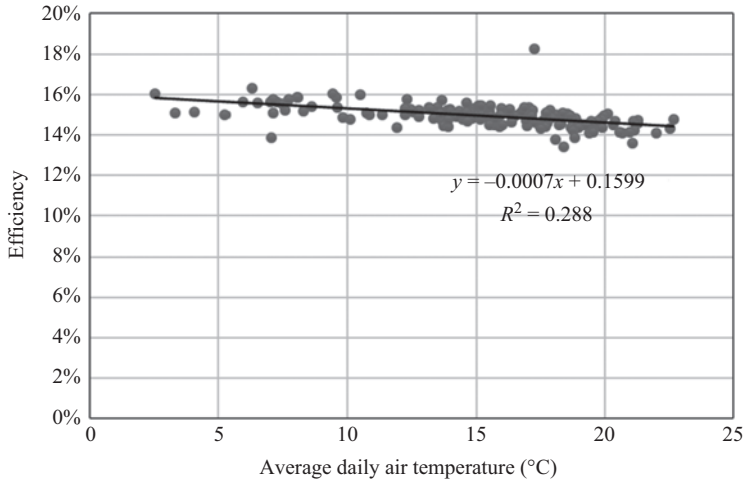

Figure 3.10 Power production as a function of ambient temperature for the year

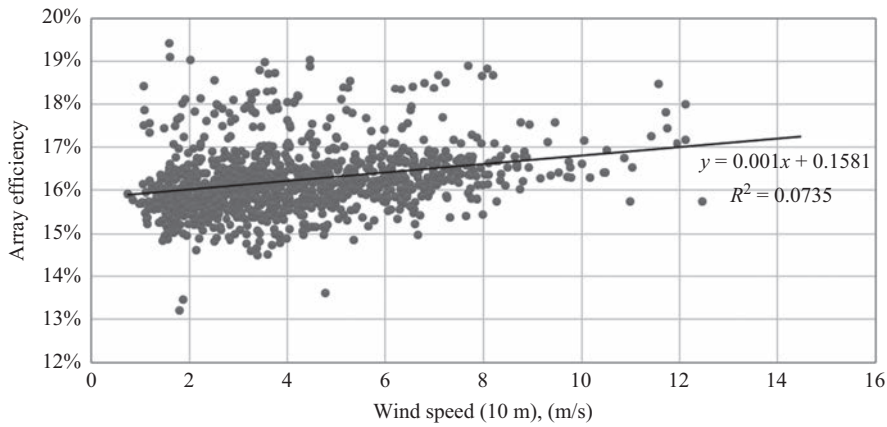

Figure 3.11 Array efficiency as a function of wind speed for the year

increasing wind speeds measured at 10 m, although the correlation is weak. Measuring cell temperature directly would be necessary to establish a stronger correlation between wind speed and PV electricity production.

Snow accumulation on the modules has a direct impact on electricity production, as illustrated in Figure 3.12. While the electricity production normally follows the solar irradiance, the correlation breaks down during and after significant winter precipitation, when electricity production can be reduced even at high irradiance levels.

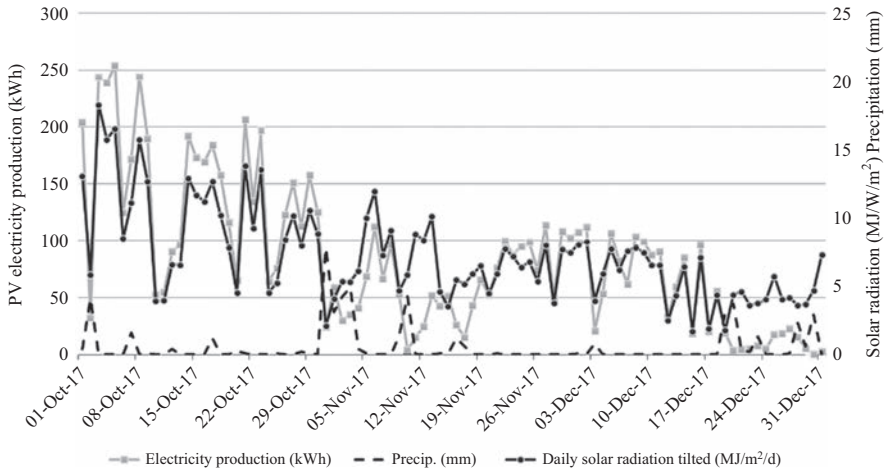

Figure 3.12 Power production as a function of snowfall. The precipitation (marked "Precip.") is entirely snow for the period shown in the figure

3.7 Simulation of system performance with actual irradiance

RETScreen was rerun using the actual monthly temperature and solar insolation averages, while adjusting the miscellaneous loss factor. A match to the actual annual electricity production of 72.54 MWh is achieved with a loss factor of 11.88%. The predicted and measured monthly production shown in Figure 3.13 demonstrates that RETscreen underpredicts the summer performance and overpredicts that in winter, because snow losses contribute significantly to the miscellaneous loss factor.

The RETScreen results can be used to infer the actual losses due to snow in 2017. It is possible to obtain a good match of electricity production from May to August 2017 by setting the miscellaneous loss factor to 0.1%, which is very low and demonstrates excellent system performance in the absence of snow. It can then be argued that most of the losses on the annual basis (11.88%), except for malfunctions (~0.4 MWh, or 0.5%), resulted from snow accumulation on the array. Therefore, the loss in energy production due to snow in 2017 is estimated to be 11.28%. To put this into perspective, NAIT's 5-year study [9] measured an average snow loss of 4% at low tilt angles, while the SAM snow loss model calculated it to be 8.36% based on the average snow depth data from the Calgary International Airport. Therefore, it appears that the empirical study results may not be applicable at the very low tilt angles (8° versus 14° for the lowest tilt angle in the NAIT study) and that year 2017 saw more snow than average.

To model the 2017 system performance in SAM, actual hourly measurements of temperature, Global Horizontal Irradiance, and wind speed from the Strathmore

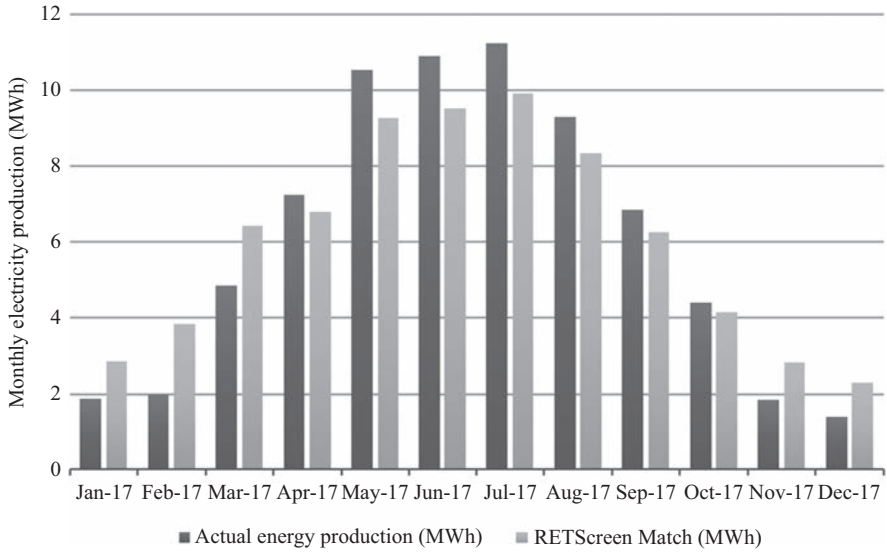

Figure 3.13 RETscreen simulation output of monthly energy production using measured irradiation for the year

weather station were combined with the 2017 daily snow depth data from Calgary International Airport, while Direct Normal Irradiance was estimated using the DISC (Direct Insolation Solar Code) model from NREL, https://www.nrel.gov/grid/solar-resource/disc.html. The results are shown in Figure 3.14. A match to the actual annual electricity production of 72.54 MWh was achieved by adjusting DC wiring and diodes/connections losses to 0.25% and 0.3%, respectively. The calculated snow loss is 11.65%, which is in good agreement with the 11.28% loss inferred from the RETScreen history match. Figure 3.14 shows a comparison between actual and calculated monthly electricity production. As can be expected with the more detailed modeling tool, there is a better match with the SAM-generated monthly predictions than with those by RETScreen. Discrepancies may be due to the lack of local snow depth data, and the low tilt angle (the SAM snow model is designed for a tilt angle of 10–45°, versus 8° in Wheatland County).

3.8 Conclusions

This evaluation of the solar PV installation in Wheatland County focused on its technical aspects and weather influences. From the energy perspective, electricity yield in the first full year of operation exceeded projections by 11.28%, achieving a capacity factor of 13.76%. This was despite the impact of snow (11.65% reduction in power output) and malfunctions (0.5% reduction). The superior performance was due to the solar resource being better than expected and the system losses being lower than anticipated.

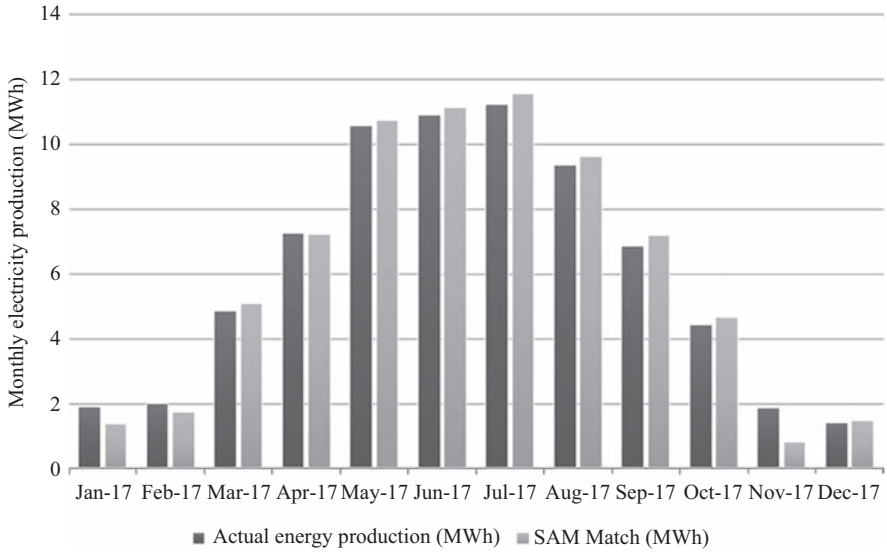

Figure 3.14 SAM simulation output of monthly energy production (top) and percentage losses (bottom) using measured irradiation for the year

Two different modeling tools were compared in effectiveness of matching actual energy production. The more detailed SAM software achieved a better match than RETScreen. Most satellite models tend to underestimate the local solar resource and should be compared to ground measurements whenever possible for more accurate performance prediction in the future.

Overall, system monitoring of the 60 kWdc rooftop solar PV system in Wheatland County demonstrated a high degree of reliability.

References

[1] Solar Energy Society of Alberta. (2017). *Generating Electricity from the Sun*. Strathmore: Solar Alberta.

[2] Alberta Energy. (2017, July 25). *Electricity Statistics. Electricity Supply*. Retrieved from Alberta Energy Website: http://www.energy.alberta.ca/Electricity/682.asp

[3] Canadian Solar. (2017, July 15). *CS6K-270|275|280M-SD*. Retrieved from Canadian Solar Website: https://www.canadiansolar.com/downloads/datasheets/na/Canadian_Solar-Datasheet-CS6KM_SmartDC_v5.4na.pdf

[4] Batzelis, E. I., Georgilakis, P. S., and Papathanassiou, S. A. (2014). Energy models for photovoltaic systems under partial shading conditions: A comprehensive review. *IET Renewable Power Generation*, 340–348.

[5] MCCAC. (2017, April). *Solar Friendly Municipalities. Solar PV Basics: Technology, Installation and Cost.* Retrieved from Municipal Climate

Change Action Center Website: http://www.mccac.ca/sites/default/files/solar_municipalities-technology_cost_0.pdf

[6] NASA. (2017, September 30). *NASA Prediction of Worldwide Energy Resource (POWER)*. Retrieved from https://power.larc.nasa.gov/cgi-bin/cgiwrap/solar/timeseries.cgi

[7] NREL. (2017, September 30). *National Solar Radiation Data Base (NSRDB)*. Retrieved from https://nsrdb.nrel.gov/international-datasets

[8] Polo, J. (2017, May 23). *Data Adaptation Techniques for Improving Data Bankability.* Retrieved from International Solar Energy Society: http://www.ises.org/sites/default/files/webinars/webinar_2017_05_polo%20Martinez.pdf

[9] NAIT. (2016). *Solar Photovoltaic Reference Array Report—March 31, 2016.* Edmonton: NAIT Alternative Energy Program.

[10] SolarEdge. (2017b, June). *Monitoring Platform Mismatch Analysis Report, Application Note*. Retrieved from www.solaredge.com: https://www.solaredge.com/sites/default/files/monitoring_platform_mismatch_analysis_report.pdf

This page intentionally left blank

Chapter 4

Environmental and economic evaluation of PV solar system for remote communities using building information modeling: A case study

Muhammad Saleem[1], Rajeev Ruparathna[2], Rehan Sadiq[1] and Kasun Hewage[1]

Photovoltaic (PV) solar energy has been a popular renewable electricity generation source at the building and community levels. With the recent rise in the demand, residential level PV installations have been under scrutiny primarily to improve their efficiency. Electricity generation potential of a roof-mounted PV system depends on the local PV potential, building orientation, shading effect, roof angle, and roof size.

Moreover, the economic viability of the PV system needs to be justified before being implemented on site. This research investigates the optimal PV solar energy potential (PvSEP) of a standalone rooftop PV system using building information modeling (BIM). Two building shapes (square and rectangular), three roof types (hip, gable, and shed), eight orientations (E, W, S, N, NE, NW, SE, and SW), and nine roof slopes (starting from 10° to 50° with an interval of 5°) were analyzed at two geographical locations in British Columbia (i.e., Kelowna and Fort St. Johns). The BIM was created in the Autodesk Revit platform, and 432 simulations were performed for each location using the Revit Architecture extension Insight. Results indicated that even though location, roof angle, orientation, and roof types are significant factors for PvSEP, building shape do not have a significant impact. This has been consistent with the published literature. The PV system with the maximum PvSEP results in the minimum payback time and greenhouse gas (GHG) emissions. This research aims to aid PV system installation decision-making by using state-of-the-art technology during the pre-construction stage.

4.1 Introduction

IPCC Special report 2018 revealed that mankind is running out of time on the battle against climate change [1]. Urgent action is required to substitute fossil fuels with

[1]School of Engineering, University of British Columbia, Canada
[2]Civil & Environmental Engineering, University of Windsor, Canada

renewable energy resources (RES). The building industry accounts for one-third of the global greenhouse gas (GHG) emissions and is the main focus area in climate change mitigation efforts. Recent policy-level developments evidenced that Net Zero Energy Buildings (NZEBs) will be the future of the building industry. In NZEBs, the building energy demand is minimized. The above-minimized energy demand is then catered by renewable energy sources. As expected, there has been a steady growth in renewable energy generation in the recent past. This growing trend toward renewable energy has been identified as the third industrial revolution [2].

Solar energy is the most abundant RES available. Therefore, photovoltaic (PV) electricity is the most popular RES in the world [3]. In most regions of the world, solar electricity costs have drastically decreased in the recent past [4]. In Canada, growth in the solar electricity sector has been rapid. In 2013, installations of solar electricity systems grew by nearly 60% compared to the previous year. Despite the challenges faced by the solar industry, Canada is today one of the top 20 solar electricity markets in the world. Canadian solar electricity industry roadmap shows that by the year 2020, 1% of electricity generation in Canada will be from solar energy technologies, with almost 6,300 MW of installed capacity [5].

PV potential depends on a number of factors including location, PV solar module angle, system efficiency, building shape, and roof types. Yet, the installation of the PV solar system has been conducted as a quick fix in the pursuit of NZEB, without following a detailed evaluation process. Optimal utilization of PV potential should be evaluated from the pre-construction stage to maximize the value of the investment while supporting the global sustainability movement. Building information modeling (BIM) is a decision support platform that can be used to determine building design with the highest solar potential. BIM is the process of developing and managing digital information-rich models for construction projects [6]. BIM offers a reliable basis for decision making over an assets' life cycle considering aspects such as cost, sustainability, and facilities management. BIM applications in the construction industry have increased significantly due to the platform's ability to integrate information and optimize processes [6,7]. The ability of BIM to conduct solar analysis would support key decision making on building orientation and design during the pre-construction stage.

While solar energy availability varies widely across Canada, and additional social, economic, and environmental factors affect the suitability of adopting a solar PV technology at a particular location. This research aims to adopt BIM to optimize the solar PV potential of residential buildings. A case study was used to analyze the impacts of multiple parameters on PV electricity generation potential. Different building designs were evaluated for two locations in British Columbia, Canada (Kelowna and Fort St. Johns). A cost–benefit analysis and a life cycle GHG emissions assessment were conducted to determine the most eco-efficient design for a selected location.

4.2 Literature review

Climate change mitigation is the major global concern in the recent past. Presently, climate change initiatives can be observed at the global level (e.g., Kyoto protocol), country level (e.g., Federal Sustainable Development Strategy Canada), local government level (e.g., BC climate action charter), and community level [8,9]. Energy sustainable communities will assist in succeeding in the above task. Energy sustainable communities are those that use RES and adopt energy-efficient measures to reduce demand [10]. Energy efficiency, energy conservation, and switching to RES are the foremost steps of establishing a sustainable energy system [11]. Hence, on-site electricity generation from RES is a central consideration in sustainable urban neighborhood development [12,13].

Regional level energy and emission plans have been prevalent in Canada during the recent past [14,15]. Long-range energy planning is vital to optimize the available energy resources and to improve system cost and reliability with maximized energy security. Climate change mitigation through renewable energy has been a popular research topic in the published literature, especially in the recent past [16–18]. Canada has a very large potential for solar energy use, and it has excellent solar resources. Since 2007, there is an estimated 544,000 m^2 of solar collectors operating in Canada. They are primarily unglazed plastic collectors for pool heating (71%) and unglazed perforated solar air collectors for commercial building air heating (26%). Annually, these installations reduce about 627 TJ of conventional energy use and reduce 38 Megatonnes of CO_2 in emissions [19].

4.3 Methodology and case study

Computer simulations were used to evaluate the PV solar energy potential (PvSEP) under various scenarios. A sample building was identified and modeled using Revit Architecture, a commonly used platform for BIM. An off-grid (often called standalone) PV system was selected for this research. The photovoltaic solar energy potential (PvSEP) at a specific location depends on orientation, azimuth, types of systems, system efficiency and available solar insolation (Kelowna and Fort St. John). The PvSEP was simulated for two locations in BC using the software Insight (an extension in RevitArchitecture). An hourly analysis was done for a whole year starting from January 1, 2017, to December 31, 2017, from sunrise to sunset using daylight saving time. PvSEP was evaluated for 432 scenarios by changing the building orientation, building shape, roof type, and roof pitch. The following assumptions were used in this study. Figure 4.1 illustrates the multiple scenarios considered for PvSEP.

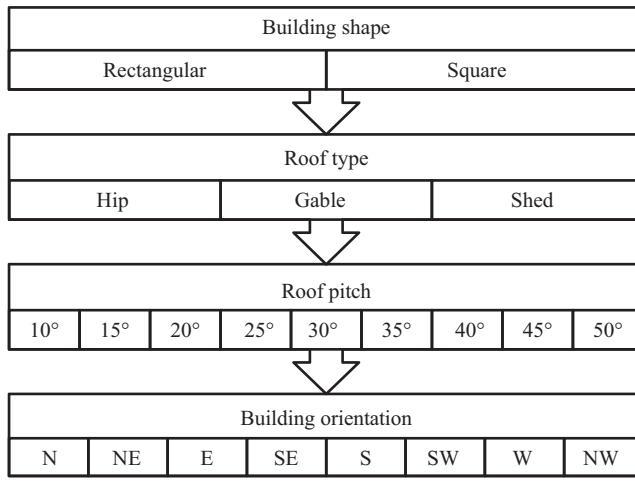

Figure 4.1 Analysis scheme to calculate optimal PV solar energy potential

(i) The roof area selected for this research was 200 m^2. It was assumed that the PV solar panels are installed on the entire roof area.
(ii) Building shape is a major determinant for solar potential. In this study, two building shapes (i.e., rectangular and square) were considered to determine the impact of building shape on PvSEP.
(iii) Different roof types have a different number of sides, which in turn impacts the PvSEP. Typical roof types such as hip roof, gable roof, and shed roof has four, two, and one sides directed toward the path of the sun, respectively. The above three roof types (hip, gable, and shed roofs) were analyzed to compare the impact of the roof type on PvSEP.
(iv) The tilt of the PV solar panel is another important determinant of PvSEP. It is important to find the optimum roof pitch. Nine roof pitch values were selected ranging from 10° to 50° with an interval of 5°.

The simulated solar performance scenarios indicated in Figure 4.1 were further evaluated using the cost–benefit analysis. A simple payback period method was selected and used to calculate cost–benefit analysis for PvSEP at the selected locations. RSMeans Data 2017 for green buildings were used to estimate the life cycle cost of a selected standalone PV solar system. Equation (4.1) was used to calculate the payback period:

$$\text{Simple payback time(years)} = \frac{\text{Total cost of the PV system}}{\text{Annual PvSEP} \times \text{Tariff rate per kWh}} \tag{4.1}$$

Despite the GHG emission avoidance during the operational stage, there is a significant embodied GHG content associated with PV panels. The GHG emission rate was selected to determine the sustainability and greenness of the system. The

GHG emission rate denotes how much GHG is emitted per unit of generated electricity. For a solar PV system, the GHG emission rate is the ratio of total GHG emissions of the PV system to the total electricity generated during its life cycle [20]. This was calculated by using (4.2). The total GHG emission values during the manufacturing phase of different solar PV system components were obtained from the published literature and life cycle impact databases:

$$\mathrm{GHG}_{\mathrm{e-rate}} = \frac{\mathrm{GHG}_{\mathrm{PV}} + \mathrm{GHG}_{\mathrm{Battery\ bank}} + \mathrm{GHG}_{\mathrm{Inverter}} + \mathrm{GHG}_{\mathrm{Supports}} + \mathrm{GHG}_{\mathrm{BOS}}}{\mathrm{E}_{\mathrm{LCA-output}}} \tag{4.2}$$

LCA software database and literature revealed the following results on the embodied GHG emissions of PV systems. The embodied GHG emissions of a PV solar system of 200 m^2 and its batteries are 15,236.40 $kgCO_2$ eq and 15,206.40 $kgCO_2$ eq, respectively.

4.4 Results

Tables 4.1 and 4.2 indicate the maximum PvSEP for the rectangular- and square-shaped buildings, respectively. The full simulation results from Insight are presented in Tables A1–A4 Appendix A. The shed roof is the most popular roof type in British Columbia. The simulation results indicated that a south-facing shed roof with 45° roof tilt can generate 46,562 kWh/year and 46,555 kWh/year at Kelowna and Fort St. John locations, respectively. The maximum PvSEP of the shed roof is 30% higher than the hip and gable roof types.

Table 4.1 PvSEP comparison between Kelowna and Fort St. John for rectangular shape building

	Rectangular shape building					
	Hip roof		**Gable roof**		**Shed roof**	
Orientation Pitch	**E, W Kelowna**	**NE, SW Fort St. John**	**E, W Kelowna**	**E, W Fort St. John**	**S Kelowna**	**S Fort St. John**
10	35,494	30,435	35,500	30,440	39,929	34,563
15	35,225	30,227	35,246	30,253	41,765	36,323
20	34,807	29,878	34,844	29,936	43,300	37,809
25	34,317	29,447	34,375	29,567	44,577	39,042
30	33,716	28,948	33,805	29,145	45,523	40,041
35	33,035	28,388	33,171	28,660	46,166	40,752
40	32,283	27,820	32,478	28,145	46,522	41,217
45	31,463	27,241	31,718	27,578	46,562	41,402
50	28,598	26,630	30,875	26,944	46,282	41,312

Table 4.2 PvSEP comparison between Kelowna and Fort St. John for square shape building

	Square shape building					
	Hip roof		Gable roof		Shed roof	
Orientation Pitch	**N, E, S, W Kelowna**	**NE, SE, SW, NW Fort St. John**	**E, W Kelowna**	**E, W Fort St. John**	**S Kelowna**	**S Fort St. John**
10	35,502	30,452	35,513	30,458	39,945	34,584
15	35,201	30,207	35,240	30,233	41,759	36,299
20	34,789	29,872	34,862	29,930	43,322	37,801
25	34,246	29,426	34,359	29,546	44,558	39,015
30	33,636	28,931	33,811	29,129	45,531	40,019
35	32,936	28,385	33,189	28,659	46,190	40,751
40	32,152	27,815	32,498	28,147	46,550	41,219
45	31,269	27,215	31,714	27,565	46,555	41,381
50	27,028	26,628	30,898	26,959	46,316	41,335

The simulations further revealed the following results related to the PvSEP.

- Location: The orientation with maximum PvSEP for the hip roof is different for the two cities. However, PV systems installed on gable and shed roofs in Kelowna and Fort St. John have a maximum PvSEP in E and W orientation and S orientation, respectively.
- The pitch of the roof: The optimum pitch of the shed roof is 45°, while hip and gable roofs have maximum PvSEP with 10° roof pitch.
- Building shape: The simulation results indicate that the building shape has a negligible impact on PvSEP.
- Roof orientation: Roof orientation has a significant impact on the PvSEP. In Kelowna, hip and gable roofs have maximum PvSEP in the E and W orientation, while the shed roof has the maximum in south-facing orientation.

The total cost of the PV solar system deployed on the rooftop was determined by adding the cost of the PV module, direct current to alternating current inverter, deep cycle solar battery system, and battery charger. The battery system is necessary for a standalone PV system. The above PvSEP results were adopted to conduct further analysis of the PV potential. According to the analysis, a shed roof at 45° has the minimum payback period at 16 years, while the hip roof at an inclination of 50° is associated with the longest payback period (28 years). The payback period could be reduced by making use of renewable energy incentive programs. However, British Columbia is one of the few provinces in Canada without a major rebate or tax credit program for renewable energy projects.

Life cycle GHG emissions potential of the PV system scenarios showed a similar variation. Simulation results revealed that the GHG emissions rate of the shed roof is 16.35 g CO_2 eq/kWh for Kelowna and 18.38 g CO_2 eq/kWh for Fort St. Johns.

4.5 Discussion and conclusions

BIM is a valuable resource to identify best design configurations for a planned building. The case study indicated multiple building design scenarios and their respective PvSEP. This information informs architects making and altering their decisions at the design stage of a building. The proposed methodology delivers a sequential decision process that enables achieving of optimal environmental performance for building-level PV systems. Other add-ons such as Talley would enable the identification of the building design with lowest life cycle impacts.

A case study approach was used to assess a standalone PV system deployed on a rooftop in two cities in British Columbia, Canada (Kelowna and Fort St. Johns). For each location, 432 simulations were run in the software Insight for a real-time analysis from dawn to dusk over the years, and the annual PvSEP was determined. Kelowna has a higher PvSEP than Fort St. John due to higher solar irradiation. It was also observed that the maximum PvSEP is obtained at different orientations for different roof types. In a rectangular-shaped building, hip and gable roof types have the maximum PvSEP in an eastern orientation, while the shed roof type has the maximum PvSEP in a southern orientation. However, the shed roof had the highest PvSEP compared to hip and gable roof types for square and rectangular building shapes in both cities. Furthermore, PvSEP for different roof types varied depending on the roof tilt or slope. PvSEP increases with an increase in the roof tilt for a shed roof, while it decreases with an increase in the roof tilt for hip and gable roofs for both building types in the case study locations. The results of this study emphasize the importance of early decision making in the design phase when installing a PV solar system on the rooftop is in consideration for the future.

A simple payback period method was used for economic analysis. The results showed that the payback time varies between 18 and 27 years for different roof types. The roof types with a higher PvSEP resulted in a lower payback time. A battery bank is required for communities where grid connectivity is unavailable. However, the battery bank accounts for approximately 36% of the total cost of the system and would substantially increase the payback time. For a grid-connected PV solar system, this payback time would be reduced up to 12 years for maximum PvSEP scenarios.

PV technologies are considered to be a more sustainable source of electricity. Compared with the traditional fossil-based power plants, one significant merit of PV power systems is the potential to mitigate GHG emissions. Even so, the manufacturing phase of PV technologies leads to significant embodied GHG emission. However, with the emerging new manufacturing technologies, the environmental and economic performance of PV technologies is expected to be further improved. This advancement would result in an even higher GHG emissions reduction from the PV solar system. Similarly, as observed in the cost–benefit analysis, a standalone PV solar system has higher GHG emission due to the battery bank compared to a grid-connected solar PV system with a similar configuration. Overall, the installation of solar PV systems in cities would assist in achieving Canada's GHG emissions reduction targets.

The rooftop PvSEP depends on the shading effect due to the nearby structures, building footprint area, and the effective PV-available roof area [21,22]. Other factors that affect the solar energy potential include the efficiencies of the solar system, which in turn is dependent on the efficiency of the adopted PV technology and physical deterioration [23]. In implementation first, it is vital to adopt the most efficient technology that is available in the market. Second, orientation and building design should be investigated to maximize the PvSEP. These factors should be considered in the pre-project planning stage with the support of the project owner's commitment to sustainable development.

Published literature on PV generation has been growing during the recent past. Several innovative research streams include light detection and ranging data, geospatial information and PV generation modeling for locational suitability for PV [24]. Developing comprehensive tools that encompass technical, environmental, and social parameters could enhance the PV energy planning in neighborhood development. Due to the variability of regional PV potential, previous research also explored the possibility of GIS-based solar mapping based on the biophysical and socioeconomic factors [25]. Software such as RETScreen would assist decision making with regard to technical parameters. Further work is necessary to develop comprehensive decision-aid tools that bring together multiple platforms such as BIM, GIS, and life cycle thinking to perform a comprehensive evaluation of the regional PV implementation.

BIM carries important add-ons for evaluating the operational performance of buildings. These features can be used to make crucial project planning and design decisions. The case study assessed the PvSEP of a building in two different locations. The analysis indicated that the location, pitch, and orientation as key parameters impacting the PvSEP. The information obtained from the simulation would provide information to adjust the building design accordingly. The BIM platform could be integrated with other software such as MATLAB. Therefore, a comprehensive design optimization tool could be developed by integrating the BIM model with economic and environmental performance evaluation algorithms. This approach would simplify the building design development and enable optimizing the solar potential in an area.

Appendix A

Table A1 Annual solar energy potential for rectangular-shaped building in Kelowna, BC (all values are in kWh/year)

Rectangular-shaped building									
	HIP roof								
Orientation	**10°**	**15°**	**20°**	**25°**	**30°**	**35°**	**40°**	**45°**	**50°**
N	35,483	35,187	34,736	34,205	33,544	32,802	31,982	31,084	25,419
NE	35,489	35,213	34,757	34,215	33,555	32,825	32,051	31,235	30,374
E	**35,494**	**35,225**	**34,807**	**34,317**	**33,716**	**33,035**	**32,283**	**31,463**	28,598
SE	35,489	35,213	34,757	34,218	33,560	32,831	32,060	31,245	**30,385**
S	35,483	35,187	34,736	34,205	33,544	32,802	31,982	31,084	25,419
SW	35,489	35,213	34,757	34,215	33,555	32,825	32,051	31,235	30,374
W	**35,494**	**35,225**	**34,807**	**34,317**	**33,716**	**33,035**	**32,283**	**31,463**	28,598
NW	35,489	35,213	34,757	34,218	33,560	32,831	32,060	31,245	**30,385**

Rectangular-shaped building									
	Gable roof								
Orientation	**10°**	**15°**	**20°**	**25°°**	**30°**	**35°**	**40°**	**45°**	**50°**
N	35,477	35,167	34,700	34,148	33,455	32,666	31,787	30,829	23,141
NE	35,489	35,213	34,756	34,214	33,553	32,820	32,045	31,229	30,367
E	**35,500**	**35,246**	**34,844**	**34,375**	**33,805**	**33,171**	**32,478**	**31,718**	**30,875**
SE	35,489	35,213	34,758	34,219	33,563	32,835	32,066	31,252	30,392
S	35,477	35,167	34,700	34,148	33,455	32,666	31,787	30,829	23,141
SW	35,489	35,213	34,756	34,214	33,553	32,820	32,045	31,229	30,367
W	**35,500**	**35,246**	**34,844**	**34,375**	**33,805**	**33,171**	**32,478**	**31,718**	**30,875**
NW	35,489	35,213	34,758	34,219	33,563	32,835	32,066	31,252	30,392

Rectangular-shaped building									
	Shed roof								
Orientation	**10°**	**15°**	**20°**	**25°**	**30°**	**35°**	**40°**	**45°**	**50°**
N	31,024	28,568	26,099	23,717	21,387	19,165	17,052	15,096	0
NE	32,358	30,581	28,705	26,857	25,029	23,296	21,700	20,262	18,984
E	35,521	35,277	34,886	34,427	33,863	33,234	32,544	31,787	30,946
SE	38,651	39,890	40,871	41,652	42,174	42,458	42,515	42,330	41,891
S	**39,929**	**41,765**	**43,300**	**44,577**	**45,523**	**46,166**	**46,522**	**46,562**	**46,282**
SW	38,621	39,844	40,807	41,571	42,077	42,345	42,391	42,196	41,750
W	35,479	35,213	34,802	34,323	33,746	33,107	32,412	31,650	30,806
NW	32,328	30,536	28,646	26,786	24,951	23,213	21,615	20,173	18,893

Note: Bold values indicate highest solar energy potential for different scenarios.

Table A2 Annual solar energy potential for square-shaped building in Kelowna, BC (all values are in kWh/year)

	Square-shaped building								
	HIP roof								
Orientation	**10°**	**15°**	**20°**	**25°**	**30°**	**35°**	**40°**	**45°°**	**50°**
N	35,502	35,201	**34,789**	**34,246**	**33,636**	**32,936**	**32,152**	**31,269**	27,028
NE	**35,503**	**35,208**	34,775	34,202	33,564	32,846	32,075	31,235	**30,402**
E	35,502	35,201	**32,789**	**34,246**	**33,636**	**32,936**	**32,152**	**31,269**	27,028
SE	**35,503**	**35,208**	34,775	34,202	33,564	32,846	32,075	31,235	**30,402**
S	35,502	35,201	**34,789**	**34,246**	**33,636**	**32,936**	**32,152**	**31,269**	27,028
SW	**35,503**	**35,208**	34,775	34,202	33,564	32,846	32,075	31,235	**30,402**
W	35,502	35,201	**34,789**	**34,246**	**33,636**	**32,936**	**32,152**	**31,269**	27,028
NW	**35,503**	**35,208**	34,775	34,202	33,564	32,846	32,075	31,235	**30,402**
	Square-shaped building								
	Gable roof								
Orientation	**10°**	**15°**	**20°**	**25°**	**30°**	**35°**	**40°**	**45°**	**50°**
N	35,490	35,162	34,717	34,132	33,461	32,683	31,806	30,824	23,158
NE	35,503	35,207	34,773	34,199	33,559	32,838	32,064	31,224	30,389
E	**35,513**	**35,240**	**34,862**	**34,359**	**33,811**	**33,189**	**32,498**	**31,714**	**30,898**
SE	35,504	35,208	34,775	34,204	33,569	32,853	32,084	31,247	30,414
S	35,490	35,162	34,717	34,132	33,461	32,683	31,806	30,824	23,158
SW	35,503	35,207	34,773	34,199	33,559	32,838	32,064	31,224	30,389
W	**35,513**	**35,240**	**34,862**	**34,359**	**33,811**	**33,189**	**32,498**	**31,714**	**30,898**
NW	35,504	35,208	34,775	34,204	33,569	32,853	32,084	31,247	30,414
	Square-shaped building								
	Shed roof								
Orientation	**10°**	**15°°**	**20°**	**25°**	**30°**	**35°**	**40°**	**45°**	**50°**
N	31,036	28,564	26,113	23,707	21,391	19,175	17,063	15,094	0
NE	32,370	30,577	28,719	26,845	25,034	23,308	21,713	20,259	18,998
E	35,534	35,272	34,904	34,411	33,869	33,252	32,564	31,782	30,968
SE	38,666	39,884	40,891	41,633	42,182	42,480	42,541	42,324	41,921
S	**39,945**	**41,759**	**43,322**	**44,558**	**45,531**	**46,190**	**46,550**	**46,555**	**46,316**
SW	38,635	39,838	40,827	41,553	42,085	42,368	42,416	42,189	41,780
W	35,492	35,209	34,819	34,308	33,753	33,125	32,432	31,646	30,828
NW	32,341	30,532	28,660	26,774	24,956	23,226	21,628	20,170	18,908

Note: Bold values indicate highest solar energy potential for different scenarios.

Table A3 Annual solar energy potential for rectangular-shaped building in Fort St. John, BC (all values are in kWh/year)

	Rectangular-shaped building								
	Hip roof								
Orientation	**10°**	**15°**	**20°**	**25°**	**30°**	**35°**	**40°**	**45°**	**50°**
N	30,431	30,227	29,886	**29,449**	28,945	28,357	22,561	22,458	22,382
NE	30,435	30,227	29,878	29,447	**28,948**	**28,388**	**27,820**	**27,241**	**26,630**
E	**30,437**	**30,244**	**29,918**	27,275	29,072	28,548	26,193	25,822	25,217
SE	30,435	30,227	29,879	29,447	28,947	28,383	27,807	27,218	26,597
S	30,431	30,227	29,886	**29,449**	28,945	28,357	22,561	22,458	22,382
SW	30,435	30,227	29,878	29,447	**28,948**	**28,388**	**27,820**	**27,241**	**26,630**
W	**30,437**	**30,244**	**29,918**	27,275	29,072	28,548	26,193	25,822	25,217
NW	30,435	30,227	29,879	29,447	28,947	28,383	27,807	27,218	26,597

	Rectangular-shaped building								
	Gable roof								
Orientation	**10°**	**15°**	**20°**	**25°**	**30°**	**35°**	**40°**	**45°**	**50°**
N	30,429	30,218	29,867	29,408	28,872	28,244	20,609	20,701	20,656
NE	30,435	30,227	29,878	29,447	28,949	28,391	27,827	27,253	26,651
E	**30,440**	**30,253**	**29,936**	**29,567**	**29,145**	**28,660**	**28,145**	**27,578**	**26,944**
SE	30,436	30,227	29,879	29,447	28,946	28,380	27,800	27,205	26,576
S	30,429	30,218	29,867	29,408	28,872	28,244	20,609	20,701	20,656
SW	30,435	30,227	29,878	29,447	28,949	28,391	27,827	27,253	26,651
W	**30,440**	**30,253**	**29,936**	**29,567**	**29,145**	**28,660**	**28,145**	**27,578**	**26,944**
NW	30,436	30,227	29,879	29,447	28,946	28,380	27,800	27,205	26,576

	Rectangular-shaped building								
	Shed roof								
Orientation	**10°**	**15°**	**20°**	**25°**	**30°**	**35°**	**40°**	**45°**	**50°**
N	26,294	24,112	21,926	19,772	17,703	15,737	0	0	0
NE	27,391	25,725	24,005	22,317	20,688	19,173	17,829	16,690	15,721
E	30,270	30,005	29,617	29,183	28,708	28,177	27,624	27,029	26,372
SE	33,239	34,376	35,293	36,023	36,569	36,893	29,537	36,970	36,685
S	**34,563**	**36,323**	**37,809**	**39,042**	**40,041**	**40,752**	**41,217**	**41,402**	**41,312**
SW	33,479	34,729	35,750	36,576	37,209	37,610	37,824	37,816	37,580
W	30,609	30,501	30,256	29,949	29,582	29,143	28,667	28,129	27,515
NW	27,632	26,079	24,456	22,871	21,323	19,868	18,563	17,441	16,468

Note: Bold values indicate highest solar energy potential for different scenarios.

Table A4 Annual solar energy potential for square-shaped building in Fort St. John, BC (all values are in kWh/year)

	Square-shaped building								
	Hip roof								
Orientation	**10°**	**15°**	**20°**	**25°**	**30°**	**35°**	**40°**	**45°**	**50°**
N	**30,453**	**30,215**	**29,896**	**29,466**	**28,992**	28,451	24,378	24,128	23,813
NE	30,452	30,207	29,872	29,426	28,931	**28,385**	**27,815**	**27,215**	**26,628**
E	**30,453**	**30,215**	**29,896**	**29,466**	**28,992**	28,451	24,378	24,128	23,813
SE	30,452	30,207	29,872	29,426	28,931	**28,385**	**27,815**	**27,215**	**26,628**
S	**30,453**	**30,215**	**29,896**	**29,466**	**28,992**	28,451	24,378	24,128	23,813
SW	30,452	30,207	29,872	29,426	28,931	**28,385**	**27,815**	**27,215**	**26,628**
W	**30,453**	**30,215**	**29,896**	**29,466**	**28,992**	28,451	24,378	24,128	23,813
NW	30,452	30,207	29,872	29,426	28,931	**28,385**	**27,815**	**27,215**	**26,628**
	Square-shaped building								
	Gable roof								
Orientation	**10°**	**15°**	**20°**	**25°**	**30°**	**35°**	**40°**	**45°**	**50°**
N	30,447	30,197	29,861	29,387	28,856	28,244	20,610	20,690	20,668
NE	30,453	30,207	29,871	29,426	28,932	28,391	27,828	27,239	26,666
E	**30,458**	**30,233**	**29,930**	**29,546**	**29,129**	**28,659**	**28,147**	**27,565**	**26,959**
SE	30,454	30,208	29,873	29,426	28,930	28,379	27,802	27,191	26,591
S	30,447	30,197	29,861	29,387	28,856	28,244	20,610	20,690	20,668
SW	30,453	30,207	29,871	29,426	28,932	28,391	27,828	27,239	26,666
W	**30,458**	**30,233**	**29,930**	**29,546**	**29,129**	**28,659**	**28,147**	**27,565**	**26,959**
NW	30,454	30,208	29,873	29,426	28,930	28,379	27,802	27,191	26,591
	Square-shaped building								
	Shed roof								
Orientation	**10°**	**15°**	**20°**	**25°**	**30°**	**35°**	**40°**	**45°**	**50°**
N	26,310	24,096	21,921	19,759	17,693	15,737	0	0	0
NE	27,340	25,708	23,999	22,301	20,677	19,172	17,830	16,682	15,729
E	30,288	29,984	29,610	29,163	28,691	28,175	27,626	27,014	26,387
SE	33,259	34,353	35,285	35,998	36,548	36,892	37,039	36,951	36,705
S	**34,584**	**36,299**	**37,801**	**39,015**	**40,019**	**40,751**	**41,219**	**41,381**	**41,335**
SW	33,499	34,706	35,743	36,551	37,188	37,609	37,826	37,796	37,601
W	30,627	30,481	30,250	29,928	29,566	29,142	28,668	28,115	27,531
NW	27,649	26,062	24,460	22,856	21,311	19,867	18,564	17,432	16,447

Note: Bold values indicate highest solar energy potential for different scenarios.

References

[1] Intergovernmental Panel on Climate Change (IPCC). (2018). *Global warming of 1.5°C*. Geneva, Switzerland.

[2] Rifkin, J. (2005). *The European Dream: How Europe's Vision of the Future is Quietly Eclipsing the American Dream*. Cornwell, UK: Polity Press.

[3] Natural Resources Canada. (2013). Solar Photovoltaic Energy. Retrieved from http://www.nrcan.gc.ca/energy/renewables/solar-photovoltaic/7303

[4] Timilsina, G. R., Kurdgelashvili, L., and Narbel, P. a. (2012). Solar energy: Markets, economics and policies. *Renewable and Sustainable Energy Reviews*, *16*(1), 449–465. https://doi.org/10.1016/j.rser.2011.08.009

[5] CanSIA. (2015). Roadmap 2020: Powering Canada's Future with Solar Electricity, Canadian Solar Industries Association, Ottawa, ON.

[6] Porwal, A. (2013). *Construction Waste Management at Source: A Building Information Modelling based System Dynamics Approach*, University of British Columbia.

[7] Porwal, A., and Hewage, K. N. (2013). Building Information Modeling (BIM) partnering framework for public construction projects. *Automation in Construction*, 31, 204–214. https://doi.org/10.1016/j.autcon.2012.12.004

[8] Ministry of Environment BC. (2010). Carbon Neutral Public Sector. Retrieved from http://www.env.gov.bc.ca/cas/mitigation/carbon_neutral.html

[9] Environment Canada. (2014). Canada's Action on Climate Change. Retrieved from http://www.climatechange.gc.ca/default.asp?lang=En&n=72F16A84-0

[10] Schweizer-Ries, P. (2008). Energy sustainable communities: Environmental psychological investigations. *Energy Policy*, *36*(11), 4126–4135. https://doi.org/10.1016/j.enpol.2008.06.021

[11] Denis, G. S., and Parker, P. (2009). Community energy planning in Canada: The role of renewable energy. *Renewable and Sustainable Energy Reviews*, *13*(8), 2088–2095. https://doi.org/10.1016/j.rser.2008.09.030

[12] Maier, S., and Gemenetzi, A. (2014). Optimal renewable energy systems for industries in rural regions. *Energy, Sustainability and Society*, *4*(1), 1–12.

[13] Costa, P. M., Matos, M. a., and Peças Lopes, J. a. (2008). Regulation of microgeneration and microgrids. *Energy Policy*, *36*(10), 3893–3904. https://doi.org/10.1016/j.enpol.2008.07.013

[14] ICLEI. (2014). Member Profiles: Community Energy Plans. Retrieved from http://www.icleicanada.org/news/item/126-member-profile-community-energy-plans

[15] Ishii, S., Tabushi, S., Aramaki, T., and Hanaki, K. (2010). Impact of future urban form on the potential to reduce greenhouse gas emissions from residential, commercial and public buildings in Utsunomiya, Japan. *Energy Policy*, *38*(9), 4888–4896. https://doi.org/10.1016/j.enpol.2009.08.022

[16] Manzini, F., Islas, J., and Martã, M. (2001). Reduction of greenhouse gases using renewable energies in Mexico 2025. *International Journal of Hydrogen Energy*, *26*(2001), 145–149.

[17] El-Fadel, M., Chedid, R., Zeinati, M., and Hmaidan, W. (2003). Mitigating energy-related GHG emissions through renewable energy. *Renewable Energy*, *28*(8), 1257–1276. https://doi.org/10.1016/S0960-1481(02)00229-X

[18] Islas, J., Manzini, F., and Martínez, M. (2003). Cost–benefit analysis of energy scenarios for the Mexican power sector. *Energy*, *28*(10), 979–992. https://doi.org/10.1016/S0360-5442(03)00048-3

[19] Natural Resources Canada. (2014). Solar Thermal. Retrieved June 15, 2015, from https://www.nrcan.gc.ca/energy/renewable-electricity/solar-thermal/7301

[20] Peng, C., Wang, L., and Zhang, X. (2014). DeST-based dynamic simulation and energy efficiency retrofit analysis of commercial buildings in the hot summer/cold winter zone of China: A case in Nanjing. *Energy and Buildings*, *78*, 123–131. https://doi.org/10.1016/j.enbuild.2014.04.023

[21] Cronemberger, J., Caamaño-Martín, E., and Sánchez, S. V. (2012). Assessing the solar irradiation potential for solar photovoltaic applications in buildings at low latitudes – Making the case for Brazil. *Energy and Buildings*, *55*, 264–272. https://doi.org/10.1016/j.enbuild.2012.08.044

[22] Singh, R., and Banerjee, R. (2015). Estimation of rooftop solar photovoltaic potential of a city. *Solar Energy*, *115*, 589–602. https://doi.org/10.1016/j.solener.2015.03.016

[23] Angelis-Dimakis, A., Biberacher, M., Dominguez, J., *et al.*, (2011). Methods and tools to evaluate the availability of renewable energy sources. *Renewable and Sustainable Energy Reviews*, *15*(2), 1182–1200. https://doi.org/10.1016/j.rser.2010.09.049

[24] Gagnon, P., Margolis, R., Melius, J., Phillips, C., and Elmore, R. (2016). *Rooftop Solar Photovoltaic Technical Potential in the United States: A Detailed Assessment*, Denver.

[25] Perpiña Castillo, C., Batista e Silva, F., and Lavalle, C. (2016). An assessment of the regional potential for solar power generation in EU-28. *Energy Policy*, *88*, 86–99. https://doi.org/10.1016/j.enpol.2015.10.004

Chapter 5

Solar energy generation technology for small homes

Santosh B. Bopche[1] and Inderjeet Singh[1]

This chapter presents concentrating collector-based technologies for capturing solar energy that may be utilized to produce power for energizing small homes (remotely located). The various types of existing solar thermal concentrating collectors, energy receivers of various shapes, sizes, and materials for selective surfaces, thermal energy storage systems, solar-powered heat engines, e.g., Stirling engine, solar-Rankine heat engine, solar-Brayton engine, are also presented thereof. The renewable hybrid technologies, e.g., solar power integration with biogas, geothermal and wind energy along with its advantages as well as limitations are discussed. It concludes with the challenges need to be faced in remote regions.

5.1 Introduction

The renewable energy is an energy obtained from natural replenishable resources. It consists of wind, water power, tidal power, solar, biomass, and energy recovered from wastes. The solar energy is available at free of cost and is the cleanest source of renewable type energy that can be utilized as a better substitute to the fossil fuel energy. It is a big challenge to extract the maximum possible heat energy from the solar irradiation. The present chapter focuses on the solar concentrating collector technology, a discussion in brief on thermal heat storage systems and an efficient solar engine technique that may be used for small-scale power generation.

5.1.1 Solar thermal power plant

A conventional coal-based power plant that works on the Rankine cycle comprises a boiler, a steam turbine, a steam condenser, a pump, feed water/condensate heaters, an economizer (for preheating feed water supplies to the boiler), and a power generator. In a solar-based thermal power plant, a steam boiler may completely be replaced by a solar-collector/reflector field during the shiny hours of the day. In the night, it can work as usual by depending on conventional fuels, e.g., coal

[1]National Institute of Technology, India

or crude oils. Such a bi-mode (conventional-fuel together with solar power-based) power generation plant is termed as a hybrid power plant.

The solar thermal power plant involves a solar concentrator field to capture as much incident solar energy as possible and to focus it onto the receivers. At the receiver, the concentrated form of solar energy is transferred to the heat transfer fluid in circulation (e.g., water, air). The working fluid is pressurized by means of a pump in an overall water–steam circuit. The steam vapors generated in the receiver are then supplied to the prime movers (steam turbine, gas turbine, and Stirling engine) directly/indirectly (indirectly via a heat exchanger and secondary fluid). The prime mover supplies the rotary power to the electric generator. The components of the solar-based thermal power plant may also comprise a provision for energy storage in order to store surplus captured solar energy during the sunshine hours and release it during the non-shiny hours.

The classes of solar thermal power plants are shown in Figure 5.1. It involves a non-concentrating-type solar chimney-driven wind turbine power plant and concentrating-type line as well as point focusing solar power plants. The photovoltaic cell-driven power plant can be energized by means of both concentrated and/or non-concentrated solar energy.

The concentrating solar power plants use line focusing collectors (linear Fresnel and parabolic trough types) to energize the Rankine cycle. A point focusing collector like central tower receiver type and parabolic dish collector type supplies energy to the power unit operating on the Brayton cycle. The Stirling engine can also be driven using the energy captured by a dish collector field [1].

A schematic showing component arrangement of a concentrating-type solar-thermal power unit is shown in Figure 5.2. These components, e.g., solar

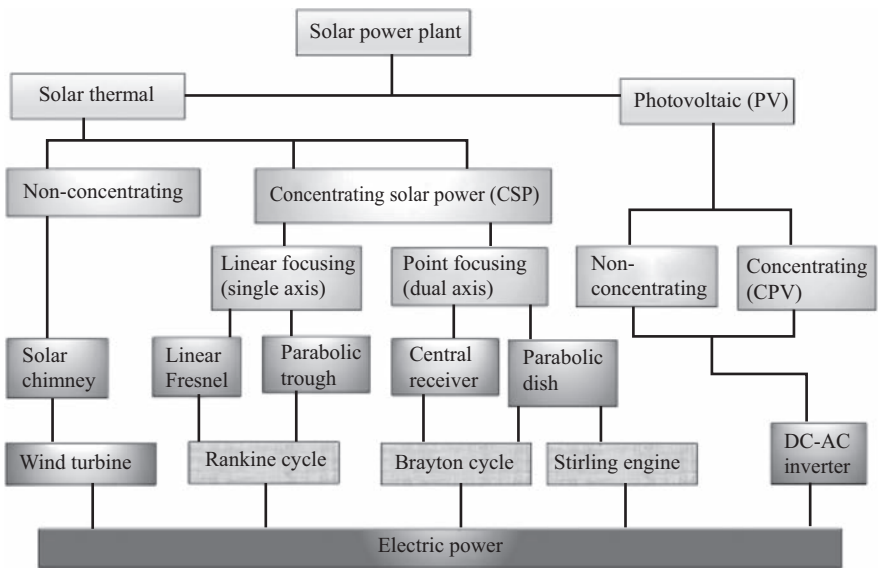

Figure 5.1 Diagram showing the classification of solar thermal power units [1]

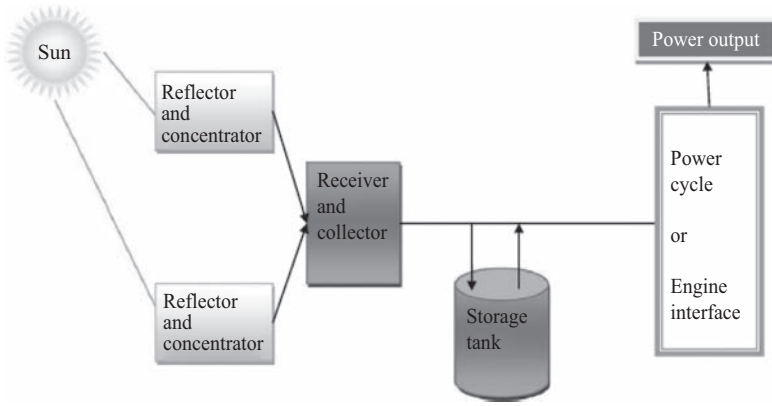

Figure 5.2 Schematic of the layout of components of a solar thermal power plant [2]

concentrator, receiver, energy storage systems, and heat engine, are discussed one by one in the subsequent sections.

5.2 Power generation technology—An overview

This section explores the concentrator designs available in the literature, which are mainly used for power generation for either a smaller power or a larger power level. The concentrating-type solar-power systems use direct solar radiation for focusing it into the receiver in a concentrated form, in order to meet higher energy densities, necessary for power generation for a smaller as well as for a larger residential community. For better results, collector arrays are generally equipped with a solar tracking system and energy storage devices or hybrid solar cum conventional thermal power generation units in order to meet the requirements during low as well as non-irradiation hours. The concentrating solar power-based energy production is pollution free and safe to handle/operate [3].

5.2.1 Classification of concentrating solar power collector systems

The concentrating solar power systems are generally classified according to the manner a collector focuses the solar irradiation and the technology preferred to capture an incident solar radiation. According to the concentration geometry, these are point focusing-type concentrators and line focusing-type concentrators. The line focusing-type concentrators are (i) parabolic profiled trough/cylindrical collectors and (ii) linear Fresnel-type collectors. The point-focus-type technology-based reflectors or concentrators include (iii) a central receiver system and (iv) a parabolic dish or Scheffler reflector system. A Scheffler collector is a smaller lateral section of a large-sized paraboloid, schematic of which is depicted in Figure 5.3. A cutting inclined plane prepares an elliptical-shaped Scheffler-reflector, which reflects an

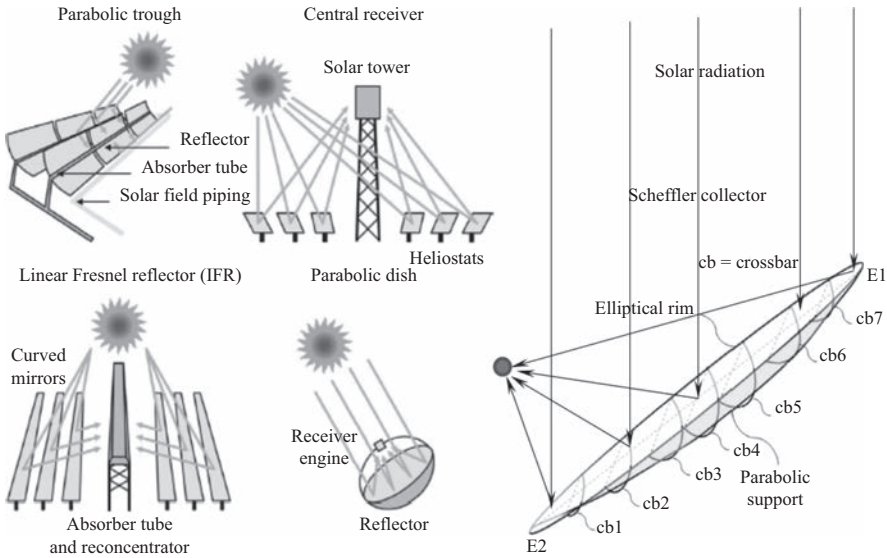

Figure 5.3 Photographs of concentrating-type collectors including the Scheffler collector [4]

incident solar radiation sideways. These reflectors are generally used for solar kitchen cooking purposes [3]. Photographs of the concentrating-type collectors are depicted in Figure 5.3.

The line focus technology-based collectors are seen to be lesser expensive and technically simpler in design but the efficiency is quite lesser as compared to point focusing collector systems [3].

5.2.1.1 Cylindrical parabolic trough type collector

A parabolic trough collector is also termed as "cylindrical parabolic collector" or "linear parabolic collector." The components include (i) an absorber tube enclosed in a concentric transparent cover, positioned at the focal axis, through which the working fluid to be heated flows and (ii) a concentrator or mirror reflector parabolic in shape. The schematic is shown in Figure 5.4.

The curved mirrors are fixed on to the parabolic trough for focusing/concentrating the solar irradiation on a receiver tube. The synthetic oil, acting as a working fluid/heat exchange medium, is circulated through the absorber tube (in a primary fluid circuit) to be heated to around 400 °C temperature suitable for various applications, viz. domestic as well as industrial purposes. According to the operating temperature range, a cylindrical parabolic collector is categorized as a low-temperature and a high temperature collector. A low-temperature range appliance operating within 100–250 °C is generally used for industrial heating purposes, and a high temperature range collector with operating temperature ranging from 300 to 450 °C is used for electrical power generation that may

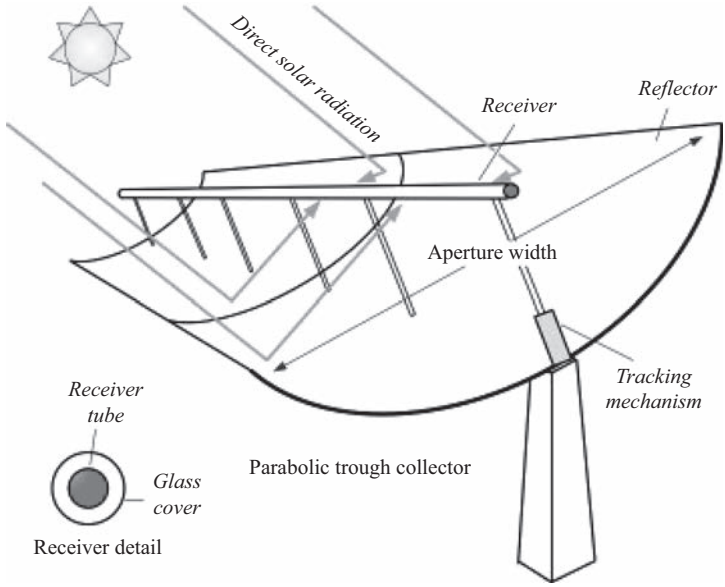

Figure 5.4 Schematic of the parabolic trough collector

be used to fulfill the demands of a larger community or a smaller individual home [3].

The generation of operating temperature is reliant on a concentration-ratio value of the solar collector system. It is stated as the ratio of the effective aperture area to the absorber tube area, as given below:

$$C = \frac{\text{Effective aperture area}}{\text{Absorber tube area}} = \frac{(W - D)L}{\pi DL} \tag{5.1}$$

where W is a collector width, D is an absorber tube diameter, and L is the length of a cylindrical parabolic collector.

With the adoption of a concentration ratio of about 70–100, an operating temperature of the order of 350–550 °C can be achieved in the system. As reported in the literature [3], a concentration that can be achieved using a parabolic trough collector is 70–80.

Then, the heated oil transfers to the heat exchangers, where feed water is preheated and evaporated which is finally supplied to a steam turbine via superheaters. The pressurized superheated-steam drives a turbine that energizes an electric generator for producing electricity. The steam is dumped into a condenser for being cooled and condensed, which is recirculated in the secondary circuit. The incorporation of a cylindrical parabolic collector's field in the steam turbine-based power generation unit is termed as the direct steam generation technology [3].

In a similar manner, collector's solar collection efficiency is described as the proportion of the heat gained by a working fluid while flowing through the

absorber tube to the solar irradiation incident at the collector aperture area, as given below:

$$\eta_{Collection} = \frac{Q_u}{I_T WL} = \frac{\left[\dot{m} Cp\left(T_{fo} - T_{fi}\right)\right]}{I_T WL} \tag{5.2}$$

where Q_u is the useful energy absorbed by a working fluid (W), $\dot{m}$ is the rate of mass flow of heat exchange fluid (kg s^{-1}), T_{fo} is an exit temperature of heat transfer fluid (°C), T_{fi} is the temperature of fluid at the inlet/entry (°C), I_T is an incident solar radiation (W/m^2), W specifies the width of the cylindrical parabolic collector and L is the collector length or the absorber tube length (m).

An absorber tube is treated with a spectrum-selective material having a higher absorptivity value. It is enclosed in an evacuated-glass tube to reduce the convective losses. Vacuum plays a leading role in preventing energy loss by convection. A slight loss of vacuum may lose heat four times more [3]. A schematic of the receiver absorber tube is presented in Figure 5.5.

This type of the solar collector needs one axis tracking mechanism to direct the solar concentrator and tube receiver toward the sun position. Generally, a parabolic trough collector is set lengthwise along the South-North path in order to follow the sun while its movement from east to west, to yield the maximum output and system efficiency [4].

The governing equation of a parabolic trough collector is stated as, $x^2 = 4fy$, where x and y are the ordinates of a parabolic collector profile. The heat transfer fluids used in solar appliances are synthetic molten salt, thermal oil, synthetic oil and water. Nickel–cadmium layers are generally preferred as selective-spectrum coating to accomplish a higher shorter wavelength solar energy absorption and a smaller longer wave infrared radiation. Such selective coatings help reducing energy losses from an absorber tube thereby increasing the collection efficiency [4].

The synthetic thermal-oil brands used in thermal power units are Therminol-VP-1, Dowtherm A, and Therminol D-12. A maximum operating temperature of thermodynamic cyclic processes is restricted to 400 °C with the use of synthetic thermal-oil. An efficiency achieved is about 38%. The hydrogen gas is generated in synthetic oil, in case if it operates above 400 °C. It may reduce the working life of synthetic oil as a heat transfer fluid. It also builds sludge or other byproducts in an

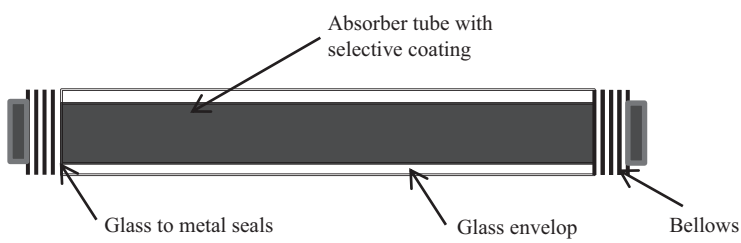

Figure 5.5 The absorber tube [3]

absorber tube which not only reduces the system's heat carrying or transfer capability and thermal efficiency but also increases the maintenance cost [4].

In a solar–thermal power unit operating on the Rankine cycle, water being used as a heat exchange fluid in an absorber tube is directly evaporated in a receiver tube. The technology is called as the directly steam/vapor generation (DSG) technology [4].

The molten salt being used as an energy transfer fluid is a combination of nitrates, e.g., sodium potassium nitrate (0.6 of $NaNO_3$ + 0.4 of KNO_3 by weight). Heat carrying/transfer characteristics of molten salt generally depend on its configuration. These salts exhibit better thermophysical characteristics at higher temperatures, e.g., large specific heat capacity, higher density, low vapor pressure, and higher thermal stability. The molten salts have higher melting points that cause a huge amount of operation and maintenance costs for providing freeze protection. The freezing of heat transfer fluids may cause damage of valves, ball joints and pumps. The synthetic oils used in solar-based plants freeze approximately at 15 °C and molten salts freeze in a temperature range of 100–230 °C. The pressurized gases may also be used as heat exchange fluids, e.g., air, CO_2, H_2, and He. An advantage of using gases is gases may operate in a wider range of temperature, abundantly available at affordable prices and have environment-friendly qualities [4]. It is also reported that the cylindrical parabolic collector-based power units with thermal storage capability may attain a year-round capacity factor of about 70% [1].

5.2.1.2 Linear Fresnel collector

In this collector, Fresnel plane mirror strips are used which reflect the rays and focus all at an elevated single straight line. It comprises an arrangement of aligned mirror stripes that behave as Fresnel reflecting lens concentrating incident solar radiation into the elevated linear receiver absorber tubes. The Fresnel reflector field may be considered as broken up parabolic trough reflectors. A schematic is presented in Figure 5.6 [3].

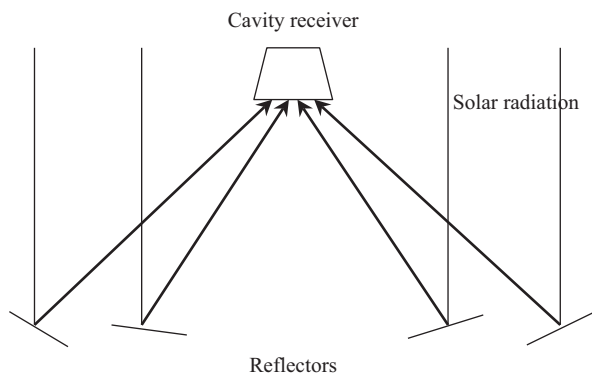

Figure 5.6 A linear Fresnel reflector [5]

All mirror strips are connected to a mechanism at the bottom of the system, which rotates them all about in independent parallel axes, in order to continuously track the sun. The photographs are shown in Figures 5.7 and 5.8.

The capacity of the linear Fresnel collector plant varies from 10 to 200 MW with a yearly solar-thermal-electric conversion efficiency fluctuating in between 8% and 10%. A Fresnel-lens-based power plant in Austria, working on a simple Rankine system, with water acting as a working fluid, is heated above 285 °C at around 70 bar [3].

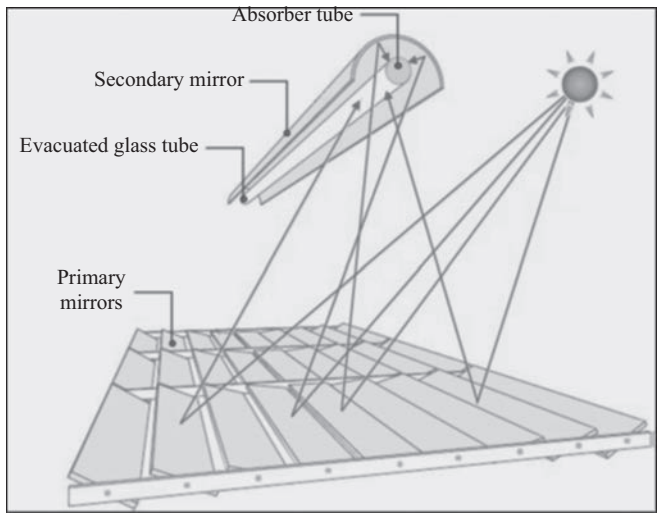

Figure 5.7 Photograph of the linear Fresnel lens [6]

Figure 5.8 The photograph of the linear Fresnel collector [2]

The problem associated with a linear Fresnel collector system is having lesser efficiency due to limited concentration (25–100). Since the concentration in the case of the linear Fresnel reflector system is lesser in comparison to the central tower and dish collector systems, the incident radiation is captured with lesser efficiency. The losses in the case of linear Fresnel reflector systems are also more compared to the central receiver systems. The losses associated with cleanliness and reflectivity of mirror, cosine effect, absorptivity of absorber tube, and transmissivity of a transparent covering of the absorber tube increase the energy cost of the linear Fresnel collector/reflector system. The linear Fresnel collector-based power units with molten salts as a heat exchange fluid may attain an operating temperature even up to 550 °C [2].

A configuration of the collectors might not have a considerable effect on the annual energy shading. It impacts on annual energy losses on account of shading as well as due to blocking. These losses may be controlled by incorporating proper spaces between the reflector rows and the collector arrangement. The densely packed mirror reflectors would not create an energy loss due to blocking and shading. The collection of heat may be improved by reducing the cost of power generation through a compact reflector configuration [1].

As compared to the cylindrical parabolic trough type collector system, a configuration of the linear Fresnel mirror reflector system is more flexible and does not need a huge capital investment that is associated with the former one. A linear Fresnel system is capable of generating steam directly in an absorber tube itself. It may also eliminate the use of thermally conductive oil as well as the heat exchanger. The technology of using the cylindrical parabolic collector and the linear Fresnel mirror type reflector/collectors in a power unit is precisely similar, especially in the case of the usage of heat transfer fluids. Conventionally, the synthetic oils have been preferred as heat exchange fluids in cylindrical parabolic-trough reflector systems which degrade chemically at higher temperature ranges, whereas the Fresnel mirror reflector systems are being used as a direct steam generation facility. The compact linear Fresnel reflector systems require a lesser ground area as compared to the cylindrical parabolic-trough type and the central receiver collector systems for the same power generation [1].

5.2.1.3 Central receiver collector or solar tower

In this type of the solar collection system, lot of reflective mirrors called as heliostats, tracking the sun in two axes, are used in order to concentrate/focus all incoming radiation into a centrally elevated tower receiver. This concept yields higher operating temperatures at the receiver for heating heat transfer fluids. The heliostats share a major single capital in the solar tower power plant. This plant is able to produce power in the range of 10–200 MW at yearly solar-electric efficiency of about 20%–30% [1].

The heliostats/mirrors are arranged in circular arcs around a central tower receiver, to capture and concentrate the solar beam irradiation at the receiver aperture. A two-axis tracking system continuously focuses the beam radiation at the receiver opening. The clean heliostats/mirrors may have an average reflectivity value of about 0.903 [7].

A schematic of the central tower collector is presented in Figure 5.9.

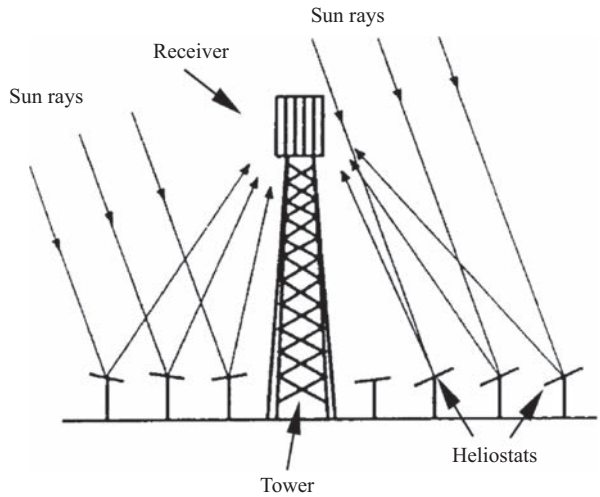

Figure 5.9 Schematic of the central receiver collector

The maximum operating temperature of the cycle is dependent on the type of heat transfer fluids being used. In the case of the Rankine-cycle-based central tower receiver-type power unit, water (steam) is preferred as a heat exchange fluid, whereas in the case of the Brayton-cycle-based unit, thermally conductive oils and molten-nitrate salts are generally used as heat transfer or working fluids. An operating temperature in the case of the solar tower-based Rankine cycle unit varies from 250–300 °C and 390 °C in the case of synthetic oil which shoots up about 565 °C for molten salt. This temperature reaches above 800 °C in the solar tower energized Brayton-cycle-based power plant. A provision of energy storage is possible with molten salts as heat transfer fluids. The molten salts or synthetic oils used in the primary circuit of the power cycle transfers energy to the secondary fluid, i.e. water in the heat exchanger, where superheated steam is generated to produce power in the turbine [1].

An average solar heat flux incident onto the receiver aperture of about 200–1,000 kW/m^2 may facilitate very high operating temperatures of about 1,500 °C. The researchers have proposed heat exchange media, e.g., water–steam, liquid Sodium, air and molten salts, for larger capacity plants of 100–200 MW [3].

The concentration ratio C in the case of the central solar tower type receiver system can be stated as a ratio of total area of the reflecting mirrors or heliostats to the aperture area of a receiver is given below. A concentration in the range of 300–1,000 can be achieved in the solar tower system [3]:

$$\text{Concentration Ratio}, C = \frac{\text{Total Area of Heliostats (m)}^2}{\text{Area of Receiver (m)}^2} \tag{5.3}$$

A receiver, in this system operating at higher temperature ranges, is complicated to design. A factor dominating the design of receiver is an ability of the

receiver to receive large and variable incident heat energy resulting from the concentration of the solar irradiation by heliostats. The values of energy fluxes varying from 100 to 1,000 kW/m^2 may cause higher thermal gradients and huge temperature stresses. Attention need to be focused while designing a receiver toward receiver shape, selection of heat transfer fluids, arrangement of absorber tubes, construction of tubes, and the material of construction. A receiver needs to be designed carefully taking into consideration the shape, wall temperature, wind-velocity, and wind direction, as it influences the combined convection as well as radiation losses [7].

The thermal stresses developed should not increase above 50% of the ultimate strength of the material of receiver in order to prevent failure due to temperature fatigue. An equation suggested by the researchers for the evaluation of the thermally developing stresses in a receiver tubing is given by [2]:

$$\sigma_{th,\max} = \frac{\Delta T_r \alpha E}{2(1-\zeta) In\left(\frac{d_o}{d_i}\right)} \left[1 - \frac{2d_i^2}{d_o^2 - d_i^2}\right] In\left(\frac{d_o}{d_i}\right) \sim \frac{E_\alpha}{2(1-\zeta)} q_{t\ jth} \tag{5.4}$$

where ζ is the Poisson coefficient (dimensionless), ΔT is the temperature difference (°C), α is the coefficient of thermal expansion (1/°C), E is the modulus of elasticity (N/m^2), d is the diameter of tubes (m) (i—inner, o—outer), k_t is the conduction through tube and q is the heat (W).

5.2.1.4 Parabolic dish collector

As discussed in Section 5.2.1, a parabolic dish type collector is a point concentrating type of radiation reflecting system, which tracks the radiation source (sun) biaxially. The concentrated energy is absorbed by a receiver situated at the focus location of the dish collector. The heat transfer fluid (water or air) is circulated in order to carry the energy absorbed so as to attain the maximum possible operating temperature. The photographs of dish collectors are shown in Figure 5.10 [1].

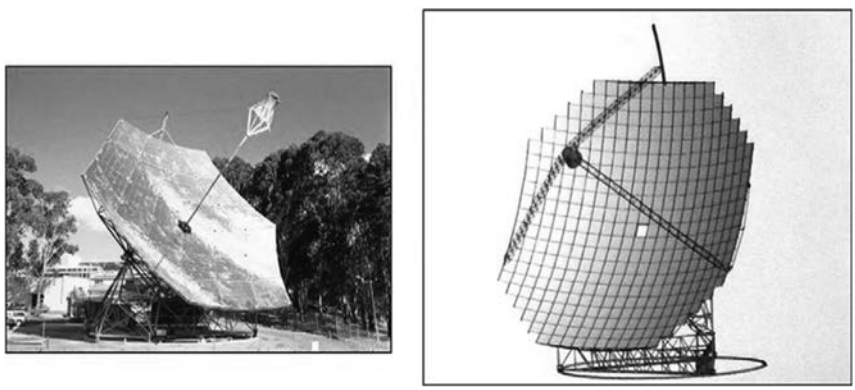

Figure 5.10 Photographs of the dish collector [2]

The parabolic profile of a collector depicted in Figure 5.11 is represented by [8]:

$$x^2 = 4yf \tag{5.5}$$

where x and y are the distances along the x and y axes, respectively; f is the focal distance from the vertex of parabolic contour. It also decides the position of a receiver for energy collection.

A focal length can also be obtained with the help of the width of the collector aperture, W, and the collector rim angle, φ, by using:

$$f = \frac{W_a}{4\tan(\varphi_r/2)} \tag{5.6}$$

The rim angle, φ_r, can be obtained by using

$$\varphi_r = \tan^{-1}\left[\frac{8(f/W_a)}{16(f/W_a)^2 - 1}\right] = \sin^{-1}\left(\frac{W_a}{2r}\right) \tag{5.7}$$

where r_r is the rim radius.

A local mirror radius, r_r, can be obtained by using

$$r_r = \frac{2f}{(1 + \cos\ \varphi_r)} \tag{5.8}$$

Equation (7) is also helpful in obtaining the radius of a collector at any location by using the rim angle at the same location. The diameter of a receiver required for capturing energy concentrated or focused by using a dish collector of width, W, and rim angle, φ_r is given by

$$D = 2\ r\sin(0.267) = \frac{W\sin(0.267)}{\sin(\varphi_r)} \tag{5.9}$$

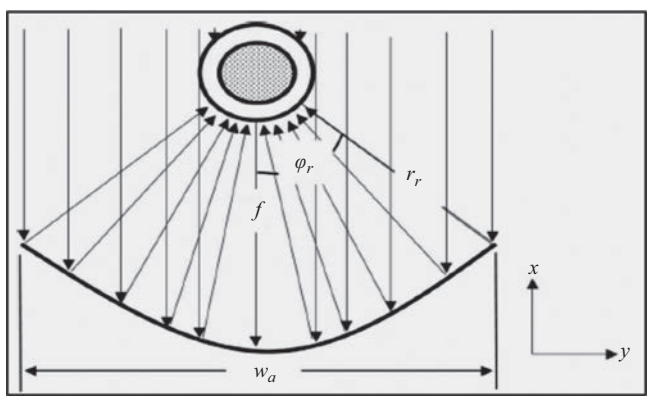

Figure 5.11 Schematic of the parabolic profile [8]

where 0.267 represents the half angle of a cone formed by incident beam radiations. These equations may be used for design and construction of a parabolic dish collector system [8].

A parabolic dish collector is used in higher temperature applications, e.g., solar to thermal vapor/steam production and solar to thermal electricity generation purposes. The operating temperature ranges from 400 °C to 750 °C, with a concentration ratio of about 3,000 and at a thermal efficiency of about 23% [3].

In addition to this, the height of a dish can be obtained by using [9]:

$$h = \frac{D_{Collector}^2}{16f} \tag{5.10}$$

The focal distance in the case of a dish collector is given by

$$\frac{f}{D_{collector}} = \frac{1}{4\tan(\varphi_r/2)} \tag{5.11}$$

A schematic showing the parabolic segments of the same focus location, but with different focal distances and dish collector diameters as well as different rim angles, i.e., various values of $f/D_{collector}$ are portrayed in Figure 5.12. In actual practices, receiver aperture is positioned at the focal point of the dish collector so as to trap the maximum incoming concentrated solar radiation.

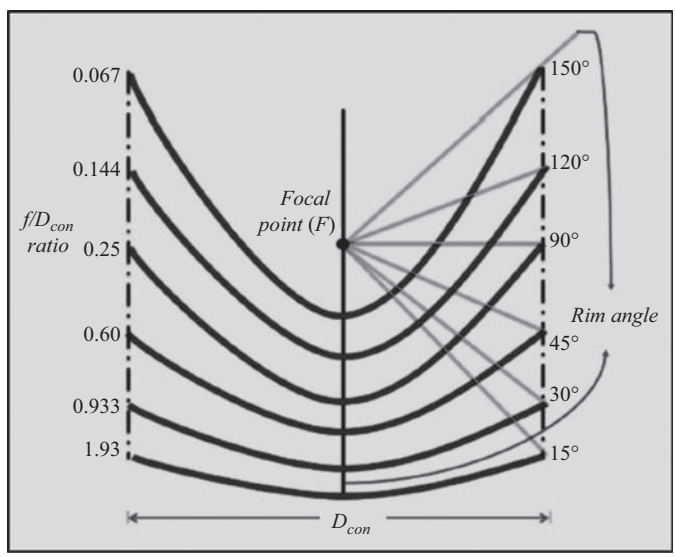

Figure 5.12 Parabolic segments with different ratios of the focal distance to the collector diameter [9]

The diameter of the focus point can be obtained using the following equation, where θ is an acceptance angle:

$$D_r = \frac{f \times \theta}{\cos\varphi_r(1 + \cos\varphi_r)} \tag{5.12}$$

The energized working fluid is utilized to drive the engine along with the generator unit to convert heat energy into mechanical energy and then to electricity. Generally, the parabolic dish-based plants have capabilities in the range of 0.01–0.4 MW. An optical efficiency of the parabolic dish reflector system is considerably higher as compared to the trough and solar tower type of concentrating systems. It is attributed to the fact that dish mirrors are continuously pointed toward the sun, while the trough collector and solar tower systems lag behind due to cosine losses. In addition to this, the dish collectors facilitate use in remote applications or in the case of smaller homes [1].

A dish collector system is reported to be a promising technology for a small-scale or distributed type electricity generation and would be a better replacement option to the diesel generator sets that may mitigate the demand load on centralized power generation units.

These systems are generally preferred to produce electricity with the help of the Stirling engine or steam turbine as a prime mover. The dish Stirling engines have demonstrated an efficiency of about 30% along with the advanced Stirling converter. The advanced Stirling converter was reported as a type of a linear alternator that produces electricity directly from reciprocating (to and fro) movement. It eliminates the mechanical transmission losses in a free piston Stirling engine. It is also reported in the literature that the free piston Stirling engine (FPSE) powered by solar dish in combination with the bio-fuel may intensely substitute the diesel generator sets. It is capable enough to generate electricity independently with no assistance of grid power supply [3].

In Stirling engines, hydrogen or helium is a commonly used working fluid. The power conversion unit of Stirling engines works on the hot air growth principle. Usually, thin glasses are used as a reflecting surface, which has solar weighted reflectance between 0.93 and 0.96. Nowadays, for maintaining the reflector surface over the collector, polymeric reflectors are used which are light in weight, flexible to fit into a curve and low cost [1].

5.2.2 Concentrating solar power (CSP) technology comparison

1. The trough collector and linear Fresnel reflector systems are used for low as well as medium temperature applications (less than 400 °C), whereas point concentrating collectors are used for higher temperature applications. In the case of direct type steam generation systems, the maximum outlet temperature of the heat exchange fluid varies from 300 °C to 680 °C [1].
2. The central receiver systems, cylindrical parabolic and Fresnel mirror type collector systems are reported to be appropriate for power production abilities in a range of 10–200 MW. A dish collector-based power plant is suitable for power

production between 0.01 and 0.4 MW. The concentration ratio value in the case of the linear Fresnel and parabolic trough collector system is under 100 (25–100). In the case of the central tower case, it is 300–1,000, and with parabolic dish collector systems, it is 1,000–3,000. In addition to this, the parabolic dish collector system exhibits an annual solar to electric conversion efficiency value of 25%–30% as compared to 15% with parabolic trough, 10% with linear Fresnel and 20%–35% with central receiver tower concepts. The requirement of ground space for the central receiver type and dish collector type is more than that in the case of cylindrical parabolic and Fresnel mirror power production systems [3].

The power production capacity of the concentrating power systems as reported by Khan *et al.* [10] is as follows: parabolic trough collector (10–300 MW), linear Fresnel reflectors and solar towers (10–200 MW) and parabolic dish collector (0.01–0.025 MW) or (10–25 kW).

5.2.3 *Advantages of CSP technologies*

The key features [10] of the solar power plants using CSP tools are as follows.

1. The efficiency of the concentration solar power technology is good due to the generation of high temperature in an operating thermodynamic cycle.
2. These collectors capture energy mostly from the incoming beam radiation. It does not involve part of diffused and reflected radiation.
3. It can operate on higher direct normal irradiation levels available.
4. It may not be appropriate for small-scale solar power generation units due to higher capital costs.

5.2.4 *Classification of concentrating solar power receiver systems*

The receivers may be classified as follows:

1. According to the *positioning* of the receiver, they are fixed receivers and movable receivers. The fixed receivers are stationary ones that do not move along the sun's position. These are used along with Fresnel mirror collectors and the central tower type receiver systems.

   The movable-receivers travel along with sun's position. They move together with the reflecting or focusing systems in order to trap the maximum possible energy. These are parabolic trough and parabolic dish types [3].
2. According to the *design* of a receiver, they are classified as the external type and the cavity type. The external type receivers are generally of cylindrical shape. The outer cylindrical surface, made up of absorber panels or a series of absorber tubes, receives an incident concentrated radiation to heat a working fluid. It has a wider range of acceptance angle. In the case of cavity receivers, the concentrated solar irradiation enters inside the receiver cavity through its opening. It may have one or more apertures to receive the concentrated energy. The acceptance angle in the case of the cavity receiver is quite lesser.

The cavity receivers are designed in such a way that it maximizes the energy absorption and minimizes losses by convection and radiation to the outer ambience. The cavity type receivers exhibit higher receiver collection efficiency as compared to external type receivers owing to more losses in the case of the latter one [7].

3. According to the *working medium* used, the receivers are classified as gas type receivers, liquid type receivers, and solid particle type receivers. The gas receivers involve volumetric type air receivers, smaller particle type air receiver, and tubular type gas receivers. In the case of volumetric air or gas receivers, porous ceramic solid medium is utilized to extract the concentrated solar energy so as to transfer it to air/gas flowing through its pores. In the case of Brayton cycle-based solar-thermal power units, these receivers are preferred. An unstable flow and nonuniform heating are the major drawbacks of these receivers. A small particle receiver uses sub-micron size particles suspended in air for absorbing solar radiation. A maximum efficiency of up to 90% at 700 °C operating temperature can be achieved using this receiver. In the case of tubular type solar receivers, a pressurized working fluid flows through the tube bank, which collects the energy transferred from the absorptive coating material provided over the tube surface.

   There are two basic kinds of the liquid receivers: (i) tubular liquid-receivers and (ii) falling-film receivers. The third type, solid particle receivers, can create temperature above 1,000 °C in the receiver. Inside the receiver chamber, free-floating ceramic particles are used to absorb directly the concentrated/focused solar energy and to transfer it to the air which fluidizes the particles.

   The selectively absorbing spectral surfaces may increase the receiver collection efficiency. The advanced selective absorber materials used to capture the maximum possible energy are tungsten, copper sulfide, zirconium diboride, cermets as intrinsic materials. Semi-conductor materials such as silicon, germanium, and lead sulfide are also used. The materials such as silicon dioxide, magnesium fluoride, titanium dioxide, aluminum oxide, and silicon nitride also exhibit absorptance values of up to 0.97. The metals having high melting point, viz. gold (Au), copper (Cu), nickel (Ni), chromium (Cr), molybdenum (Mo), tungsten (W), and cobalt (Co), also exhibit good absorption characteristics along with oxides such as silica, alumina, and magnesia. The recently developed materials, e.g. $Cr–Cr_2O_3$ and $Ni–Al_2O_3$, portray spectrally averaged absorptance of about 0.94 with a spectrally averaged emittance of 0.07 [11]. The spectral, hemispherical reflectance curves for selective surfaces, e.g. black nickel, black chrome, 301 stainless steel, and white epoxy paint on aluminum, are shown in Figure 5.13 [12]. The hemispherical reflectance values are higher for the radiation wavelength range of 0.5–3 μm.

   The spectral emittance for selected materials, e.g., carbon, copper, aluminum, gold, tungsten, nickel, aluminum oxide white enamel, and magnesium oxide, are shown in Figure 5.14 and for aluminum with different surface finishes are depicted in Figure 5.15 [12].

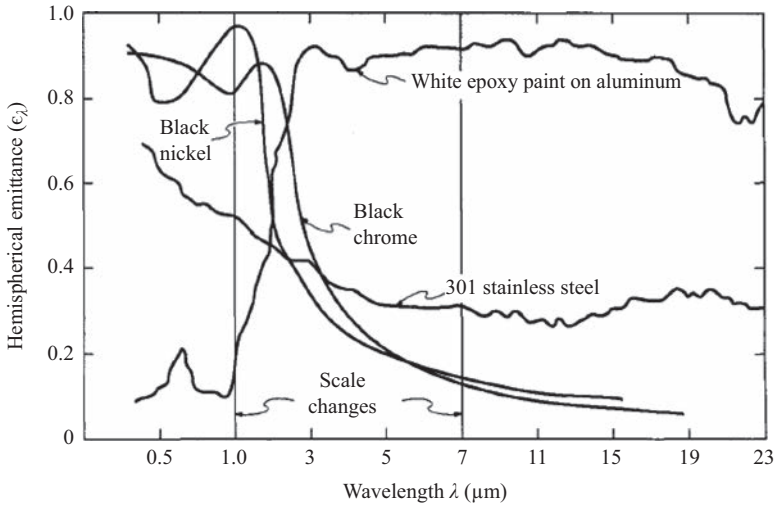

Figure 5.13 Spectral, hemispherical reflectance for several selective surfaces [12]

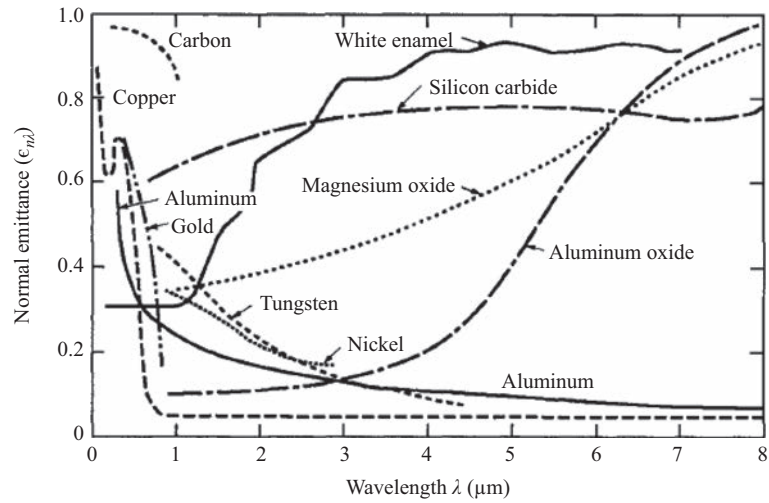

Figure 5.14 Spectral emittances for various materials [12]

The hemispherical reflectance spectrum for copper-coated material with various roughness and coating thickness values is depicted in Figure 5.16. It is seen that the samples with similar roughness values exhibit a very similar spectrum, whereas the influence of coating thickness is very poor on the reflectance value [13].

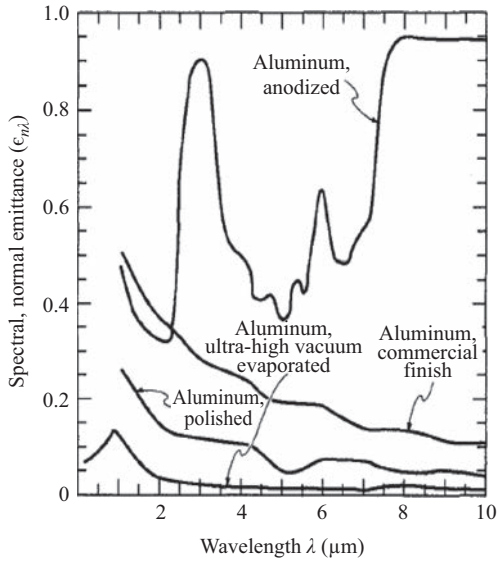

Figure 5.15 Spectral emittance for aluminum with different surface finishes [12]

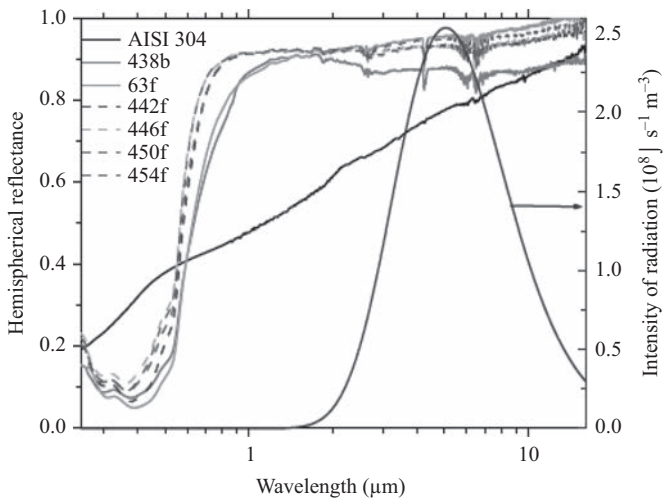

Figure 5.16 Hemispherical reflectance spectrum of copper-coated samples and AISI 304 [13]

4. Other types comprise heat pipe type and Bio-dish type hybrid receiver. A receiver is an important part of the solar thermal Stirling engine-based power system. It comprises an absorber with an aperture, which is positioned at the focus point of the parabolic dish type collector system. These days, heat pipe receivers are mostly used in the solar-Stirling engine technology [14].

It uses sodium (Na) and potassium (K) mixture as heat carrying and transfer fluids inside the receiver to transfer heat to the engine heater head. Another type is the bio-dish type hybrid receiver, which is made up of ceramic material, meant for receiving concentrated power from one side and burns a biomass on another side of a receiver. An absorbing surface of a receiver is the ceramic hemisphere with a provision for the internal inbuilt channels. The concentrated solar energy is getting absorbed on the internal surface of the hemisphere. On another side, a biogas combustor is located which is surrounded by a cylindrical-shaped air-preheater and ceramic made cylindrical shell for transferring the combustion gases. This is how hybrid operation executes in a bio-dish hybrid receiver. The losses from the cavity receivers reported to be about 20% of the total power input into the system [15]. The performance of the collector is given by (5.13) as follows, which is dependent on the ability of the working fluid to extract energy from the involved absorber metallic surfaces as well as the losses from the absorber surface. So, the incident concentrated solar energy is equal to the energy gained by the working fluid and the losses emitted by the hot cavity (absorber) surface:

$$\eta_{th} = \frac{Q_u}{(I_R \times A_C)} = \frac{(I_R \cdot A_C - Q_{losses})}{(I_R \times A_C)} = 1 - \frac{Q_{losses}}{(I_R \times A_C)} \tag{5.13}$$

where

I_R Solar incident radiation (W/m^2)
Ac Aperture area of the collector (m^2)
Q_u Useful heat gain of the coolant $= \dot{m}C_p(\Delta T)$
Q_l Heat losses due to conduction, convection, reflection, and emission

The concentrated energy incident into the cavity receiver is utilized to increase the internal energy of the working fluid in the form of temperature rise, crossing the resistances involved in the path of heat flow. The temperature rise of working fluid depends on the temperature rise of the absorber surface or selective coating. Further, when the temperature of the selective coating is higher, the emission losses to the environment are also higher that degrades the performance of the collector, as given by (5.13). As reported [15], the emission losses are more at higher temperature levels.

The thermal resistance diagram of the solar thermal collector with the central receiver system is shown in Figure 5.17. The solar energy incident onto the concentrating collector or heliostats liberate in the form of losses due to the resistances involved in the path of heat flow, e.g., optical resistance of reflective collector/heliostat, receiver/absorber surface resistance, reradiative, convective/conductive resistances, conductive resistances through the metallic wall, conduction, and convective resistances of insulating material.

Various concentrating type solar collectors used for power generation are discussed in subsequent sections.

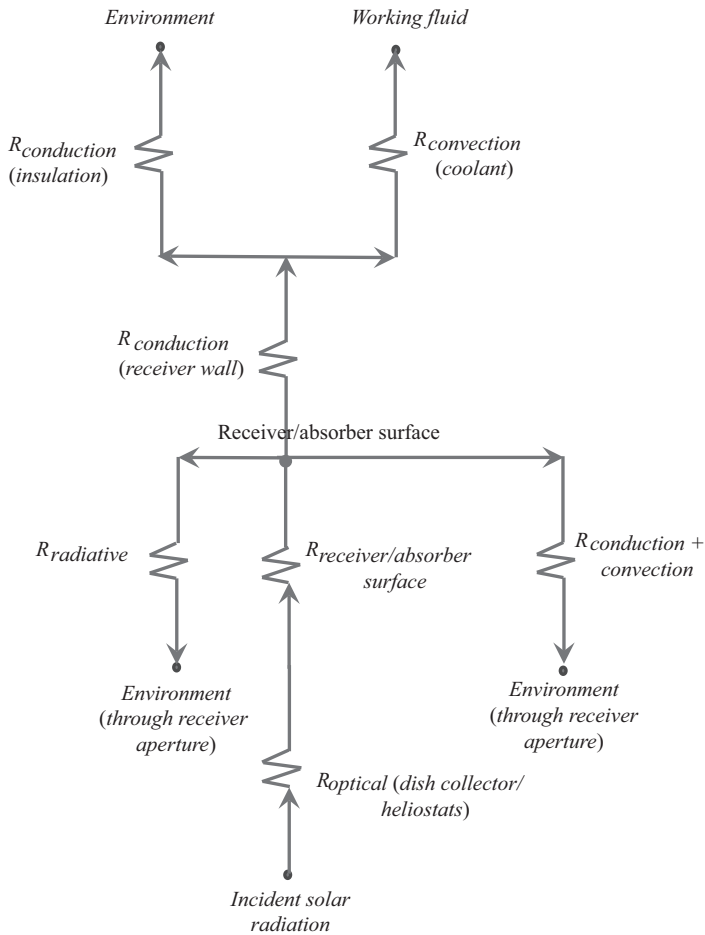

Figure 5.17 Thermal resistance diagram of the solar thermal collector

5.3 Thermal energy storage

A concentrating type solar power unit may be generally worked with and without energy storage. A small storage is required in a solar-based power plant in the form of a warm power block for quicker startup and efficient functioning of the plant. During the startup of the plant from the cold condition, a larger amount of energy is needed as compared to warm startup of the plant, which is possible with small energy storage facility. The provision of energy storage in the plant reduces the interruptions of power supply which generally occurs due to irregular sunshine hours during the day. For energy storage, a power unit needs to keep separate tanks for thermal energy storages [2]. The thermal heat/energy storing systems are essential for storing heat during sunny hours and releasing it during the poor sunny hours or no sunshine hours [16].

Generally, the solar irradiation captured by the solar field is absorbed by the heat transfer fluid. The solar field may consist of so many collectors either

parabolic dish collectors, linear Fresnel collectors, or heliostats spread over a larger ground area. During extensive sunshine hours, energy in addition to the energy required for power generation is stored in the thermal heat/energy storing system, as depicted in Figure 5.18. This additional energy to be stored in the energy storage system is released during the wee hours of solar irradiation or night hours so as to meet up the power demand [17].

The efficiency encountered in delivering energy from solar collector to receiver generally ranges from 50% to 60% as well as the receiver thermal collection efficiency ranges from 80% to 90% [17].

Though the solar energy is free of cost, the present solar collection systems are costly and price per unit electricity production from solar input is higher. Thus, solar energy captured and collected from the solar collector field must be preserved by adopting better thermal energy storage systems and through executing efficient solar-thermal-electricity cycles. This is important pertaining to the economics of concentrating solar power plant deployment.

5.3.1 Types of energy storage

There are basically three types of energy storages, e.g., (i) sensible energy storage, (ii) latent energy storage, and (iii) thermochemical type storage system.

5.3.1.1 Sensible energy storage

The storage of energy using materials such as air, water oil, rock-beds, concrete/sand, and bricks is known as sensible energy storage. An extent of heat energy accumulated in the storage material is dependent on temperature growth, mass of

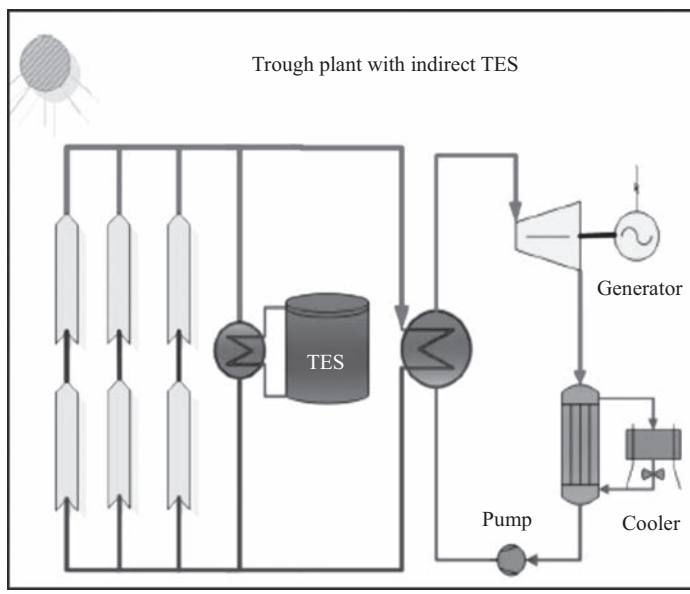

Figure 5.18 Schematic of the indirect solar power unit along with energy storage system [17]

material, and also specific heat of an energy storing medium. In general, the selection of a medium depends upon the specific heat of medium, variations of temperature in an operating cycle and availability of space. In concentrating solar power unit operation, a sensible energy storage technique is widely adopted owing to its reliability, cost-effective, and easy to use/handle, and huge experimental information is available in the literature [16].

Most of the solid form materials have varied the operating temperature range of 200–1,200 °C and a higher value of thermal conductivity, e.g., about 40 W/m K. The materials, which are of low cost, can sustain higher working temperatures, yield better performance and are environment friendly, suggested by the researchers are concrete/polypropylene fibers, graphite, pebble stone, asbestos contained waste, and sand rocks [16]. It may not be true for all low cost materials.

In the case of sensible heat storage systems, generally pebble (solid) packed bed is preferred. For a packed bed energy storage system, the sensible heat stored can be calculated using [18]:

$$E = \beta(1-\varepsilon)\rho_s V\left[(C_s T)_h - C_s T\right)_c] \tag{5.14}$$

where

ρ_s Density of solid
C_s Specific heat of solid
ε Void fraction (fraction of space not being occupied by solid particles)
T Temperature (h—hot, c—cold)
V Volume
β Thermal factor

5.3.1.2 Latent heat storage

The method of storing and releasing thermal energy by the phase change materials at constant temperature is known as a thermal energy storage technique. It does not involve any chemical reaction during energy storage and release and comprises latent energy of fusion for a conversion from solid–liquid and latent energy/vaporization heat for conversion from liquid to vapor transition [16].

The advantages of using phase changing materials for latent energy storage are (i) its charging and discharging property in a narrow range of temperature quite closer to its phase change temperature, (ii) larger energy densities due to their higher latent heat of phase change as compared to sensible energy storage materials. Since volume as well as pressures is almost constant, the change of phase might be either solid to liquid or solid to solid [16].

Along with advantages, the phase change materials have some limitations also. It has a lower value of thermal conductivity (0.2–0.8 W/mK) that slows down the charging as well as discharging process. The incorporation of an additive, e.g., graphite, metallic matrix/foam, fins, dispersions of conductive particles (nanoparticles), microencapsulation of phase changing materials, and modification in the energy-storage system design (embedding of finned heat pipes), may improve its thermal conductivity of thermal energy storage system [16].

The metal alloys, e.g., magnesium, zinc, and aluminum, may also exhibit higher thermal conductivity (twice of molten salts) and also show good thermochemical stability, but these are quite costly. The inorganic and organic energy storage materials have higher melting point temperatures say between 100 °C and 900 °C [16].

In the case of cylindrical parabolic trough collector, Fresnel mirror collector, and parabolic-dish collector-based power systems, the phase change materials having the lowest phase change temperatures (100–300 °C) can be used. In the case of solar power tower (central tower system) and parabolic dish collectors system, the phase changing materials with phase change temperatures greater than 400 °C (where temperature shoots up to 600 °C or 1,500 °C in central tower type and parabolic-dish collector system, respectively) are generally used [16].

5.3.1.3 Thermochemical energy storage

The thermochemical energy storing systems depend on reversible chemical reactions that cause combination or decomposition of reactants. The solar energy is used here to initiate a chemical reaction that is endothermic. A higher energy density and longer storage durations are the advantages of thermochemical energy storage system over latent energy storage systems.

For medium and higher operating temperatures, i.e., 300–1,000 °C, the thermochemical energy storage materials suggested are metallic hydrides, hydroxides, carbonates, redox, and ammonia systems [16].

5.3.1.4 Advantages of thermal energy storage in the case of CSP generation

The incorporation of thermal energy storage system may help attaining higher operating temperatures (greater than 800 °C) and yielding improved solar thermal efficiency in an economic manner [17].

1. It helps in providing electricity on demand to the connected electric power grid. It allows solar concentrating power plants to generate electricity even during the weak sunshine hour, when demand is at its peak thereby makes power plant extra cost effective.
2. It mitigates the solar irradiation variation and also confirms the non-stopping power generation. It helps increase in power generation time on demand.
3. The power generation based on concentrating solar systems with provision of thermal energy storage system is lesser susceptible to changing weather situations due to its inbuilt thermal inertia.

5.4 Solar-powered heat engines

5.4.1 Stirling engine

The most efficient way to produce solar thermal-powered electricity is parabolic dish-Stirling technology. The parameters playing an important role in examining the performance of a dish-Stirling engine system are average working pressure, dead volume, type of working fluid, effectiveness of regenerator, cold end temperature, hot end

temperature, receiver temperature, and concentration ratio. The maximum possible solar thermal efficiency portrayed for dish-Stirling system is about 32% with an absorber temperature of about 850 K at a concentration ratio of 1,300 approximately. The receiver thermal efficiency up to 84% may be achieved. Such a type of power systems first transforms thermal energy into mechanical energy with the help of concentrating reflector surfaces and Stirling engine. The mechanical power is converted into electricity using generators. The use of hybridization and energy storage facility would be a favorable option for facilitating prolonged uninterrupted power supply [19].

The Stirling engine is an externally combustion type heat engine. It allows working on heat energy obtained from various sources, e.g., burning of any combustible material, agricultural waste, methane obtained from biomass, and solar irradiation [20]. The Stirling systems are the devices that can operate on a wide variety of working fluids, e.g., air, hydrogen, helium, nitrogen, and steam. There are three major Stirling engine designs exist: alpha, beta, and gamma engines. Out of which gamma type shows a maximum theoretical mechanical efficiency value. This type of parabolic dish-powered Stirling engine consists of dish collector systems, receiver, Stirling engine, and electricity generator. A heat exchange fluid energized inside the solar-thermal receiver is used to drive the Stirling engine which later drives a generator. A line diagram of the dish-Stirling power system is depicted in Figure 5.19 [19].

The Stirling engine operates on the Stirling thermodynamic power cycle, comprising two isotherms (T = c) and two isochoric (V = c) processes. The thermodynamic P–V cycle on which Stirling engines operate is shown in Figure 5.20. The movement of working/heat transferring fluid between the cold and hot spaces of an engine causes

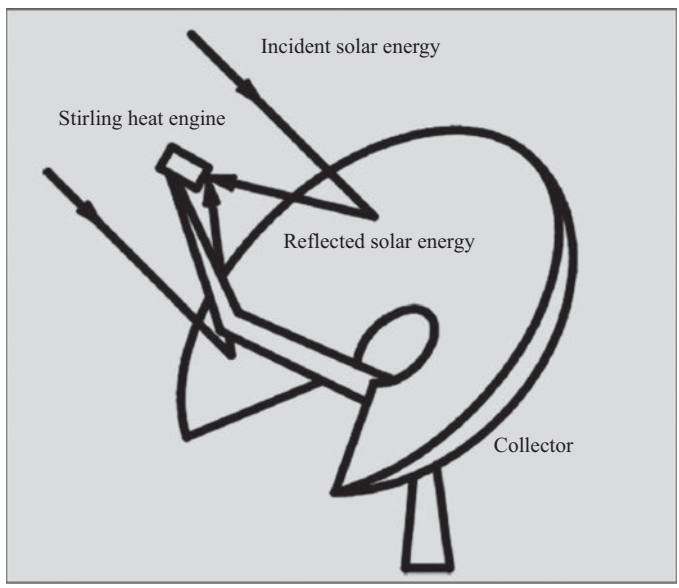

Figure 5.19 Line diagram of the dish collector-based Stirling engine system [19]

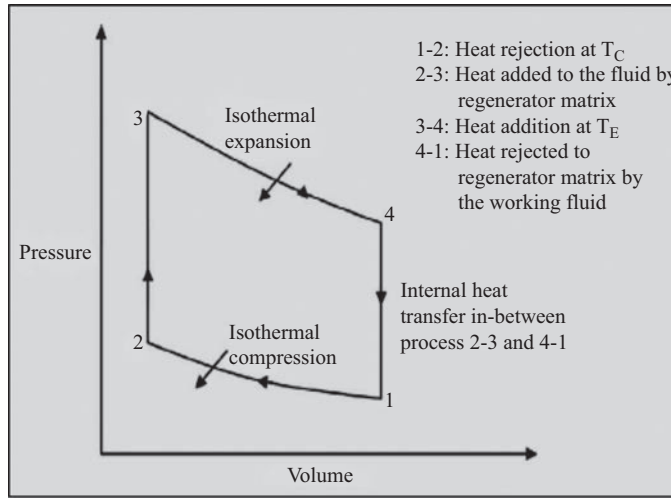

Figure 5.20 Thermodynamic Stirling P–V cycle [21]

constant volume process of the cycle to occur. The compression and expansion of working fluid causes the occurrence of compression and expansion processes at constant temperature, respectively [20].

The heat input to the cycle is met using the regenerative heat exchanger which absorbs energy from a heat transfer fluid (4-1 process) heated up in the receiver element. The heat is rejected to the operating fluid during process 2-3. The solar parabolic dish can be utilized to supply heat necessary to run the Stirling engine. The factors resulting the maximum efficiency of the Stirling engine are better regenerator efficiency, higher values of heat transfer coefficients, lesser work of compression, higher work of expansion, better sealing of working fluids preventing leakage from compression space to the crankcase. It requires working fluids having higher thermal diffusivity and lower viscosity values, e.g., hydrogen is generally preferred in the Stirling engine system among air, hydrogen, and helium fluids [21].

5.4.1.1 Working/operation

The cylindrical arrangement in which working fluid flows/moves is a closed type system. This eliminates a drawback of working fluid contamination and loss. The working fluid is energized with the help of incident solar-radiative flux. The heat carrying and releasing characteristics of working fluids are reported to be a very important aspect. Higher mass flow rates assist the heat exchange/transfer phenomenon. A requirement of higher mass flow of working fluid can be reduced using higher pressure and/or lesser viscosity. An operation involves four processes in the cycle, working of which is represented by Figure 5.21 [20].

1. **Isothermal compression process (1-2):** In this process, heat is being carried by an external cooling medium from the heat transfer fluid, at a lower temperature. A displacer stops at its top dead center after pushing working

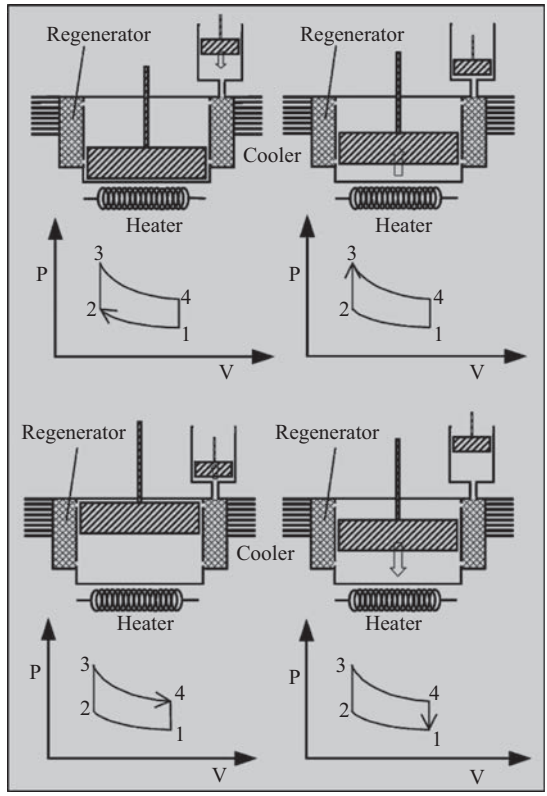

Figure 5.21 Working of Stirling engine [20]

medium in the cold region of a cylinder. It is state 1 with pressure P_1. The flywheel thrust pushes a power piston from bottom dead center to top dead center (BDC to TDC), assisted by a vacuum created during cooling of working medium. A working medium is under compression in the cold region of the power cylinder. This work of compression is indicated by process (1-2).

2. **Isochoric heat adding process (2-3):** In this process, heat is transferred to a working medium from the regenerator. A displacer moves from TDC to BDC and transfers working medium from the cold region to the hot region. During this heating process, power piston retains at its TDC. Heat (in storage) supplied by a regenerator increases the temperature as well as pressure of the working medium from 2-3 at constant volume.
3. **Constant temperature expansion process (3-4):** The heat is transferred to a working fluid by an external heat resource (e.g., concentrated solar energy). A displacer pushes the working medium into the hot region (while moving from TDC to BDC) along with the resultant rise in pressure to its maximum in an operating cycle. The displacer later rests at its BDC. This state is point 3. In a

hot region, the working medium expands to pressure P_4 maintaining the temperature constant. The power piston moves from TDC to BDC due to improved pressure and supplies mechanical energy to flywheel, which is being used throughout the continuing processes of a cycle. The area under 3-4 signifies the work performed by a working medium in the cycle.

4. **Isochoric cooling process (4-1):** Heat is being transferred by the working medium to the regenerator. During this process, the flywheel momentum as well as vacuum formed by the reduced pressure; a displacer moves from BDC to TDC. It transfers the working medium to a cold region, via regenerator, where pressure is low and little creation of vacuum in the space. This process is represented by 4-1, at constant volume. The working medium transfers energy to the regenerator.

5.4.1.2 Advantages of Stirling engine

A theoretical ideal Stirling cycle exhibits three advantages, dictated as follows.

1. It is reported that the presence of ideal regenerator makes thermal efficiency of the Stirling engine approach the Carnot cycle efficiency. It also reduces the quantity of input energy required from external sources for operating the cycle, which ultimately enhances the Stirling cycle efficiency [20].
2. The replacement of two isentropic processes of Carnot cycle by two isochoric processes increases the area of PV diagram. At higher cyclic peak pressures and larger swept volumes, substantial work is being developed by the Stirling engine. The increased quantum of work is denoted by marked areas as depicted in Figure 5.22. Processes 1-2-3-4 represent the Stirling cycle and 1-2C-3-4C represents the Carnot cycle [20].
3. As compared to almost all reciprocating piston engines operating at the same temperature levels, compression ratios, mass flow rates, and the same peak pressures, the ideally working Stirling engine depicts the maximum mechanical efficiency [20].

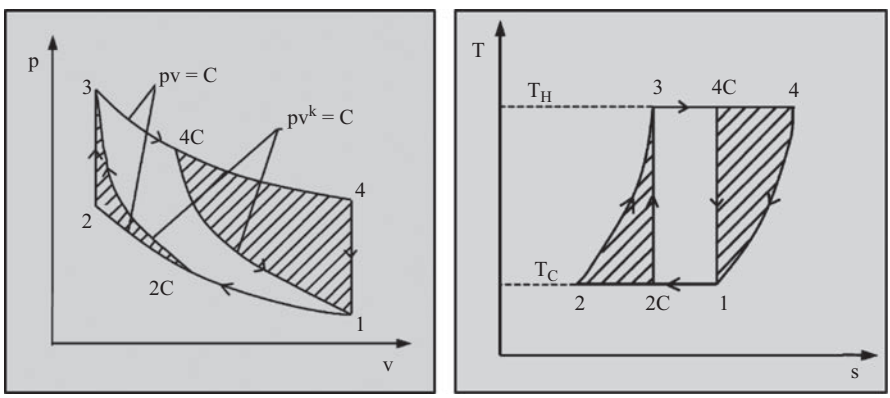

Figure 5.22 Schematic shows PV and TS diagram of the Stirling cycle [20]

5.4.1.3 Types of Stirling engine

The isothermal compression as well as isothermal expansion processes happens inside the power cylinder of an engine with the help of power piston. The role of the displacer is to move the working fluid backward and forward through the engine components, e.g., generator, heater, and cooler at constant volume [20]. The Stirling engine is classified as alpha, beta, and gamma configuration. All the three types of engines work on the same thermodynamic cycle despite having different component design and arrangement. The schematics of these types are shown in Figure 5.23 [20].

The displacer is absent in the alpha-type Stirling engine. The hot and cold pistons are situated on both sides of the heater-generator-cooler assembly. They travel consistently in a similar direction in order to deliver isochoric cooling or heating processes of the working fluid. One piston is fixed and another moves after transferring the whole working fluid into the cylinder to compress or expand it. The hot piston does the expansion task, while the cold piston does the compression work [20].

Both the piston and displacer have been included in the same power cylinder, in the case of a beta-type Stirling engine. The displacer is intended to move the working fluid from the hot end to the cold end via cooler, regenerator, and heater. The power piston situated at the cold end of the power cylinder does the job of compressing the working fluid when it is available at the cold end of the power cylinder. Similarly, it does a task of expanding a working fluid when it moves at the hot region of a power cylinder [20].

In the gamma type of Stirling engine, a displacer and piston moves in different cylinders which are in connection with each other. The working medium available between the hot and cold zones of a displacer cylinder is moved through the heater, a regenerator, and a cooler assembly by the displacer. The power piston does the job of both compressing as well as expanding the working medium. The gamma

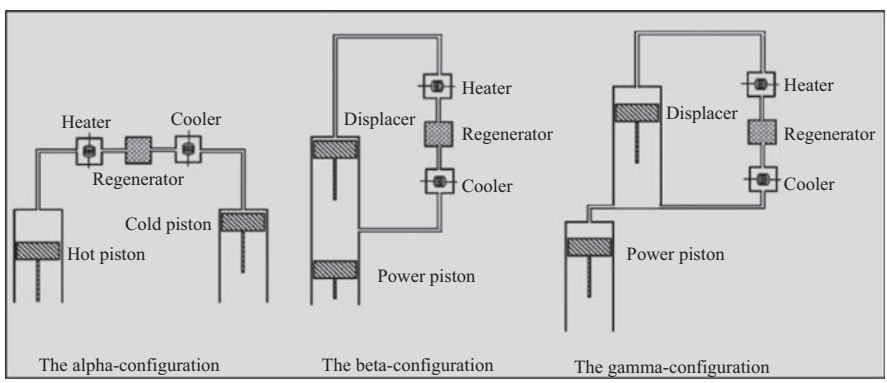

Figure 5.23 Configurations of Stirling engine [20]

type arrangement having double acting piston design exhibits a higher theoretical value of mechanical efficiency [20].

As reported in the literature [20], for an operating temperature range of 923–1,073 K and for speed ranging from 2,000 to 4,000 rpm, the Stirling engine exhibits an efficiency of about 30%–40%.

It is also reported [21] that the power generation capacity of worldwide installed dish-Stirling power plants varies from 1 to 25 kW, attaining a maximum efficiency of about 29.4%. The Stirling engine operating using helium as a working/heat transfer fluid is reported to yield high efficiency. It is also seen that the nonmetallic polymeric film reflectors are found appropriate for dish reflector materials that may give as high as 97% optical efficiency. The research prospects are there in an area of phase changing materials for their economics, identification, and compatibility [21].

The solar concentrator size generally varies from 3 to 15 m for power generation. The steps involved in designing the solar dish-driven Stirling Engine are as follows [22].

(i) Shape selection and type of dish, (ii) selection of dish reflecting material, (iii) estimation of diameter of dish, size, and focal distance, size of focal point, (iv) concentration ratio calculation, (v) type of absorber or receiver, material, and shape, and (vi) Stirling engine design along with the electric generator.

The Stirling engines have been reported to be inexpensive as compared to PV-based energy production units of 1,500 W electrical and of higher capacity. These engines can be employed for use in remote or hilly regions for meeting small requirement of power of individual home. In remote areas, it can be used for applications, e.g., illuminating lamps, fans, driving small machines and small capacity water pumps, charging of batteries, especially in remote areas [21].

The direct solar-driven Stirling engines are of utmost importance at locations where solar irradiation intensity is available in plenty. In order to use directly the solar energy captured, a concentrating reflector and an absorber are integrated with the Stirling engine. The Stirling engine-based solar power unit that can be used in various household applications is suitable at locations where quite lower temperature cooling sink is available, silent operation at a lower speed is mandatory or acceptable, continuous and constant power generation is required and a longer warming period is allowed [23].

5.4.2 Solar-Rankine cycle

In addition to the solar Stirling engine, the Rankine cycle is also a competitive power producing cycle for electricity generation from solar thermal energy. The major equipment of solar Rankine cycle power unit is (i) solar reflector or concentrator, (ii) thermal energy storage system, and (iii) Rankine cycle components (boiler, turbine, condenser, and pump). According to the type of working fluids, it can be a steam Rankine cycle or organic Rankine cycle. The line schematic of solar Rankine cycle is shown in Figure 5.24, which can be used for water pumping applications [23].

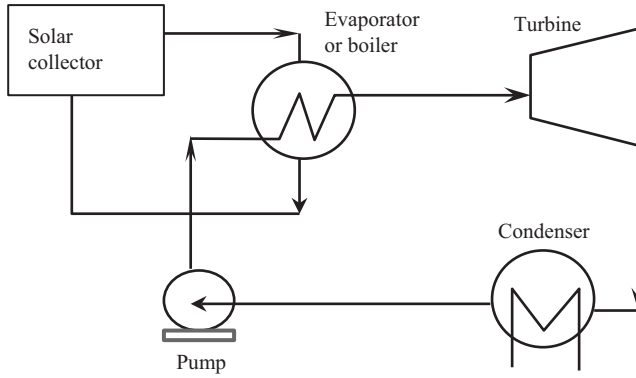

Figure 5.24 Schematic of Solar Rankine cycle [23]

The thermal energy collected from solar radiation is used to heat up water in the evaporator (boiler) section. The pressurized steam may be used directly to run the steam turbine or indirectly through the heat transfer fluid. The fluids used in the latter case are water and Therminol-VP1. The indirect heating of heat transfer fluid method is adopted in order to prevent the mechanical restrictions that occur with direct heating technique and to have a provision of thermal energy storage in an operating cycle. The working medium selection for solar-based Rankine cycles working in a low-temperature range is very important. Generally, they are categorized as wet fluid, isentropic type fluid and dry fluids. The wet fluids must enter into turbine in a superheated state, since liquid formation causes erosion of turbine blades. The isentropic fluids need not be in a superheated state at the entry to the turbine. It is in a saturated or superheated state at the turbine exit. The similar conditions apply to the dry fluids [23].

5.4.3 Solar-Brayton cycle

The solar-only electrical power plant is quite competitive with solar systems operating at higher temperatures. The maximum the working temperature attained in the circuit, the better the performance of a plant. Sometimes, part of an energy supplied into the combustion chamber of gas turbine power cycle can be make up using capturing solar irradiation on the collector field. Such a combination is termed as integration of the solar parabolic dish collector into the Brayton cycle, which can be a better option for transforming solar irradiation into electricity. A schematic of solar preheating Brayton-based power unit is shown in Figure 5.25, where “SF” represents the solar field, “P” the pump, “EV” the evaporator, “K” the compressor, “T” the turbine, and “HX” the heat exchanger, “CC” the combustion chamber and “G” represents the generator. The compressed air at the compressor exit is preheated by the heat energy captured using concentrating solar dish field. An additional heat exchange is incorporated into the Brayton cycle circuit ahead of the combustion chamber to transfer energy from the solar circuit to the Brayton gas circuit [23].

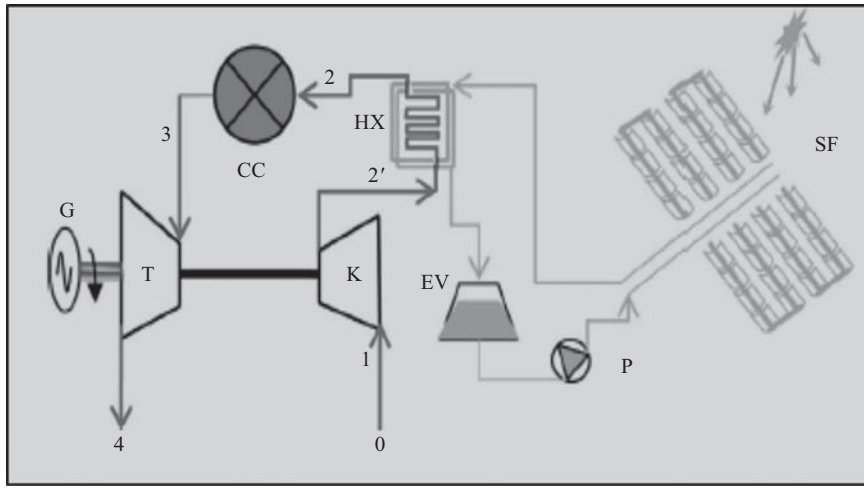

Figure 5.25 Schematic of the integrated solar Brayton cycle components

5.5 Integration of solar to thermal power with the conventional generating unit

The renewable hybrid technologies have been divided into three categories: low, medium, and high hybrid system, which are dependent upon their energy generation capabilities. Low renewable energy technologies deliver better efficiency as compared to the medium and high renewable hybrid technologies. These low renewable energy technologies are Solar-Brayton cycles (as discussed earlier), solar-assisted coal power units, and integrated solar combined cycles (ISCC). The medium class renewable energy systems have some limitations such as low efficiency and are less economical, e.g., the solar thermal power unit with natural gas fuel for backup. High renewable hybrid technologies are environment-friendly, having less impact on the environment. These are the combinations of concentrating solar power with biogas, geothermal, and wind energy [24,25].

5.5.1 Low renewable energy hybrid technologies

In this case, the solar energy is utilized in fossil fuel-based power units for assisting secondary tasks like preheating of working fluid entering into the Boiler. A share of the same in the case of low renewable integration system is usually less than 20% of the total energy supplied.

5.5.1.1 Solar-Brayton cycles

In the Brayton cycle-based gas turbine unit, a captured solar energy is used to heat up the compressed air, prior passing it to the combustion unit/chamber. It may also be used to create a steam that is to be supplied into the combustion unit/chamber as a functional/working fluid, as shown in Figure 5.25. The cycle efficiency increases

in both the cases due to increased working fluid temperature at the inlet to a combustion chamber. The solar-thermal to electricity conversion efficiency of such plants exhibits an increasing trend due to a rise in working fluid temperature of the Brayton cycle at the entry to the turbine. This mode of hybridization permits uninterrupted plant working even during the absence of solar energy.

5.5.1.2 Solar-assisted coal power units

Solar-assisted coal-fired thermal power units make use of concentrated/absorbed solar energy for the purpose of preheating as well as boiling. It is known that in the case of coal-fueled power plants, the generated superheated steam in a boiler is supplied into the high-pressure stages of the turbines. An intermediate and lower pressure turbine stages are driven by the steam leaving from high-pressure turbine, and by the steam supplied after being reheated in the boiler which finally condensed into the condenser. The condensate enters into a boiler via. three low pressure heaters, deaerator, and three high pressure heaters as depicted in Figure 5.26. The condensate as well as feed water is heated with the help of steam extracted from various stages of the steam turbine.

An energy extracted from the sun is utilized in such a way that, during sunny hours, the steam extracted from one of the turbine stages is cut-off and the feed-water may be heated by utilizing heat absorbed from solar-energized feed water heater (FWH). In case when the solar irradiation is inadequate to completely cut off the steam extraction, the total flow of feed water is heated partially by extracted steam and partially by solar-driven heat exchanger, as depicted in Figure 5.26 [26]. The abbreviation "SWH" represents solar water heater in the schematic.

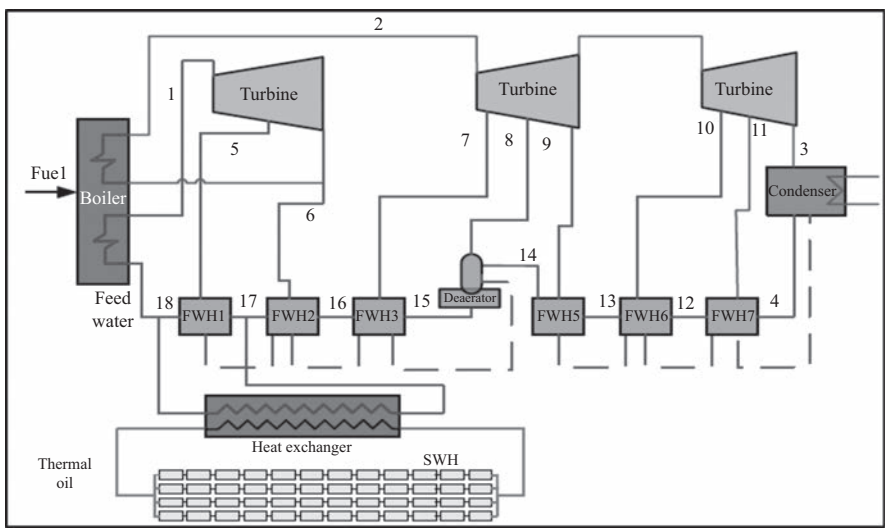

Figure 5.26 Solar-assisted coal-fueled power unit [26]

5.5.1.3 Integrated solar combined cycles (ISCC)

The ISCC is defined as a combined cycle technology that offers higher performance as compared to the individual Rankine and Brayton cycle-based power units. The hybridization of combined cycle can be brought into practice through the two cycles, e.g., topping cycle and bottoming cycle. The example of topping cycle is solar-Brayton cycle power units and an example of bottoming cycle is a solar-assisted coal-fired plants. It is observed from the literature that topping cycle-based hybridization technology have lots of key features as compared to the bottoming cycle integration [24].

5.5.2 Medium-renewable hybrids

The drawback of a standalone solar power plant, i.e., low capacity factor, can be overcome by using thermal energy storage system. It has been noticed that many standalone solar thermal power units use fossil fuels, e.g., natural gas as a reserve to retain the plant functional during duration of low insolation periods. The solar power plants in the Spain can contribute 12%–15% of gross power generation output using fossil fuels, and in the United States this ratio is close to 25%. The systems include (i) combined solar-coal Rankine energy generation system and (ii) solar power plant with natural gas. The combined solar-coal Rankine energy generation system is discussed in earlier section. The solar power unit with natural gas is discussed ahead.

5.5.3 High renewable hybrid technologies

The high renewable hybrids technology includes concentrating solar power system combined with biogas unit, with geothermal unit and wind turbine unit.

5.5.3.1 Concentrating solar power-biogas

In the present scenario, it is observed from the literature that concentrating solar power-biogas hybrid technology delivers a promising option of generating uninterrupted electricity, especially in remote and hilly areas [24].

One such solar-power-based biogas unit presented by Zhang *et al.* [27] is discussed. In this system, the heat sources such as solar tower/collector field and biogas boiler are coupled in parallel. During the day time, the power is generated by using both the energy resources solar and biogas, while only biogas is active during the night time, without stopping the power unit. An excess biogas produced during sunshine hours is collected in the container tank which is utilized for electricity generation during insufficient supply of solar energy. A steam turbine is then driven solely by a biogas unit continuously on cloudy days [27].

5.5.3.2 Concentrating solar power-geothermal

The geothermal technology is a new nonfossil fuel resource that is holding potential of hybridization with concentrating solar power. Generally, geothermal power units extract thermal energy from the ground to produce electrical power. The flash kind of geothermal systems is the most well-known type of geothermal

power units. Generally, the flash system utilizes hotter water at higher pressure to produce vapor in a flash chamber, which runs the turbine. Another kind of power units is based on the low-temperature geothermal resources to produce vapors of a fluid having a low boiling point. These systems also work on the Rankine cycle. Due to constant supply of energy, geothermal power plants are working as a base load unit with high energy capacity factor. The performance of the geothermal power plant also reduces with enhancement in the atmospheric temperature. But hybridization with concentrating solar power can mitigate some of its difficulties presently being faced on an individual level. The assistance of solar energy in the geothermal power cycle is mainly for (i) super heating of steam before supplying it to the turbine and (ii) preheating of geothermal brine [24].

Generally, geothermal liquids/gases are being drawn from so many wells at various temperatures. The geo-fluid obtained from low-temperatures is additionally heated in the solar-driven heat exchange unit. It is then utilized to evaporate the operational heat transfer fluid in thermodynamic cycles to generate electricity [28].

5.5.3.3 Concentrating solar power-wind

The hybridization of concentrating solar power plants with wind power is presently the most cost-effective renewable energy available, which is widely adopted in the world. The hybridization technology of a concentrating solar power with the wind energy needs lot of research attention for its improvements. It is because both do not have widespread synergy in the point of sharing of system arrangement, especially unlike the other thermal energy sources, for example, biomass and geothermal. On the other hand, solar energy naturally helps wind energy in producing power without interruptions. The wind speed is generally low during the day time and during the summer season as compared to during nights as well as winter seasons. The investigations have showed that the best ideal location of wind and concentrating solar power units may lessen the limitations of standalone concentrating solar power units and wind plants. The integration may supply constant base load electrical power [24].

Multiple options of utilizing solar energy are discussed in this chapter in order to portray the probability of utilizing these integrated resources for providing energy to many remotely located smaller homes.

5.5.4 Advantages of hybridization of solar power systems with other technologies

As observed from the literature survey, several CSP systems with the integration of other technologies have been investigated in the recent years, some important advantages are found:

1. Hybridization technologies accelerate more nonstop operation of the power generation plants arrangements and also decrease the need for the obtainability of the sun shining hours.
2. The hybridization of solar combined cycle's power plants can lead to obtaining higher conversion efficiencies of solar energy into electrical energy at lesser costs.

3. The energy storage system is a key alternative to reduce the drawback of the standalone solar power plant such as a low capacity factor. It is observed that many standalone solar power units use fossil fuels, such as natural gas as a reserve to keep a unit functional during low insolation periods.
4. The key significance of hybridization of the solar-assisted coal-fired power production system is to reduce carbon dioxide emission and gives some of its share for environment protection.
5. The environmental and global warming issue can easily be handled using this kind of hybrid technologies.

5.6 Concluding remarks

The thermal efficiency of a solar thermal power unit is stated as a ratio of the difference of two terms (i) solar energy absorbed by the solar thermal absorber and (ii) the energy losses via radiation and convective modes of heat transfer; to the incident solar energy on the collection system. It is expressed as [11]:

$$\eta_{th} = \frac{\alpha Q_{in} - Q_{loss}}{Q_{in}} = \alpha - \frac{\varepsilon \sigma F_{view} T_R^4 + h(T_R - T_{amb})}{\eta_{field} \times E_{DNI} \times C} \tag{5.15}$$

where

α Solar absorptance of the photothermal absorber
ε Thermal emittance of the solar thermal absorber
σ Constant-Stefan Boltzmann (5.67×10^{-8} W/m^2 K^4)
F_{view} Configuration factor between absorber surface and surroundings
T_R Temperature of absorber surface (K)
h Heat transfer coefficient of convection mode (W/m^2 K)
T_{amb} Surrounding temperature (K)
η_{field} Efficiency of collector field (incorporating losses by cosine factor, spillage, and reflectance)
E_{DNI} Direct normal irradiance flux (W/m^2)
C Concentration ratio

5.6.1 Ways to improve the efficiency of solar-based power plant/efficiency improvement

The ways which may augment the efficiency of a solar-based power plant are discussed as follows.

1. To enhance the power plant performance, it is required to prevent dust accumulation on the reflectors and also regular dry cleaning is recommended by many researchers. Since it is reported that the transmittance of glass plates reduces by 39.4%, on an average on exposing it to the solar radiation for 38 days. To inherit self-cleaning and anticontamination properties in the concentrating solar power mirror, superhydrophobic material coatings are recommended [11].

2. The heat transfer fluids with higher thermal stability of temperatures may also improve solar collection system performance. The low viscosity of heat transfer fluid reduces the pumping power, whereas higher values of specific heats of fluid reduce the size of a thermal energy storage tank. These two factors also help in augmenting the efficiency of a solar thermal system [11].
3. The replacement of the aluminum concentrator by galvanized steel structure, aluminum polymeric reflector by thin-silvered glass reflector and applying selective surface coatings on the receiver help improving the system performance. The use of steel and thin glass reflector improves the system performance by about 12% that may lessen the cost of energy to be delivered by about 25% [29].
4. The use of high mirror quality that allows more than 98.5% reflectivity to the solar rays incident on the reflector surface, also help in improving system's efficiency [29].

5.6.2 Challenges/limitations of concentrating power technology in remote as well as desert regions

Despite concentrating solar power technology is realistic and convincing in remote areas for individual home power generation, lots of challenges are to be faced for its efficient and uninterrupted operation. It involves water consumption/availability, electricity transmission, energy supply security, materials design, selection of energy exchange fluids, feasibility of thermal energy storage, and design of receiver subsystems in addition to commercial feasibility and ecological effects. Some of the technical challenges are deliberated as follows [11].

1. **Water consumption**
   Huge quantity of water is essential for cooling of receiver (solar power component) and for cleaning of mirrors/other reflecting surfaces. The availability of water is a major concern in some remotely located regions. The predicted water need ranges from 3 to 3.50 m^3/kW. The 95% of total water requirement is used at cooling tower and 5% is consumed in general for mirror cleaning. The adoption of dry mirror cleaning approaches are essentially helpful in reducing the use of water consumption in solar-based power plants.
2. **Dry cooling**
   Most of the commercialized concentrating solar power plants are associated with the conventional Rankine cycle steam power plant. The cooling of turbine outlet steam is to be achieved using cooling water. The lower the steam-condensation temperature, the better the plant efficiency. A cooling task in the steam condenser is better achieved by using ordinary cooling water, which helps in quicker cooling and that to at lower temperature. Studies of National Renewable Energy Laboratory (NREL) have revealed that dry-cooling might preserve water usage by more than 90%. However, the difference of temperature between the cooing water and the dry cooling medium may differ the yield of cycle thermal efficiency.
3. **Dustcleaning**
   The reflectivity of the heliostats, parabolic concentrator, and the transmissivity of the solar absorber reduces due to accumulation of dust particles and therefore

the efficiency. The studies have revealed that about 40% of the solar-thermal to electric power conversion decreases due to formation of a dust layer of size 4.844 gm per sq. meter. It also influences the optical performance of the concentrating solar power reflector. It is seen that 1% decrease in the reflectivity increases the levelized cost of electricity by about 1%. The most effective way is to wash mirrors with detergent and water. At rural or remotely deserted area it's a challenge to arrange water for the task.

4. **CSP-desalination cogeneration**
   The concentrating solar power generation with desalination is nowadays an attractive option in remotely located desert areas. The steam generated in the concentrating solar power cycle is used to support the desalination process, which may also fulfill the water demands of the remote population facing shortages.
5. **Heat transfer fluid**
   The heat transfer fluid is a vital part of the concentrating solar power plant which does a job of transferring heat effectively from the concentrated radiation to the steam generator. The heat transfer fluids used in concentrated solar to electricity power unit are air, water (steam), thermal-oils, organic, as well as molten salts. It not only serves the purpose of transferring energy but also serves the job of storing energy without thermal energy storage tank. The desired features of the heat transfer fluids are low melting point (in order to minimize the risk of freezing) and higher thermal stability (to enhance system performance). In the case of solar power systems, the heat transfer fluids need to be stable upto 700 °C and should have corrosion-resistant property also not to corrode the material of container or pipelines. The low viscosity reduces the pumping power, whereas higher specific heat is good to lessen the size of the tanks meant for energy storage purposes. Keeping in view all above aspects, the air has been reported as a best option for the same. The thermal oils, e.g., mineral oil, synthetic oils, and silicon oil, have very narrow operating ranges, i.e., between 200 °C and 400 °C.
6. **Environmental impacts**
   It is reported that the concentrating solar power systems are environment friendly and are commercially feasible. The development of efficient concentrating solar power systems may capture maximum freely available and clean source of solar radiation for illuminating and energizing small or remotely located homes or communities. It may also reduce emission of hazardous gases.

   In the case of solar tower installations, living creatures like flying birds get injured badly due to concentrated solar radiation beams focusing toward solar tower.

   The effluent of harmful heat transfer fluids (organic fluids, thermal synthetic oils, molten salts, hydraulic fluids, lubricants, and coolants) into the atmosphere after usage from the concentrating solar power systems may not be environment friendly. Proper preparation and better practices need to be followed to shrink the environmental impacts caused using these materials. The organics biphenyl/diphenyl oxide used in concentrating power systems are very toxic and may have a probability to catch fire.

7. **High capital costs**
   Other significant matter with the CSP system is the commercial feasibility. The capital costs of concentrated solar technology-based power unit is high. The pursual of mass production techniques and technology innovations/advancements in heat transfer fluids, high temperature storage systems and in thermodynamic cycles may decrease the capital, running, and maintenance cost by around 60% in near future.

   So, it is observed that setting up of solar thermal power units in remotely placed areas for a bigger capacity, say, above 100 kW is problematic to maintain and operate. In such areas, solar thermal power plant of less than or equal to 5 kW capacity for an individual home may prove beneficial to meet the routine/daily household needs.

5.7 Summary

A brief of local energy generation technologies specifically the "concentrating solar power" is described in the chapter along with the different types of solar thermal collector systems and the power generation cycles that can be used for power generation. It also includes the ways to improve the performance of solar thermal power systems and challenges to be faced for remote power generation in order to meet the individual's daily energy needs.

References

[1] O. Ogunmodimua and E. C. Okoroigweb, Concentrating solar power technologies for solar thermal grid electricity in Nigeria: A review, Renewable and Sustainable Energy Reviews 90 (2018) 104–119.
[2] J. P. Bijarniya, K. Sudhakar, and P. Baredar, Concentrated solar power technology in India: A Review, Renewable and Sustainable Energy Reviews 63 (2016) 593–603.
[3] A. Ummadisingu, and M. S. Soni, Concentrating solar power – Technology, potential and policy in India, Renewable and Sustainable Energy Reviews 15 (2011) 5169–5175.
[4] W. Fuqiang, C. Ziming, T. Jianyu, Y. Yuan, S. Yong, and L. Linhua, Progress in concentrated solar power technology with parabolic trough collector system: A comprehensive review, Renewable and Sustainable Energy Reviews 79 (2017) 1314–1328.
[5] S. S. Sahoo, S. Singh, and R. Banerjee, Thermal hydraulic simulation of absorber tubes in linear Fresnel reflector solar thermal system using RELAP, Renewable Energy 86 (2016) 507–516.
[6] A. Buscemi, D. Panno, G. Ciulla, M. Beccali, and V. Lo Brano, Concrete thermal energy storage for linear Fresnel collectors: Exploiting the South Mediterranean's solar potential for agri-food processes, Energy Conversion and Management 166 (2018) 719–734.

[7] S. P. Sukhatme, Solar Energy: Principles of Thermal Energy Collection and Storage, Second Edition, Tata McGraw Hill, New Delhi, 2000.
[8] I. H. Yılmaz and A. Mwesigye, Modeling, simulation and performance analysis of parabolic trough solar collectors: A comprehensive review, Applied Energy 225 (2018) 135–174.
[9] A. Z. Hafez, A. Soliman, K. A. El-Metwally, and I. M. Ismail, Solar parabolic dish Stirling engine system design, simulation, and thermal analysis, Energy Conversion and Management 126 (2016) 60–75.
[10] J. Khan and M. H. Arsalan, Solar power technologies for sustainable electricity generation – A review, Renewable and Sustainable Energy Reviews 55 (2016) 414–425.
[11] X. Xu, K. Vignarooban, B. Xu, K. Hsu, and A. M. Kannan, Prospects and problems of concentrating solar power technologies for power generation in the desert regions, Renewable and Sustainable Energy Reviews 53 (2016) 1106–1131.
[12] M. F. Modest, Radiative Heat Transfer, Second Edition, Academic Press, San Diego, CA, 2003.
[13] T. K. Tsai, Y. H. Li, and J. S. Fang, Spectral properties and thermal stability of CrN/CrON/Al_2O_3 spectrally selective coating, Thin Solid Films, 615 (2015) 91–96.
[14] U. R. Singh and A. Kumar, Review on solar Stirling engine: Development and performance, Thermal Science and Engineering Progress 8 (2018) 244–256.
[15] T. Mancini, P. Heller, B. Butler, *et al.*, Dish-Stirling systems: an overview of development and status, Journal of Solar Energy Engineering, 125 (2) (2003) 135–151.
[16] U. Pelaya, L. Luoa, Y. Fana, D. Stitoub, and M. Rood, Thermal energy storage systems for concentrated solar power plants, Renewable and Sustainable Energy Reviews 79 (2017) 82–100.
[17] Z. Ma, G. Glatzmaier, and M. Mehos, Fluidized bed technology for concentrating solar power with thermal energy storage, Journal of Solar Energy Engineering, 136 (2014) 031014.
[18] J. D. McTigue, J. Castro, G. Mungas, N. Kramer, J. King, and C. Turchi, Hybridizing a geothermal power plant with concentrating solar power and thermal storage to increase power generation and dispatch ability, Applied Energy, 228 (2018) 1837–1852.
[19] U. R. Singh and A. Kumar, Review on solar Stirling engine: Development and performance, Thermal Science and Engineering Progress 8 (2018) 244–256.
[20] B. Kongtragool and S. Wongwises, A review of solar-powered Stirling engines and low temperature differential Stirling engines, Renewable and Sustainable Energy Reviews, 7 (2003) 131–154.
[21] D. J. Shendage, S. B. Kedare, and S. L. Bapat, Cyclic analysis and optimization of design parameters for Beta-configuration Stirling engine using rhombic drive, Applied Thermal Engineering 124 (2017) 595–615.

[22] A. Z. Hafez, A. Soliman, K. A. El-Metwally, and I. M. Ismail, Solar parabolic dish Stirling engine system design, simulation, and thermal analysis, Energy Conversion and Management 126 (2016) 60–75.
[23] O. Behar, Solar thermal power plants – A review of configurations and performance comparison, Renewable and Sustainable Energy Reviews 92 (2018) 608–627.
[24] S. Pramanik and R. V. Ravikrishna, A review of concentrated solar power hybrid technologies, Applied Thermal Engineering, available online, doi: 10.1016/j.applthermaleng.2017.08.038.
[25] J. Qin, E. Hu, G. J. Nathan, and L. Chen, Mixed mode operation for the solar aided power generation, Applied Thermal Engineering, DOI: 10.1016/j.applthermaleng. 2018.04.118.
[26] H. Hong, S. Peng, Y. Zhao, Q. Liu, and H. Jin, A typical solar-coal hybrid power plant in China, Energy Procedia 49 (2014) 1777–1783.
[27] G. Zhang, Y. Li, Y. J. Dai, and R. Z. Wang, Design and analysis of a biogas production system utilizing residual energy for a hybrid CSP and biogas power plant, Applied Thermal Engineering 109 (2016) 423–431.
[28] M. C. Bassetti, D. Consoli, G. Manente, and A. Lazzaretto, Design and off-design models of a hybrid geothermal-solar power plant enhanced by a thermal storage, Renewable Energy 128 (2018) 460–472.
[29] H. Price, E. Lupfert, D. Kearney, E. Zarza, G. C. R. Gee, and R. Mahone, Advances in parabolic troughsolar power technology, Journal of Solar Energy Engineering ASME, 124 (2002) 109–125.

Chapter 6

Numerical analysis of phase change materials for use in energy-efficient buildings

Swapnil S. Salvi[1,2] and Himanshu Tyagi[1]

Due to the efficient performance in energy storage density, solar thermal energy storage (TES, especially latent type) applications are drawing more attention in the research field of solar energy. Among all of the types of solar thermal storage technologies, the latent heat storage system using phase change materials is the most efficient way of storing thermal energy. It has some dominant factors such as high density energy storage and isothermal operations, i.e., very small temperature range for heat storage and removal. Thus, latent heat storage systems have greater applicability over the other types of TES systems.

This chapter initially presents an analysis of a latent-type solar thermal energy storage (TES) system involving some of the important cases carried out comprising the application of ambient conditions with various geometries and working conditions. The analysis is carried out in MATLAB® and COMSOL®, which contains transient simulations of latent heat storage functioning with 1D and 2D modeling. It comprises the validation of numerical 1D analysis with corresponding analytical solution, observation of the change in thermophysical properties at the melting point, etc.

Further in this study, the phase change material (PCM) is assumed to be incorporated in a brick wall structure, which can improve its thermal performance. A 1D numerical model on COMSOL Multiphysics is developed to analyze the thermal performance of the PCM-filled brick wall unit. The numerical model and the adopted hypotheses are illustrated in detail. The comparison between temperature distributions of a simple brick wall and a brick wall with a PCM layer is presented. The results show that using the numerical tool, it can be observed that the thermal performance of the PCM-filled brick wall is efficient over the simple brick wall without PCM. This concept of the PCM-impregnated building structure is found to be successful in shifting the energy requirement of the equipped building sector from a high peak electricity demand period to an off-peak period.

[1]Department of Mechanical Engineering, Indian Institute of Technology Ropar, India
[2]Department of Mechanical and Aerospace Engineering, University of Texas at Arlington, USA

6.1 Introduction

6.1.1 Motivation

Solar energy is the most abundant energy source and it has the highest potential to be the most effective energy source among all other conventional energy sources such that out of the total solar energy intercepted by earth, i.e., approximately $1.8 \times 1{,}014$ kW, only one-thousandth part of solar energy with 10% efficient energy conversion devices will produce 400% of the total world's energy generation rate [1]. The higher usage of fossil fuels is due to its comparatively lower price and easy accessibility. But, due to burning, fossil fuels will produce harmful and, up to some extent, poisonous emissions into the atmosphere, affecting various critical environmental factors from the human health and global warming point of view. Also, the depletion rate of fossil fuel is faster than its production due to over exploitation. Thus, we must research and improve the most promising alternate energy resources, and the solar photovoltaic (PV) and solar thermal energy are the best-suited options for the future energy requirements of the developing world due to its clean and nonpolluting nature.

Solar thermal collectors are the heat exchangers in which heat transfer fluid (HTF) transforms the solar thermal energy absorbed by the collector in order to use it in the applications such as water heating, steam generation, drying, and desalination [1]. Solar thermal collectors can be classified on the basis of two factors, viz., concentration of solar radiation and operational temperature of the solar collector [2]. Non-concentrating and concentrating collectors are the further categorization on the grounds of the concentration of solar radiation absorbed. Flat plate type and evacuated tube type collectors are included in non-concentrating collectors, whereas concentrating collectors will be further classified on the basis of the method of concentrating solar radiation, viz., line focused (linear Fresnel, parabolic trough collector, etc.) and point focused (parabolic dish reflector, power tower, etc.) type collectors. According to the operational temperatures of the specified collectors, it is classified as low-, medium, and high-temperature solar collectors [3].

It has been well understood by the researchers that there is a significant scope of enhancement in solar energy harvesting. The functional working of the components of solar collectors must be improvised with the help of the continuous research in order to enhance the overall performance of the solar thermal systems. The researchers have shown their keen interest in the optimization of conventional solar harvesting techniques, also in the enhancement of overall solar power plant as well as individual components of the solar thermal collectors. Numerous inventions have been successfully attempted in order to increase the solar selectivity of the absorber, increasing the heat transfer coefficient of the working fluid or HTF, reducing the thermal losses, etc. In recent years, some researchers have deliberately published some reviews on improvisation of solar thermal power plants. Reddy *et al.* [4] studied different case studies of solar thermal power plants in the Indian climatic conditions in order to efficiently design the functional requirements and operating parameters of solar thermal power plants. Suman *et al.* [5] presented an

overview of different methods used in order to enhance the performance of solar thermal energy harvesting.

The enhancement in the efficiency of individual components of the solar thermal collector will ultimately improve the overall performance of the solar thermal system. Amri *et al.* [6] presented a review on improvisations in the solar selective coatings in the case of a flat plate type solar collector specifically manufactured by sol–gel methods. For high-temperature applications, Cao *et al.* [7] reviewed cermet-based absorber coatings including the performance of different materials, manufacturing methods, etc. with considerations of solar selectivity requirements. Moreover, Atkinson *et al.* [8] studied and reported the research studies which state the improvisation of absorbers as well as reflectors of solar thermal collectors by applying solar selective coatings best suited for concentrated solar thermal systems.

The improvement in the heat transfer coefficient of HTF directly by introducing nano-sized particles in it, collectively called nanofluid, is ultimately used for improving the heat transfer mechanism in solar thermal systems. Taylor *et al.* [9] presented an extensive review of nanofluids in the field of high flux solar thermal collectors. Mahian *et al.* [10] and Kasaeian *et al.* [11] focused their review on applications of nanofluids in the field of solar energy considering economical and environmental aspects, along with the possible challenges for the same. Further, there is a considerable research work going on in the field of direct absorption of solar energy into volumetric absorbers. Phelan *et al.* [12] elaborated the past record of direct absorption solar collectors (DASC) as well as their future scope in different applications, highlighting the potential of solar energy conversion using the DASC. Gomez-Garcia [13] focused on the ceramic-based volumetric absorbers including various structures and manufacturing methods. Gorji *et al.* [14] presented an extensive review of the integration of nanofluids in the DASC including the preparation of nanofluids and optical characterization of the same along with the challenges and difficulties faced. The researchers are also working on the integration of TES into solar thermal power plants, which leads to the prevention of fluctuations in solar energy supply due to day–night cycles and unexpected cloud covers [15]–[17].

Energy used to maintain the ambient air conditions in the building sector shares a significant part of the total energy being used worldwide. Moreover, due to the recent increase in population and improvement in living standards of people, the overall energy requirements by the building sector are continuously increasing. Phase change material (PCM)-assisted TES can be considered as an efficient solution to control the surge in building energy demands. PCM incorporated envelopes in brick walls or gypsum boards can be used to reduce the energy demands which ultimately improve the energy efficiency of buildings. PCM incorporation enhances the thermal energy capacity of construction materials (concrete, brick, stone, etc.).

6.1.2 Background

Global problems such as increasing fossil fuel use and higher greenhouse gas emissions could be tackled by effective utilization of renewable energy forms. Earth's surface experiences solar radiation for a significant time period of the day,

which can be converted into thermal energy directly or into electricity using solar PV. Solar TES techniques are becoming a fundamental requisite to reduce the adverse effects of fluctuations in solar radiative energy due to cloud cover, day–night cycle, seasonal variations, etc.

It has been recognized by Kuravi *et al.* [16] that TES incurs a lower capital cost as compared to mechanical and electrical energy storage technologies, along with higher operational efficiencies. TES is implemented to balance out the low solar energy supply and periodic higher demand rates. Zalba *et al.* [18] stated that TES also ensures the security of energy supply and storage. The TES system can allow the power plant to run on its full capacity regularly, even if the demand rate is not matching with the thermal energy production. Due to the highly efficient properties of PCM, it can also be used for the PV thermal management [19].

Different forms of TES are sensible heat storage, latent heat storage and thermochemical storage [15]. The detailed classification of energy storage materials is depicted in Figure 6.1 [20]. The storage of energy by any means other than thermal requires the usage of an extra equipment such as electric battery, whereas in the case of latent heat storage, it can be reduced or eliminated [18].

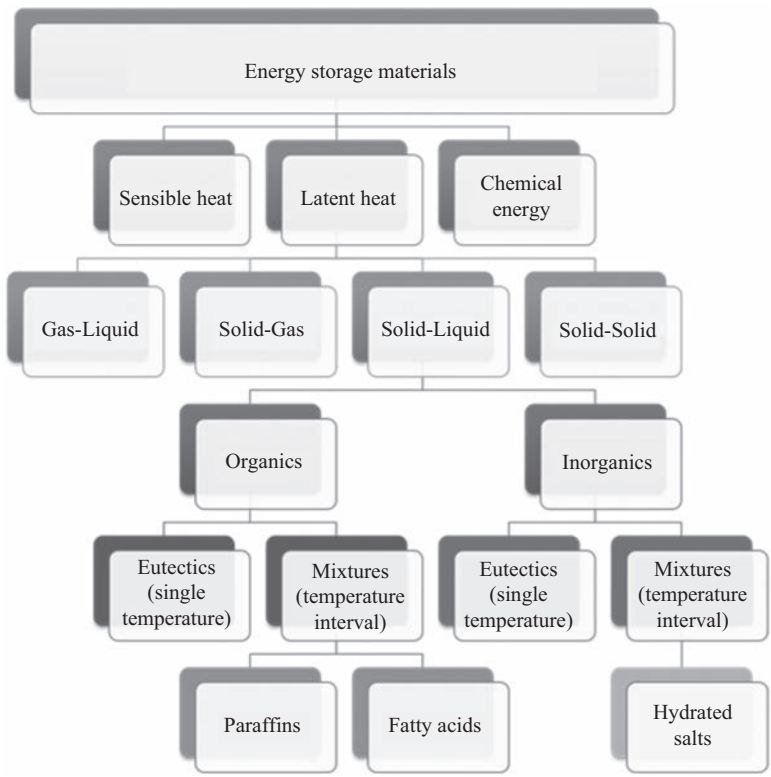

Figure 6.1 Classification of energy storage materials. Adapted from Ref. [20]

Zhao *et al.* [21] stipulated that the major issue regarding the PCM is its low thermal conductivity, which usually ranges from 0.2 to 0.7 W/m K. This is much lower as compared to heat storage mediums in sensible heat storage systems. Low thermal conductivity will result in a slow disposal rate of the stored heat energy, and thus it leads to the sub-optimal performance of the PCM-latent heat storage system. It is a very important and desired quality required as far as thermal storages are concerned. For improving the thermal performance of the PCM storage system, fins are incorporated in the system [22] or high thermal conductivity particles are introduced into the PCM.

In this study, we will be focusing on the analysis of latent thermal storage models in Section 6.2. Various cases including different working conditions are applied on the 1D and 2D geometries. Initially, the validation of the numerical solution has been carried out with the analytical solution of simple 1D Cartesian as well as cylindrical geometries, using COMSOL and MATLAB codes. Further cases comprehend the temperature distribution for the conditions to a higher temperature above PCM's melting point. The corresponding results are presented and illustrated in the problems mentioned.

There are numerous applications of TES incorporating PCM [18,23] such as TES for shifting the peak loading conditions, energy-efficient buildings, transport of temperature-sensitive goods, hot water PCM tanks, etc. It has been estimated that most of the energy is used for cooling and heating of the buildings (commercial and residential) because of climate change, social and economical changes, transformation of life style, etc., especially in developing countries such as India and China. In these developing countries, up to one-third of the total primary energy gets consumed for the construction of the buildings and usage of the occupants.

For comfortable residential and commercial buildings, cooling and heating of the building are necessary. For most of these end-uses (such as lighting, fans, appliances, heating, and cooling), electrical energy is required, for which fossil fuels have been used. So, one should focus on the usage of clean and free energy (such as solar energy) resources for comfortable buildings. Solar energy is freely available on the earth, and a huge amount of solar energy incident on the surface of earth. It has been estimated that around 5.6 million exajoules of sunlight incident on earth's surface, which is 1,000 times the current global energy consumption [24]. The value of the incident solar radiation varies from one terrestrial location to another.

Thermal energy storage for maintaining the ambient conditions inside the buildings is becoming increasingly important due to the surge in fossil fuel prices and environmental concerns. The properties such as high thermal storage density as well as the isothermal nature of the operation leads to employ PCMs in the latent heat storage system. New and intelligent materials, such as PCM, can store latent heat energy in addition to the typical sensible energy capacity, allowing one to store significantly more energy as compared to conventional building materials. This kind of (latent heat type) TES is preferred more and more in the case of buildings built with energy-saving purposes.

The PCM-Brick wall system can offer some competitive advantages over the traditional brick wall [20], listed as follows:

1. The ability to save the operative fees by shifting the peak electricity demand to off-peak periods, since electricity cost is much lower at night as compared to that of the day.
2. Continuous storage of solar energy during the day, and releasing it at night, thus improvising the thermal comfort level.
3. Storage of natural cooling through ventilation at night in summer, which can be released to the room air during day time, thus reducing the cooling load of air conditioning.

There are various ways to incorporate the PCM into building structures which have been investigated in the literature [25], viz., direct incorporation, immersion, and encapsulation. The present study describes the application of PCM in the sector of energy-efficient buildings. The topic with validation of COMSOL simulations over a brick wall with the analytical method for the identical conditions will be initialized. One special case is also carried out in order to check whether gravitational effects are advantageous for the PCM incorporated bricks walls or not, so as to decide whether we have to enhance or suppress the gravitational effects inside melting PCM by accounting volumetric construction of PCM storage. Generally, the PCM included in the wall is in the form of microencapsulated particles in a thin, high-molecular-weight polymeric film, thus leading to the prevention of any significant buoyancy effects inside the PCM layer and enhanced heat transfer [26]. Moreover, microencapsulation offers numerous advantages such as the increase in the effective heat transfer surface area, enhancing PCM inertness with the respect to the surrounding environment and restricting the major changes in the bulk volume due to phase change [23]. Further, numerical modeling of a brick wall containing the PCM layer in between has been done to check the effectiveness of the PCM layer. It has also been compared with the conventional case of the simple brick wall (without PCM) experiencing similar realistic boundary conditions. Additionally, the major findings or conclusion of the study as well as some possible future scope regarding the same are detailed.

6.1.3 Prior work

For the harnessing of the solar irradiation, solar thermal collectors absorb the solar energy, convert it into heat and transfer the heat to the working fluid (air, water, PCM, etc.). Li *et al.* [27] numerically showed that 64.6% heating demand and 20.2% of cooling requirement in buildings can be met by using solar energy. Tsalikis and Martinopoulos [28] suggested that the solar energy systems are capable of covering more than 76% of the total primary energy demand and in some cases up to 97%, while presenting a Discount Pay Back Period of less than 6 years (with a minimum of 4 in some cases) with an initial investment cost of 10,000–12,250 €. Kyriaki *et al.* [29] presented the overall evaluation of the solar thermal system and its contribution in the improvement of building's energy and environmental

performance. They have concluded that with solar thermal systems, there has 67% less CO_2 emission to the environment. The building sector is predicted to be the fourth largest contributor to CO_2 emissions [30]. In order to minimize the energy consumption for the building sector, the development of new energy storage devices must be developed where the PCMs get to be the most suitable candidate [30].

During the past one or two decades, an extensive research has been carried out in order to achieve a highly efficient latent heat energy storage which can be utilized in the scope of energy-efficient buildings. However, as per the literature, it is found that there are some hurdles to make this technology totally compatible with the practical applications. Zhang *et al.* [25] analyzed the application principles of PCM-integrated building walls and also have discussed different applications and the trends of PCM utilization in the building sector. Vicente *et al.* [31] experimentally tested the capabilities of PCM to be used as a thermal regulator for indoor building spaces. They compared among different combinations of clay masonry, PCM macrocapsules and extruded polystyrene (XPS) form as a thermal insulation. Cabeza *et al.* [32] demonstrated the utilization of the microencapsulated PCM impregnated into the concrete walls in order to achieve cold inside building conditions and enhanced thermal inertia. Moreover, Izquierdo-Barrientos *et al.* [33] numerically studied the PCM properties in order to determine the optimum phase change temperature for the highest possible heat capacity. They have concluded that the PCM envelope inside the wall increases the thermal load during the day time and decreases during the night time.

Zhu *et al.* [34] experimentally analyzed a wallboard in a common concrete wall integrated with shape-stabilized PCMs. They found that the melting temperature and thicknesses of the PCM layer are most significant factors to be focused on while designing the similar system. They also analyzed the peak load reductions for cooling and heating using numerical techniques. With optimum parameters chosen, authors have concluded that the energy savings for a year were 3.4%–3.9%. Sayyar *et al.* [35] carried out a comparative study based on the experimental and numerical analysis of shape-stabilized phase change nanocomposites to achieve the aim of energy-efficient building constructions. They have reported that the integration of a nano-PCM into the building envelopes will maintain the required average interior temperatures and reduce the overall energy consumption by 79%. Further, Kuznik *et al.* [36] carried out an experimental comparative study on the PCM wallboard in order to achieve minimum fluctuations in thermal behavior of wallboard using a wooden wallboard with and without PCM. They also compared the experimental results with the numerical simulations carried out with identical boundary conditions. Biswas *et al.* [37] utilized a nano-PCM enhanced wallboard to carry out experimental as well as numerical evaluation. They studied the two different setups kept side by side, one with simple gypsum wallboard and another incorporated with PCM, analyzed for a whole year. After carrying out the mentioned comparative study, the authors concluded that the nano-PCM wallboard reduced the thermal fluctuations as well as the peak heat gains by delaying the heat transferred into the interior of the building space. Moreover, Biswas *et al.* [38]

experimentally analyzed the probability of utilizing a novel PCM made of glycerides engraved into high density polyethylene pellets into the building envelopes. They have also validated the experimental results with an identical numerical model by carrying out the annual simulations. This study concludes that the modified PCM building envelope system can yield better thermal performance at a lower cost.

Bastani *et al.* [39] investigated the incorporation of the PCM into the wallboard inside the building envelope in order to shift the peak energy load of the building sector to the off-peak load period. They concluded that the two most important factors would be the PCM thickness and its thermophysical properties, which must be appropriately quantified to satisfy the design objective. Further, Castell *et al.* [40] carried out an experimental comparative study for the purpose of building cooling, in which they compared the working of PCM with two construction materials, viz., conventional and alveolar brick to be tested in real conditions. This study demonstrated that there were approximately 15% energy savings for setups with the PCM as compared to that of without the PCM. Alvarez *et al.* [41] presented an innovative solution to enhance the building night cooling application utilizing the PCM. They reported that positioning PCM inside ventilated air layers of building wall sections leads to a significant increase in the convective heat transfer coefficient along with the hike in the utilization factor. Shilei *et al.* [42] investigated the effect of incorporating the PCM into simple gypsum wallboards and hanging them up on the interior side of the wall in order to achieve the minimum thermal fluctuations in the winter season. They reported that the impact of PCM wallboards inside the room when experiments were carried out inside the room can weaken the indoor air fluctuations and can reduce the heat transfer through building walls. Further, Ahmad *et al.* [43] carried out a comparative study between experimental investigation and computerized simulation of PCM wallboards by analyzing thermal behavior of the system. This study showed that the polyvinyl chloride panels filled with PEG 600 is a suitable candidate for our objective of the building material with higher heat capacity storage and light weight construction. Shi *et al.* [44] experimentally assessed the position of macro-encapsulated PCM integrated with concrete walls for analyzing indoor temperatures as well as humidity contents. They reported that the proposed PCM models are thermally efficient by reducing the maximum temperatures around 4 °C. It also provides required comfort by reducing the inside humidity levels by 16%.

Some of the researchers also attempted to mix the nano/micro-PCM with concrete, in order to use it directly as a construction material. Schossig *et al.* [45] investigated the probability of using the technology of microencapsulation of PCM in the field of energy-efficient buildings. They carried out numerous simulations to find out the useful material parameters in order to use them for reasonable known applications. Sa *et al.* [46] presented the development of a new composite material based on the incorporation of microencapsulated paraffin in cement-based plastering. Firstly, this setup was experimentally analyzed, and further in order to

validate the same, the finite element method was applied to the thermal analysis. From these studies, it has been stated that the appropriate base for numerical simulations of real-scale buildings has been set, encompassing the use of PCM-based plasters in order to evaluate the corresponding optimum solution. Further, Sage-Lauck *et al.* [47] studied the modelling of the construction of a passive cooled duplex house, whose design incorporates the PCM inside the building structures. The results of the corresponding building energy simulations signify that the integration of 0.9 kg/m^2 surface area of the PCM in building structures with a melting temperature of around 25 °C can reduce the overheat by about 50%. Moreover, Kheradmand *et al.* [48] evaluated the thermal behavior of cement-based plastering mortars with and without the microencapsulated PCM. It was reported that the use of more than one type of PCM in the mortar has revealed appropriate thermal behavior. However, the thermal characterization testing gave confirmation for the feasibility of hybrid PCMs in mortars (Table 6.1).

Table 6.1 Summary of the literature for PCM applications

Sr. no.	Author (year)	Type of PCM	Wall composition	Method of incorporation	Development
1.	Sayyar *et al.* (2014)	Fatty acid based	Concrete	Shape-stabilized PCM	Reduced energy consumption by 79%
2.	Zhu *et al.* (2015)	Paraffin based	Concrete	Shape-stabilized PCM	Achieved annual energy savings for cooling and heating purposes around 3.4%–3.9% and 14.8%–18.8%, respectively
3.	Kuznik *et al.* (2009)	ENERGAIN®	Wooden wallboard	Micro-encapsulate	Validation of experimental data with numerical solution considering hysteresis
4.	Biswas *et al.* (2014)	Glycerides	Cellulose insulation	Macro-encapsulation	Better thermal performance at lower cost with considerable energy savings
5.	Castell *et al.* (2010)	RT 27 and SP-25 A8	Brick and Alveolar brick cubicles	Macro-encapsulation	15% additional energy savings can be achieved

6.2 Analysis of latent heat TES

In this section, we will carry out a thermal analysis for various combinations of different geometries, in 1- or 2D system and with the Cartesian or cylindrical coordinate system. This section will be initialized with the basic validation of 1D Cartesian as well as cylindrical PCM geometries. Further, it will be continued with varying boundary conditions and addition of more realistic boundary conditions (Table 6.2).

The PCM for all described cases selected except case 2 and case 3 from this section is octadecane ($C_{18}H_{38}$) which is being used as encapsulated PCM in building structures [26], having the properties described in Table 6.3 [49,50].

All the cases except the last contain a numerical study which considers only conduction as a mode of heat transfer and neglects the effect of natural convection. The assumption of only conduction is valid for small PCM passages.

Table 6.2 List of cases and their details

Case no.	Geometry	Coordinate system	Boundary conditions	Brief details
1.	1D	Cartesian	Constant temperature	Comparison of analytical vs. numerical solutions for a case of PCM melting
2.	1D	Cylindrical	Constant heat (extraction) flux	Comparison of analytical vs. numerical solutions for a case of PCM freezing
3.	1D	Cylindrical	Constant temperature	Comparison of analytical vs. numerical solutions for a case of PCM freezing
4.	1D	Cartesian and cylindrical	Constant temperature	Observing the change in slope in transient temperature distribution at melting temperature
5.	2D	Cylindrical	Convective heat transfer	Observing the effects of gravity/natural convective currents

Table 6.3 Thermophysical properties of octadecane

Properties	Solid	Liquid
Melting temperature (T_m)	27.5 °C	
Latent heat of fusion (L)	244 kJ/kg	
Density (ρ)	814 kg/m^3	774 kg/m^3
Dynamic viscosity (μ)	10^8 Pa s (infinite)	0.0039 Pa s
Thermal conductivity (k)	0.358 W/m K	0.152 W/m K
Specific heat (C_P)	2,150 J/kg K	2,180 J/kg K

6.2.1 Case 1 (Cartesian coordinates—analytical vs. numerical)

In order to start the thermal analysis of various PCM geometries, we will be first focusing on a simple 1D case of Cartesian as well as cylindrical coordinates. In this case, the validation of numerical against analytical solution for a rectangular slab is carried out. The schematic for the same is shown in Figure 6.2.

Analytical solution for the 1D model [51] gives the following temperature distribution equation (6.1) for the liquid region in the PCM slab:

$$T_l(x,t) = T_W + (T_m - T_W) \times \frac{erf\left[\frac{x}{2\sqrt{\alpha_l \times t}}\right]}{erf[\beta]} \tag{6.1}$$

where T_l is the spatial temperature of liquid PCM, T_W and T_m are the left side wall temperature and the melting point of PCM, respectively, α_l is the thermal diffusivity of liquid PCM, and x and t are spatial and time variables, respectively.

β is the root of interfacial melting front equation:

$$\beta e^{\beta} erf(\beta) = \frac{C_{Pl}(T_W - T_m)}{L\sqrt{\pi}} \tag{6.2}$$

where C_{Pl} is the specific heat of the liquid PCM and L is the latent heat of fusion.

Phase front location $X(t)$ also depends on β:

$$X(t) = 2\beta\sqrt{\alpha_l t} \tag{6.3}$$

Selected parameters for the problem in case 1 for numerical as well as analytical solution are as follows:

- Length = 3 m
- Initial temperature, $T_i = 27.5$ °C
- Left wall temperature, $T_W = 50$ °C
- Mesh = Custom (Max element size = 0.5 mm)
- Time range = (0:5:600) s

From the results, we can validate the numerical method. Figures 6.3 and 6.4 show that the temperature distribution and the phase front location of the numerical method are fairly matching with the analytical solution.

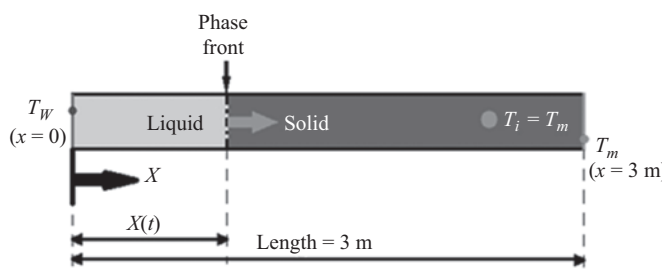

Figure 6.2 Schematic model for case 1

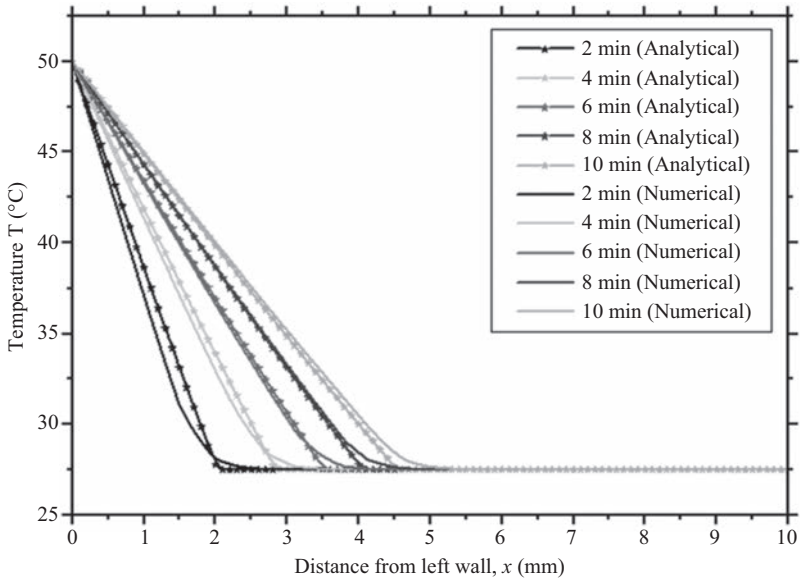

Figure 6.3 Comparison of temperature distribution of numerical vs. analytical method—case 1

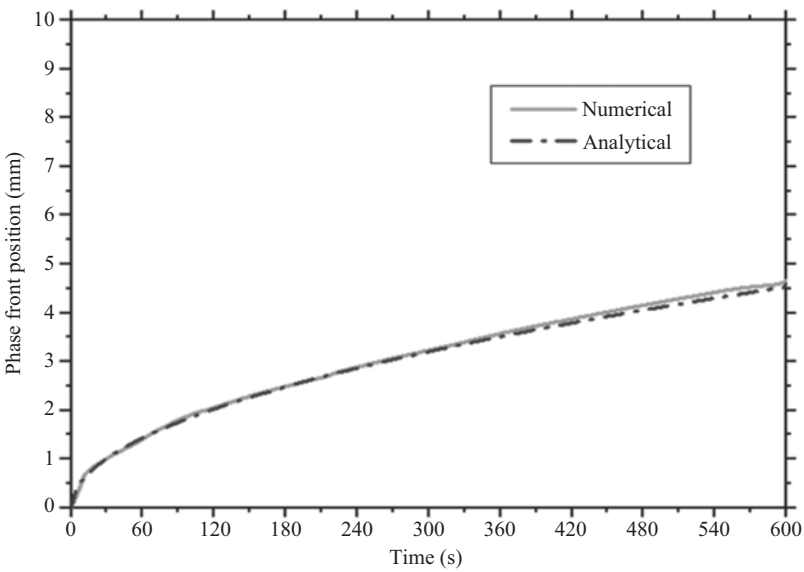

Figure 6.4 Comparison of phase front position of numerical vs. analytical method—case 1

The results of the comparison of analytical and numerical solution in case 1 show that the numerical results are fairly validated using the analytical method results.

6.2.2 *Case 2 (cylindrical coordinates—analytical vs. numerical—constant heat extraction freezing)*

As we have analyzed the 1D case for Cartesian coordinates, we will now carry out the analysis of 1D cylindrical coordinates with two different source boundary conditions. Case 2 specifies the constant heat extraction as a source boundary condition, whereas for the next case (case 3) the constant temperature boundary condition is taken as the source term. In case 3, the validation of numerical against analytical solution for a semi-infinite cylinder is carried out. The schematic for the same is shown in Figure 6.5.

Analytical solution for the 1D model [51] gives the following temperature distribution equation (6.4) for the liquid region in the cylindrical pipe of PCM:

$$T_l(r,t) = T_i + (T_i - T_m) \times \frac{Ei\left[\dfrac{-r^2}{4\alpha_l \times t}\right]}{Ei\left[-\lambda^2 \dfrac{\alpha_s}{\alpha_l}\right]} \tag{6.4}$$

where T_l is the spatial temperature of liquid PCM, T_i and T_m are the initial temperature of liquid and the melting point of PCM, respectively, α_l is the thermal diffusivity of liquid PCM, α_s is the thermal diffusivity of solid PCM, and r and t are spatial and time variables, respectively.

λ is the root of interfacial melting front equation (6.5):

$$\lambda^2 \alpha_s L\rho = \frac{Q}{4\pi} e^{-\lambda^2} + \frac{k_l(T_i - T_m)}{Ei\left[-\lambda^2 \dfrac{\alpha_s}{\alpha_l}\right]} e^{-\lambda^2(\alpha_s/\alpha_l)} \tag{6.5}$$

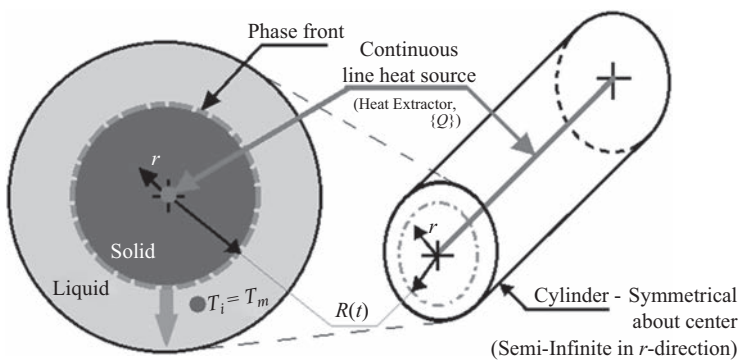

Figure 6.5 Schematic model for case 2

where Q is the heat extraction rate per unit time, L is the latent heat of fusion, k_l is the thermal conductivity of liquid, and ρ is the density of PCM.

Phase front location $R(t)$ also depends on λ:

$$R(t) = 2\lambda\sqrt{\alpha_s t} \tag{6.6}$$

Selected parameters for the problem in case 2 for numerical as well as analytical solution are as follows:

- Material = Water
- Radius = 1 m
- Initial temperature, $T_i = 0$ °C
- Constant heat extraction at center, $Q = -100$ W/m
- Mesh = Custom (Max element size = 0.5 mm)
- Time range = (0:5:600) s

From the results, we can validate the numerical method. Figures 6.6 and 6.7 show that the temperature distribution and the phase front location of the numerical method are fairly matching with the analytical solution.

The results of the comparison of analytical and numerical solutions in case 2 shows that the numerical results are fairly validated using the analytical method results.

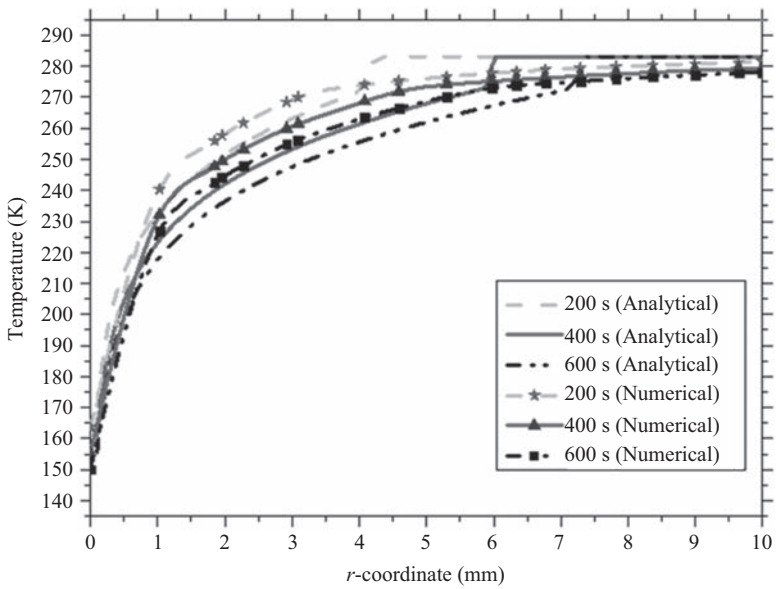

Figure 6.6 Comparison of temperature distribution of numerical vs. analytical method—case 2

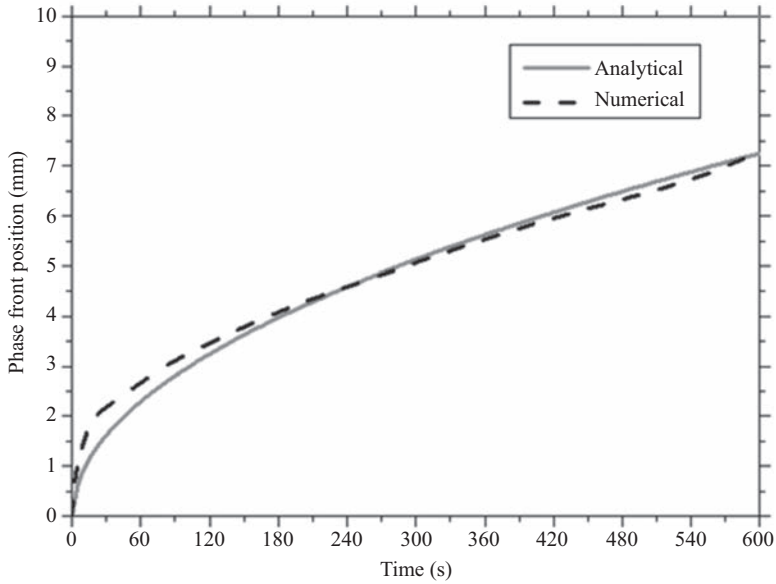

Figure 6.7 Comparison of the phase front position of numerical vs. analytical method—case 2

6.2.3 Case 3 (cylindrical coordinates—approximate vs. numerical—constant temperature freezing)

Since we are done with the analysis of 1D cylindrical coordinates with a constant heat extraction source boundary condition, we will now analyze and validate this case for a constant temperature source boundary condition (a case for freezing of PCM). The only change with respect to the previous case is the source boundary condition. In this case, the validation of numerical against approximate solution for a semi-infinite cylinder is carried out. The schematic for the same is shown in Figure 6.8.

Approximate solution for the 1D model [51] gives the following temperature distribution equation (6.7) for the solid region in the cylindrical pipe of PCM:

$$T_s(r,t) = T_S + (T_m - T_S) \times \frac{\ln\left[\frac{r}{a}\right]}{\ln\left[\frac{R}{a}\right]} \tag{6.7}$$

where T_s is the spatial temperature of solid PCM, T_S and T_m are the inner pipe surface temperature and the melting point of the PCM, respectively, a is the inner pipe radius, and r and t are spatial and time variables, respectively.

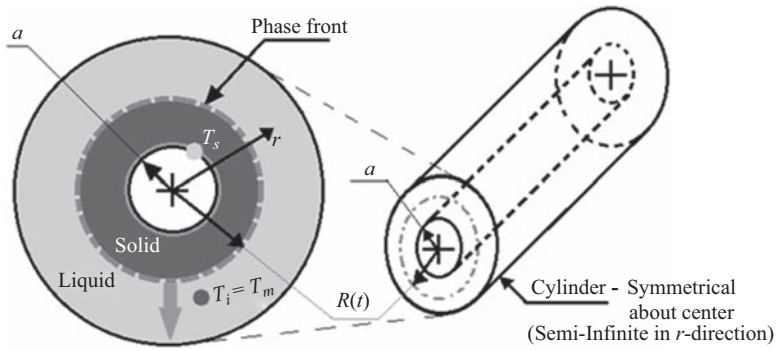

Figure 6.8 Schematic of case 3

Phase front location $R(t)$ can be find out using the following equation:

$$2R^2 \ln\left[\frac{R}{a}\right] - R^2 + a^2 = \frac{4k_s(T_m - T_S)}{L\rho} \tag{6.8}$$

The selected parameters for the problem in case 3 for numerical as well as analytical solution are as follows:

- Material = Water
- Radius = 1 m
- Radius of inner pipe (a) = 0.01 m
- Initial temperature, $T_i = 0$ °C
- Inner pipe surface temperature, $T_S = -10$ °C
- Mesh = Custom (Max element size = 0.5 mm)
- Time range = (0:5:600) s

From the results, we can validate the numerical method. Figures 6.9 and 6.10 show that the temperature distribution and the phase front location of the numerical method are fairly matching with the approximate solution.

The results of the comparison of approximate and numerical solution in case 3 show that the numerical results are fairly validated using the analytical method results. The graph of temperature distribution (see Figure 6.9) shows that there is a significant error between approximate and numerical solution, because a steady-state condition is being considered in the approximate solution, whereas in the numerical solution it is considered as transient. The phase front position (see Figure 6.10) got a fair match between approximate and numerical methods with minimal errors.

6.2.4 *Case 4 (Cartesian and cylindrical coordinates—ambient—change in slope)*

After carrying out validations of numerical techniques applied to the basic geometries in Cartesian as well as cylindrical coordinates, we will now focus on the

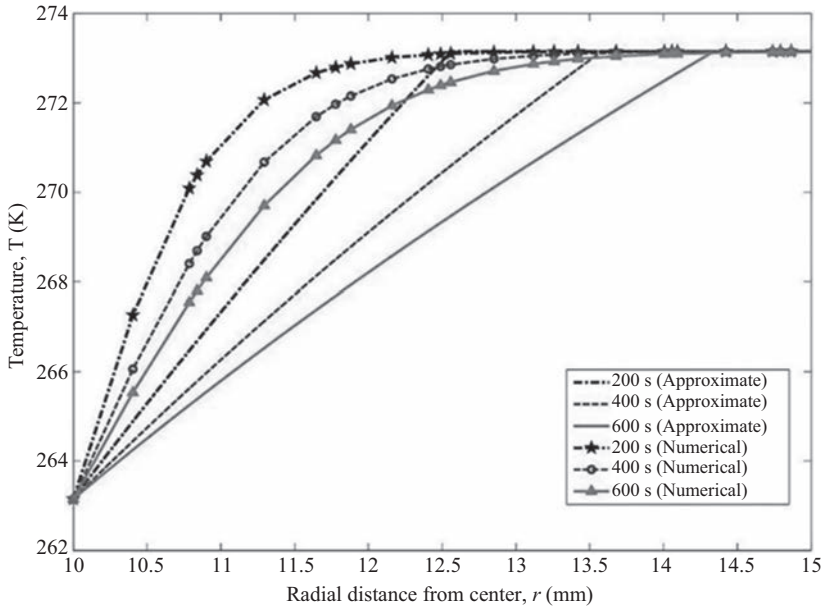

Figure 6.9 Comparison of temperature distribution of numerical vs. approximate method—case 3

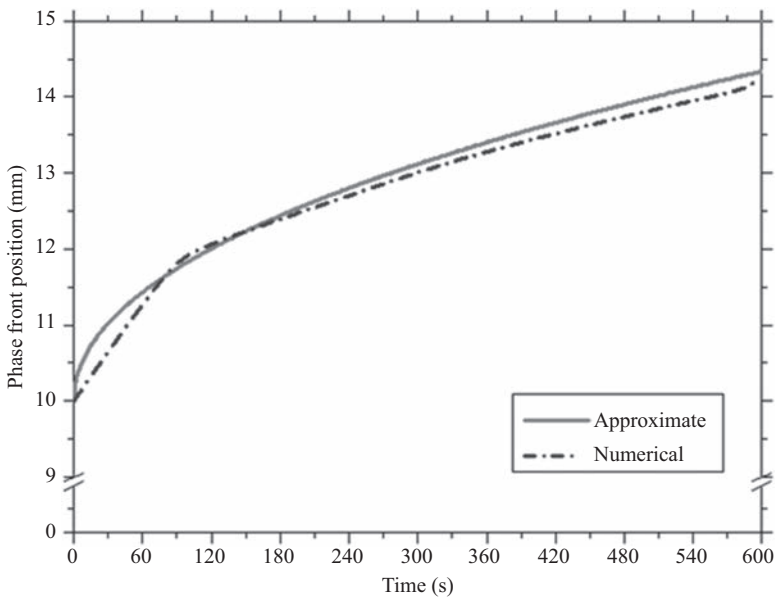

Figure 6.10 Comparison of phase front position of numerical vs. approximate method—case 3

further cases in which we will be introducing more and more realistic boundary conditions. In this case, the numerical solution gives the temperature distribution for Cartesian and cylindrical coordinates, melting the PCM from ambient-like conditions to a higher temperature. Both the problems described in this case are considered as problems of melting of PCM. The schematics for Cartesian and cylindrical problems are illustrated in Figures 6.11 and 6.12, respectively, where X and R are phase front locations in Cartesian and cylindrical coordinates, respectively.

Technical parameters for the problem in case 4 for numerical analysis are as follows:

Cartesian coordinates:

- Length = 200 mm
- Initial temperature, $T_i = 20$ °C
- Left wall temperature, $T_W = 40$ °C
- Mesh = Extremely fine
- Time range = (0:20:2,400) s

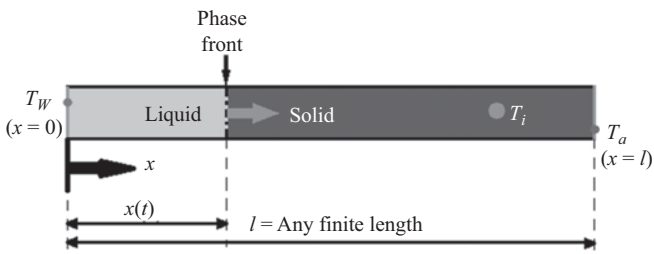

Figure 6.11 Schematic for Cartesian problem case 4

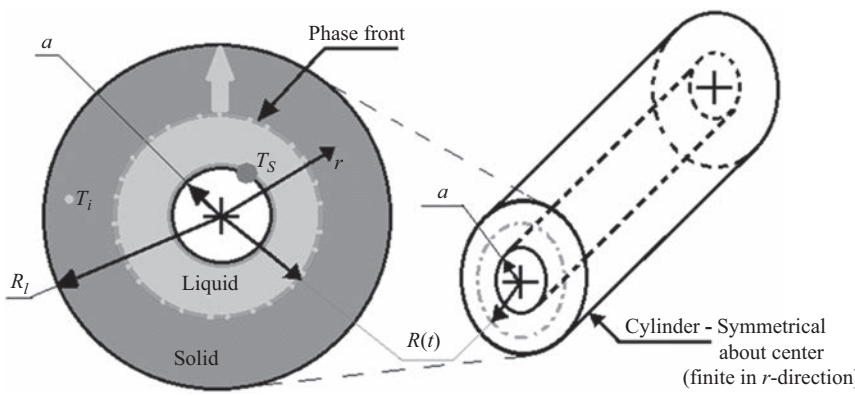

Figure 6.12 Schematic for cylindrical problem case 4

Cylindrical coordinates:

- Inner radius = 10 mm
- Outer radius = 30 mm
- Initial temperature, $T_i = 20$ °C
- Inner wall temperature, $T_S = 40$ °C
- Mesh = Extremely fine
- Time range = (0:20:2,400) s

In this case, we can observe the change in the slope in temperature distribution curves at the melting point of the PCM as the thermophysical property changes when the state of the PCM changes from solid to liquid (see Figures 6.13 and 6.14).

Case 4 shows the change in the slope in temperature distributions at the melting temperature of PCM due the change in properties of the PCM while converting from the solid to liquid state.

6.2.5 Case 5 (Cylindrical coordinates—2D—Gravity)

Models used for the analysis purpose of case 5 are "laminar flow" and "heat transfer in fluid" with transient analysis, which will be compared with a problem with conduction only (neglecting convection). Laminar flow is driven by the body force due to natural convection.

It is being assumed that the cylinder is kept in the horizontal position lengthwise, and thus the buoyancy forces are developed in the plane perpendicular to the

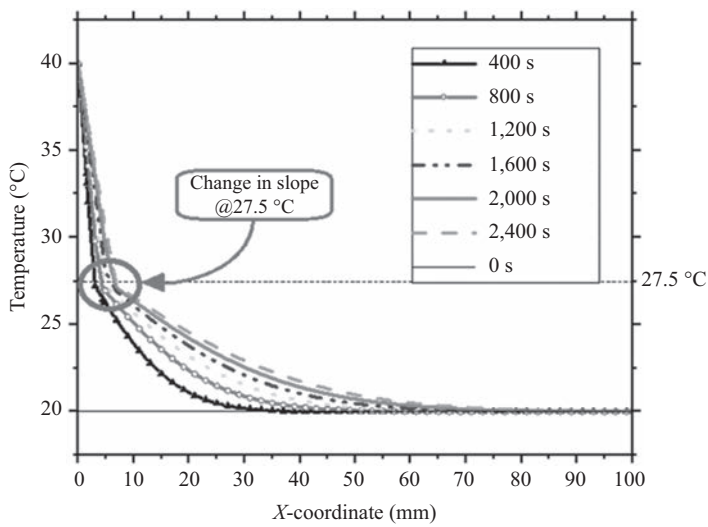

Figure 6.13 Temperature distribution for PCM (Cartesian coordinates)—case 4

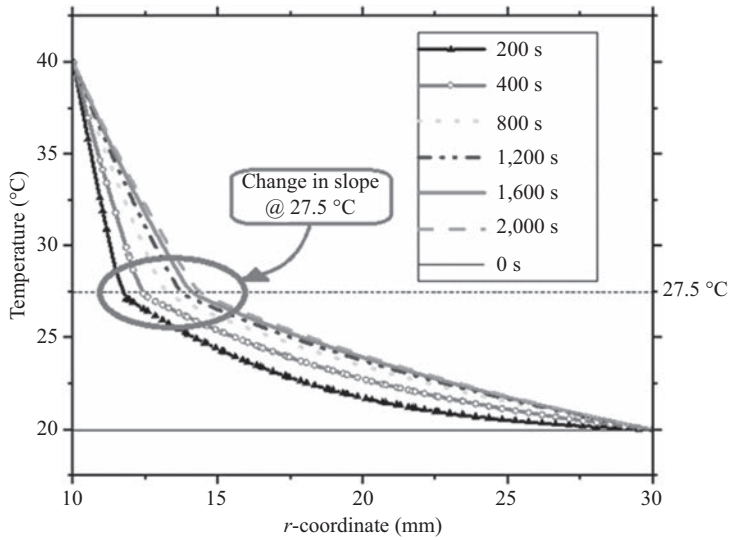

Figure 6.14 Temperature distribution for PCM (cylindrical coordinates)—case 4

axis of cylinder (in the vertical direction). Selected parameters while defining the problem are as follows:

- Inner radius = 25 mm
- Outer radius = 50 mm
- Initial temperature, $T_i = 27.5$ °C
- Inner wall temperature, $T_{in} = 60$ °C
- Outer wall temperature, $T_{out} = 30$ °C
- Convective heat transfer coefficients, h
- $h_{in} = 20$ W/m^2 K and $h_{out} = 10$ W/m^2 K
- Mesh = Finer
- Time range = (0:1:200) min

The only case in this chapter which includes natural convection is accounted with phase transformation process. This case gives the comparison of phase transformation with and without the consideration of natural convection.

It can be observed from Figure 6.15 that initially due to dominant convective currents, the melting rate is higher in the problem in which gravity is accounted. However, in the problem accounting natural convection, the heat accumulates in the upper part of the geometry. Due to which the bottom part of the cylinder takes comparatively more time to melt than that of the upper part, because most of the heat transferred to the bottom part is through conduction only.

Case 5 depicts the effects of considering natural convection or the effects of gravity with cylindrical 2D geometry. It has been observed that the hot liquid octadecane is getting accumulated in the upper area due to the setup of convective

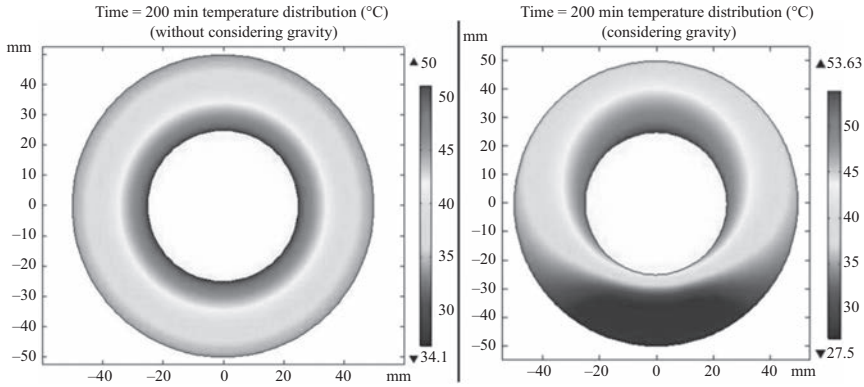

Figure 6.15 Comparison of temperature distributions—case 5

eddy currents/density differences, and thus it results in the maximum solid octadecane melting in the upper region first.

6.3 Energy-efficient buildings: An application of latent heat TES

The aim of energy-efficient buildings can be achieved using either the concept of PCM impregnated into the wallboards, concrete blocks, or underfloor heating with PCM [26]. In this section, we will be carrying out COMSOL simulations over a brick wall with PCM envelopes with more and more realistic boundary conditions progressively.

6.3.1 Validation of COMSOL simulations for a simple brick wall

In this problem, a simple brick wall is being analyzed and the solution form COMSOL will be compared to that of the analytical method with identical boundary conditions which consider the solar heat gain from the right side of the wall (Figure 6.16).

Table 6.4 states the properties for air and brick.

Transient parameters for analysis:

- Time for analysis $t = 24$ h
- Time steps $dt = 0.1$ h

Assumptions:

- Brick wall (Cartesian coordinates).
- One dimensional.
- Only conduction is considered with a heat generation term which is required for a phase transformation process.

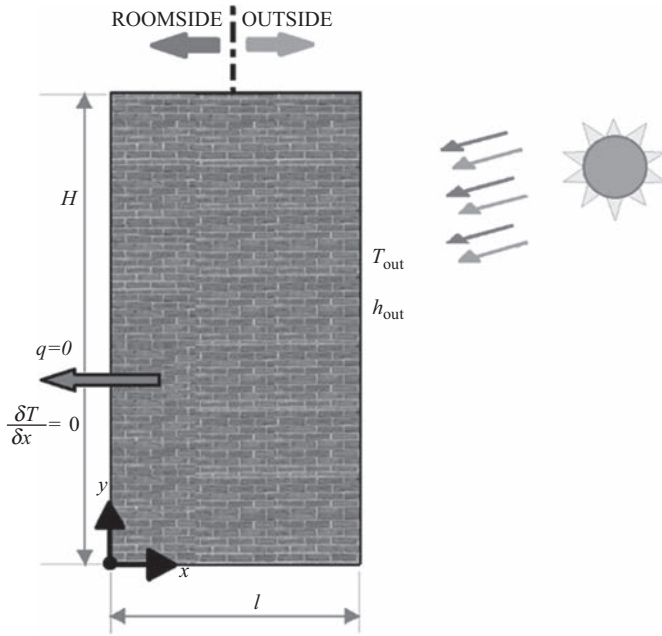

Figure 6.16 Schematic of model for analytical validation

Table 6.4 Properties of air and brick

Properties	Air	Brick
Thermal conductivity (k)	0.0257 W/m K	0.5 W/m K
Density (ρ)	1.205 kg/m^3	2,000 kg/m^3
Specific heat (C_P)	1,005 J/kg K	900 J/kg K

- Free convection/gravitational effect is not considered in this problem.
- Length of the wall (in the plane perpendicular to the paper) is assumed to be infinite.

Boundary conditions:

- At $x = 200$ mm, $T_{out} = 45$ °C, $h_{out} = 10$ W/m^2 K
- At $x = 0$, $\frac{\partial T}{\partial x} = 0$
- At $t = 0$ s, $T_i = 25$ °C

Dimensions:

- $l = 200$ mm
- $H = 1{,}000$ mm (semi-infinite dimension)

The approximate analytical solution [51] can be depicted by

$$\theta(x,t) = Ae^{-\gamma^2\tau}\cos\left(\gamma\frac{x}{l}\right) \tag{6.9}$$

The obtained graphs show the temperature distributions along the thickness of the brick wall. The validation of the COMSOL solution with the analytical method can be easily observed from Figure 16.17.

The temperature distribution curve at 4 h of analytical solution is the curve with the highest error among all other curves. It is due to the approximate nature of the solution which imposes a limitation over the result such that nondimensional time (τ, also termed as Fourier number) should be more than 0.2 value for getting accurate results with less amount of error.

6.3.2 *Numerical model for thermal analysis of PCM in brick walls*

In this problem, the brick wall is incorporated with a PCM layer in between with a specific thickness. Analysis carried out will be used to compare the results of transient temperature distributions of brick walls with PCM experiencing solar heat gain against the results of transient temperature distributions of simple brick walls (without PCM) experiencing similar boundary conditions (Figure 6.18).

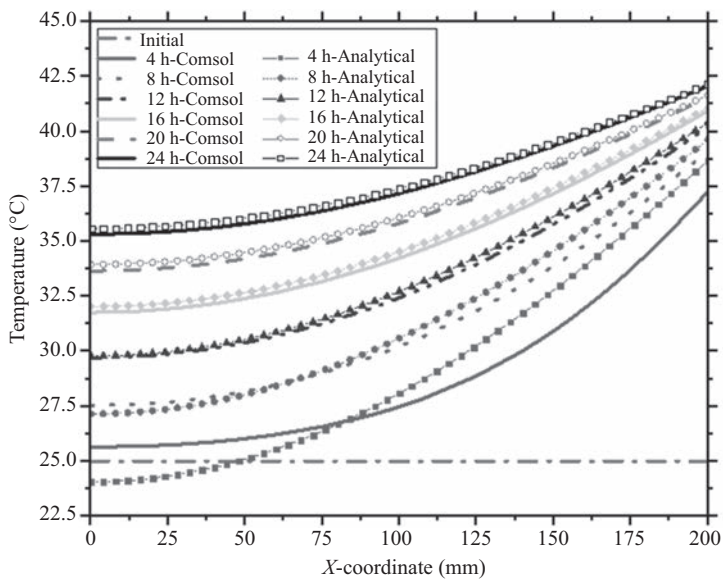

Figure 6.17 Temperature distribution for brick wall: comparison of COMSOL vs. analytical (approximate) method

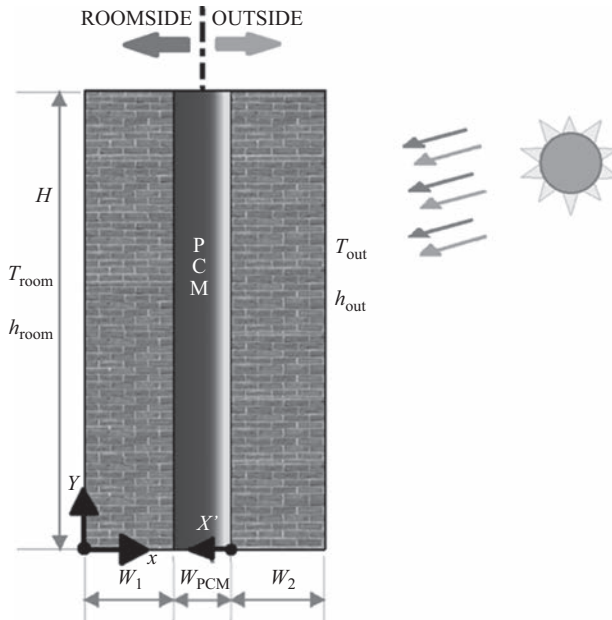

Figure 6.18 Schematic of the model for thermal analysis of brick wall with PCM

Transient parameters for analysis:

- Time for analysis $t = 24$ h
- Time steps $dt = 0.1$ h

Assumptions:

- One dimensional.
- Only conduction is considered with a heat generation term which is required for a phase transformation process.
- Free convection/gravitational effect is not considered in this problem.
- Length of the wall (in the plane perpendicular to the paper) is assumed to be infinite.

Boundary conditions:

- At $x = 200$ mm, $T_{out} = 45$ °C, $h_{out} = 10$ W/m^2 K
- At $x = 0$ mm, $T_{room} = 25$ °C, $h_{room} = 5$ W/m^2 K
- At $t = 0$ s, $T_i = 25$ °C

Dimensions:

- $W_1 = W_2 = 75$ mm (brick wall thickness)
- $W_{PCM} = 25$ mm (PCM layer thickness)
- $H = 1{,}000$ mm (semi-infinite dimension)

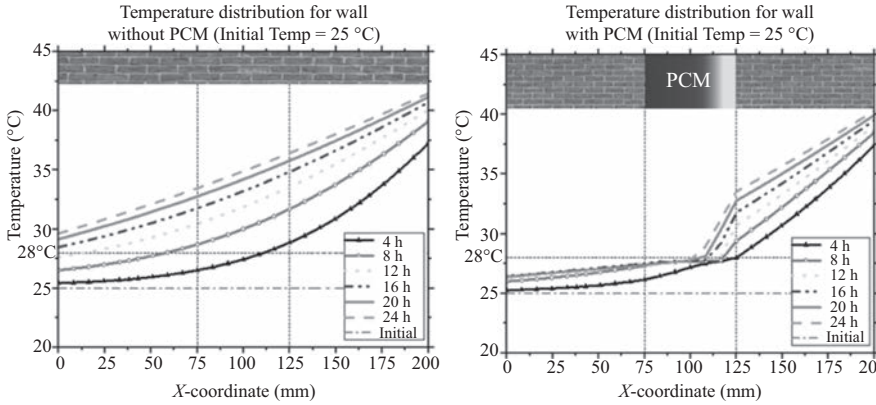

Figure 6.19 Comparison of temperature distributions

We can observe that in Figure 6.19, the results of temperature distributions of the brick wall with the PCM case is compared with the simple brick wall case. In both the cases, similar boundary conditions have been taken.

The results reveal that the problem of brick wall containing the PCM layer after comparing to a simple brick, change in room-side temperature can be easily observed, i.e., approximately a 4 °C reduction in room temperature is achieved in the case of brick wall with PCM.

6.3.3 Numerical model for thermal analysis of PCM in brick walls (considering gravitational/buoyancy effects)

In this problem, we will be considering the buoyancy forces produced due to density differences inside the molten liquid PCM. The remaining problem will be as same as Section 6.3.2. Analysis carried out will be used to observe the effects of gravitational forces on the overall performance of a PCM incorporated brick wall in which PCM is utilized as a thermal barrier. The results of this subsection will be compared with that of the previous subsection for better understanding.

Transient parameters for analysis:

- Time for analysis $t = 24$ h
- Time steps $dt = 0.1$ h

Assumptions:

- Two dimensional.
- Free convection/gravitational effect is considered for this problem.
- Length of wall (in the plane perpendicular to the paper) is assumed to be infinite.

Boundary conditions:

- At $x = 200$ mm, $T_{out} = 45$ °C, $h_{out} = 10$ W/m^2 K
- At $x = 0$ mm, $T_{room} = 25$ °C, $h_{room} = 5$ W/m^2 K
- At $t = 0$ s, $T_i = 25$ °C

Dimensions:

- $W_1 = W_2 = 75$ mm (brick wall thickness)
- $W_{PCM} = 25$ mm (PCM layer thickness)
- $H = 1{,}000$ mm (semi-infinite dimension)

From Figures 6.20–6.22, we can observe that there is a change in the temperature profile due to the consideration of gravitational forces. The temperature profile is tilted/inclined inside the PCM passage inside the wall gap. As we know that in both the cases, similar boundary conditions have been taken, the following comparison will lead us to a meaningful observation.

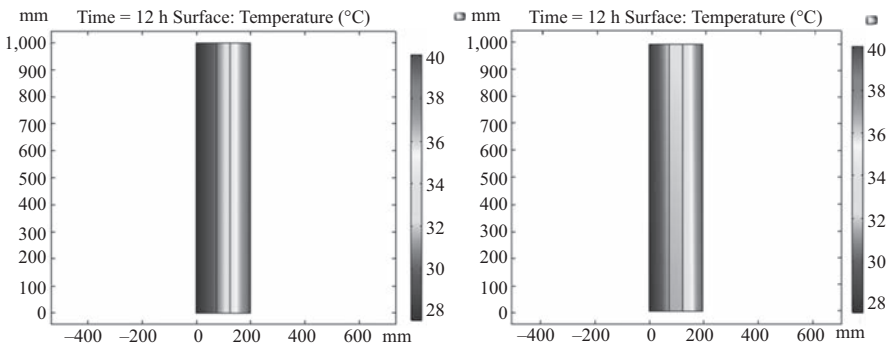

Figure 6.20 Comparison of temperature distributions (@ $t = 12$ h)

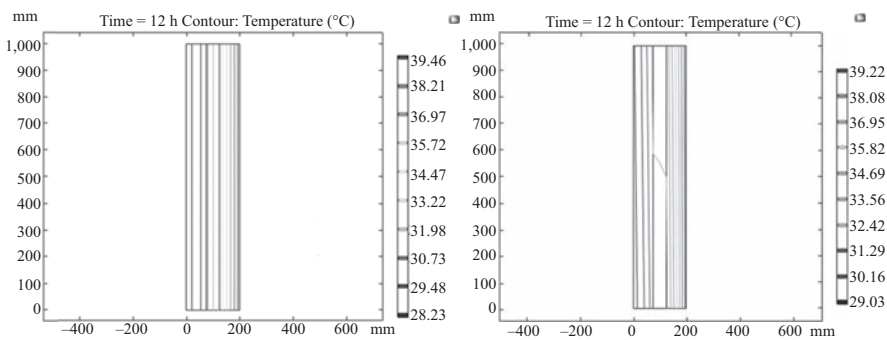

Figure 6.21 Comparison of isotherms distributions (@ $t = 12$ h)

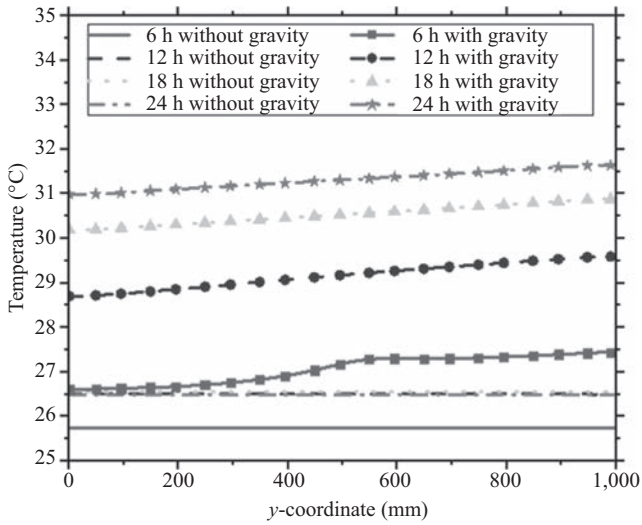

Figure 6.22 Comparison of temperature distribution within the brick wall (@ x = 10 mm)

From Figure 6.22, we can observe the difference between the transient temperature distribution within 24 h in both conditions, first without considering gravity and the latter one considering gravity. The results reveal that the problem of brick wall containing the PCM layer considering gravitational effects will transfer the heat more effectively, and thus it is not advised to enhance the gravitational phenomenon inside the PCM passages.

With the consideration of gravity in the problem, it results in the increase in the inside wall temperature as compared to the earlier case—with no consideration of gravity. Rigorous buoyant forces speed up the melting process in the upper part of the PCM layer, which results in the increase in heat being transferred to the inside wall. In order to prevent enhanced heat transfer due to any significant buoyancy effect inside the PCM layer, generally microencapsulated PCM particles are used which will successfully suppress the major gravitational effects.

6.3.4 Numerical model for thermal analysis of PCM in brick walls (with more realistic boundary conditions)

In this problem, the brick wall is incorporated with a PCM layer in between with a specific thickness, the same as that of the previous subsections. The only difference in this case is—the dimensions chosen are taken from the literature and the boundary conditions applied on both inside and outside with respect to the wall are more realistic. This problem can give us a substantial understanding of the effective utilization of PCM with the walls in order to lower down the in-house cooling load. Analysis carried out will be used to compare the results of transient temperature distributions of the brick wall with PCM experiencing solar heat gain against the

results of transient temperature distributions of simple brick wall (without PCM) experiencing similar boundary conditions.

Transient parameters for analysis:

- Time for analysis $t = 24$ h
- Time steps $dt = 0.1$ h

Assumptions:

- One dimensional.
- Only conduction is considered with a heat generation term which is required for a phase transformation process.
- Free convection/gravitational effect is not considered in this problem.
- Air is assumed as a stationary medium, i.e., without convection.
- Length of the wall (in the plane perpendicular to the paper) is assumed to be infinite.

Boundary conditions:

- At $x = 150$ mm, $q = 500$ W/m^2 and $T_{out} = 45$ °C, $h_{out} = 10$ W/m^2 K
- At $x = -150$ mm, $\frac{\partial T}{\partial x} = 0$
- At $t = 0$ s, $T_i = 25$ °C

Dimensions:

- $W_1 = W_2 = 60$ mm (brick wall thickness)
- $W_{PCM} = 30$ mm (PCM layer thickness)
- $W_{air} = 150$ mm (air layer thickness)
- $H = 500$ mm (semi-infinite dimension)

Dimensions used in the problem are taken after referring some similar problems from the literature [31,52] (Figure 6.23).

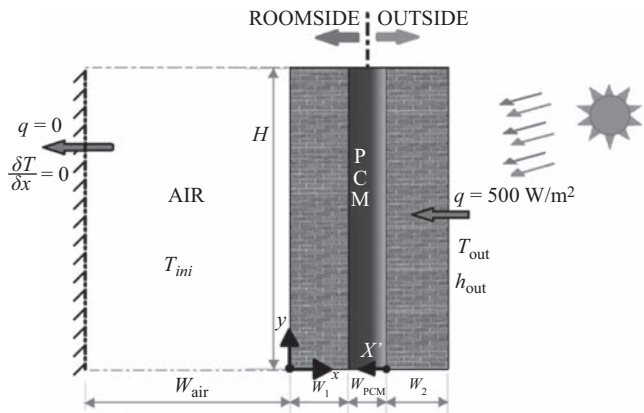

Figure 6.23 Schematic of model for thermal analysis of brick wall with PCM

First, results will be plotted depicting temperature distributions along the bricks and air passage in Figure 6.24. We can observe that the phase front crosses the thickness of 30 mm in approximately 10 h, after which all the PCM layer converts into liquid. However in Figure 6.25, results of temperature distributions of brick wall with the PCM case is compared with the simple brick wall case. In both the cases, similar boundary conditions have been taken.

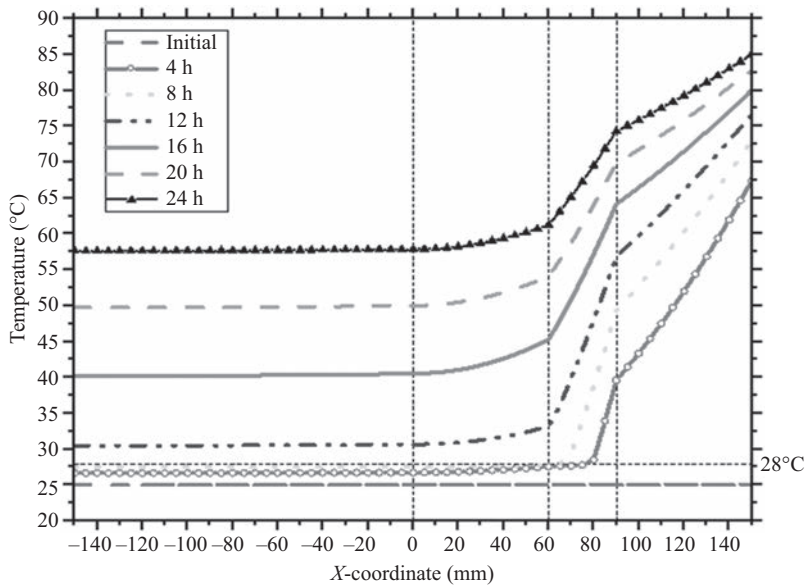

Figure 6.24 Temperature distributions for brick wall with PCM (including air passage)

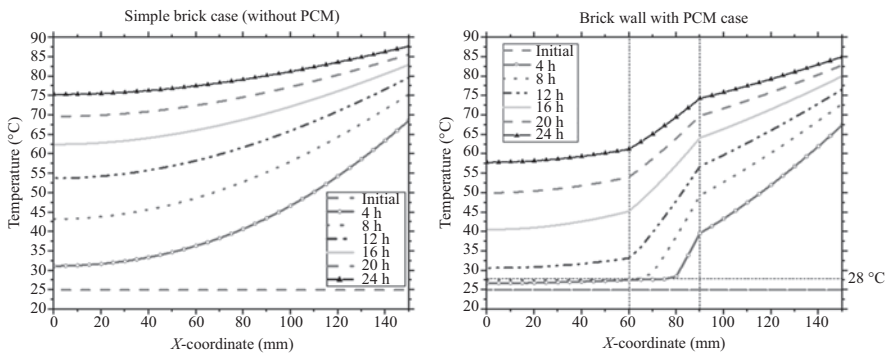

Figure 6.25 Comparison of temperature distributions (inside wall only)

The results reveal that the problem of brick wall containing the PCM layer after comparing to a simple brick, change in room-side temperature can be easily observed, i.e., approximately 15 °C reduction in room temperature is achieved in the case of brick wall with PCM.

6.4 Conclusion

The PCM appears to be a promising solution, since in latent form it can store and release more energy than the sensible energy stored by most of the construction materials. Initially, in this study (Section 6.2), the focus is kept on the thermal analysis of latent heat thermal storages using PCM, with different combinations of various geometries and boundary conditions. From Section 6.2, we have studied about the behavior of PCM with various combinations of surrounding environments. According to the study carried out in Section 6.3, it was an attempt to make use of PCM and their behavioral properties in some practical life application like energy-efficient buildings. It can be clearly observed that PCM helps regulating the thermal load on the building walls in order to maintain the average indoor temperature around the required room temperature.

Thermal analysis showed that the utilization of PCM into building wall envelopes is effectively successful in shifting cooling as well as heating load to off-peak of the electricity demand period from the high peak demand period. It is also capable of efficient storage of thermal energy through solar radiations which will be useful during cloudy days or at night. From the results after designing the problem of the PCM layer in the brick wall, we can conclude that PCM can improve the thermal behavior and energy efficiency of the building.

From the results after designing various problems of PCM, we can conclude that PCM can improve the thermal behavior and energy efficiency of building. The results reveal the following:

- Different effects of various boundary conditions on PCM structures.
- In the problem of brick wall containing the PCM layer after comparing to brick wall without PCM, the change in room-side temperature can be easily observed (approximately 15–25 °C).

In the case of energy-efficient buildings, PCM is utilized as a thermal barrier in combination with the wall. Thus, gravitational effects which lead to rigorous heat transfer must be suppressed using PCM microencapsulation techniques. The selection of PCM must be done according to their phase change temperature; it should be closer to the required average room temperature with appropriate properties such as latent heat and thermal conductivity. This kind of technology can save a large amount of energy usage in the building sector. The focus must be kept on designing an efficient construction planes with PCM incorporated into the walls (concrete or brick) with the proper consideration of the corresponding thermal aspects.

6.5 Future scope

- Enhancing the effective properties of PCM which will ultimately increase the effectiveness of solar TES systems. By using the techniques such as
  - Encapsulation
  - Cascaded TES
  - Addition of nucleating agents (e.g., Borax)
- Performing experiments in order to validate the simulations.
- Analysis of nano-encapsulated PCM structures, which can be suspended in fluids to be used for TES as well as heat transfer fluids.

References

[1] S. A. Kalogirou, "Solar thermal collectors and applications," *Prog. Energy Combust. Sci.*, vol. 30, no. 3, pp. 231–295, 2004.

[2] V. Bhalla and H. Tyagi, "Parameters influencing the performance of nano-particles-laden fluid-based solar thermal collectors: A review on optical properties," *Renew. Sustain. Energy Rev.*, vol. 84, no. 2017, pp. 12–42, 2018.

[3] C. Kennedy, "Review of mid-to high-temperature solar selective absorber materials," *NREL Tech. Rep.*, pp. 1–58, 2002.

[4] V. S. Reddy, S. C. Kaushik, K. R. Ranjan, and S. K. Tyagi, "State-of-the-art of solar thermal power plants—A review," *Renew. Sustain. Energy Rev.*, vol. 27, pp. 258–273, 2013.

[5] S. Suman, M. Kaleem, and M. Pathak, "Performance enhancement of solar collectors—A review," *Renew. Sustain. Energy Rev.*, vol. 49, pp. 192–210, 2015.

[6] A. Amri, Z. Tao, T. Pryor, and C. Yin, "Developments in the synthesis of fl at plate solar selective absorber materials via sol – gel methods: A review," *Renew. Sustain. Energy Rev.*, vol. 36, pp. 316–328, 2014.

[7] F. Cao, K. Mcenaney, G. Chen, and Z. Ren, "Environmental Science A review of cermet-based spectrally selective solar absorbers," *Energy Environ. Sci.*, vol. 7, pp. 1615–1627, 2014.

[8] C. Atkinson, C. L. Sansom, H. J. Almond, and C. P. Shaw, "Coatings for concentrating solar systems – A review," *Renew. Sustain. Energy Rev.*, vol. 45, pp. 113–122, 2015.

[9] R. A. Taylor, P. E. Phelan, T. P. Otanicar, *et al.*, "Applicability of nanofluids in high flux solar collectors," *J. Renew. Sustain. Energy*, vol. 3, no. 2, p. 23104, 2011.

[10] O. Mahian, A. Kianifar, S. A. Kalogirou, I. Pop, and S. Wongwises, "A review of the applications of nanofluids in solar energy," *Int. J. Heat Mass Transf.*, vol. 57, no. 2, pp. 582–594, 2013.

[11] A. Kasaeian, A. T. Eshghi, and M. Sameti, "A review on the applications of nano fluids in solar energy systems," *Renew. Sustain. Energy Rev.*, vol. 43, pp. 584–598, 2015.

[12] P. Phelan, T. Otanicar, R. Taylor, and H. Tyagi, "Trends and opportunities in direct-absorption solar thermal collectors," *J. Therm. Sci. Eng. Appl.*, vol. 5, no. 2, p. 021003, 2013.

[13] F. Gomez-garcia, J. González-aguilar, G. Olalde, and M. Romero, "Thermal and hydrodynamic behavior of ceramic volumetric absorbers for central receiver solar power plants: A review," *Renew. Sustain. Energy Rev.*, vol. 57, pp. 648–658, 2016.

[14] T. B. Gorji and A. A. Ranjbar, "A review on optical properties and application of nanofluids in direct absorption solar collectors (DASCs)," *Renew. Sustain. Energy Rev.*, vol. 72, pp. 10–32, 2017.

[15] J. Duffie and W. Beckman, *Solar Engineering of Thermal Processes*, 4th ed., Hoboken, NJ: John Wiley and Sons, vol. 116, 2013.

[16] S. Kuravi, J. Trahan, D. Y. Goswami, M. M. Rahman, and E. K. Stefanakos, "Thermal energy storage technologies and systems for concentrating solar power plants," *Prog. Energy Combust. Sci.*, vol. 39, no. 4, pp. 285–319, 2013.

[17] Y. Tian and C. Y. Zhao, "A review of solar collectors and thermal energy storage in solar thermal applications," *Appl. Energy*, vol. 104, pp. 538–553, 2013.

[18] B. Zalba, J. M. Marín, L. F. Cabeza, and H. Mehling, "Review on thermal energy storage with phase change: Materials, heat transfer analysis and applications," *Appl. Therm. Eng.*, vol. 23, no. 3, pp. 251–283, 2003.

[19] M. C. Browne, B. Norton, and S. J. Mccormack, "Phase change materials for photovoltaic thermal management," *Renew. Sustain. Energy Rev.*, vol. 47, pp. 762–782, 2015.

[20] A. Sharma, V. V. Tyagi, C. R. Chen, and D. Buddhi, "Review on thermal energy storage with phase change materials and applications," *Renew. Sustain. Energy Rev.*, vol. 13, no. 2, pp. 318–345, 2009.

[21] C. Y. Zhao, W. Lu, and Y. Tian, "Heat transfer enhancement for thermal energy storage using metal foams embedded within phase change materials (PCMs)," *Sol. Energy*, vol. 84, no. 8, pp. 1402–1412, 2010.

[22] R. Velraj, R. V. Seeniraj, B. Hafner, C. Faber, and K. Schwarzer, "Heat transfer enhancement in a latent heat storage system," *Sol. Energy*, vol. 65, no. 3, pp. 171–180, 1999.

[23] M. M. Farid, A. M. Khudhair, S. A. K. Razack, and S. Al-Hallaj, "A review on phase change energy storage: Materials and applications," *Energy Convers. Manag.*, vol. 45, no. 9–10, pp. 1597–1615, 2004.

[24] S. Kondaraju, E. K. Jin, and J. S. Lee, "Direct numerical simulation of thermal conductivity of nanofluids: The effect of temperature two-way coupling and coagulation of particles," *Int. J. Heat Mass Transf.*, vol. 53, no. 5–6, pp. 862–869, 2010.

[25] Y. Z. Ã, G. Zhou, K. Lin, Q. Zhang, and H. Di, "Application of latent heat thermal energy storage in buildings: State-of-the-art and outlook," vol. 42, pp. 2197–2209, 2007.

[26] A. M. Khudhair and M. M. Farid, "A review on energy conservation in building applications with thermal storage by latent heat using phase change materials," *Energy Convers. Manag.*, vol. 45, no. 2, pp. 263–275, 2004.

[27] L. Li, M. Qu, and S. Peng, "Performance evaluation of building integrated solar thermal shading system: Active solar energy usage," *Renew. Energy*, vol. 109, pp. 576–585, 2017.

[28] G. Tsalikis and G. Martinopoulos, "Solar energy systems potential for nearly net zero energy residential buildings," *Sol. Energy*, vol. 115, no. 2015, pp. 743–756, 2015.

[29] E. Kyriaki, E. Giama, A. Papadopoulou, V. Drosou, and A. M. Papadopoulos, "Energy and environmental performance of solar thermal systems in hotel buildings," in *Procedia Environmental Sciences*, 2017, vol. 38, pp. 36–43.

[30] A. K. Pandey, M. S. Hossain, V. V. Tyagi, N. Abd Rahim, J. A. L. Selvaraj, and A. Sari, "Novel approaches and recent developments on potential applications of phase change materials in solar energy," *Renew. Sustain. Energy Rev.*, vol. 82, no. 2017, pp. 281–323, 2018.

[31] R. Vicente and T. Silva, "Brick masonry walls with PCM macrocapsules: An experimental approach," *Appl. Therm. Eng.*, vol. 67, no. 1–2, pp. 24–34, 2014.

[32] L. F. Cabeza, C. Castellón, M. Nogués, M. Medrano, R. Leppers, and O. Zubillaga, "Use of microencapsulated PCM in concrete walls for energy savings," *Energy Build.*, vol. 39, no. 2, pp. 113–119, 2007.

[33] M. A. Izquierdo-Barrientos, J. F. Belmonte, D. Rodríguez-Sánchez, A. E. Molina, and J. A. Almendros-Ibáñez, "A numerical study of external building walls containing phase change materials (PCM)," *Appl. Therm. Eng.*, vol. 47, pp. 73–85, 2012.

[34] N. Zhu, P. Liu, P. Hu, F. Liu, and Z. Jiang, "Modeling and simulation on the performance of a novel double shape-stabilized phase change materials wallboard," *Energy Build.*, vol. 107, pp. 181–190, 2015.

[35] M. Sayyar, R. R. Weerasiri, P. Soroushian, and J. Lu, "Experimental and numerical study of shape-stable phase-change nanocomposite toward energy-efficient building constructions," *Energy Build.*, vol. 75, pp. 249–255, 2014.

[36] F. Kuznik and J. Virgone, "Experimental investigation of wallboard containing phase change material: Data for validation of numerical modeling," *Energy Build.*, vol. 41, no. 5, pp. 561–570, 2009.

[37] K. Biswas, J. Lu, P. Soroushian, and S. Shrestha, "Combined experimental and numerical evaluation of a prototype nano-PCM enhanced wallboard," *Appl. Energy*, vol. 131, pp. 517–529, 2014.

[38] K. Biswas and R. Abhari, "Low-cost phase change material as an energy storage medium in building envelopes: Experimental and numerical analyses," *Energy Convers. Manag.*, vol. 88, pp. 1020–1031, 2014.

[39] A. Bastani, F. Haghighat, and J. Kozinski, "Designing building envelope with PCM wallboards: Design tool development," *Renew. Sustain. Energy Rev.*, vol. 31, no. 2014, pp. 554–562, 2014.

[40] A. Castell, I. Martorell, M. Medrano, G. Pérez, and L. F. Cabeza, "Experimental study of using PCM in brick constructive solutions for passive cooling," *Energy Build.*, vol. 42, no. 4, pp. 534–540, 2010.

[41] S. Álvarez, L. F. Cabeza, A. Ruiz-pardo, A. Castell, and J. Antonio, "Building Integration of PCM for natural cooling of buildings," *Appl. Energy*, vol. 109, pp. 514–522, 2013.

[42] L. Shilei, Z. Neng, and F. Guohui, "Impact of phase change wall room on indoor thermal environment in winter," *Energy Build.*, vol. 38, no. 1, pp. 18–24, 2006.

[43] M. Ahmad, A. Bontemps, H. Sallée, and D. Quenard, "Experimental investigation and computer simulation of thermal behaviour of wallboards containing a phase change material," *Energy Build.*, vol. 38, no. 4, pp. 357–366, 2006.

[44] X. Shi, S. A. Memon, W. Tang, H. Cui, and F. Xing, "Experimental assessment of position of macro encapsulated phase change material in concrete walls on indoor temperatures and humidity levels," *Energy Build*, vol. 71, pp. 80–87, 2014.

[45] P. Schossig, H. M. Henning, S. Gschwander, and T. Haussmann, "Micro-encapsulated phase-change materials integrated into construction materials," *Sol. Energy Mater. Sol. Cells*, vol. 89, no. 2–3, pp. 297–306, 2005.

[46] A. V. Sá, M. Azenha, H. De Sousa, and A. Samagaio, "Thermal enhancement of plastering mortars with Phase Change Materials: Experimental and numerical approach," *Energy Build.*, vol. 49, pp. 16–27, 2012.

[47] J. S. Sage-Lauck and D. J. Sailor, "Evaluation of phase change materials for improving thermal comfort in a super-insulated residential building," *Energy Build.*, vol. 79, p. 32, 2014.

[48] M. Kheradmand, M. Azenha, J. L. B. De Aguiar, and K. J. Krakowiak, "Thermal behavior of cement based plastering mortar containing hybrid microencapsulated phase change materials," *Energy Build.*, vol. 84, pp. 526–536, 2014.

[49] B. D. V Hale, M. M. J. Hoover, N. Lockheed, *et al.*, *Nasa Contractor Report Nasa Cr-51363*, 2017.

[50] W. R. Humphries and E. I. Griggs, *A design handbook for phase change thermal control and energy storage devices-NASA*, 1977.

[51] Y. Cengel and A. Ghajar, *Heat and Mass Transfer*, 4th ed., New York: McGraw-Hill Education, 2011.

[52] A. Carbonari, M. De Grassi, C. Di Perna, and P. Principi, "Numerical and experimental analyses of PCM containing sandwich panels for prefabricated walls," *Energy Build.*, vol. 38, no. 5, pp. 472–483, 2006.

Chapter 7

Insulation materials

Özgür Bayer[1]

Insulation is a key component of green building design. A well-insulated home should keep your space warm in the winter and cool in the summer, and this in turn cuts down carbon emissions linked to global climate change. In terms of energy efficiency, investing in high levels of insulation materials for your home is more cost-effective than investing in expensive heating technologies. Insulation materials work by resisting heat flow, measured by an *R*-value (the higher the *R*-value, the greater the insulation). *R*-value depends on the type of insulation, its thickness, and its density. In this sight, this study draws attention to the importance of building insulation materials in green buildings' sustainable energy performance.

7.1 Introduction to insulation materials in green buildings

The concept of green building can be defined as the precautions which increase the efficiency of usage of water, energy and material while decreasing the building's impacts on the environment. When looking at a residential building from outside, insulation of the building is not one of the stunning components that attract attention. However, the insulation of the building is the most important component which is the effect of the building being more comfortable and having higher performance. Insufficient insulation of the building leads to energy loss during heating and cooling processes, resulting in an inefficient system. Green building insulation leads to saving energy consumption and also helps in regulating the health of the people. Problems that threaten human health such as mould problems arise as a result of inappropriate insulation. Therefore, insulation of buildings is an important issue, many of which have to be emphasized.

Most of the heat losses appear on the largest external part of residential buildings including walls, roofs, foundations and floors. Not only do proper insulations keep excess heat out in hot weather and limit the heat loss in cold

[1]Dept. of Mech. Eng., Middle East Technical University, Turkey

conditions, but they also provide comfort indoors. There are various kinds of insulation materials for different applications.

The healthiest insulation type for human as well as the most favourable one for the environment is Green Building Insulation. Although it is not exactly a type of insulation, it is a perspective that allows the building to be more comfortable, more economical and longer lasting from the construction of the building to its daily use in daily life. Therefore, in order to protect sustainability, natural and local materials with less waste are used so that the pollution during construction and after construction is reduced to a minimum [1–3].

In short, insulation is the key to energy preservation, a headstone of green buildings. Insufficiently insulated or uninsulated buildings waste lots of energy. On the other hand, well-insulated buildings save energy and set down operating costs but also keep places more comfortable and healthy for people.

Comparing *R*-values is one way of choosing one type of insulation over another, these numbers can be misleading when site conditions and construction techniques are not factored in. Insulation is a basic building component that is difficult to alter after the fact. Although houses can be retrofitted to add more insulation, the process is expensive and often difficult. Recommended *R*-values from such sources as in the US Department of Energy should be viewed as bare minimums, not maximums. Well-insulated, well-sealed houses need effective ventilation. Buildings without insulation located specifically in cold climates provide maximum potential to save energy, because one can get the highest level of energy savings from the first set up of insulation. From new buildings in developing countries without insulation, we can also save important amount of energy [3].

7.2 Evolution of insulation materials

7.2.1 Historical development of insulation materials in green building concept

Although in the last decade green building movement gained momentum, the first applications can be tracked to the nineteenth century. Regarding David Gissen, who is an architect in National Building Museum in Washington, DC, structures such as Crystal Palace in London used methods which aim to lower the effect of building on environment [4,5]. For some old buildings, ventilation systems attached on the roofs and air conditioners located underground had been used to adjust inside air temperature. In addition, deep-set windows were used in New York Times building in New York. Both of these techniques were very useful for conditioning the indoor temperature while reducing the buildings' effect on environment. The cooling methods mentioned above led the architecture from the 1930s through 1960s. With the onset of air-conditioning devices, construction steels and special glasses, glass-covered and steel buildings became popular. These buildings can be air-conditioned

with enormous HVAC systems, consuming huge amounts of cheap fossil fuel. The significant energy consumption in these buildings made the residents very curious and careful about the budget.

Around the 1970s, environmental concerns and increasing fuel costs inspired some architects, ecologists and environmentalists. These two issues have started the green building movement. The First World Day gave this inexperienced building concept an opportunity, but in 1973, the oil embargo provided the environmental movement that meant the struggle of the green building. With the gas lines for the blocks, people began to question whether they should trust the fossil fuels very independently for their energy. As a result of oil embargo, American Institute of Architects formed two subgroups about energy. The first group was responsible for saving energy by exploring the concept of useful positioning of reflective roofing materials and buildings in terms of environment, while the other group was looking for technological solutions like three-glazed windows. The green building movement slowed down for some periods in which energy concepts were not popular, but it is possible to talk about some green building applications that were developed during the 1970s such as Gregory Bateson building which was driven by environmental-friendly and energy-sensitive solar batteries in California, using underground lawns and sunlight, and underground rock storage cooling systems and field climate control equipment. From the end of the 1970s to 1990s, research on the concept of the green building accelerated and focused on the efficiency. These investigations have resulted in new design solar panels, special building units, prefabricated wall systems and the use of light in weight windows for saving energy throughout the day [4,5].

Thermal insulation materials which are not natural need energy mostly obtained from fossil fuels in their production stages. Therefore, demand for natural thermal insulation materials is increasing. It is possible to divide the development of thermal insulation materials into three different time periods. Each period began with an important step in the historical development of mankind, science or industry [5].

The first period reflects the industrial revolution. In this period; natural and artificial insulation materials started to appear and bricklaying elements were developed. In the second half of 20th century, plastics became popular and plastic foams instead of natural insulation materials were widely used. After 2000, revival of natural materials was observed with new materials based experimental research [5].

7.2.2 Research and development efforts

Everyday new technologies produce new insulation materials. New ones are thinner, have lower value, are more resistant to demolishing powers (bacteria, humidity, higher temperature, etc.) and composite (at least two or more materials). Future insulation materials will allow buildings to breathe better which affects human health

positively. Thermal resistance gets stronger with the help of a thick insulation layer and by reducing thermal conductivity [6].

Thermal insulation materials as well as solutions must have as low conductivity as possible, and they should not increase much in 100 years or longer periods. Besides, even piercing these materials by some objects such as nails should not change the low level of conductivity except for local heat bridges. Vacuum-based technologies may not work well in this sense for a long time because of loss of vacuum and moisture uptake.

It is important for the future heat insulation materials to be cut off as an adoption site without losing anything from the thermal insulation performance. Some other features also need to be addressed. These include, but are not limited to, mechanical strength (e.g. compressive and tensile strength) or other protective ways, emitting smoke during fires, preferably during those which do not release toxic gases, fires where toxic gases should not be released, resistance to climatic conditions with various climate exposures, dissolution cycles and water and competitive prices against other thermal insulation materials. Summarized information for various features with the requirements recommended can be found in literature [7,8].

For instance, being able to reduce the λ of a material cannot be considered as an innovative act when the resistance of fire becomes worse or when there is a significant increase in the cost. What will be regarded as an innovation is reducing the λ value up to 10%. The followings should be the topics of further research for other features:

- For the fibre materials that are inorganic/not organic, there should be more focus on limiting dust and fibre emissions as well as on the use of binders. Moreover, materials may help decreasing the consumption of energy in production.
- For organic foamed materials like extruded polystyrene (XPS), removal of chlorofluorocarbons (CFCs) and hydrochlorofluorocarbons (HCFCs) from the feedstock is critical, so as to cancel CFCs and HCFCs, which are as yet utilized by numerous makers, and to diminish the utilization of CO_2 as a substitute of the CFCs and HCFCs. A conceivable cost decrease would be a noteworthy point in making this material more competitive.
- Another research point for both expanded polystyrene (EPS) and XPS is the development of a possible fire reaction by using certain additives. Nevertheless, they contribute to a rise in the λ value. Care on the toxicity should be considered especially in the case of polyurethane and fire [3].
- For existing buildings, some skilful and flexible composite materials such as, plaster, foils, particle and chipboard, aluminium plates may be a necessity. At this point determination of the mechanical properties of these insulation materials will be researched. In this regard, the most significant aspects of new developments are placed into insulation products. In order for these interventions which are always sensitive issues depending on the present energy prices to be feasible, this step is particularly important.

- As the last point, the level of progress in harmonizing the methodologies and concerns for environmental effects of all materials should be considered. Adaptation of the technique and energy usage in production are obvious concerns for insulation materials just as in other aspects when a life cycle analysis is applied [9,10].

7.3 Categorization of insulation materials

Insulation materials diverge into different groups such as synthetic, natural and novel new technology materials (Figure 7.1).

7.3.1 Natural insulation materials

7.3.1.1 Sheep's wool

Regarding insulation, sheep's wool is additionally handled with borate in order to withstand heat, mould and pests. Sheep's wool can hold big amount of water in it. This might be an advantage for some applications. On the other hand, borate can leave the system through the wet and dry cycles, and this phenomenon is not desired. Sheep's wool can be in different stat-framed wall structure with different *R* values [12].

The elastic characteristic of the material results in different usage as floating floors. Sheep's wool thermo physical properties may vary. Density of it is at most 0.054 W/mK and specific heat value for it is between 1.3 and 1.7 kJ/kgK. One can rely on sheep's wool thermal insulation characteristics in winter conditions, but for summer, insulation behaviour might be poor [13].

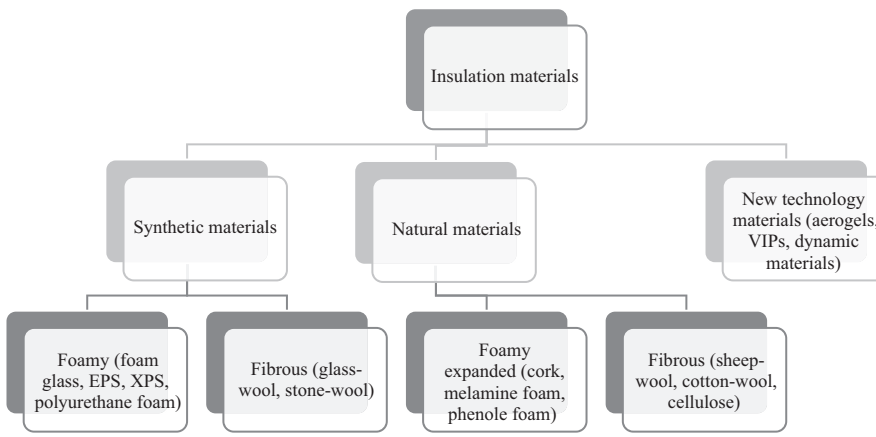

Figure 7.1 Most commonly used insulation materials (Adapted from [11])

Recycled wools are used for the manufacturing insulation materials; also, fibres can be combined with polyester or polypropylene grid [14].

The acoustic absorption property of these materials is quite stunning. The measurements showed that for frequencies above 500 Hz, the samples had sound absorption coefficient greater than 0.8, and they led to an improvement of sound-reduction index with a value of 6 dB. These insulation materials have high hygroscopicity values as well [15].

7.3.1.2 Flax and hemp

Linum usitatissimum L. and *Cannabis sativa* L. known as flax and hemp, respectively, are fibre plants. These plants have stems with surface layers, bark layer with bundles up to 50 layer and the core layer. The bast fibre bundles forming the bark layer of the plant are commonly used thermal insulation materials. However, in old buildings, the core layer had been used as insulation material as well. Additionally, tow of flax and hemp fibres are known to be used in insulation tapes between timbers of early constructions [16]. Both insulation materials have thermal conductivity, density and specific heat values in the range of 0.038–0.060 W/mK, 20–90 kg/m^3 and 1.6–1.7 kJ/kgK, respectively [13]. Similar to natural materials, hemp-based insulation substances absorb humidity of the air which leads to an increase in thermal conductivity. Related studies on hydrophobic additives and biodegradability were carried out in literature [17,18]. Acoustic characterization of an innovative combination of binder, hemp chips, and water was also performed by Glé *et al.* [19]. The waste of these insulation materials can be recycled, disposed of at refineries or at regular storage sites in energy facilities [19].

7.3.1.3 Cellulose

Cellulose is a – for the most part – reused item produced using the daily papers and other cellulose filaments. It is a standout amongst the most favoured materials of regular manufacturers. As a free fill, it may be utilized for walls, floors and rooftops very well; and is likewise accessible in blankets, sheets and batts. It contains borate as an additive such as hemp and flax. There are many brands which use cellulose as insulation materials such as Warmcell and Ecocell.

7.3.1.4 Cotton

Cotton insulation contains mostly recycled cotton and a small amount of fibre. Cotton insulating borate is used since it retards flames, repels insects and rodents as in cellulose insulation. Because of the high content of recycled materials, minimum energy is used to produce this product. Cotton insulation should be made in batts and the price of it is about 15%–20% higher than glass fibre insulation [12].

7.3.1.5 Straw

In the exquisite plains of the United States 150 years ago, the renowned straw bale construction attracted renewed interest. The system of forming boards from straw with no adhesives was developed within the 1930s. Thickness of straw panels is changing between two and four inches. The forums tended to make successful sound-absorbing

boards for inside segments. A few producers have advanced basically insulated boards from a few layered and compressed straw boards [12].

7.3.1.6 Wood fibre

It is produced by using wood chips that are made of wood and compressed into sheets or batts by utilizing regular resin or water as a cover. It has low exemplified vitality and uses outgrowth from the forest service industry. Precedents include pavatex, thermowall and homatherm.

7.3.1.7 Expanded clay aggregate

It is small fired clay pellets that develop into lightweight, permeable and weight-bearing when they extend at high temperatures. These materials can be utilized in foundations as an insulator and aggregate. They have high embodied energy but excellent thermal insulation properties.

7.3.2 Synthetic insulation materials

Synthetic insulation materials are man-made. Synthetic insulation materials are generally better than the natural ones due to the fact that synthetic materials have higher humidity resistance, lower conductivity (heat transfer ratios are lower), bacteria resistance and better durability.

7.3.2.1 Polystyrene insulation materials

Foam board, bead board insulation and concrete insulation materials are mostly produced from polystyrene which is a colourless, transparent thermoplastic. Moulded extended polystyrene, in forms of small foam beads, is the raw material for foam board insulation. They are mostly poured into wall cavities or blocks of concrete. Luckily, foam beads are very light, without any static electric problem and tough enough to manipulate [12].

Other polystyrene insulation materials are EPS and XPS. EPS is again formed as small plastic beads, but XPS is a molten fabric that is produced as sheets [20,21]. XPS is commonly handled as foam board insulation, whereas EPS is mostly applied in blocks. After production, the *R*-value of XPS insulation may decrease due to the fact of replacement of gasoline by air. It is not possible to mention any stunning acoustic characteristics of it since it has low density and closed porosity. The raw material is flammable; therefore, a fire retardant is frequently used during production. One can find these insulation materials in panels in the market, so they can easily be handled and shaped [13]. Researchers figured out that thermal conductivity of EPS changes drastically with humidity. The more the humidity, the higher the thermal conductivity of EPS is [22]. Compared to EPS, XPS absorbs less moisture with higher specific heat (1.3–1.7 kJ/kgK). XPS costs more than EPS.

7.3.2.2 Polyurethane insulation materials

Obtained by an exothermic reaction between special compounds, polyurethane foam is basically a poly-isocyanic combination and is available in rigid board or

liquid spray foam forms [23]. R11, CO_2 and C_8H_{18} which are used as propellants in polyurethane insulation material production affect the thermal conductivity [11].

Polyurethane has cellular structure including gas inside with closed mobile and open cellular forms. Closed mobile foam includes fuel-filled cells with nearly no gaps, whereas open cellular foam has air-filled cells resulting in lower thermal insulation characteristic. Thermal resistance of the material may decrease within the first a few years but stays unchanged then. Additionally, *R* values can be kept nearly constant if coatings like foil and plastic are applied. Moreover, in some applications, reflective foil might help the radiation insulation. In practice spraying, liquid foam works better since moulding helps efficient insulation. Following the new production stages, closed-cell polyurethane foam insulation does not require HCFC nowadays.

Having low density, open-cell polyurethane foam has nearly constant *R* values with time. Some forms may have CO_2 as agent [12].

Sprayed polyurethane foam has the ability to fill the voids with permitting water vapour passage and still immune to moisture. Providing good airtightness, this insulation material is fire resistant [12,24]. Its thermal conductivity, density and specific heat values may range in between 0.022 and 0.040 W/mK, 15 and 45 kg/m^3, and 1.3 and 1.45 kJ/kgK, respectively [13,25].

Polyurethane in foam board or liquid foam forms can also be handled as structural insulation panels with standardized dimensions. These panels have better water vapour diffusion resistance and thermal insulation characteristics than EPS but are more expensive [12].

7.3.2.3 Polyisocyanurate insulation materials

Produced by a similar chemical reaction of polyurethane, polyisocyanurate or polyiso is fuel-included closed cell foam structure with low thermal conductivity value [12,26,27].

The insulation material is available in rigid board, liquid, spray foam or laminated panel forms. Similar to XPS, the *R*-value of polyisocyanurate insulation decreases with years due to the same phenomenon. Usage of foil and plastic facings helps to keep the *R*-value stable up to even 10 years. In practice, successful application of reflective foil on polyiso, especially on the external surfaces of the buildings, acts as a radiant barrier. Some manufacturers also use polyisocyanurate in structural insulated panels.

Like polyurethane, polyisocyanurate in foam board or liquid foam forms can also be used to produce structural insulation panels with standardized dimensions. Although polyisocyanurate insulation materials are more expensive, they have better thermal insulation, fire and water vapour-diffusion characteristics when compared to EPS [12].

7.3.2.4 Vermiculite and perlite insulation materials

Containing asbestos, vermiculite and perlite were used as attic space insulation materials before the 1950s. They are in small and light pellet forms and need special attention in handling. Application might be by pouring into the zone or using with cement to increase the thermal resistance [12].

7.3.2.5 Urea-formaldehyde (UF) foam insulation materials

Urea-formaldehyde (UF) foam came into use in residential buildings in between the 1970s and early 1980s, but after that, the usage for residential buildings of the insulation material became very limited since it emits formaldehyde and shrinks. Recent applications are mostly for covering walls of industrial sites. The foaming agent is pressurized air which needs 2–3 weeks for proper curing. UF foam will not expand because of the treatment plans, like polyurethane. UF foam allows the passage of water vapour through it and the structure of insulation material denaturizes at elevated temperatures [12].

7.3.3 Novel insulation materials

The goal was to achieve the lowest thermal conductivity for the materials and the lowest thermal transmittance values, thus achieving the highest possible thermal insulation values for the buildings. The traditional building insulation materials and results for today have handicap that they require rather thick building envelopes keeping in mind the end goal to meet the undeniably requesting thermal protection. As a solution, the researchers focused on novel insulation materials.

7.3.3.1 The vacuum insulation panels (VIPs)

The vacuum insulation panel (VIP) is made from an open-pored core material that is airtight and vacuum-proof with water vapour-proof foil. VIPs are the latest state-of-the-art thermal insulation. Their thermal conductivities range from 3 to 4 mW/mK, typically 8 mW/mK owing to air and water vapour. The wet thermal conductivity will change. It will be inevitably much higher than that value after 50 and 100 years depending on the VIP envelope type, which presents an important drawback for all VIPs. If nails (and the similar) happen to pierce the VIP inlet, thermal conductivity increases to about 20 mW/mK. As a result, cutting the VIP becomes impossible to set on the premises. Besides, they are pierced, they lose their thermal insulation performance to a great degree, which is another limitation of VIPs. Many features such as thermal conductivity, penetration of air and humidity, service life, compatibility of VIPs are studied by some authors [28–33].

In spite of their limitations, including their relatively high costs, still, VIPs are still a big step forward regarding the thermal insulation of buildings. Lower λ value of VIP than the conventional materials such as mineral wool and polystyrene products will be specifically important, depending on the aging time, once passive house standard and requirements as well as zero energy or emissions are pursued.

Even though VIPs are an absolute answer for the future, they are currently considered to be the best solution for a lot of thermal building envelopes and they will continue to be so in the near future in economic sense, from the perspective of thermal energy savings. Developing envelopes which stop VIP and air fumes from penetrating the VIP core and thus maintaining low conductivity for at least 50 or 100 years should be the topic of further VIP-related research. Research and implementation on such issues will lead to boosted knowledge and understanding on the solutions of possible future problems on thermal insulation [28–33].

7.3.3.2 Gas-filled panels

In principle, compared to air, filling lower thermal conductivity gases like argon, krypton and xenon is the innovation of gas-filled panels (GFPs). To protect the low conductive gas concentration in GFPs and prevent the air and humidity pervasion into GFPs, the thermal performance of this panel is vital. Naturally, vacuum's thermal insulation is better than many gasses that are used in GFPs. On the other hand, network structure of GFP does not have to withstand an internal vacuum as VIPs. Surfaces that have low emissivity in GFP reduce the transfer of radial heat. Despite the calculated lower theoretical values, the thermal conductivities for prototype GFP are quite high as 40 mW/mK. Therefore, GFPs have most of the merits and demerits of VIPs. Yet, VIPs appear to be a better choice for now and tomorrow once the GFPs future is considered [34–36].

A gas insulation material (GIM) is not so different from a vacuum insulation material except for the fact that a low-conductivity gas replaces (takes the place of) the vacuum in the closed pore structure. This means, GIM is a homogeneous material with a closed porous form closed with a low thermal conductivity gas which has very low thermal conductivity in the intact state.

7.3.3.3 Aerogels

Aerogels are novel thermal insulation solution with the highest potential examined by researchers. It would be possible to get low thermal conductivities of up to 4 mW/mK at lower pressures once the carbon black is used to suppress the transfer of radiation. Nevertheless, in ambient pressures, aerogels that are sold have been told to have up to 13 mW/mK thermal conductivities. For aerogels, costs of production are still high. Although their compression strength is relatively high, they are very sensitive to strengths of very low tensile. Integrating a tensile matrix can increase the tensile strength. As an interesting fact, it is possible to produce aerogels as opaque, translucent or transparent materials, so a wide variety of building applications are possible. How spacious and comprehensive they will be is to be seen in the future [37,38].

7.3.3.4 Dynamic insulation materials

Generally, heat insulation materials are considered (believed) to be static, that is, they have a fixed value. The normal selection is then made as physically in the lowest possible level for thermal conductivity as well as economic and building constraints. However, a building envelope can be treated as a structure which can adjust thermal properties according to the varying energy needs. This can be done with the help of a dynamic insulation material (DIM) in which it is possible to control the thermal conductivity within the desired range. Another name could be controllable insulation material.

DIMs, as a part of intelligent new buildings, may include phase change and electrochromic materials. DIMs including innovative solutions can manage the solar energy in solar systems, storage and release of renewable energies and dynamic control. Intensive study and research on intelligent products such as electrochromic windows have been conducted, and the first products are available in the market [38,39].

7.4 Characterization, application and selection methodology of insulation materials for green buildings

7.4.1 Characterization of insulation materials: optimal insulation level concept

Climate, the energy value, type of the heating gadget and efficiency and the price of the insulation established are the major drivers (motives) determining the most effective ranges of insulation. At both national and local levels, the required building codes and required insulation levels are determined in accordance with building policies. With the help of specific climatic data and energy costs expected, optimal insulation levels for a plenty of cities were derived from a European study (ECOFYS, 2007) [40]. Using insulation materials in construction keeps buildings warm in winters and cool in summers. In order to get the optimal level of insulation, critical issues related to some properties of insulating materials should be considered.

7.4.1.1 Thermal conductivity

Thermal conductivity, often denoted by the symbol k or λ, is the property of material to conduct heat that is a constant for any given material and is measured in W/mK. For some common materials at room temperature conditions, the thermal conductivity value may vary between 0.025 and 1,000 W/mK [41]. The thermal conductivity increases as the moisture content increases in traditional thermal insulation materials. From the aspect of the green building applications, including passive and zero energy or emission buildings in cold climates, selection of insulation materials with proper thermal conductivity values is critical.

7.4.1.2 Thermal resistance

The measure of opposing effect on heat flow by diffusion and radiation is named as thermal resistance which is a function of material thermal conductivity, thickness and density. Thermal resistance, R-value, is expressed in m^2K/W. Higher thermal resistance means that it is easy to maintain the temperature difference for a long time. Resistance network scheme of material is showed in Figure 7.2. R_{so} and R_{si}

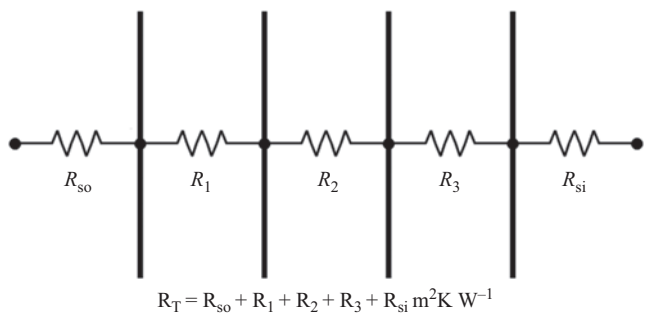

Figure 7.2 Thermal resistance diagram

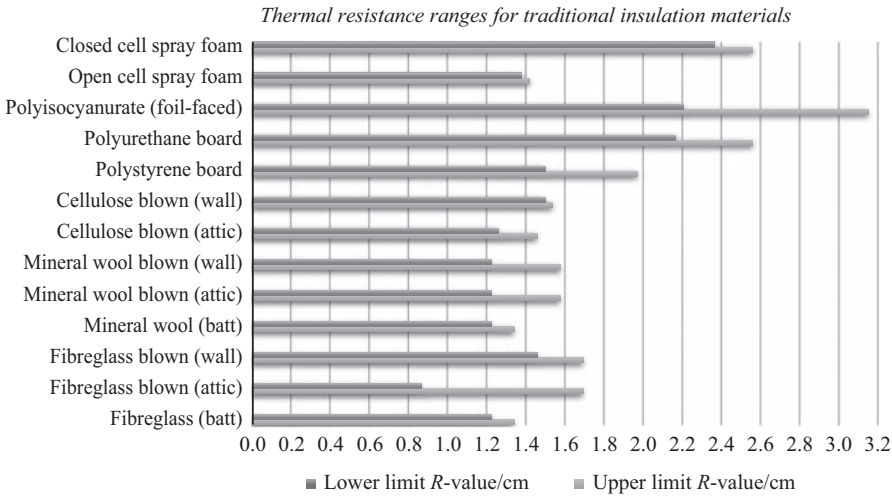

Figure 7.3 R-value per (5 cm thickness) of some common insulation materials (Adapted from [41])

are the thermal resistance of the outside and inside surrounding, respectively. A material with higher thermal resistance is a better insulator [42–45] (Figure 7.3).

7.4.1.3 Overall heat transfer coefficient (*U*)

Overall heat transfer coefficient is also known as *U*-value or the thermal transmittance. It is the amount of heat which flows through a certain element per unit area and time. *U*-value is used to determine the heat transfer through a building. *U*-value can be determined by different methods such as

- estimated methods,
- the heat flow meter method and
- quantitative methods-infrared thermography: In situ estimation of the component *U*-values with heat flowmeter method is not generally conceivable because of the immense number of constraints. An elective strategy is the infrared thermovision.

There are many discussions and studies about the validity of these methods in literature. These studies show that the measurements cannot set standards about the validity of methods. However, professionals and many laboratories use these methods to determine the *U*-value [46–55].

7.4.2 Application of insulation materials

7.4.2.1 Walls

Wall is the structure providing safety and shelter; so insulation of the outer wall is significant. Most wall structures in the world are either ‘stick built’ framing forms

or 'high thermal mess' ones. Despite the existence of framing structures allowing voids to be filled with insulation, the structural elements still behave like thermal bridges or areas with considerably higher heat transfer properties. On the other hand, in most high thermal mass walls, insulation is not used as they benefit from their thermal inertia. In the old-framed structure cavities, there is no insulation material [56–60].

Exterior wall insulation

Insulated walls are commonly used in most developed countries and are well built. The most effective approach has been to cover all the walls with insulation, and studies on this subject are continuing. An additional external structural insulation coating should ideally be made before the wall rain curtain or coating is added. In the newest buildings in Europe and North America, an external thermal insulation composite system is also added under plaster or cementitious finishing [57–60].

7.4.2.2 Roofs

There are two common roof geometries such as pitched (sloped) roofs and flat roofs (or low-sloped roofs). In some countries, mechanical equipment is placed in the roof cavities to reduce the thermal effect of the roofs in pitched roofs. This mechanical equipment can cause problems in an unconditional hot environment. The biggest challenge for thermal insulation of roofs is observed in applications of pitched roofs with no attic space like in cathedral ceilings. Pitched roofing is more common in places where there is a lot of snow. The use of flat roofs is common in many urban buildings and industrial buildings around the world [56,61].

Flat roofs

Depending on where the thermal insulation is, flat roof constructions are generally grouped as cold or hot. Though still used in some places, cold flat roofing is not suggested to apply. In these roofs, insulation is applied between the beams under the structural deck. Thermal motion can seriously affect the structural elements of a cold ceiling, and the insulation layer can accumulate moisture more. In the other form, i.e. warm roof, insulation is placed on the structural deck. It is not necessary to ventilate the insulation layer. As the roof structure or the height of the beam do not determine the limits on thermal performance, this approach is considered to be effective. Optimal thickness of the insulation is mostly determined based on the effectiveness of life cycle cost. For the existing roofs, additional insulation thickness can be limited by parapets and access doors, but insulation can be easily added to most parts of the roof without over-cost. One quite common practice is addition of insulation to the roofs of sloped slabs. Because of the effect of the chimney, wiring, piping, access to the chimney as well as the roof and the interfaces with the partition walls, leakage of air between the building and the conditioned space between the building and the attic can be crucial. For both new constructions and refurbishment operations, proper insulation and ceilings are airtight. Despite applied by some builders and plumbers, this is not the most approved process [56,61].

Pitched roofs

With the ceilings of cathedrals for curved roofs, the insulation is placed between the beams. On top of and perpendicular to the beams, additional insulation can be done as they do not have enough depth to provide high levels of insulation (or to raise the insulation level). Using foam in the beams to get high-performance insulation is another approach. Depending on the roof material and the design of the roof for the ventilation of the accumulation, closed or open-cell foam must be used. Owing to the high cost and moisture issues, the insulation of the cathedral ceilings with very sloped roofs is less than the other roof designs. However, a solution to this problem can be adding insulation inside the structural elements. It is necessary to take all curtains into consideration for added insulation and making the airtightness of the roof stronger as these measures have return rates to guarantee before retrofitting or major renovations. This is consistently a prioritized and cost-effective measure, but it is not commonly used [56,61].

Cool roofs

It is desirable to avoid as much heat as possible in hot climates from the surface of the roof, in the furnace or on the conditioned space. The white colour cool roof can reflect the visible and near-infrared light well. Performance of the roof gets lower by time with the pollution of particles and biological growth. Therefore, elderly grades are indicated in policy programs to guarantee that the energy-saving measures are accurate. Lately, a cold roof concept has had roof-grading requirements in detail, providing solar reflection and thermal-emission performance criteria after a roof sample has been aged for a certain period of time, such as 3 years (weathering tests at various climates). The oldest white roofs at the highest level reflect 80% of the solar energy, while black roofs range from 5% to 10% (CRRC, 2013). There also exist cold-coloured products that look exactly like the typical roofs but reflecting the near-infrared portion of the sunlight. These products represent about 30%–50% of solar energy depending on performance and colon [56,61].

7.4.2.3 Foundations and floors

The base includes various basic configurations including complete basements, interlaced fields and class plates. All configurations are available, but some are more common in specific regions. Adding insulation in all applications should be considered as an important point, but in colder climates, it is particularly important. In warmer regions, foundations can be heat-rejection sources, and they provide ground union. The greatest concerns are the basement, creep area or upholstery exposed to weathering. Most screening areas and basements in cold climates require reinstallation. It is possible to apply insulation on the walls inside, but moisture problem must be taken care of. This has been a topic of debate among construction researchers worldwide and draws attention owing to the resolution of issues with other components of the building envelope.

For new constructions and some equipment, the insulating floors on the basement or interspaced areas are easy measures. The basement is translating into a half-air-conditioned place by that, serving as a buffer zone which is useful.

Before the insulation, ground must be properly sealed. In the same way, the canal should be insulated and sealed appropriately in case it is in the basement or creep cavity [3,56].

7.4.3 Selection criteria for insulation material

Choosing the optimum insulation materials and amount is a crucial step in designing green building insulation. The factors to be considered are fire resistance, compressive strength, durability, water vapour absorption and transmission, ease of application, cost and thermal conductivity.

Although there are many factors involved, thermal performance is the most important step in selecting the insulating materials. Most of building components do not have different overall thermal resistance with respect to same insulation type and thickness. The overall thermal resistance can be the same regardless of where the insulation material holds; however, some other issues may change. If insulation is applied on interior walls, the building might be protected by mass against outside, more thermal bridges will be available and minimized heating benefits will be observed. On the other hand, with insulation on exterior walls, the building may easily store solar energy with less durability, and cooling and heating effects will be valid on summer and winter, respectively. Apart from exterior or interior wall applications, insulation placed in the middle results in even distribution with a trade-off between the benefits of the cost and insulation thickness [41,62].

7.4.3.1 Thermal performance

Thermal performance can be decided by three factors: namely thermal resistance, thermal bridging and thermal storage. First, as far as thermal resistance is concerned, high *R* value insulation materials (e.g. polyethylene, rock wool, fibreglass, polystyrene) should be selected. The relations between material thickness, density, operating temperature range and thermal resistance should be carefully calculated to achieve the optimum performance. Second, to prevent thermal bridge, a complete application of thermal insulation around the walls/roof should be performed. Also, there should be no or least amount of framing. Finally, for the thermal storage, in order to benefit from it, large and dense walls made of concrete are to be used.

7.4.3.2 Cost

The cost of insulating a building is composed of several segments: materials, installation, auxiliary costs as air sealing and waste disposal, and cumulative energy costs through the lifetime of the structure. Whenever the design of green building insulation is made, care should always be given to special high-performance insulation material selection resulting in extra cost and labour cost (Figure 7.4).

7.4.3.3 Ease of construction

Not all the designs are easy to construct. Ease of construction should be planned according to the workmanship requirement, speed of construction, operation, maintenance and replacement.

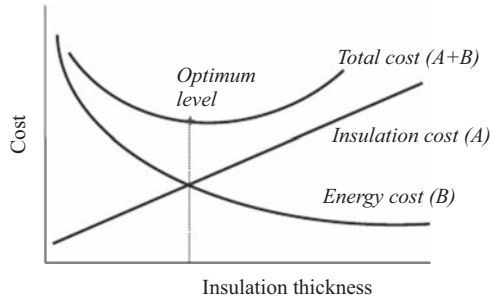

Figure 7.4 Optimum insulation material thickness (Adapted from [41])

7.4.3.4 Building standards requirements

To ensure safety and prevent medical issues, building standards/codes requirements should be met by checking the fire, health, mechanical strength expectations.

7.4.3.5 Durability

Insulation material should be durable, too. To satisfy this, the facts of changing *R* value, water permeability and absorption effects, stability on dimensions and strength should be considered.

7.4.3.6 Air tightness

The material should act as vapour/infiltration barrier to improve insulation quality for the walls, roof, etc. It should also be weather friendly and not have any cracks to ensure good insulation.

7.5 Insulation materials in green residential buildings

Green buildings' aim is to have less negative impact on nature and environment. Therefore, selected insulation materials with small *U* values should be eco-friendly. Also, green buildings use sunlight quite efficiently. They breathe by the help of wind but not lose heat and using some complicated system like special air conditioners, they may save afternoon heat for later use at night. Traditional structures use energy, soil, water and raw materials in large quantities in construction and operation. They are responsible for emissions of major greenhouse gases and pollutants. Besides, they produce large amount of wastes affecting plants and wildlife [63].

Buildings consume large quantities of energy. According to the United Nations Environment Program report, buildings use 30%–40% of the major energy produced worldwide [64]. The United States uses twice and three times as much energy as each unit in Germany and Japan, respectively [64]. The 2008 report of the International Energy Agency stated that existing buildings consume 40% of the world's total energy resulting in 24% of global CO_2 emissions [65]. Fortunately, it is possible to improve the energy efficiency in buildings with many methods.

Simple measures, such as air dressing, maintenance of entry gate closers, and changing available windows with storm windows as a low-cost alternative, are often a low hanging condition in the weather. Besides, once cooling and heating is concerned, a valid and rather inexpensive method of improving efficiency is applying insulation materials to new and existing buildings. To reduce the amount of energy used in production of insulation and allow recycling or biodegradation, innovations would be helpful. For insulation, materials such as mineral, fibrous and cellulose-derived products exist [62,66].

7.5.1 Standards and certificates for insulation materials used in green buildings

Raw materials cost and waste are produced in the construction, use, renovation and demolition stages of the buildings. These facts required some regulations which were evolved to the green building standards, certifications and grading systems aiming to reduce adverse effect on nature with sustainable design. There are some of the certification and rating systems used in the United States. Energy Star, LEED, Green Globes, Living Building Challenge, NZEB, Passive House Institute US, SITES and WELL Building Standard are the important ones. International certification and rating systems like BCA Green Mark Scheme, Beam, BREEAM, CASBEE, EDGE, Green Star SA, Pearl Rating System for Estidama are eligible worldwide [67–82].

In addition to building standards, there are also standards and certificates for insulation materials. For thermal insulation, accepted seven ecolabel criteria sets are defined by New Zealand, Canada, Australia, Korea, Taiwan, United Kingdom and USA. EU Ecolabel will also be modified by adding a criterion about insulation which will be a priority for the future [83].

The Good Environmental Choice Australia (GECA) Standard was introduced in 2007. It is valid for insulation materials such as panels, blankets, felts, loose fillers and sprayed thermal insulation. The standard does not define specific procedure for installation of materials and does not give a range for thermal conductivity or *R* values. For GECA certification, all products must meet the relevant national standard (AS4859.1: 2006 in case of insulation) [83].

Environmental Choice New Zealand Label criteria were published in 2004. They clarify the environmentally friendly products which meet the requirements of the test. During the certification process, an observation plan is submitted to relevant environmental controls and production records. Similar to GECA, the New Zealand Label covers all bulk, resistant insulation materials but does not cover foil-type insulators and is delayed for pipe works and ductwork [83].

Canada's related departments published the criteria for heat and insulation products first in 1997. It is necessary for the products to meet all possible government and industrial standards regarding safety and performance, including the regulations related to disposal of wastes left out from the production process. As in the New Zealand scheme, it is a must to have access to quality control, verification and production records as well as manufacturing issues [83].

The Taiwan Green Mark Logos was introduced in 1992, and it includes more than 100 products including heat-insulation materials. Although it has less details than the other features, it meets the requirements of thermal conductivity, material restrictions and packaging rules [83].

Korean Ecolabel, which is a voluntary standard carried out by government, was also launched in 1992. Korean public services were made to buy products with eco-label by the law to motivate people to use eco-friendly products. In the criteria, waste materials in the insulation products, limitations on the material and the quality requirements are covered [83].

7.5.1.1 Product characteristics

Thermal resistance levels are not specified by The Canadian and Australian criteria and the UK Energy Saving Recommended (ESR) but instead existing standards are referred. Summarized methodologies are used to test and validate standards. These standards must be met by before applying for eco-label status. In addition to the British Standards and Building Regulations, the proposed thermal conductivity levels for roof insulation works not captured by the Building Code are between 0.044 and 0.037 W/mK. For and overall heat transfer coefficient value of 0.16 W/m^2K, the required thickness of the insulating material may change from 270 to 150 mm for thermal conductivity values of 0.044–0.024 W/mK, respectively [83].

Further to the Korean Industrial Standards and Taiwan Green Mark, the thermal conductivity should be less than 0.044 W/mK. Within the New Zealand Environmental Selection criteria, wall and ceiling products should have *R* value of 2.5 and 3, respectively.

7.5.1.2 Material requirements

All standards dictate the usage of recycled content and reduce waste whenever possible and ask manufacturers to label the packaging for useful information to consumers. Recycling conditions for different countries' regulations are summarized in Table 7.1. Detailed explanations with extended comparison for recycling content and prohibited substances in insulation materials can be found in literature [83].

Table 7.1 Recycling content in insulation materials (Adapted from [83])

Product type	Korea Ecolabel	GECA	Canadian specification (according to type and fill/spray applied)
Natural insulation materials (%)	≥ 40	≥ 25	≥ 35
Synthetic insulation materials (%)	≥ 20	≥ 85	≥ 5

References

[1] Building Design and Construction, "White Paper on Sustainability", page 4, November (2006).
[2] Office of the Federal Environment Executive, "The Federal Commitment to Green Building: Experiences and Expectations," 18 September (2003).
[3] Johnston D., and Gibson S. Green from the ground up, sustainable, healthy and energy efficient home construction. Newtown, CT: Tounton Press Inc, (2008).
[4] Good to know: Green building incentive strategies. (2014, May 02). Retrieved from https://www.usgbc.org/articles/good-know-green-building-incentive-strategies-0.
[5] Bozsaky D. The historical development of thermal insulation materials. Periodica Polytechnica Architecture, 41(2), pp. 49–56. doi: https://doi.org/10.3311/pp.ar.(2010)-2.02.
[6] Al-Ajlan S.A. Measurements of thermal properties of insulation materials by using transient plane source technique. Applied Thermal Energy, 26 (2006), pp. 2184–2191.
[7] Jelle B.P., Gustavsen A., and Baetens R. The path to the high performance thermal building insulation materials and solutions of tomorrow. Journal of Building Physics, 34 (2010), pp. 99–123.
[8] Baetens R. (2009) Properties, requirements and possibilities for highly thermal insulating materials and solutions in buildings – State-of-the-art and beyond'. M.Sc. thesis, Catholic University of Leuven - Department of Architecture, Urban Design and Regional Planning (Leuven, Belgium), SINTEF Building and Infrastructure – Department of Building Materials and Structures (Trondheim, Norway) – Norwegian University of Science and Technology – Department of Civil and Transport Engineering (Trondheim, Norway).
[9] Papadopoulos A.M., Theodosiou T., and Karatzas K. Feasibility of energy saving renovation measures in urban buildings: the impact of energy prices and the acceptable payback time criterion. Energy and Buildings, 34 (2002), pp. 455–466.
[10] SAPPEK, 2004. Report of the technical standards of the materials' properties, SAPPEK programme: Design and Development of Innovative Stone-wool Products for the Energy Upgrading of Existing and New Build-ings, LHTEE, Aristotle University Thessaloniki, Greece (in Greek).
[11] Papadopoulos A.M. State of the art in thermal insulation materials and aims for future developments. Energy and Buildings, 37 (2005), pp. 77–86.
[12] Insulation Materials. (2018). Retrieved from https://www.energy.gov/energysaver/weatherize/insulation/insulation-materials.
[13] Schiavoni S., Donirgysaver F., Bianchi F., and Asdrubali F. Insulation materials for the building sector: a review and comparative analysis. Renewable and Sustainable Energy Reviews, 62 (2016), pp. 988–1011.
[14] Fassi A., and Maina L. L'isolamento ecoefficiente, Edizioni Ambiente, Milano (2009) (in Italian).

[15] Zach J., Korjenic A., Petránek V., Hroudová J., and Bednar T. Performance evaluation and research of alternative thermal insulations based on sheep wool. Energy and Buildings, 49 (2012), pp. 246–253.
[16] Kymäläinen H.-R., and Sjöberg A.-M. Flax and hemp fibres as raw materials for thermal insulations. Building and Environment, 43 (2008), pp. 1261–1319.
[17] Zach J., Hroudova J., Brožovskýc J., Krejzad Z., and Gailiuse A. Development of thermal insulating materials on natural base for thermal insulation systems. Procedia Engineering, 57 (2013), pp. 1288–1294.
[18] Korjenic A., Petránek V., Zach J., and Hroudová J. Development and performance evaluation of natural thermal-insulation materials composed of renewable resources. Energy and Buildings, 43 (2011), pp. 2518–2523.
[19] Glé P., Gourdon E., and Arnaud L. Acoustical properties of materials made of vegetable particles with several scales of porosity. Applied Acoustics, 72 (2011), pp. 249–259.
[20] R. Fangueiro Fibrous and composite materials for civil engineering applications. Cambridge, UK: Woodhead Publishing Limited, (2011).
[21] Bunge C.V.F., Duffy J., and Hood L. Advances in thermal insulation of extruded polystyrene foams. Cellular Polymers, 30 (2011), pp. 137–156.
[22] Lakatos A., and Kalmár F. Analysis of water sorption and thermal conductivity of expanded polystyrene insulation materials. Building Services Engineering Research and Technology, 34 (2013), pp. 407–416.
[23] Kuhn J., Ebert H.P., Arduini-Schuster M.C., Büttner D., and Fricke J. Thermal transport in polystyrene and polyurethane foam insulations. International Journal of Heat and Mass Transfer, 35 (7) (1992), pp. 1795–1801.
[24] Webster D.K.C. Thermal stability and flame retardancy of polyurethanes. Progress in Polymer Science, 34 (10) (2009), pp. 1068–1133.
[25] Wu C.W., Sung W.F., and Chu H.S. Thermal conductivity of polyurethane foams. International Journal of Heat and Mass Transfer, 42 (12) (1999), pp. 2211–2217.
[26] Zhao C., Yan Y., Hu Z., Li L., and Fan X. Preparation and characterization of granular silica aerogel/polyisocyanurate rigid foam composites. Construction and Building Materials, 93 (2015), pp. 309–316.
[27] Pescari S., Tudor D., Tölgyi S., and Maduta C. Study concerning the thermal insulation panels with double-side anti-condensation foil on the exterior and polyurethane foam or polyisocyanurate on the interior. Key Engineering Materials, 660 (2015), pp. 244–248.
[28] Fricke J. (2005) From dewars to VIPs – One century of progress in vacuum insulation technology. In: Proceedings of the 7th International Vacuum Insulation Symposium, EMPA, Dübendorf, Switzerland, 28–29 September, 5–14.
[29] Fricke J., Schwab H., and Heinemann U. Vacuum insulation panels – exciting thermal properties and most challenging applications. International Journal of Thermophysics, 27 (2006), pp. 1123–1139.
[30] Schwab H., Heinemann U., Beck A., Ebert H.-P., and Fricke J. Permeation of different gases through foils used as envelopes for vacuum insulation

panels. Journal of Thermal Envelope & Building Science, 28 (2005), pp. 293–317.

[31] Simmler H., and Brunner S. Vacuum insulation panels for building application – basic properties, ageing mechanisms and service life. Energy and Buildings, 37 (2005a), pp. 1122–1131.

[32] Simmler H., and Brunner S. (2005) Ageing and service life of VIP in buildings. In: Proceedings of the 7th International Vacuum Insulation Symposium, EMPA, Dübendorf, Switzerland, 28–29 September, 15–22.

[33] Jelle B.P., Gustavsen A., and Baetens R. (2009) Beyond vacuum insulation panels – How may it be achieved?. In: Proceedings of the 9th International Vacuum Insulation Symposium (IVIS 2009), London, England, 17–18 September.

[34] Yarbrough D.W., Petrie T.W., Kinninger D., and Graves R.S. (2007) Thermal performance of gas-filled panels with reflective surfaces installed in an attic. In: Proceedings of the Thermal Performance of the Exterior Envelopes of Whole Buildings X International Conference (Buildings X), Clearwater Beach, Florida, USA, 2–7 December.

[35] Mills G.L., and Zeller C.M. The performance of gas filled multilayer insulation. Advances of Cryogenic Engineering: Transactions of the Cryogenic Engineering Conference, 53 (2008), pp. 1475–1482.

[36] Baetens R., Jelle B.P., Gustavsen A., and Grynning S. Gas-filled panels for building applications: a state-of-the-art review. Energy and Buildings, 42 (2010), pp. 1969–1975.

[37] Aspen Aerogels, Spaceloft® 3251, 6251, 9251 (2008) Flexible Insulation for Industrial, Commercial and Residential Applications. Available at: www.aerogel.com.

[38] Aspen Aerogels, Spaceloft^{TM} 6250 (2008b) Extreme Protection for Extreme Environments. Available at: www.aerogel.com.

[39] Granqvist C.G., Green S., Niklasson G.A., Mlyuka N.R., von Kræmer S., and Georén P. Advances in chromogenic materials and devices. Thin Solid Films, 518 (2010), pp. 3046–3053.

[40] International Energy Agency Transition to sustainable buildings: strategies and opportunities to 2050. International Energy Agency (2013).

[41] Al-Homoud M.S. Performance characteristics and practical applications of common building thermal insulation materials. Building and Environment, 40 (2005) p. 357.

[42] Bergman T.L., Lavine A.S., Incropera F.P., and DeWitt D.P. Fundamentals of heat and mass transfer, 7th Edition, Singapore: John Wiley & Sons Inc, (2011).

[43] Jelle B.P. Traditional, state-of-the-art and future thermal building insulation materials and solutions – properties, requirements and possibilities. Energy and Buildings, 43 (2011), pp. 2549–2563.

[44] International Organization for Standardization. ISO 6946:2007—building components and building elements—thermal resistance and thermal transmittance—calculation method, International Organization for Standardization, Geneva, Switzerland (2007).

[45] International Organization for Standardization. ISO 9869-1:2014—thermal insulation—building elements—in situ measurement of thermal resistance and thermal transmittance. Part 1: Heat flow meter method, International Organization for Standardization, Geneva, Switzerland (2014).
[46] Scholl W., and Maysenhölder W. Impact sound insulation of timber floors: interaction between source, floor coverings and load bearing floor. Building Acoustics, 6 (1999), pp. 43–61.
[47] Thermal Conductivity of common Materials and Gases (2013). Retrieved from https://www.engineeringtoolbox.com/thermal-conductivity-d_429.html.
[48] Albatici R., and Tonelli A.M. Infrared thermovision technique for the assessment of thermal transmittance value of opaque building elements on site. Energy and Buildings, 42 (2010), pp. 2177–2183.
[49] Dall'O G., Sarto L., and Panza A. Infrared screening of residential buildings for energy audit purposes: results of a field test. Energies, 6 (2013), pp. 3859–3878.
[50] Fokaides P.A., and Kalogirou S.A. Application of infrared thermography for the determination of the overall heat transfer coefficient (*U*-Value) in building envelopes. Applied Energy, 88 (2011), pp. 4358–4365.
[51] Tejedor B., Casals M., Gangolells M., and Roca X. Quantitative internal infrared thermography for determining in-situ thermal behaviour of façades. Energy and Buildings, 151 (2017), pp. 187–197.
[52] Evangelisti L., Guattari C., Gori P., De Lieto and Vollaro R. In situ thermal transmittance measurements for investigating differences between wall models and actual building performance. Sustainability, 7 (2015), pp. 10388–10398.
[53] Ficco G., Iannetta F., Ianniello E., D'Ambrosio Alfano F.R., and Dell'Isola M. *U*-value in situ measurement for energy diagnosis of existing buildings. Energy and Buildings, 104 (2015), pp. 108–121.
[54] Choi D.S., and Ko M.J. Comparison of various analysis methods based on heat flowmeters and infrared thermography measurements for the evaluation of the in situ thermal transmittance of opaque exterior walls. Energies, 10 (2017), pp. 1019.
[55] Nardi I., Paoletti D., Ambrosini D., De Rubeis T., and Sfarra S. *U*-value assessment by infrared thermography: a comparison of different calculation methods in a Guarded Hot Box. Energy and Buildings, 122 (2016), pp. 211–221.
[56] Baetens R., Jelle B.P., and Gustavsen A. Properties, requirements and possibilities of smart windows for dynamic daylight and solar energy control in buildings: a state-of- the-art review. Solar Energy Materials & Solar Cells, 94 (2010b), pp. 87–105.
[57] Thamer A.D., Hafiz M.H., and Mahdi B.S. Mechanism of building-up deposited layer during electro-spark deposition. Journal of Surface Engineered Materials and Advanced Technology, 2 (2012), pp. 258–263.
[58] Herrera R.I., Vielma J.C., Ugel R., Martinez Y., and Barbat A. Optimal design and earthquake-resistant design evaluation of low-rise framed RC structure. Natural Science, 4 (2012), pp. 677–685.

[59] Suwanbamrung C., Tapalak N., Jitchun C., *et al*. Student capacity building of dengue prevention and control: a study of an Islamic school, Southern Thailand. Health, 4 (2012), pp. 366–376.
[60] Chakraborty S., Kumar P., and Chakraborty S.K. Neural network approach to response of buildings due to earthquake excitation. International Journal of Geosciences, 3 (2012), pp. 630–639.
[61] Castleton H.F., Stovin V., Beck S.B.M., and Davison J.B. Green roofs; building energy savings and the potential for retrofit. Energy and Buildings, 42 (2010), pp. 1582–1591.
[62] Kruger A., and Seville C. Green building: principles and practices in residential construction, international edition. USA: Cengage Learning, (2013).
[63] Howe J.C., and Gerrard M.B. The law of green buildings regulatory and legal issues in design, construction, operations, and financing. USA: American Bar Association, (2010).
[64] U.S. Dept. of Energy Buildings Technology Program. Obama administration launches new energy efficiency efforts (June 29, 2009). Available at http://www1.eere.energy.gov/buildings/news_detail.html?news_id=12607.
[65] International Energy Agency. Promoting energy efficiency investments: case studies in the residential sector (2008).
[66] Papadopoulos A.M., and Giama E. Environmental performance evaluation of thermal insulation materials and its impact on the building. Building and Environment, 42 (2007), pp. 2178–2187.
[67] Wbdg.org. (n.d.). Green Building Standards and Certification Systems | WBDG Whole Building Design Guide. [online] Available at: https://www.wbdg.org/resources/green-building-standards-and-certification-systems [Accessed 13 Aug. 2018].
[68] Energystar.gov. (n.d.). Green Buildings and ENERGY STAR. [online] Available at: https://www.energystar.gov/buildings/about-us/how-can-we-help-you/energy-star-action/green-buildings-and-energy-star [Accessed 13 Aug. 2018].
[69] New.usgbc.org. (n.d.). LEED | USGBC. [online] Available at: https://new.usgbc.org/leed [Accessed 13 Aug. 2018].
[70] Greenglobe.com. (n.d.). Green Globe | Green Globe Certification – Certified Sustainability. [online] Available at: https://greenglobe.com/ [Accessed 13 Aug. 2018].
[71] International Living Future Institute. (n.d.). Living Building Challenge | International Living Future Institute. [online] Available at: https://living-future.org/lbc/ [Accessed 13 Aug. 2018].
[72] International Living Future Institute. (n.d.). Zero Energy | International Living Future Institute. [online] Available at: https://living-future.org/net-zero/ [Accessed 13 Aug. 2018].
[73] Institute, P. (n.d.). Passivhaus Institut. [online] Passivehouse.com. Available at: https://passivehouse.com/ [Accessed 13 Aug. 2018].
[74] Gbci.org. (n.d.). About SITES | GBCI. [online] Available at: http://www.gbci.org/press-kit-sites [Accessed 13 Aug. 2018].

[75] Anon, (n.d.). [online] Available at: https://www.wellcertified.com/ [Accessed 13 Aug. 2018].
[76] Bca.gov.sg. (n.d.). Building & Construction Authority. [online] Available at: https://www.bca.gov.sg/greenmark/green_mark_buildings.html [Accessed 13 Aug. 2018].
[77] Bec.org.hk. (n.d.). Business Environment Council 商界環保協會. [online] Available at: http://bec.org.hk/articles/beam—green-building-labelling [Accessed 13 Aug. 2018].
[78] BREEAM. (n.d.). BREEAM. [online] Available at: https://www.breeam.com/ [Accessed 13 Aug. 2018].
[79] Ibec.or.jp. (n.d.). Welcome to CASBEE website. [online] Available at: http://www.ibec.or.jp/CASBEE/english/ [Accessed 13 Aug. 2018].
[80] EDGE Buildings. (n.d.). EDGE Buildings | Build and Brand Green. [online] Available at: https://www.edgebuildings.com/ [Accessed 13 Aug. 2018].
[81] GBCSA. (n.d.). Green Star Tools. [online] Available at: https://gbcsa.org.za/certify/green-star-sa/ [Accessed 13 Aug. 2018].
[82] Department of Urban Planning and Municipalities. (n.d.). Department of Urban Planning and Municipalities – The Pearl Rating System for Estidama. [online] Available at: https://www.upc.gov.ae/en/estidama/estidama-program/the-pearl-rating-system-for-estidama [Accessed 13 Aug. 2018].
[83] Harwell E.A. Green public procurement thermal insulation technical background report for the European Commission – DG Environment (June 2010).

Chapter 8

Latent relationships between construction cost and energy efficiency in multifamily green buildings

Andrew McCoy[1], Dong Zhao[2], Yunjeong Mo[2], Philip Agee[3], and Freddy Paige[4]

Residential buildings have accounted for more than 20% of total energy usage in the United States over the last decade. Reducing household energy consumption has environmental and economic impacts. Building scientists and construction engineers have attempted to obtain accurate energy use prediction; however, few have focused on the relationship between construction cost and energy use. This chapter investigates the associations among detailed construction cost takeoffs and actual energy use in multifamily green buildings. The researchers employ advanced machine-learning analytics to model the correlations between construction costs and energy use data collected from multifamily residential units. The findings identify cost divisions in the construction stage that significantly correlate with energy use in the operational stage. The model allows developers to predict energy consumption based on construction costs and enables them to adjust their investment strategies to amplify the energy efficiency of green building technologies.

8.1 Introduction

Building innovation is increasingly critical for meeting challenges of energy conservation and climate change. Kok *et al.* [1] addressed a shift toward green building innovation diffusion for affordable housing through the diffusion of building certifications in the commercial building market. They noted the importance of occupied structures in aggregate energy consumption and greenhouse gas emissions as well as the so-called energy paradox that juxtaposes slow levels of adoption in new buildings against the profitability of more energy-efficient (EE) technologies.

[1]Myers-Lawson School of Construction, USA
[2]School of Planning, Design & Construction, Michigan State University, USA
[3]Grado Department of Industrial Systems Engineering, USA
[4]Department of Civil and Environmental Engineering, USA

As of 2012, residential buildings in the United States consume over 20% of energy [2] used countrywide, representing a cost of approximately $416 billion [3]. Although new and weatherized housing units are becoming more efficient, today it is still a significant source of US energy consumption. The US Department of Energy (DOE) reports that the housing stock has become increasingly EE since 1980: houses built most recently are 14% and 40% more EE than homes built 30 and 60 years ago, respectively. More recently, the residential and commercial sectors accounted for 40% of total US energy consumption, with residential accounting for 22% alone [4]. Nevertheless, housing has also experienced an energy paradox: homebuilders are resistant to use EE innovations and have scarce information regarding their payback.

Since the 2008 Great Recession, regulatory changes in building codes and efficiency requirements in both Europe and the United States have increased their pace of EE diffusion. Expected performance and initial cost of adoption have increased the probability of realizing anticipated returns on investment, primarily using proven technologies [5,6], and there is mounting evidence that these gains are capitalized in the prices of residential buildings [7,8]. Household energy prediction is significant to policies and strategies that affect energy use reduction, economic development, and environmental sustainability [9]. Many studies have investigated building energy performance and its associated factors, such as construction technology, thermal property, building envelope, heating, ventilating, and air-conditioning (HVAC), indoor temperature, thermostat setpoints, schedules, lighting and appliances, weather, and occupant behavior [10]. However, few have focused on the relationship between construction cost and energy use.

This study contributes to knowledge on energy consumption, capital costs, and payback by focusing on the latent relationship between cost and actual energy consumption in high-performance housing (HPH). The work focuses on multifamily buildings using a machine-learning (ML) approach. The results from this study reinforce the ability to use cost data for energy prediction, identify the appropriate ML algorithm and model for energy prediction, and determine critical variables for energy prediction [11]. The work advances information exchange regarding actual costs of green buildings and the ability to capitalize on possible gains while identifying the need to address key barriers to HPH diffusion in the housing market.

8.2 Literature review

A review of the literature suggests that there is no standard definition of HPH. All previous studies have emphasized EE, sustainability, and environmentally friendly products [12]. In general, homes that can be described as high performance are (1) safer and healthier, (2) more energy and resource-efficient, (3) more durable and resilient, and (4) more comfortable.

8.2.1 Green design and construction

Green design and construction criteria and research are closest in scope to our definition of HPH. Ng *et al.* [13] defined green building as “improving the way that

homes and homebuilding sites use energy, water, and materials to reduce impacts on human health and the environment." While the intent and concept of green building is straightforward, early adopters among designers, building contractors, and tradesmen recognized a need for communicating standards of quality that could be tied to economic value. As a result, green stakeholders developed multiple certifications and rating systems worldwide that lent confidence to the risks in implementing a new and relatively unknown system. The industry has rapidly addressed perceptions of green buildings as well as the benefits and risks involved. However, actual data on implementation costs are lacking [14].

8.2.2 Residential certifications and rating systems

ENERGY STAR™ for Homes was established in 1996 as a joint effort of the US EPA and DOE. Based on program rigor, national brand recognition, and established training quality and qualifications of third-party Home Energy Raters (HERS), the ENERGY STAR certification has become a core component of many residential green building programs. The ENERGY STAR program[1] maintains a focus on building science and analyzes buildings as integrated energy systems. Other residential green building certification programs include LEED for Homes (LEED-H) and the ICC 700 National Green Building Standard (NGBS). These programs differ in their emphasis and accountability of green design and building practices owing to the differences in their origination and user base: LEED is designer-focused and NGBS is developer–builder-focused.

The EarthCraft program, created in 1999 by a partnership between Southface Energy Institute and the Greater Atlanta Homebuilders Association, is regionally specific to the Southeast United States. The program focuses on performance and measurement. According to the program's website, it "introduces green building to the construction industry in a way that could be easily integrated into the building process," which makes it accessible to builders. Since 1999, EarthCraft has become one of the largest regional certification systems in the country. EarthCraft buildings have measured results [15,16], and the focus program for HPH units measured in this work.

8.2.3 Certifying residential buildings

Although an HPH unit may be certified, not every certified building is necessarily a high-performing one. According to Korkmaz *et al.* [17], green, sustainable, and HPH units are designed and constructed to maximize the energy efficiency of envelope, mechanical, and lighting systems to provide superior quality in the indoor environment for enhancing occupant wellbeing. Such buildings are being widely adopted for their potential to reduce energy costs and improve the health and productivity of occupants. However, there are costs involved. One of the primary barriers in the market is the owner's perception of high initial costs associated with these homes resulting from higher labor hours and the use of innovative materials and technologies [18].

[1]ENERGY STAR has implemented an update titled "version 3," which was not included in this sample. Version 3 expands the scope of the program's focus to encompass indoor air quality, water distribution, and renewable energy.

8.3 Sustainable development trends

Much of the green building literature details benefits for owners, society, the environment, and users [19]. Furthermore, momentum exists toward sustainable development within various industries: construction and development, real estate, and regulatory organizations. In general surveys representing several industries, most respondents felt that trends in sustainable building were growing [20,21]. In addition, many representatives within the construction and building industry have been exposed to green building projects and sources of green building knowledge continue to expand [22]; however, the costs for green building are perceived to be higher [23].

According to the US Green Building Council (USGBC), the number of LEED-certified projects is growing [24]. EarthCraft is also growing, especially in the multifamily, low-income housing market [24].

8.4 Construction costs, green premiums, and paybacks

The cost of producing a house has risen 206% since 1998. Using National Association of Homebuilders (NAHB) Construction Cost Survey national data (www.nahb.org), Figure 8.1 shows that total costs associated with building a single family

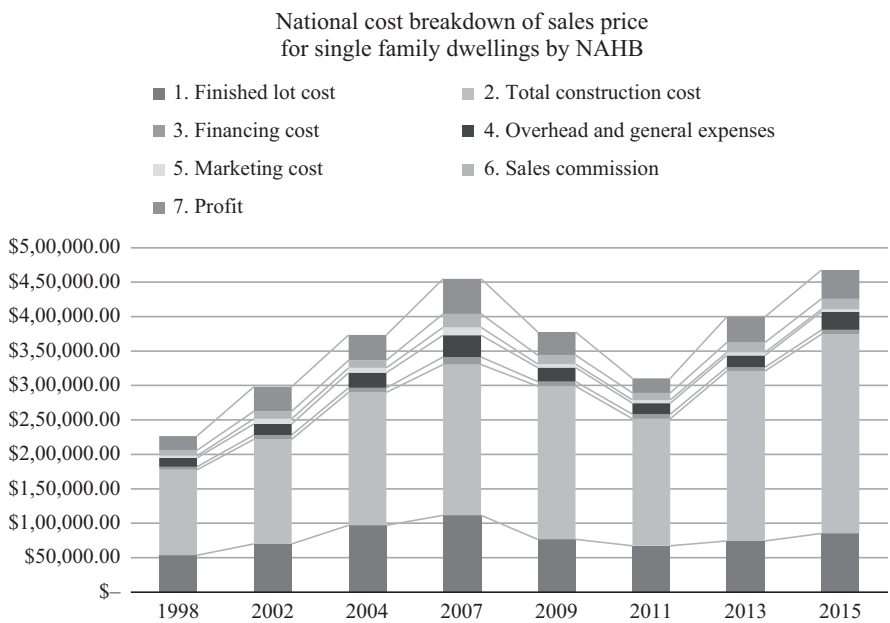

Figure 8.1 Total Cost Associated with Building a Single Family Dwelling unit Source: National Association of Homebuilders (NAHB), New Construction Cost Breakdown, 1998–2015

dwelling unit (indirect, direct, and soft costs) increased until the Great Recession, decreased until 2011, and then rebounded. New standards for mechanical and electrical systems and high-performance technologies have strained traditional cost models in terms of specific areas such as direct, indirect, and soft costs, depending on location and type of construction.

The costs for HPH services and products imply that upfront investing and payback decisions are difficult because of a lack of comparable industry data. Perceptions have led to the belief that green premiums tend to be approximately 11% greater for LEED and ENERGY STAR projects, but actual numbers show that such construction premiums can be as low as 1% and 0.5%, respectively [20]. Ahn and Pearce [22] reported that 1.84% of LEED certification levels and their associated premium costs were from installation.

Initial upfront costs for HPH projects might seem higher than standard new construction (i.e., code-built), but paybacks on the operational side are achievable. For example, LEED and ENERGY STAR buildings often command higher rental rates, have lower vacancies, and have higher resale values than the alternatives [25]. Rent and occupancy premiums can range from 4.4% to 51% and 4.2% to 17.9%, respectively [20].

The misalignment between who invests in energy efficiency and who receives the benefit of the investment creates a split-incentive in multifamily housing. The split-incentive issue has been described in the literature as a market barrier to HPH in multifamily housing stock [26,27]. The split-incentive and lack of energy performance data following the investment in energy efficiency creates uncertainty and risk for owners, widening the energy efficiency gap in multifamily housing.

More recently, Southface [24] reported that

> experienced green developers have found ways to incorporate green elements into their affordable housing projects in cost effective ways. Many experienced developers carefully select sites to benefit costs, by choosing a site that is very walkable to transit and services. Also, some developers have been able to invest in water conservation elements for each affordable housing unit with as little as $83 per unit. In general, projects with higher return on investments and shorter payback periods are achieved through efficient systems and thus lower utility costs.

Like the commercial market, HPH multifamily housing provides a payback opportunity through reduced operating and maintenance expenses, including utilities (i.e., electricity, gas, water, and waste removal), cleaning practices, energy-saving devices, efficiency in infrastructure, downsizing mechanical and electrical equipment, using natural light, efficient plumbing fixtures, reclaiming and recycling materials, and operational savings [28,29].

Wollos [30] found that buildings implementing above-code green building measures could reduce energy use by 10%–40%, and Campbell [31] found that affordable housing developments implementing above-code green design and construction measures increased resident retention [31]. Studies of buildings that follow leading certification practices indicate lower operating expenses [28], which equates to stronger cash flow [32]. Nalewaik and Venters [29] found that green

retrofits used 42% less energy and 34% less water than conventional buildings, reducing costs.

Other barriers to HPH development include lack of knowledge and information, unreliable performance metrics, and inadequate data collection [24]. Industry fragmentation, multiple project stakeholders, path dependency, and experience levels with green building practices produce a large disparity within project teams [33]. HPH developer-builders likely encounter inconsistent federal, state, and local regulations, whereas publicly funded affordable housing developments can face additional, more stringent requirements [33].

To justify initial investments and paybacks for HPH projects, industry stakeholders and owners need to be informed using actual data [25]. Only Matthiessen and Morris [34] have attempted to focus on comparing green versus nongreen building costs. These studies found no cost difference and focused on commercial or institutional facilities, not residential [34]. Rehm and Ade [14] note that other studies do not explicitly test for cost premiums or omit critical elements, such as soft costs. The remainder of this chapter addresses the information gap, and the following sections comprehensively measure actual costs of green and nongreen buildings within one certified program.

8.5 Methodology

8.5.1 Variables

This study contains 72 variables for energy use prediction. Electricity use by the square foot per residential unit (kWh/sf) is the dependent variable. The 71 independent variables are grouped as (i) basic building information, (ii) construction cost information, and (iii) technical information. Table 8.1 lists the four basic information variables describing the characteristics of residential units. Table 8.2 lists the 24 construction cost variables—12 describing direct costs and 12 describing indirect costs. Table 8.3 lists the 43 technical variables describing the building envelope, HVAC systems, lighting, and appliances.

8.5.2 Data

The researchers collected construction cost data from 24 developers on 236 Low-Income Housing Tax Credit (LIHTC) multifamily residential units in Virginia. Costs were sub-categorized by construction cost divisions, including both direct costs of facilities and buildings and indirect and soft costs of sites and

Table 8.1 Basic information variables

Code	Description	Code	Description
HERS*	HERS score (1–100)	SrNsr	Senior(0), non-senior(1)
NewReno	New(0), renovation(1)	Area	Square footage of each unit

*HERS (Home Energy Rating System).

Table 8.2 Construction cost information variables

Code	Description (direct cost)	Code	Description (indirect cost)
A00	Substructure	S01	Site development
B10	Shell: superstructure	S02	Acquisition
B20	Shell: exterior enclosure	S03	Overhead
B30	Shell: roofing	S04	Profit
C00	Interiors	S05	General requirement
D10	Services: conveying	S06	Bonding fee
D20	Services: plumbing	S07	Professional services
D30	Services: HVAC	S08	Pre-development
D40	Services: fire protection	S09	Construction period financing
D50	Services: electrical	S10	Permits and fees
E00	Equipment and furnishings	S11	Developer fee
F00	Special construction	S12	Start-up and reserves

Table 8.3 Technical information variables

Code	Description	Code	Description
T01	Period of collection	T24	Sealed attic *R*-value
T02	Conditioned area	T25	Above grade walls *R*-value
T03	Conditioned volume	T26	Foundation walls
T04	Number of bedrooms	T27	Slab
T05	House type	T28	Edge slab *R*-value
T06	Foundation type	T29	Under slab *R*-value
T07	Air-source heat pump fuel type	T30	Window U-value
T08	Air-source heating efficiency	T31	Window solar heat gain coefficient
T09	Air-source cooling efficiency	T32	Infiltration rate, heating
T10	Water heater type	T33	Infiltration rate, cooling
T11	Water heater fuel type	T36	Infiltration measurement method
T12	Water heater energy factor	T37	Percent interior lighting
T13	Water heater tank size	T38	Percent garage/exterior lighting
T14	Duct leakage	T39	Refrigerator energy usage
T15	Ventilation system type	T40	Dishwasher energy factor
T20	Programmable heat	T41	Range/oven fuel type
T21	Programmable cool	T42	Clothes dryer fuel type
T22	Ceiling flat *R*-value	T43	Clothes dryer energy factor
T23	Sealed attic		

organizations. The research team collected monthly energy consumption over 3 years. This study used full data from 159 residential units from 9 developments located in 9 cities (Table 8.4). The construction cost, basic building information, and technical building data were collected in 2014 and 2015 through multiple site visits with the aid of property managers. Monthly energy consumption was collected through a partnership with industry collaborators [35].

Construction cost data were collected from the developers' proforma sheets and categorized by the research team. The cost per square foot was gained by

Table 8.4 Summary of sample residential units

Development code	City	Cost certified year	Number of units
D1	King George	2012	18
D2	Chesapeake	2012	32
D3	Richmond	2008	29
D4	Arlington	2011	5
D5	Orange	2012	19
D6	Scottsville	2012	13
D7	Richmond	2012	22
D8	Lynchburg	2011	14
D9	Hampton	2011	7

dividing the total construction cost by total development square footage. Because the buildings were completed from 2008 to 2012, construction cost data were adjusted using the Producers Price Index (PPI) to 2013-dollar values, similar to a previous methodology by Ang *et al.* [36].

Energy use data for each residential unit were averaged from January 2013 to June 2016. The average energy use per unit was normalized by the square footage of the unit in a similar method to that used for cost data normalization. In addition, 38 instances (residential units) without electricity data were removed from the initial dataset of 197 instances. Seven independent variables of technical information where more than 50% of the data were missing were omitted. Five independent variables of technical information with a lower rate of missing data (18% for T13, 22% for T14, 1% for T22, and 11% for T32/33) were interpolated using mean imputation.

8.5.3 Data analysis

Three analytic models were designed in this research to (i) explore the cost data ability to predict energy use, (ii) identify the appropriate ML algorithm, and (iii) define the critical variables:

- Model 1: Cost variables only (24 variables)
- Model 2: Basic and cost variables (28 variables)
- Model 3: Basic, cost, and technical variables (71 variables)

Algorithm comparison and feature selection were performed for each model using 10-fold cross validation. In total, 28 ML algorithms were tested and the top 5 algorithms were selected for each model. Some of the algorithms used were sequential minimum optimization (SMO) regression, linear regression, random subspace, addictive regression, Gaussian processes, and K-star. Algorithm performance was evaluated using criteria such as the correlation coefficient and root mean square error (RMSE). Correlation-based feature selection (CFS) subset evaluation with a greedy stepwise method was used for feature selection for each

model. CFS evaluates subsets of features by considering both individual predictive ability of each feature and the interrelations among them. Greedy stepwise implements greedy forward or backward search through feature subsets [37]. For the selected features, Pearson's *R* value between the dependent and independent variables and the Pearson correlation were tested.

8.5.4 Findings

Data on construction costs of Virginia LIHTC multifamily projects support previous research indicating that developer/builder organizations continue to adopt new technology and adjust to associated costs. The difference in the total cost between green and nongreen developments is not statistically different across the entire sample of development total costs. The data indicate a higher average total cost for nongreen developments of 6.2% or \$7.15 per square foot (ft^2; Table 8.3). LIHTC green development data indicate a lower average cost of 13% or \$10.08 per square foot of indirect or "hard" costs and a higher average by 6.9% or \$2.93 per square foot in indirect and soft costs (Table 8.5).

Sample data require higher resolution to go beyond the square foot comparison level. Nevertheless, nongreen LIHTC developments cost more per square foot but contained smaller total unit sizes and comprised fewer developments built after 2008, when green rating systems were integrated into Virginia LIHTC policy. Because green developments occurred primarily after 2008, costs across the entire sample were analyzed using two methods: (i) *without* PPI inflation for nongreen developments after 2008 and (ii) *with* PPI inflation for nongreen developments after 2008. *Without* PPI inflation for nongreen developments, green developments cost more in 2013 dollars. *With* PPI inflation for nongreen developments, green developments cost less in 2013 dollars. The resulting difference in cost per square foot between the nongreen and the green developments was 6.9% less for green in 2013 dollars. However, none of these differences are statistically significant.

The data indicate higher average soft cost (Table 8.6) in the areas of professional services, financing, permits and fees, developer fees, and start-up and reserves and lower average soft cost in the areas of services, bonding fees, and pre-development. Professional services include Architects, Engineers, Real Estate Agents, and Consultants, including Green Building Consultants (Table 8.7). Financing refers to costs associated with financing the construction process, including loan fees, loan interest, legal fees, real estate tax, insurance, and bridge loans. Permits and fees are relative to

Table 8.5 Development costs: green vs. nongreen

	Average cost per ft^2		
	Green	**Nongreen**	**Diff. (± %)**
Direct (hard)	\$66.21	\$76.29	−13
Indirect (soft)	\$42.37	\$39.44	6.9
Total	\$108.59	\$115.74	−6.2

Table 8.6 Detailed soft costs ($/ft^2): green vs. nongreen

Soft cost	Green	Nongreen	Diff. (± %)	Sig.
Services	$8.16	$10.44	−21	0.10
Bonding fee	$0.30	$0.45	−33	0.41
Prof. services	$5.59	$3.57	36	0.13
Pre-development	$0.93	$0.96	−3	0.95
Financing	$4.12	$4.07	1.2	0.51
Permits and fees	$3.84	$3.34	13	0.38
Developer fee	$13.46	$11.69	13	0.45
Start-up and reserves	$5.13	$3.72	27	0.9

Table 8.7 Green building consultant fee overview

Unit of analysis	Green building consultant fee
Percentage of total cost	0.38%
Percentage of indirect cost	0.93%
Percentage of professional services (indirect cost)	16.34%
Fee $/ft^2	$0.36
Fee $/unit	$336.66

the locality of the construction and refer to local government fees and permanent financing fees. Developer fees refer to allowed overhead costs for the builder-developer organization and start-up and reserves include marketing, rent-up, operating deficits, replacement reserves, furniture, and equipment.

Services within general contractor services include overhead, profits, and general requirements. Bonding fees refer to costs associated with performance and bidding bonds, and pre-development fees include market study, appraisal, environmental reports, and tax credits.

The results suggest that the average cost per square foot is not significantly statistically different across time and across the entire set of developments sampled (green and nongreen). Therefore, both nongreen and green developments do not deviate significantly enough from the overall average over time to indicate that one sample set has higher costs per square foot. This implies that over time, green development costs per square foot (especially hard costs) have diffused into the industry at a similar level to nongreen construction developments.

The literature suggests that technology innovation diffusion must overcome developer-builder resistance for success [16]. The result of increased professional services and reduced general contracting (GC) services suggests that risk in this sample of LIHTC green developments is shared across multiple key stakeholders in the project delivery process. Traditionally, in the nongreen sample, lower professional fees and higher general contracting (GC) services are indicative of risk being

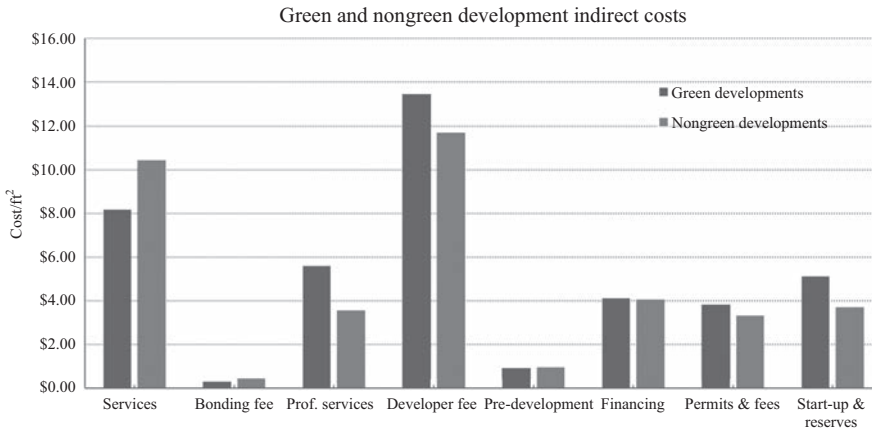

Figure 8.2 Green and nongreen development indirect costs

carried by the GC more than other stakeholders, which has historically generated resistance to new technologies.

Owing to the higher cost of "services" in Figure 8.2, a detailed analysis of the contribution of green building consultant fees to soft costs was undertaken in Table 8.7. These fees do not appear to be a primary contributor to higher soft costs in the green developments sampled.

8.6 Energy use and development costs

Although the cost comparison was critical to this work, the major aim was to determine whether a positive relationship exists between green construction costs and energy saved by residents. The design and construction process often requires a "bottomline" approach that could influence the likelihood of certain processes, technologies, or products over others. However, our analysis does not indicate this influence.

8.7 Model 1: Cost information only

8.7.1 Algorithm comparison

Model 1 uses only cost information (Table 8.8) to predict energy use based on direct and indirect costs of the multifamily units. The direct and indirect cost variables described in Table 8.2 were used for this model. Table 8.8 summarizes the top 5 algorithms among 28 algorithms sorted by correlation coefficient in descending order. SMO regression shows the best result with the highest correlation coefficient and the lowest RMSE, followed by linear regression. Random committee, K-nearest neighbors, and k-star perform similarly. Therefore, Model 1 findings are presented based on SMO regression results.

Table 8.8 Top algorithm comparison for Model 1

Algorithms	Corr. coeff.	RMSE
SMO regression	0.5146	0.2222
Linear regression	0.4963	0.2241
Random committee	0.4865	0.2258
K-nearest neighbors (K = 1)	0.4864	0.2258
K-star	0.4864	0.2258

Table 8.9 Feature selection for Model 1

Code	Description	Corr. coeff.	Absolute corr. coeff.	*p*-Value
S08	Pre-development	0.3289	0.3289	<0.0001
S04	Profit	0.3186	0.3186	<0.0001
S12	Start-up and reserves	−0.2957	0.2957	0.0002
S05	General requirement	−0.2772	0.2772	0.0004
S06	Bonding fee	0.2271	0.2271	0.0040

8.7.2 Feature selection

Among the 24 cost variables, the model selected 5 cost information features with strong prediction power (Table 8.9). The five selected features rank the top five variables with the highest absolute correlation coefficient values. At the 95% significance level, *p*-values of all selected features were less than 0.004. All the selected features are indirect costs. The pre-development, profit, and bonding fee features show a positive relationship with energy usage in the multifamily units used in this study. Start-up and reserves and general requirement show a negative relationship with energy usage. This finding suggests that higher indirect investment may lead to better energy performance, although further investigation is required.

8.8 Model 2: Basic and cost information

8.8.1 Algorithm comparison

Model 2 selects both basic information (Table 8.1) and cost information (Table 8.2) to predict energy use. Variables in Tables 8.1 and 8.2 were used for this model. Table 8.10 summarizes the top five algorithms for this model. Additive regression showed the best result with the highest correlation coefficient and the lowest RMSE, followed by SMO regression. Therefore, additive regression was selected for Model 2 with slightly better performance slightly than Model 1.

8.8.2 Feature selection

Five features were selected (Table 8.11). The selected features are the same as those in Model 1, suggesting that additional basic information variables do not

Table 8.10 Algorithm comparison for Model 2

Algorithm	Corr. coeff.	RMSE
Additive regression	0.5375	0.2181
SMO regression	0.5294	0.2195
K-star	0.5200	0.2249
Random subspace	0.5107	0.2216
Linear regression	0.5091	0.2226

Table 8.11 Feature selection for Model 2

Code	Description	Corr. coeff.	Absolute corr. coeff.	*p*-Value
S08	Pre-development	0.3289	0.3289	<0.0001
S04	Profit	0.3186	0.3186	<0.0001
S12	Start-up and reserves	−0.2957	0.2957	0.0002
S05	General requirement	−0.2772	0.2772	0.0004
S06	Bonding fee	0.2271	0.2271	0.0040

significantly contribute to prediction performance for the multifamily units in this study. Nevertheless, these results also suggest that higher indirect investment may lead to better energy performance. Again, more investigation is needed.

8.9 Model 3: Basic, cost, and technical information

8.9.1 Algorithm comparison

Model 3 uses basic information (Table 8.1), cost information (Table 8.2), and technology information (Table 8.3) to predict energy usage in the multifamily units of this study. All variables in this study are used for this model selection. Table 8.12 summarizes the top five selected algorithms. SMO regression shows the best results with the highest correlation coefficient and the lowest RMSE, followed by the Gaussian processes. The overall performance of Model 3 significantly exceeds that of prior models. Model 3 findings are therefore presented using SMO regression results.

8.9.2 Feature selection

Nine features are selected among the 71 variables, as listed in Table 8.13. When all variables are independently evaluated using the absolute correlation coefficient, the selected features rank within the top 16. The four most significantly correlated variables are the ceiling flat *R*-value (T22), profit (S04), water heater fuel type (T11), and general requirements (S05). No basic information features were selected in Model 3. Three cost information (Table 8.2) features were selected in Model 3: (S04, S05, and S06). Six technical information (Table 8.3) features were selected in

Table 8.12 Algorithm comparison for Model 3

Algorithm	Corr. coeff.	RMSE
SMO regression	0.5648	0.2141
Gaussian processes	0.5427	0.2172
Additive regression	0.5422	0.2178
Linear regression	0.5386	0.2231
Random subspace	0.5224	0.2199

Table 8.13 Feature selection for Model 3

Code	Description	Corr. coeff.	Absolute corr. coeff.	*p*-Value
T22	Ceiling flat *R*-value	−0.3552	0.3552	<0.0001
S04	Profit	0.3186	0.3186	<0.0001
T11	Water heater fuel type	0.2865	0.2865	0.0003
S05	General requirements	−0.2772	0.2772	0.0004
T37	Percent interior lighting	−0.2531	0.2531	0.0013
T09	Air-source heat pump cooling seasonal efficiency	−0.2476	0.2476	0.0017
S06	Bonding fee	0.2271	0.2271	0.0040
T26	Foundation walls	0.2197	0.2197	0.0054
T31	Window SHGC	−0.2002	0.2002	0.0114

Model 3 (in order of significance): ceiling flat *R*-value (T22), water heater fuel type (T11), percent interior lighting (T37), air-source heat pump cooling seasonal efficiency (T09), foundation walls (T26), and window SHGC (T31).

Table 8.14 compares the selected algorithms for the three models. SMO regression offers the best performance in Models 1 and 3 and the second best in Model 2. Support vector machines are often used in research because they can solve nonlinear models effectively even with a small training data sample size [38]. SMO is an algorithm implemented using the um tool and is broadly used for SVM training [39]. In this study, it works well in correlating energy use with cost and building technology information. The findings show that prediction performance continuously improves from Model 1 to Model 3, suggesting that model performance strengthens when more meaningful features are added.

The results from Table 8.14 indicate that the cost-only model (Model 1) demonstrates a comparable performance to other two models. This finding is consistent with existing research that building technologies are highly correlated with energy consumption. The finding reveals the latent correlation between construction cost during the construction process and energy consumption during the operational stage and suggests the critical capability of cost data in predicting energy use.

Among the three models, Model 3 contains the highest number of indicators and thus demonstrates the best prediction performance. Figure 8.3 charts the Model 3 prediction, which is accurate for values in the moderate range and slightly weak

Table 8.14 Performance comparison among models

Model	Best algorithms	Corr. coeff.	RMSE
1: Cost only	SMO regression	0.5146	0.2222
2: Info + cost	Additive regression	0.5375	0.2181
3: Info + cost + tech	SMO regression	0.5648	0.2141

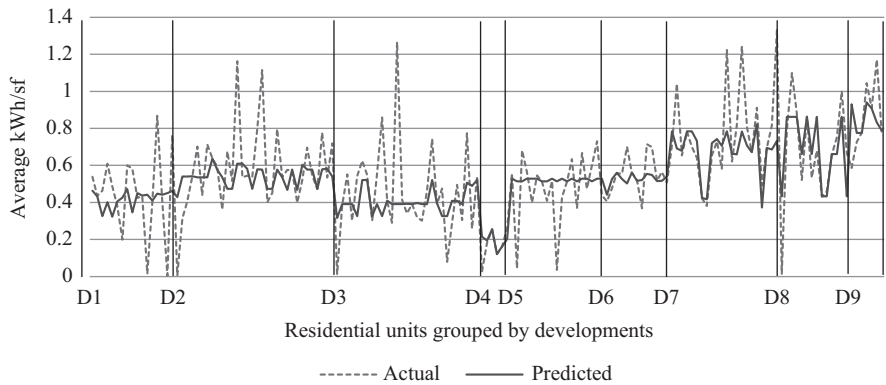

Figure 8.3 Energy consumption prediction

for peak values. As with all models in this work, the delta between peak values indicates the potential for improvement in future studies.

8.10 Conclusions

This work shares findings from a multi-year study that measured the energy performance of Virginia's green building multifamily housing stock. Over the last 10 years, the LIHTC program has encouraged EE in the affordable rental stock. This research addresses key issues related to EE and affordable housing by measuring actual, unit-level energy use. The study analyzes 24 developments containing 236 apartments and 72 variables for energy use prediction to compare the cost for building green versus nongreen evaluates for effects of annual operation and energy use.

The difference in the total construction cost between green and nongreen developments is not statistically significant. Furthermore, cost does not statistically correlate to energy usage in the unit. The data indicate a higher average total cost for nongreen developments of 6.2% or $7.15 per square foot compared to green developments. Data for LIHTC green developments indicate a lower average cost by 13% or $10.08 per square foot in direct (i.e., "hard") costs and a higher average by 6.9% or $2.93 per square foot in indirect (i.e., "soft") costs. Green building consultant fees represent $0.36 per square foot or 0.38% of total development costs.

These fees do not appear to be a main contributor to higher soft costs in green developments sampled. The 3-year energy usage study results did not indicate a significant correlation between development costs and energy usage. Low-cost green buildings realized just as much energy savings for residents as high-cost ones.

Findings from this work have identified a significantly latent relationship between construction costs and energy consumption in multifamily green buildings. Our analytic model uncovers cost and technological factors that correlate energy efficiency in residential buildings. As a result, developers can predict energy use based on construction costs. The model is a valuable tool for developers to assess or adjust their investment strategy, and it contains practical significance for planners and policy makers in pursuing a resilient and sustainable built environment. For example, energy consumption prediction allows for life cycle cost analysis at the preconstruction phase.

This study was limited to LIHTC housing units in Virginia and does not incorporate behavioral data of occupants, which may provide more accurate analysis for energy consumption. Future studies will include behavioral data and more refined ML techniques, such as error analysis and feature engineering, to refine the models. Future works will also explore the effects of weather differences on energy consumption owing to variance in development of geographic location.

References

[1] Kok, N., McGraw, M., and Quigley, J. M. (2011). "The diffusion of energy efficiency in building." *The American Economic Review 101*(3), 77–82.

[2] Jones, P. H., Taylor, N. W., Jennison Kipp, M., and Knowles, H. S. (2010). "Quantifying household energy performance using annual community baselines." *International Journal of Energy Sector Management 4*(4), 593–613.

[3] Zhao, D., McCoy, A., and Du, J. (2016). "An empirical study on the energy consumption in residential buildings after adopting green building standards." *Procedia Engineering 145*, 766–773.

[4] U.S. Energy Information Administration (EIA). (2016). *Electricity Data*. Retrieved from http://www.eia.gov/tools/faqs/faq.cfm?id=86&t=1.

[5] Beerepoot, M., and Beerepoot, N. (2007). "Government regulation as an impetus for innovation: Evidence from energy performance regulation in the Dutch residential building sector." *Energy Policy 35*(10), 4812–4825.

[6] Harvey, L. D. (2013). "Recent advances in sustainable buildings: review of the energy and cost performance of the state-of-the-art best practices from around the world." *Annual Review of Environment and Resources 38,* 281–309.

[7] Bloom, B., Nobe, M. E. C., and Nobe, M. D. (2011). "Valuing green home designs: A study of energy star homes." *The Journal of Sustainable Real Estate 3*(1), 109–126.

[8] Dastrup, S., Zivin, G. J., Costa, D. L., and Kahn, M. E. (2012). "Understanding the solar home price premium: Electricity generation and, green, social status." *European Economic Review 56*(5), 961–973.

[9] Zhao, D., McCoy, A. P., and Smoke, J. (2015). "Resilient built environment: New framework for assessing the residential construction market." *Journal of Architectural Engineering 21*(4), B4015004.

[10] Tavares, P., and Martins, A. (2007). "Energy efficient building design using sensitivity analysis—A case study." *Energy and Buildings 39*(1), 23–31.

[11] Dong, B., Cao, C., and Lee, S. E. (2005). "Applying support vector machines to predict building energy consumption in tropical region." *Energy and Buildings 37*(5), 545–553.

[12] Adomatis, S. K. (2012). "Residential appraising-describing the green house made easy." *Appraisal Journal 80*(1), 21.

[13] Ng, E. (2010). *Designing High-Density Cities for Social and Environmental Sustainability.* London: Earthscan.

[14] Rehm, M. and Ade, R. (2013). "Construction costs comparison between 'green' and conventional office buildings." *Building Research and Information 41*(2), 198–208.

[15] McCoy, A. P., Koebel, C. T., Sanderford, A. R., Franck, C. T., and Keefe, M. (2015). "Adoption of high performance housing technologies among US homebuilding firms 2000-2010." *Cityscape: A Journal of Policy Development and Research 17* (2), 157–178.

[16] McCoy, A. P., Pearce, A. R., and Ahn, Y. (2012). "Toward establishing attributes for innovative green building products: A survey of SIPS builders." *Journal of Green Building 7*(3), 153–176.

[17] Korkmaz, S., Messner, J., Riley, D., and Magent, C. (2010). "High-performance green building design process modeling and integrated use of visualization tools." *Journal of Architectural Engineering 16*(1), 37–45.

[18] Konchar, M., and Sanvido, V. (1998). "Comparison of US project delivery systems." *Journal of Construction Engineering and Management 124*(6), 435–444.

[19] Baird, G. (2010). *Sustainable Buildings in Practice*. London: Routledge.

[20] Jackson, J. (2009). "How risky are sustainable real estate projects? An evaluation of LEED and energy star development options." *Journal of Sustainable Real Estate 1*(1), 91–106.

[21] Yudelson, J. (2008). *Marketing Green Building Services*. Architectural Press, an Imprint of Elsevier: Oxford, UK.

[22] Ahn, Y. H., and Pearce, A. R. (2007). "Green construction: Contractor experiences, expectations, and perceptions." *Journal of Green Building 2*(3), 106–122.

[23] Kats, G. (2003). The Costs and Financial Benefits of Green Buildings. A Report to California's Sustainable Building Task Force.

[24] Trachtenberg, A., Hill, S., McCoy, A., and Ladipo, T. (2016). "The Impact of Green Affordable Housing." *A Study by Southface and the Virginia Center for Housing Research*. February 1, 2016. DOI: 10.13140/RG.2.1.1179.4960

[25] Choi, C. (2009). "Removing market barriers to green development: Principles and action projects to promote widespread adoption of green development practices." *Journal of Sustainable Real Estate 1*(1), 107–138.

[26] Bird, S., and Hernández, D. (2012). "Policy options for the split incentive: increasing energy efficiency for low-income renters." *Energy Policy 48*, 506–514. doi:10.1016/j.enpol. 2012.05.053.

[27] Hynek, D., Levy, M., and B. Smith. (2012). "Follow the Money: Overcoming the Split Incentive for Effective Energy Efficiency Program Design in Multi-family Buildings." Retrieved 1 Jan 2017 from http://aceee.org/files/proceedings/2012/data/papers/0193-000192.pdf.

[28] Miller, N., Pogue, D., Saville, J., and Tu, C. (2010). "The operations and management of green buildings in the United States." *Journal of Sustainable Real Estate 2*(1), 51–66.

[29] Nalewaik, A., and Venters, V. (2008). "Cost and Benefits of Building Green." *IEEE Engineering Management Review 38*(2), 77–87. DOI: 10.1109/EMR.2010.5497026

[30] Wollos., K. G. (2011). Enhancing Energy Efficiency and Green Building Design in Section 202 and Section 811 Programs. Washington, DC: U.S. Department of Housing and Urban Development. Print. 17-49.

[31] Campbell. E. J. (n.d.). Affordable Housing Adapts to New Building Trends. bdmag.com n.d. web. Oct. 2014.

[32] Pivo, G. (2013). "The effect of transportation, location, and affordability related sustainability features on mortgage default prediction and risk in multifamily rental housing." *Journal of Sustainable Real Estate 5*(1), 50–67.

[33] Watson, R. (2009). "The Green Building Impact Report 2008." *Journal of Sustainable Real Estate 1*(1), 241–243.

[34] Matthiessen L., and Morris P. (2007). Cost of Green Revisited: Reexamining the Feasibility and Cost Impact of Sustainable Design in the Light of Increased Market Adoption. *Davis Langdon*: New York.

[35] Zhao, D., McCoy, A. P., Du, J., Agee, P., and Lu, Y. (2017). "Interaction effects of building technology and resident behavior on energy consumption in residential buildings." *Energy and Buildings 134*, 223–233.

[36] Ang, A., Bekaert, G., and Wei, M. (2007). "Do macro variables, asset markets, or surveys forecast inflation better?" *Journal of monetary Economics 54*(4), 1163–1212.

[37] Hall, M. A. (1999). *Correlation-based Feature Selection for Machine Learning.* Doctoral dissertation, The University of Waikato, Hamilton

[38] Zhao, H. X., and Magoulès, F. (2012). "A review on the prediction of building energy consumption." *Renewable and Sustainable Energy Reviews 16*(6), 3586–3592.

[39] Chang, C. C., and Lin, C. J. (2011). "LIBSVM: A library for support vector machines." *ACM Transactions on Intelligent Systems and Technology (TIST) 2*(3), 27.

Chapter 9

Secondary battery technologies: a static potential for power

Pavlos Nikolaidis[1] *and Andreas Poullikkas*[2]

Electrical energy storage (EES) systems provide various benefits of high energy efficiency, high reliability and controllability, low cost and environmental impact, and so on, by storing and retrieving energy on demand. Historically, electrochemical battery storage systems have by far spurred the greatest interest of research, offering immediate response times, medium-to-long term storage duration and no power-rate limitations. Based on electrochemical oxidation–reduction reversible reactions, batteries can convert chemical energy stored in their active materials directly into electricity and vice versa. In this work, the most important battery technologies are reviewed and compared along with their contribution in global battery market. Lithium-ion monopolize in portable electronic devices, whereas lead–acid holds the exclusivity in automotive starting, lighting and ignition (SLI) applications and is considered as the best choice for small-to-medium scale stationary applications of uninterruptible power supply (UPS) and buck-up power. In terms of safety and simplicity, both systems are considered viable options for small-scale residential applications, while advanced lead–acid and high-temperature batteries are suited in medium-to-large scale applications including commercial and industrial consumers. The most discussed aspects relating to electrochemical storage are the exhaustible material reserves which may cause their cost to increase and battery disposition which locally affects consumers and globally the whole of mankind. However, a key solution exists, namely recycling, and is supported by various processes. Once the impacts from the collection and transportation of all types of spent batteries are minimized, the field of electrochemical EES integration will be expanded more and more, resulting in a sustainable development.

9.1 Introduction

EES finds ready application in a diverse range of sectors including portable electronics, transportation and stationary systems, providing traction and propulsion,

[1]Department of Electrical Engineering, Cyprus University of Technology, Cyprus
[2]Cyprus Energy Regulatory Authority, Cyprus

the ubiquitous automotive starting, lighting and ignition (SLI), standby power, remote area power supply, etc. [1]. Apart from their potential support in mobile devices, automotive vehicles, space applications and the rest of autonomous or isolated systems, for several years now, EES systems are attracting increasing interest for power-quality regulation, bridging power and energy-management applications in power system operations. Optimal planning of such systems can enhance grid stability, increase penetration of renewable energy sources (RES), improve the efficiency of energy systems, conserve fossil fuel reserves and reduce environmental impact of energy generation, separating the power production from its consumption, both in space and time [2,3].

Classified by the form of stored energy into mechanical, chemical, electrochemical and electromagnetic, the term of storage refers to a wide variety of techniques and technologies. Historically, electrochemical battery storage systems have by far spurred the greatest interest of research, demonstrating many different chemistries to meet the ever-increasing demand. Possessing immediate response times, medium-to-long term storage duration and no power-rate limitations, they are capable of participating in almost all realistic EES applications. In the beginning, batteries were used by scientists to study and understand electricity. After their discovery, they became a power for telegraphs, first telephones and other early electrical devices, generating soon a need for more compact prototypes with better capacity and stable voltage and current [4]. The first conventional secondary battery, lead–acid (Pb–acid), was invented in 1859. Since the beginning of the next century (and specifically in 1915), nickel–cadmium (NiCd) batteries have been used commercially, followed by the introduction of sodium–sulfur (NaS) in the 1960s. Although lithium-ion (Li-ion) battery was first proposed in the same year, the first was produced 31 years later. Sodium–nickel chloride (NaNiCl or ZEBRA) technology was acquired by MES (Swiss) in the early 1999 [5]. Although many other chemical topologies, including secondary batteries, flow batteries and fuel cells, have been investigated and found technically feasible, they are still under development.

Extensive research has revealed that a single storage device cannot meet the requirements of a whole power system; however, the later may qualify more than one applications either directly if it is operated in different modes providing individual storage functions or indirectly by just avoiding the need to apply additional devices to meet an event. According to the application that the battery energy storage (BES) systems are intended for use, they are presented favorable or unfavorable as to some performance characteristics, namely, power and energy rating, volumetric and gravimetric power and energy density, discharge time and time of response, operating temperature, self-discharge rate, round-trip efficiency, critical battery voltage, calendric and cyclic lifetime, investment and whole life cost, spatial requirement, environmental impact, recharge time and storage duration, memory effect, technical maturity, scalability, recyclability, transportability [6]. All information found in the literature is listed in Table 9.1, providing the technical and operational performance characteristics of the most important battery technologies.

Table 9.1 Characteristics of secondary battery technologies [5,7–20]

	Pb–acid	**NiCd**	**NiMH**	**Zn–air**	**NaS**	**ZEBRA**	**Li-ion**
Power rating (MW)	0–20	0–40	0.01–3	0–0.01	0.05–8	0–0.3	0–0.1
Energy capacity (MW h)	0.001–40	6.75	–	–	0.4	–	0.004–10
Power capital cost ($/kW)	300–600	500–1,500	270–530	100–250	>1,000	150–300	1,200–4,000
Energy capital cost ($/kW h)	200–400	800–1,500	200–730	10–60	300–500	100–200	600–2,500
O&M cost ($/kW year)	50	20	–	–	80	–	–
Specific power (W/kg)	180	140–180	220	60–225	150–240	174	500–2,000
Specific energy (W h/kg)	30–50	35–60	50–75	450–650	120	120	100–200
Power density (kW/m^3)	10–400	38–141	8–588	10–208	1.3–50	54.2–300	56–800
Energy density (kW h/m^3)	25–90	15–150	39–300	22–1,673	150–345	108–190	94–500
Technical maturity	Mature	Commercialized	Mature	Developing	Commercialized	Commercializing	Commercialized
Daily self-discharge (%)	0.1–0.2	0.1–0.2	5–20	Almost 0	Almost 0	20	0.03
Depth of discharge (%)	80	100	50	–	100	–	80
Lifetime (years)	5–15	10–20	2–15	0.17–30	10–15	10–14	5–15
Cycling times	200–2,000	1,500–3,000	1,200–1,800	100–300	1,500–5,000	1,000	3,000–10,000
Round-trip efficiency (%)	85–90	60–90	50–80	50	89–92	70–85	~100
Response time	Millisecond	Millisecond	–	–	Millisecond	–	Millisecond
Suitable storage duration	Minutes–days	Minutes–days	–	Hours–months	Seconds–hours	Seconds–hours	Minutes–days
Autonomy	Seconds–hours	Seconds–hours	–	Seconds–24 h	Seconds–hours	Seconds–hours	Minutes–hours

In Section 9.2, the state-of-the-art battery technologies are classified and discussed in detail. Section 9.3 refers to the battery market and contribution of each individual technology, while recycling aspects are conducted in Section 9.4. Finally, the conclusion is summarized in Section 9.5.

9.2 Principles of operation

Batteries are classified as primary which are not rechargeable and secondary which can be recharged. BES refers to the secondary batteries which consist of cells each comprising a pair of opposite electrodes immersed in an electrolyte, and they can store and provide energy through electrochemical reversible reactions. Depending on the materials used as electrodes and electrolytes, BES systems are divided into lead–acid, alkaline, metal–air, high temperature and lithium-ion [7,21,22].

9.2.1 Lead–acid

As the oldest type of rechargeable batteries, lead–acid (Pb–acid) is widely used in vehicles and boats for engine starting and a host of other facilities and is therefore considered as one of the best suited for stationary applications as it can supply excellent pulsed power [17,22,23]. A schematic diagram of a Pb–acid battery operation is shown in Figure 9.1. In the charged state, the battery consists of lead

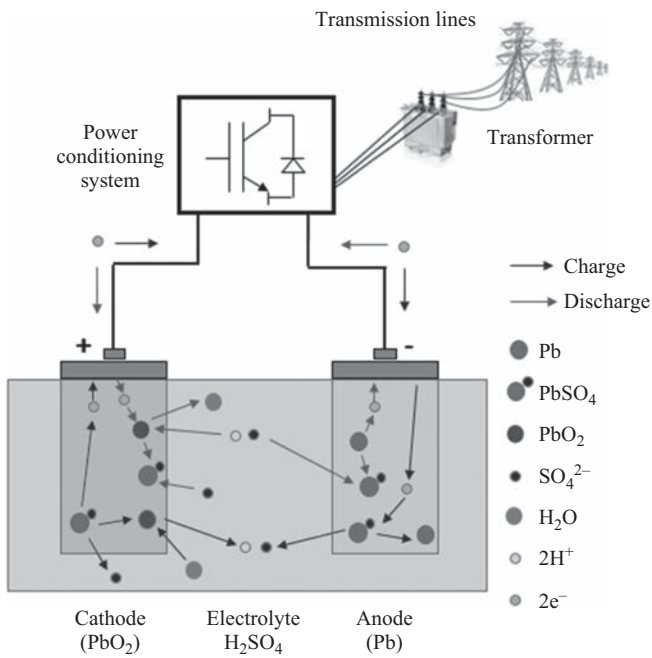

Figure 9.1 Demonstration of Pb–acid battery cell [39]

(Pb) and lead oxide (PbO_2) both in 37% sulfuric acid (H_2SO_4), whereas in the discharged state, lead sulfate ($PbSO_4$) is produced both at the anode and the cathode while the electrolyte changes to water [24]. The chemical reactions at the anode and cathode are presented by (9.1) and (9.2), respectively [25]. The rated voltage of a Pb–acid cell is 2 V and capable of operating in the range of −5 °C and 40 °C [7,9,26]:

$$Pb + SO_4^{2-} \rightleftharpoons PbSO_4 + 2e \tag{9.1}$$

$$PbO_2 + SO_4^{2-} + 4H^+ + 2e^- \rightleftharpoons PbSO_4 + 2H_2O \tag{9.2}$$

Although lead–acid technology has maturity of over a century and low manufacturing cost, the lead and sulfuric acid used to form the anode and the electrolyte, respectively, are toxic and its cycle life is relatively limited. In addition, flooded type devices require periodic water maintenance and large footprint due to their low specific energy (25 W h/kg) and discharging depth (70%), thus they become unfavorable for large-scale applications. From the invention of valve regulated lead–acid (VRLA) batteries, banks of up to 36 MW are already being utilized for power generation from RES, as they achieve higher specific energy (30–50 W h/kg) and depths of discharge (80%) with negligible maintenance requirements [9,10]. More recently, an advanced Pb–acid system with a split design has been demonstrated and is able to provide significantly longer cycle life in the order of ~17,000 cycles compared to 200–2,000 of VRLA, enabling its application in large scales [25]. Regardless of improvements, lead toxicity and sulfuric acid are still the main concerns and may restrict this battery type from being indefinitely used.

9.2.2 Alkaline

Nickel–cadmium (NiCd) and nickel–metal hydride (NiMH) represent the alkaline batteries comprising nickel oxide for cathode and potassium hydroxide for electrolyte. Nickel–cadmium batteries are widely used in both portable and stationary applications providing chief advantages compared to lead–acid such as higher specific energy (60 W h/kg), longer cycle life (1,500–3,000 cycles) and lower water-maintenance requirements, against the higher manufacturing cost [1]. At the charging state, they consist of a nickel oxyhydroxide NiOOH cathode, a metallic cadmium Cd anode, a separator and an alkaline electrolyte [5]. During the discharging process, the cathode NiOOH reacts with water which exists in the aqueous potassium hydroxide ($KOH{\cdot}H_2O$) to produce $Ni(OH)_2$ and hydroxide ion at the anode. The reversible reactions are given in (9.3) and (9.4) for the anode and cathode, respectively, while a better explanation can be obtained by Figure 9.2 through a flow diagram:

$$Cd + 2OH^- \rightleftharpoons Cd(OH)_2 + 2e^- \tag{9.3}$$

$$2NiOOH + 2H_2O + 2e^- \rightleftharpoons 2Ni(OH)_2 + 2OH^- \tag{9.4}$$

On the contrary, except from the higher cost, both its maximum capacity and whole life are subject to memory effect and thus cannot be repeatedly recharged after

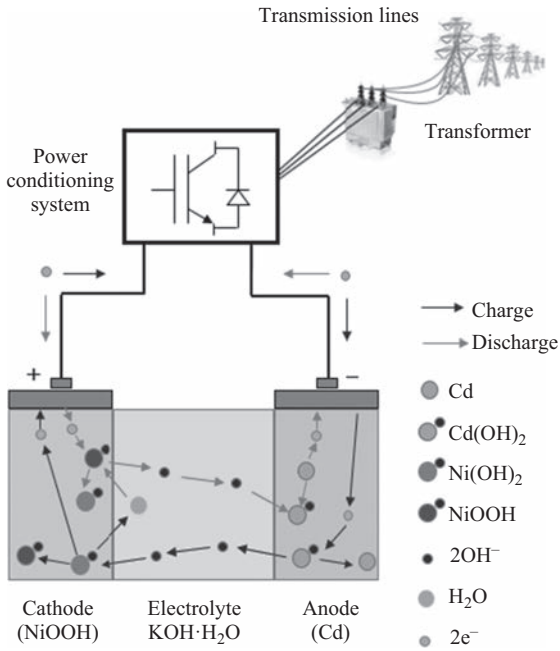

Figure 9.2 Demonstration of Ni–Cd battery cell [39]

being partially discharged [27]. Similar to lead–acid, nickel–cadmium spent batteries create environmental concerns because of cadmium and nickel toxicity and consequently are largely displaced [28]. As regards nickel–metal hydride (NiMH), it defers in which a hydrogen-absorbing alloy is used to form the electrode instead of cadmium. The electrochemical reactions at the anode and cathode of such a device are represented by (9.5) and (9.6), respectively. Possessing the same with NiCd cell voltage of 1.2 V, NiMH can achieve higher specific energy (up to 75 W h/kg) and reduced memory effect. In the contrary, it suffers from severe self-discharge issues (20% per day) and lower efficiency; thus, it becomes an undesirable candidate for electrical storage from RES [8,11,12,29]:

$$MH_x + OH^- \rightleftharpoons M + H_2O + e^- \tag{9.5}$$

$$NiO(OH) + H_2O + e^- \rightleftharpoons Ni(OH)_2 + OH^- \tag{6.6}$$

Nevertheless, the distinct advantage of the wide temperature-range of operation (from a minimum of −40 °C to 50 °C) of Ni-based batteries, make their use possible for some utility-scale EES applications [13].

9.2.3 Metal–air

Metal–air batteries can be considered as special types of fuel cell which use metal instead of fuel and air as the oxidant. The anodes in these batteries are commonly

available metals with high energy density such as lithium (Li), aluminum (Al) or zinc (Zn), while the cathodes are made of either porous carbon or metal mesh capable of absorbing oxygen (O_2) from air. The liquid or solid electrolytes are mainly good hydroxide ion (OH^-) conductors like potassium hydroxide (KOH) [9]. Although Li–air has a theoretical specific energy as high as 11,140 W h/kg, there are concerns about a probable fire due to the high reactivity of Li with humid air [25,30]. Moreover, it possesses a much more expensive cell compared to Zn–air, which is environmentally benign and exhibits long storage life while un-activated [27]. Hence, Zn–air represents the only technically feasible example of metal–air batteries up to date, offering a high energy density (650 W h/kg). It provides a cell voltage of 1.6 V, temperature range from −20 °C to 50 °C and negligible self-discharge rate. On the contrary, it is difficult to be recharged and offers a limited cycling capability of a few hundred cycles along with a quite low efficiency of fairly 50% [5]. However, Zn–air constitutes a developing technology that occurs promising and is able to contribute in future energy-management applications. The chemical reactions, at the anode and cathode of a Zn–air cell shown in Figure 9.3, are provided in (9.7) and (9.8), respectively. Other metals proposed to form the anode of a metal–air cell can be represented by a similar manner. Equations (9.9) and (9.10) are given as an example of an under-research metal–air battery of aluminum (Al) anode:

$$Zn + 2OH^- \rightleftharpoons Zn(OH)_2 + 2e^- \tag{9.7}$$

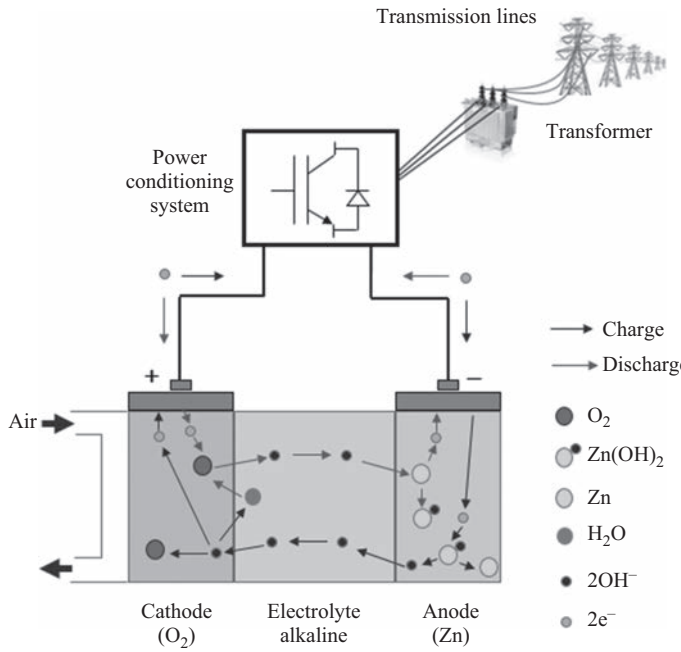

Figure 9.3 Demonstration of Zn–air battery cell [39]

$$H_2O + O_2 + 2e^- \rightleftharpoons 2OH^- \tag{9.8}$$

$$Al + 4OH^- \rightleftharpoons Al(OH)_4 + 3e^- \tag{9.9}$$

$$O_2 + H_2O + 3e^- \rightleftharpoons 3OH^- \tag{9.10}$$

9.2.4 High temperature

High temperature batteries consist of molten sodium anode material, a solid electrolyte of beta-alumina and according to the cathode solid reactant they are subdivided into sodium–sulfur (NaS) and sodium–nickel chloride (NaNiCl or ZEBRA) [31]. NaS batteries are constructed from inexpensive materials and are considered as an attractive option for large-scale stationary electrical storage applications since they offer high energy density (150–345 kW h/m^3) and cycle efficiency (89%–92%), long cycle life (1,500–5,000 cycles) and they are much smaller and lighter than NiCd, NiMH and Pb–acid [8,10,32]. The main disadvantages of NaS technology are the corrosive nature of manufacturing materials and the requirement for constant heat input in order to maintain the electrolyte's molten state which is ensured at 300 °C–350 °C increasing the hazard of probable reaction between electrode materials and associated fire [22]. A demonstration of a charge/discharge cycle concerning a NaS cell is illustrated in Figure 9.4 while the

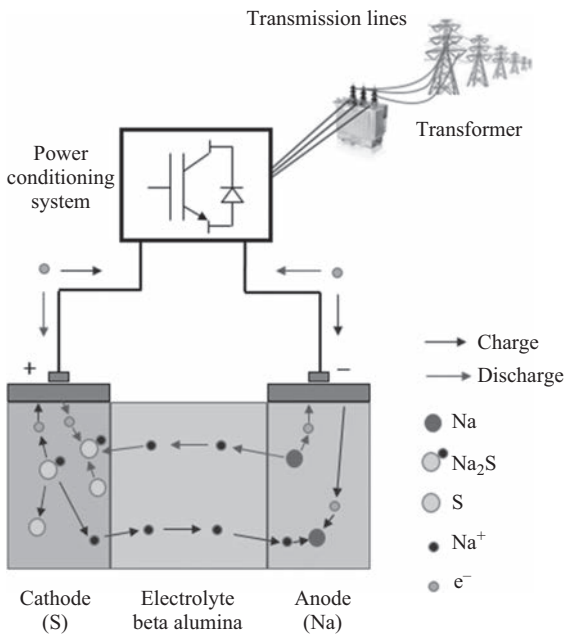

Figure 9.4 Demonstration of Na–S battery cell [39]

reactions realized at the negative and positive electrodes are shown in (9.11) and (9.12), respectively:

$$2Na \rightleftharpoons 2Na^{+} + 2e^{-} \tag{9.11}$$

$$S + 2e^{-} \rightleftharpoons S^{2-} \tag{9.12}$$

On the other hand, ZEBRA technology has some advantages relative to NaS systems including lower mean temperature of 250 °C–350 °C and a much safer cell, no corrosion problems, high cell voltage (2.58 V) and the ability to withstand limited overcharge and discharge [1,14]. The overall chemical reaction occurs in a ZEBRA battery is represented by (9.13):

$$2NaCl + Ni \rightleftharpoons NiCl_2 + 2Na \tag{9.13}$$

9.2.5 Lithium-ion

The last major type of battery storage technology is lithium-ion (Li-ion) system containing a graphite anode, a cathode formed by a lithium metal oxide ($LiCoO_2$, $LiMO_2$, $LiNiO_2$, etc.) and an electrolyte consisting of a lithium salt dissolved in an organic liquid (such as $LiPF_6$); thus, electrodes can reversibly accommodate ions and electrons [33]. Finally, a separator is deployed to prevent a short-circuit between the electrodes and associated hazard of flame burst. A typical structure of a Li-ion battery with a cathode made of $LiCoO_2$ is demonstrated in Figure 9.5. During discharging, lithium atoms (Li) are oxidized to lithium ions (Li^{+}) releasing electrons. While the electrons are flowing through the external circuit to reach the cathode, Li^{+} are moving through the electrolyte to the cathode where they react with the cobalt oxide (CoO_2) and electrons to form lithium cobalt oxide ($LiMO_2$) [34]. Equations (9.14) and (9.15) show the chemical reactions realized at the anode and cathode of the demonstrated example. However, the reactions can be generalized into (9.16) and (9.17) to explain the similar operation occur if different lithium metal oxides ($LiMO_2$) are used to form the cathode [5,13]:

$$LiC_6 \rightleftharpoons Li^{+} + e^{-} + 6C \tag{9.14}$$

$$CoO_2 + Li^{+} + e^{-} \rightleftharpoons LiCoO_2 \tag{9.15}$$

$$Li_xC \rightleftharpoons xLi^{+} + xe^{-} + C \tag{9.16}$$

$$LiMO_2 + xLi^{+} + xe^{-} \rightleftharpoons Li_{1-x}MO_2 \tag{9.17}$$

Lithium-ion batteries offer chief advantages over the nickel–cadmium and lead–acid, as they provide the highest specific energy (200 W h/kg), specific power (500–2,000 W/kg) and nominal voltage (3.7 V), energy storage efficiency of close to 100%, lower self-discharge rate (0.03% per day), no memory effect and extremely low maintenance requirements [7,24]. Despite the above advantages, the high cost as well as the prohibitive for their lifetime deep discharging are the main drawbacks of lithium-ion batteries that restrict their use in large-scale applications [8].

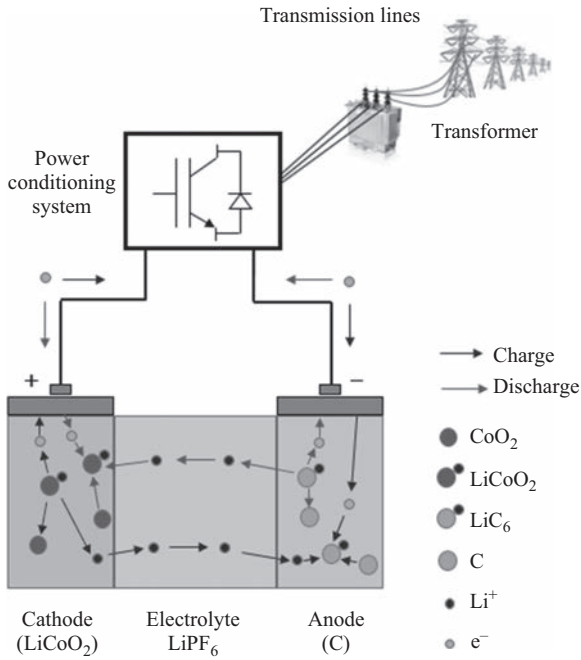

Figure 9.5 Demonstration of Li-ion battery cell [39]

Although considerable efforts are paid to lower the cost, concerns still exist relating to an increasing consumption in the future, since the depleting worldwide lithium reserves may lead to increasing raw material costs [15,35]. A further disadvantage is the sensitivity they provide to high temperatures and thus are equipped with a battery-management system to at least provide overvoltage, over-temperature and overcurrent protection [15,36]. Their suitable temperature range of operation is rated between −30 °C and 60 °C [9].

9.3 Battery market and public concerns

With the fast-paced changing technologies in the battery industry, new chemistry references addressing new technologies are coming to the market. Increasing need for mobile devices along with the electrification of transportation sector and the tendency of modern power systems to shift toward decarbonization lead to the differentiation of batteries into various types providing different properties to successfully match distinguished applications to individual technologies. The EES application field along with the main advantages and disadvantages relating to each battery technology are presented in Table 9.2.

Typical household-type batteries are used in consumer items such as telephones, flashlights, radios, watches and so on. At the end of the twentieth century,

Table 9.2 Comparisons of secondary battery technologies

	Typical use	**Advantages**	**Disadvantages**	**Operating temperature range (°C)**
Pb–acid	Power quality support, starting/ lighting/ignition services	Most mature technology, low manufacturing cost	Environmental concerns about lead toxicity and sulfuric acid	−5 to 40
NiCd	Power quality support, automotive support	Low maintenance requirements	Memory effect, environmental concerns about nickel and cadmium toxicity	−40 to 50
NiMH	Power quality support, automotive support	Absence of toxic metal, reduced memory effect versus to Ni–Cd cell	Severe self-discharge rate	−40 to 50
Zn–air	Energy-management services	Environmentally benign, negligible self-discharge rate	Difficult recharging, limited cycling capability	−20 to 50
NaS	Decentralized power quality support, centralized energy management	Inexpensive manufacturing materials, small and light designs	Corrosive nature of manufacturing materials, heat input requirement, fire hazard	300 to 350
ZEBRA	Decentralized power quality support, centralized energy management	No corrosion problems, safer cell versus Na–S cell	Severe self-discharge rate	250 to 350
Li-ion	Portable devices, electric vehicles	High specific energy and power, increased nominal voltage, efficiency of near 100%	High capital cost, sensitivity to high temperatures	−30 to 60

the rechargeable batteries occupied 8% of the European portable market. Among them, NiCd owned 38%, followed by NiMH with a share of 35% and Li-ion near 18% of the European market [37]. In the beginning of the twenty-first century, Li-ion batteries surpassed other cells in various parameters. With high power and energy per unit mass and volume, Li-ion monopolize today in portable electronic devices (such as in smartphones and laptops). Although it currently outperforms other systems dominating the battery market with a high market share of 63% worldwide, it is by far the most expensive to be applied in stationary larger scale EES applications [38]. On the other hand, Pb–acid holds the exclusivity in automotive SLI applications and is considered as the best choice for small-to-medium scale stationary applications of UPS and buck-up power [39]. Globally, Pb–acid contributes with about 18% of the quantity of energy stored using electrochemical storage systems, while NaS accounts for 24%, confirming their suitability for large-scale applications [2].

Our entry into the fourth industrial revolution set to modernize our daily life, notably with the booming of digital technologies (communications, artificial intelligence, the Internet of Things (IoT), 3-D printing or nano/biotechnologies), requires us to integrate sustainable development goals and actions to address the critical damage caused by the previous industrial revolutions [40]. The increasing presence of batteries, both primary and secondary, in daily human-life, make them almost invisible to people. However, potential environmental concerns relating to their production and disposal are of vital importance. In terms of sustainability, life cycle analyses should include production, operation, maintenance, disposal and replacement, in order to assess both the environmental and economic improvements. Aiming to study the production of batteries, the majority of studies focus on energy demand and greenhouse gas emissions. Other environmental impacts such as toxicity, acidification, abiotic depletion, eutrophication and ozone degradation are considered less often [41].

Regarding the disposition of batteries, there are different alternatives involving landfill, stabilization, incineration and recycling. In a landfill, mercury (Hg) and cadmium (Cd) are the main source causing soil and underground water contamination when washed out by the rain [42]. Stabilization constitutes a high-costly process involving a pretreatment of batteries to avoid any direct conduct of contained metals with the environment in landfills, while incineration can take place once the batteries are disposed of and sent to a municipal waste combustion facility, introducing hazardous emissions into the atmosphere including mercury, lead and dioxins. Recycling differs from its alternatives giving credits for recycled materials, since primary resources are saved and demand for new virgin materials is decreased. In addition, it possesses a key solution to pollution control at landfills and incinerators, due to the impact of hazardous metals (mercury, lead, copper, zinc, cadmium, manganese, nickel and lithium) present in batteries [37].

9.4 Recycling of batteries

Besides the impact on space requirements, metal intensity for each battery technology has a considerable influence on world metals availability for EES [43,44]. Considering also the environmental disasters due to improper disposition of batteries, several countries' objectives are to limit the concentration of mercury, cadmium and lead in the devices, to standardize the identification of recyclable technologies and to develop efficient recycling programs.

Nanoengineering do show promise for combining the electrochemical advantages of different materials, yielding composite designs with satisfactory performance in terms of safety and sustainability [23]. Aiming to continuously increase the energy density, the development of secondary batteries based on metal anodes (e.g., Li, Na, Mg, Zn and Al) are among the sought-after candidates for next-generation mobile and stationary storage systems [45]. Because of their reliability, stability, safety and general excellent cycling behavior and performance at various temperatures, Li-ion batteries are considered one of the most important successes of modern electrochemistry, dominating portable electronics market and now expanding to large-scale EES applications, in particular, electric vehicles (EVs) and renewable power stations [46]. However, lithium (Li) is a rare metal element and its most easily accessible reserves are in remote or in politically sensitive areas [47]. Sodium (Na) and zinc (Zn) are considered as the most promising alternatives due to the wide availability, environmental friendliness and the low cost of their abundant resources [48].

Recycling plays a critical role in reducing the demand and the impacts associated with mining and resource extraction for the battery active materials. The comprehensive procedure involves the collection, transportation, storing, reutilization, recycling, treatment and the environmentally correct final disposal of batteries [42]. Collection is a very complex aspect since its activities (especially those associated with transportation) may turn the overall operation unfeasible. In addition, for a safe final disposal, it is necessary to know the composition of the used batteries which is unrelated to their size or shape. Battery-recycling can be realized through the basic methods of separation of components via unity operations of mining treatment, pyrometallurgy and hydrometallurgy, supported by several different processes which either are designed for specific kind of battery or can be applied together with other types of materials. The first and cheapest method is realized using physical mechanisms to separate the materials of interest or to concentrate such materials for further recovering giving the turn to other methods to take place. Pyrometallurgy essentially consists of recovering materials by using high temperatures with the help of rotary, shaft or reverberatory furnace, whereas hydrometallurgy retrieves the metals that have been first dissolved in solutions, by electrolysis or precipitation [49].

9.5 Conclusion

A wide variety of battery technologies and concepts are available while others will emerge in the future. Advanced energy storage devices are playing an increasingly important role in modern society, including portable devices, EVs and large-scale smart grids. With high power and energy per unit mass and volume, Li-ion monopolizes in portable electronic devices but is by far the most expensive to be applied in stationary larger-scale EES applications. As the cheapest battery option, Pb–acid holds the exclusivity in automotive SLI applications and is considered as the best choice for small-to-medium scale stationary applications of UPS and buck-up power. Other technologies, such as high-temperature and metal–air battery storage systems, need more time to become mature and economical, and without appropriate storage opportunities, their future contribution will be caused to slow down.

On larger scales, to make intermittent power sources capable of delivering reliable baseload electricity, new findings on inexpensive and durable materials could help opening up new avenues for battery design. Such approaches include metal mesh membrane applicable to a wide variety of molten-electrode battery chemistries and other ultracapacitor-based energy storage solutions applied at both sides of the meter, extending the lifespan of batteries. The highest priority must be given to the preparation of specific recycling goals, associated with a management structure which will minimize the collection and transportation impacts while enabling the recycling of all types of spent batteries. Finally, sufficient algorithms and tools capable of capturing the whole range of both the benefits and environmental impacts of battery applications are needed in order to facilitate consumers select the best fit technology option and encourage them to do so in a sustainable manner.

References

[1] J. Baker, "New technology and possible advances in energy storage," *Energy Policy*, vol. 36, no. 12, pp. 4368–4373, 2008.

[2] M. Aneke and M. Wang, "Energy storage technologies and real life applications – A state of the art review," *Appl. Energy*, vol. 179, pp. 350–377, 2016.

[3] R. Amirante, E. Cassone, E. Distaso, and P. Tamburrano, "Overview on recent developments in energy storage: Mechanical, electrochemical and hydrogen technologies," *Energy Convers. Manage.*, vol. 132, pp. 372–387, 2017.

[4] M. Křepelková, "Evolution of batteries: From experiments to everyday usage," pp. 1–7, 2017.

[5] H. Chen, T. N. Cong, W. Yang, C. Tan, Y. Li, and Y. Ding, "Progress in electrical energy storage system: A critical review," *Prog. Nat. Sci.*, vol. 19, no. 3, pp. 291–312, 2009.

[6] A. Chatzivasileiadi, E. Ampatzi, and I. Knight, "Characteristics of electrical energy storage technologies and their applications in buildings," *Renew. Sustain. Energy Rev.*, vol. 25, pp. 814–830, 2013.

[7] I. Hadjipaschalis, A. Poullikkas, and V. Efthimiou, "Overview of current and future energy storage technologies for electric power applications," *Renew. Sustain. Energy Rev.*, vol. 13, no. 6–7, pp. 1513–1522, 2009.

[8] P. J. Hall and E. J. Bain, "Energy-storage technologies and electricity generation," *Energy Policy*, vol. 36, no. 12, pp. 4352–4355, 2008.

[9] K. C. Divya and J. Østergaard, "Battery energy storage technology for power systems—An overview," *Electr. Power Syst. Res.*, vol. 79, no. 4, pp. 511–520, 2009.

[10] A. Poullikkas, "A comparative overview of large-scale battery systems for electricity storage," *Renew. Sustain. Energy Rev.*, vol. 27, pp. 778–788, 2013.

[11] W. H. Zhu, Y. Zhu, Z. Davis, and B. J. Tatarchuk, "Energy efficiency and capacity retention of Ni-MH batteries for storage applications," *Appl. Energy*, vol. 106, pp. 307–313, 2013.

[12] A. K. Shukla, S. Venugopalan, and B. Hariprakash, "Nickel-based rechargeable batteries," *J. Power Sources*, vol. 100, no. 1–2, pp. 125–148, 2001.

[13] X. Luo, J. Wang, M. Dooner, and J. Clarke, "Overview of current development in electrical energy storage technologies and the application potential in power system operation," *Appl. Energy*, vol. 137, pp. 511–536, 2015.

[14] M. Beaudin, H. Zareipour, A. Schellenberglabe, and W. Rosehart, "Energy storage for mitigating the variability of renewable electricity sources: An updated review," *Energy Sustain. Dev.*, vol. 14, no. 4, pp. 302–314, 2010.

[15] S. Vazquez, S. M. Lukic, E. Galvan, L. G. Franquelo, and J. M. Carrasco, "Energy storage systems for transport and grid applications," *IEEE Trans. Ind. Electron.*, vol. 57, no. 12, pp. 3881–3895, 2010.

[16] S. Sabihuddin, A. E. Kiprakis, and M. Mueller, "A numerical and graphical review of energy storage technologies," *Energies*, vol. 8, no. 1, pp. 172–216, 2015.

[17] J. McDowall, "Integrating energy storage with wind power in weak electricity grids," *J. Power Sources*, vol. 162, no. 2 SPEC. ISS., pp. 959–964, 2006.

[18] Z. Wen, J. Cao, Z. Gu, X. Xu, F. Zhang, and Z. Lin, "Research on sodium sulfur battery for energy storage," *Solid State Ionics*, vol. 179, no. 27–32, pp. 1697–1701, 2008.

[19] A. Khaligh, S. Member, Z. Li, and S. Member, "Battery, ultracapacitor, fuel cell, and hybrid energy storage systems for electric, hybrid electric, fuel cell, and plug-in hybrid electric vehicles: State of the art," *IEEE Trans. Veh. Technol.*, vol. 59, no. 6, pp. 2806–2814, 2010.

[20] F. Rafik, H. Gualous, R. Gallay, A. Crausaz, and A. Berthon, "Frequency, thermal and voltage supercapacitor characterization and modeling," *J. Power Sources*, vol. 165, no. 2, pp. 928–934, 2007.

[21] P. Nikolaidis and A. Poullikkas, "Cost metrics of electrical energy storage technologies in potential power system operations," *Sustain. Energy Technol. Assess.*, vol. 25, pp. 43–59, 2018.

[22] R. M. Dell and D. A. J. Rand, "Energy storage, a key technology for global energy sustainability," *J. Power Sources*, vol. 100, no. 1, pp. 2–17, 2001.

[23] S. Xin, Y. You, S. Wang, H. Gao, Y. Yin, and Y. Guo, "Solid-state lithium metal batteries promoted by nanotechnology: Progress and prospects," *ACS Energy Lett.*, vol. 2, pp. 1385–1394, 2017.
[24] D. O. Akinyele and R. K. Rayudu, "Review of energy storage technologies for sustainable power networks," *Sustain. Energy Technol. Assess.*, vol. 8, pp. 74–91, 2014.
[25] J. Cho, S. Jeong, and Y. Kim, "Commercial and research battery technologies for electrical energy storage applications," *Prog. Energy Combust. Sci.*, vol. 48, pp. 84–101, 2015.
[26] K. S. Ng, C. S. Moo, Y. C. Lin, and Y. C. Hsieh, "Investigation on intermittent discharging for lead–acid batteries," *PESC Rec. – IEEE Annu. Power Electron. Spec. Conf.,* vol. 3839, no. 5, pp. 4683–4688, 2008.
[27] G. M. Ehrlich, *Lithium-Ion Batteries*. McGraw-Hill, New York, 2002.
[28] A. L. Salgado, A. M. O. Veloso, D. D. Pereira, G. S. Gontijo, A. Salum, and M. B. Mansur, "Recovery of zinc and manganese from spent alkaline batteries by liquid-liquid extraction with Cyanex 272," *J. Power Sources*, vol. 115, no. 2, pp. 367–373, 2003.
[29] M. A. Fetcenko, S. R. Ovshinsky, B. Reichman, *et al*., "Recent advances in NiMH battery technology," *J. Power Sources*, vol. 165, no. 2, pp. 544–551, 2007.
[30] D. Larcher and J.-M. Tarascon, "Towards greener and more sustainable batteries for electrical energy storage," *Nat. Chem.*, vol. 7, no. 1, pp. 19–29, 2015.
[31] B. L. Ellis and L. F. Nazar, "Sodium and sodium-ion energy storage batteries," *Curr. Opin. Solid State Mater. Sci.*, vol. 16, no. 4, pp. 168–177, 2012.
[32] S. J. Kazempour, M. P. Moghaddam, M. R. Haghifam, and G. R. Yousefi, "Electric energy storage systems in a market-based economy: Comparison of emerging and traditional technologies," *Renew. Energy*, vol. 34, no. 12, pp. 2630–2639, 2009.
[33] B. Scrosati and J. Garche, "Lithium batteries: Status, prospects and future," *J. Power Sources*, vol. 195, no. 9, pp. 2419–2430, 2010.
[34] J. G. Kim, B. Son, S. Mukherjee, *et al*., "A review of lithium and non-lithium based solid state batteries," *J. Power Sources*, vol. 282, pp. 299–322, 2015.
[35] I. Råde and B. A. Andersson, "Requirement for metals of electric vehicle batteries," *J. Power Sources*, vol. 93, no. 1–2, pp. 55–71, 2001.
[36] J. McDowall, P. Biensan, and M. Broussely, "Industrial lithium ion battery safety—What are the tradeoffs?," *Telecommun. Energy Conf.*, pp. 701–707, 2007.
[37] A. M. Bernardes, D. C. R. Espinosa, and J. A. S. Tenório, "Recycling of batteries: A review of current processes and technologies," *J. Power Sources*, vol. 130, pp. 291–298, 2004.
[38] X. Chen, T. Hou, K. A. Persson, and Q. Zhang, "Combining theory and experiment in lithium – Sulfur batteries: Current progress and future perspectives," *Mater. Today*, vol. 22, pp. 34–37, 2018.
[39] P. Nikolaidis and A. Poullikkas, "A comparative review of electrical energy storage systems for better sustainability," *J. Power Technol.*, vol. 97, no. 3, pp. 220–245, 2017.

[40] P. Poizot, F. Dolhem, and J. Gaubicher, "Progress in all-organic rechargeable batteries using cationic and anionic configurations: Toward low-cost and greener storage solutions?," *Curr. Opin. Electrochem.*, vol. 9, pp. 1–11, 2018.

[41] J. F. Peters, M. Baumann, B. Zimmermann, J. Braun, and M. Weil, "The environmental impact of Li-Ion batteries and the role of key parameters – A review," *Renew. Sustain. Energy Rev.*, vol. 67, pp. 491–506, 2017.

[42] D. Crocce, R. Espinosa, A. Moura, J. Alberto, and S. Tenório, "Brazilian policy on battery disposal and its practical effects on battery recycling," vol. 137, no. 1, pp. 134–139, 2004.

[43] I. Ra, "Requirement for metals of electric vehicle batteries," *J. Power Sources*, vol. 93, pp. 55–71, 2001.

[44] M. Beaudin, H. Zareipour, A. Schellenberglabe, and W. Rosehart, "Energy storage for mitigating the variability of renewable electricity sources: An updated review," *Energy Sustain. Dev.*, vol. 14, no. 4, pp. 302–314, 2010.

[45] L. Fan, S. Wei, S. Li, Q. Li, and Y. Lu, "Recent progress of the solid-state electrolytes for high-energy metal-based batteries," *Adv. Energy Mater.*, vol. 1702657, pp. 1–31, 2018.

[46] F. Schipper, P. K. Nayak, E. M. Erickson, *et al*., "Study of cathode materials for lithium-ion batteries: Recent progress and new challenges," *Inorganics*, vol. 2, p. 32, 2017.

[47] H. Wang, W. Li, D. Liu, X. Feng, J. Wang, and X. Yang, "Flexible electrodes for sodium-ion batteries: Recent progress and perspectives," *Advanced Materials*, vol. 1703012, pp. 1–8, 2017.

[48] J. Fu, Z. P. Cano, M. G. Park, A. Yu, M. Fowler, and Z. Chen, "Electrically rechargeable zinc–air batteries: Progress, challenges, and perspectives," *Advanced Materials*, vol. 1604685, pp. 1–34, 2017.

[49] D. Crocce, R. Espinosa, A. Moura, J. Alberto, and S. Tenório, "An overview on the current processes for the recycling of batteries," *J. Power Sources*, vol. 135, pp. 311–319, 2004.

This page intentionally left blank

Chapter 10

A critical review with solar radiation analysis model on inclined and horizontal surfaces

Figen Balo[1] and Lutfu S. Sua[1]

Utilization of renewable energy resources is gradually increasing in developing countries as well as the developed ones. Although the use of these resources is becoming increasingly important to meet energy demands, efficient use of limited resources requires planning and in-depth analysis beforehand. Correspondingly, in recent years, countries have started to work on increasing the share of renewable energy among other energy-production methods to ensure energy independence. In this study, in order to design PV system for maximum efficiency under certain climatic conditions, a comparative analysis of solar energy potential for two cities in certain climatic conditions is conducted. Based on the calculations, the values of the indicators show that potential for photovoltaic systems in both cities correspond to expected levels. The study aims to determine the most efficient solar panel by utilizing the real solar radiation values obtained for the photovoltaic system design.

10.1 Introduction

The solar energy potential in replacing a considerable portion of energy demand fuels the research efforts toward increasing the efficiency of solar systems. Diminishing amount of conventional energy sources and increasing environmental concerns also add to the value of this research. Solar radiation is one of the most determining factors on the climate and environment. Energy flows in the climate system is displayed in Figure 10.1.

Figure 10.2 shows global net radiation (insolation and longwave (LW) radiation). Radiative cooling by outgoing LW radiation is the primary way the Earth loses energy. In this figure, blue fields represent sites where more energy is leaving than incoming energy, while the red fields are sites where more energy is coming in than what is leaving. Thus, the blue fields are running a deficit in regards to insolation, while the red fields have a surplus of insolation.

[1]Industrial Engineering Department, Firat University, Turkey

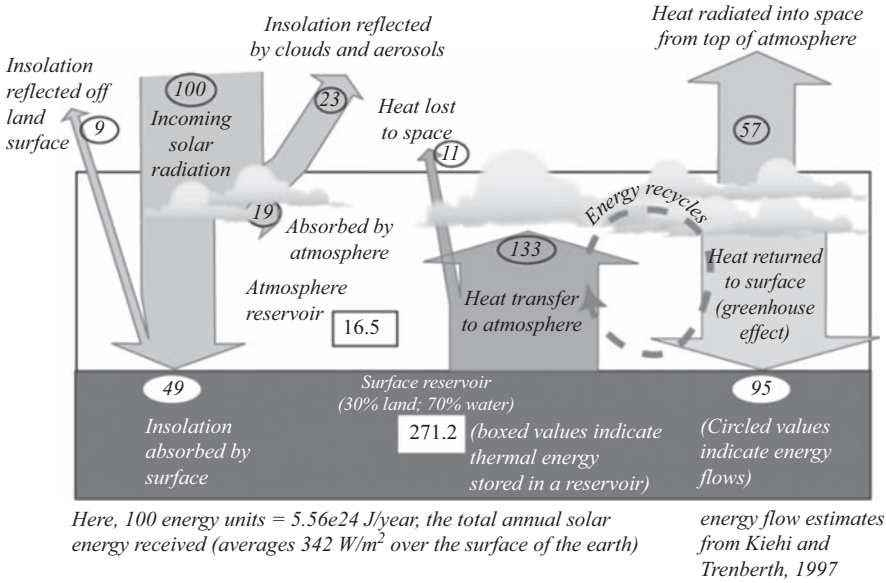

Figure 10.1 Energy flows in climate system [1]

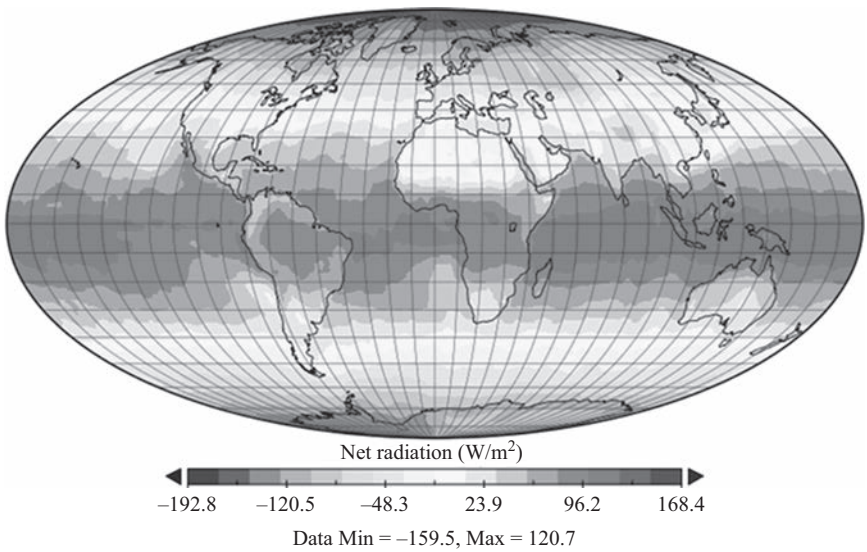

Figure 10.2 Global net radiation: insolation and LW radiation [2]

Considering the limited number of meteorological stations with consistent observations, making use of estimation models in estimating the radiation levels is quite important. Variations in solar radiation keep attracting many researchers due to its environmental, economic, and other consequences. Measuring solar radiation levels is significantly important as necessary information about climate changes can be extracted from it which in return can determine the viability of solar energy investments. The deterministic models are developed to estimate the radiation depending on the climatic conditions; thus it is important to choose the specific model to be installed based on the specifics of the region. Many articles pointed out that artificial neural network (ANN) methodology is better than empiric models [3–5]. For 11 meteorological sites on Tibet, Pan *et al.* investigated the exponential model based on temperature. The temperature difference is used as input. To calibrate the model, data for 35 years were applied. For testing, data for 5 years were applied [6]. For 22 sites in South Korea, Park *et al.* searched linear empiric model [7]. Gorka *et al.* compared three temperature-based empirical models for Spain: ANNs, adaptive neuro-fuzzy inference system, and gene expression programming. For testing purposes, 2,855 observations from four stations were utilized and 4,420 observations were utilized to train these models. The models used the combinations of the parameters (maximum and minimum air temperature, clear sky radiation, extraterrestrial radiation, and day number) [8]. Korachagaon *et al.* investigated 16 non-sunshine duration models to predict monthly average clearness values. As inputs, the moisture, wind speed, altitude, longitude, relative humidity, and five other temperature-related characteristics are used. Data for 875 sites are evaluated to analyze the models [9]. For 17 cities in Iran, Behrang *et al.* searched 11 models by applying particle swarm optimization technique [10]. To predict average hourly sun irradiation, Janjai *et al.* obtained a satellite-based model [11]. For Dezful, Iran, Behrang *et al.* investigated multilayer perceptron network along with radial basis function network. The parameters' six combinations used wind speed, day number, evaporation, relative humidity, sunshine duration, and mean air temperature. To train these models, 1,398 days were used. For testing, 214 days were used [12]. For four sites in Tunisia, Chelbi *et al.* researched five empiric models [13]. For Akure in Nigeria, Adaramola searched six non-sunshine duration models to predict long-term monthly average sun irradiation and Angström–Page model. In non-sunshine duration models, precipitation, relative humidity, and ambient temperature were used [14]. For 69 sites in China, Jin *et al.* analyzed six sunshine duration fraction (SDF) models and used three SDF models to predict monthly average sun irradiation. Altitude and latitude are added as parameters in modified models. The coefficient values are derived separately [15]. Bakirci investigated 60 empiric models developed to predict global monthly with average daily sun irradiation, in which many of the predictions had same formulas just with diverse regressive constant parameters. However, according to the conclusions of many articles, these constant parameters are generally based on the investigation areas [16]. To predict hourly solar irradiation, Shamim *et al.* used a fixed technique. To obtain the relative humidity and air pressure, they used a mesoscale meteorological model for diverse atmospheric

layers. By using available measured data, they computed the cloud cover index with the relative humidity and air pressure. By an empirical correlation, they determined clear sky radiation and transmission factor to compute levels of actual hourly solar irradiation. The clear sky radiation was predicted by applying irradiation transfer model. For training, data for 1 year were used [17]. For six provinces in Iran, Khorasanizadeh *et al.* assessed three mean SDF (MSDF) models and three non-sunshine duration models (NSDM) to project the monthly average global sun irradiation. In MSDF models, the relative humidity and temperature are added as parameters. Compared with SDF models, the root mean square error of all models changed from 0.82 to 0.47 MJ/m^2 day [18]. For Shiraz in Iran, Shahaboddin *et al.* used the ANN and extreme learning machine algorithm. The relative humidity, average air temperature, temperature difference, and SDF are applied as inputs. For testing, 3 years of data are used [19]. For Isfahan in Iran, Mohammadi *et al.* presented four SDF models with data for 9 years. Data for 4 years are utilized to test the data [20]. For seven sites in Spain, Almorox *et al.* researched eight non-sunshine duration models which were primarily based on the minimum and maximum temperature. In some models, the characteristics of latitude, altitude, mean temperature, and the day of the year were involved [21]. Dumas *et al.* designed a linear formula to correlate sun irradiation with the daily temperature variation and product of sunshine duration by using the power balance between adjacent atmosphere layer and soil layer [22].

For seven locations in Turkey, Duzen *et al.* investigated five SDF models to predict monthly average radiation [23]. For four provinces in Turkey, Teke *et al.* researched cubic, linear and quadratic empiric models [24]. For Turkey, Ozgoren *et al.* used the ANNs model of multi nonlinear regression to obtain the best independent characteristics for the input layer. They selected ten characteristics: soil temperature, altitude, sunshine duration, cloudiness, minimum and maximum atmospheric temperature, mean atmospheric temperature, latitude, wind speed month of the year. Levenberg–Marquardt optimization algorithm is utilized to train the ANN [25]. For Saudi Arabia, El-Sebaii *et al.* performed three MSDF models, three SDF models and NSDF models to project average monthly global sun irradiation. The characteristics grouped in MSDF models were cloud cover, temperature, and relative humidity. To derive novel empirical coefficient values, the data of 9 years are employed [26,27]. For 79 sites in China with data for 10 years, Li *et al.* [28] applied a combined model (sine and cosine functions). For four cities in India, Katiyar *et al.* [29] searched the quadratic, cubic, and linear models to predict monthly average radiation using annual data. Wan Nik *et al.* analyzed six mathematical expressions of the hourly solar radiation's ratio to daily radiation. For monthly average hourly irradiation, the prediction was made. From three sites of Malaysia, data for 3 years were utilized to test the models [30]. For Shanghai in China, Yao *et al.* evaluated 89 monthly average radiation models. Using various coefficients, many models are applied with same mathematical expressions. For five SDF models in Shanghai, they derived new fitting coefficients [31]. For four stations, Li *et al.* assessed eight SDF models in China.

For calibration, data for 11 years are used. Data of 4 years are used for validation. The root mean square error is used as statistical indicator [32]. For 25 sites in Spain, Manzano *et al.* assessed the linear Angström–Prescott model. More than 10 years of data are used for calibration purposes [33]. In the ANNs model, Linares-Rodriguez *et al.* applied the satellite data. The performance obtained is reported to be very good [34]. Besharat *et al.* searched 78 empiric models. They grouped them into four classes of models based on sun ray, cloud, meteorological characteristics, and temperature. To develop a case study, they applied a few models from each of the classes for Iran. The best performance is determined through a sun ray-based model with exponential expression [35]. For four provinces in Iran, Khorasanizadeh *et al.* [36,37] analyzed six models. The first model is based on exponential, the second on polynomial and other four models on cosine and sine functions. For Yazd in Iran, Besharat *et al.* analyzed the cloud-based model and Hargreaves model. The data of 16 years are utilized to obtain empiric constants [38]. For Shiraz in Iran, Besharat *et al.* assessed two SDF models, two MSDF models, and one NSDF model [39]. For nine sites in China, Zhao *et al.* researched the linear model and RMSE varied between 1.72 and 5.24 MJ/m^2 day [40]. Qin *et al.* used Levenberg–Marquardt algorithm with inputs of mean area temperature, difference of area temperature between night and daytime, air pressure rate number of days, vegetation index, and monthly precipitation. For Tibetan Plateau, data of 7 years from 22 sites are used to train the ANNs [41]. For 41 sites in China, Wan *et al.* applied linear Angström–Prescott model to predict global daily sun irradiation. Those sites divided into seven sun climate regions and nine thermal climate regions depending on diverse criteria, respectively. They applied the ANN model with inputs of latitude, altitude, longitude, day number, SDF, and daily mean temperature [42]. Şenkal proposed ANN model with altitude, longitude, latitude, land surface temperature, and two diverse surface emissivity as inputs. The last three characteristics were determined using satellite data. To train the ANN, 1 year of data from ten sites is used. The root mean square error in testing and training stage was reported as 0.32 and 0.16 MJ/m^2 day, respectively [43]. For two sites in Iran, Piri *et al.* researched one modified SDF model and three SDF models. They used the method of support vector regression. RMSE of them ranged between 2.14 and 3.70 MJ/m^2 day. The minimum and maximum temperature, relative humidity, and sunshine duration selected as inputs of kernel function [44]. For Gaize in Tibetan, Liu *et al.* investigated three non-sunshine duration models, two SDF models and three modified SDF models. For calibration, 1,085 days of data was analyzed. Data of 701 days were utilized for validation purposes. Root mean square error varied from 1.68 to 3.13 MJ/m^2 day. For various seasons, they argued that deriving coefficient values respectively was unnecessary [45]. For Saudi Arabia, Mohandes applied particle swarm optimization to train the ANN. As inputs, latitude, altitude, longitude, sunshine duration, and month of the year were used. However, prediction was for monthly average global sun irradiation. To train the ANNs, 31 sites' data are utilized. The average mean absolute percentage error is obtained as 8.85% [46]. Şenkal *et al.* studied

ANNs model for 12 provinces in Turkey. The mean beam radiation, mean diffuse radiation, altitude, longitude, and latitude were utilized as inputs. The satellite-based method to predict the average monthly irradiation is proposed. Root mean square error changed from 2.75 to 2.32 MJ/m^2 day [47]. To obtain the most effecting input characteristics for prediction, Yadav *et al.* performed the Waikato Environment's software. They determined the minimum and maximum temperature, average temperature, sunshine duration, and altitude as input characteristics, while longitude and latitude were the least effective characteristics. However, the prediction was for average monthly global sun irradiation. By the ANNs, the maximum mean absolute percentage error is obtained as 6.89% [48,49]. Yadav *et al.* searched numerous articles using ANN to project sun irradiation in three reviews and predict sun irradiation on horizontal surfaces. They pointed out that ANN models perform better compared to the empiric ones [50]. Olatomiwa *et al.* used the adaptive neuro-fuzzy inference system and ANN for Iseyin, Nigeria. Maximum and minimum temperature and sunshine duration were used as inputs. Data of 15 years were utilized for testing purposes while data of 6 years were used to train the model. In testing and training stages, RMSE varied between 1.76 and 1.09 MJ/m^2 day, respectively [51]. Jiang *et al.* performed to a priori association rules and Pearson correlation coefficients to choose the relevant input characteristics. The wind speed, total average opaque sky cover, precipitation, opaque sky cover, minimum and maximum temperature, relative humidity, average temperature, daylight temperature, heating and cooling degree days are chosen as parameters [52]. For 35 sites in China, Zang *et al.* [53] researched the same model by reducing two coefficients [54]. Mean absolute percentage error and RMSE for the 35 sites ranged between 16.22% and 4.33% and from 1.88 to 1.10 MJ/m^2 day, respectively. For four sites in Thailand and five sites in Cambodia, Janjai *et al.* researched a satellite-based model. RMSE is obtained as 1.13 MJ/m^2 day [55]. For three sites in Liaoning City, China, Chen *et al.* researched five SDF models. From each site, data for 35 years were obtained. To derive empirical coefficient values, 70% of the data were analyzed. For testing, 30% of the data were used. For each station, the empirical coefficient values are determined [56]. To predict sun irradiation, Sun *et al.* assessed the influence of autoregressive moving average model. They investigated the data of 20 years from two sites in China [57]. Bakirci studied seven different SDF models with data measured from 18 sites in Turkey. For the prediction of long-term monthly average daily global solar radiation, he used models including exponential, logarithmic, quadratic, and linear equations. For the same sites, the performances of the applied models are obtained with slight differences [58]. In a year, Ayodele *et al.* performed a function to present the clearness index's distribution. By using 7 years, the coefficient values determined daily sun irradiation data. Except for October, the effectiveness values of all months are obtained [59]. Park *et al.* [60] used support vector machine and wavelet transform algorithm. Data for 10 years are used to train the models. The difference between minimum and maximum ambient temperatures, SDF, water vapor pressure, relative humidity, extraterrestrial global sun irradiation, and average ambient temperature are used as parameters.

The next section provides a review of the radiation models developed in the literature, followed by the comparative analysis of two selected provinces in second climatic regions to reveal their potential for solar energy.

10.1.1 Climate, solar energy potential and electric production in Gaziantep and Şanlıurfa

Equipment limitations along with the high maintenance cost of them have limited the number of stations measuring solar radiation. Thus, calculating the solar radiation levels using meteorological variables is a common application [61–63]. The land and sunshine period are of great significance for facilities to be established based on solar energy. Thus, comprehensive investigation need to be undertaken about climate, solar energy potential, and current facilities.

Solar radiation map for Gaziantep and Şanlıurfa are displayed in Figure 10.3. In terms of solar energy potential, both cities are classified under second climatic region.

Average solar radiation, radiation function frequency, radiation function phase shift and latitude values for both cities are shown in Table 10.1.

In the next section, a comparative analysis is conducted on MATLAB® platform for both cities to reveal their solar radiation characteristics and potential.

10.2 Solar radiation intensity calculation

10.2.1 Horizontal surface

10.2.1.1 Daily total solar radiation

Various models are being developed to calculate the amount of solar radiation reaching any surface. The need for utilizing such models stems from the lack of data for solar radiation on surface. Thus, many researchers try to come up with solar radiation models depending on the conditions of specific regions.

Angström and Prescott have led the way of generating linear solar radiation models that are used in many regions [64]. Glover and McCulloch have come up with a radiation model by adding the latitude of region as well [65]. Rietveld proposed a model to calculate the solar radiation on horizontal surfaces by using data from 42 stations located in different countries and argued that the model can be used in every region [66]. Newland used a linear logarithmic model to obtain the best function in calculating the solar radiation on horizontal surfaces [67].

Total solar radiation on horizontal surfaces on a given day can be calculated through the following equation [68]:

$$I = I_{ort} - FGI \cos\left[\frac{2\pi}{365}(n + FKI)\right] \tag{10.1}$$

where n is the days, FKI is the radiation function phase shift, FGI is the radiation function frequency, and I_{ort} is the annual average of daily total radiation.

Figure 10.3 Solar radiation map for Gaziantep and Şanlıurfa

Table 10.1 Radiation values

City	Iort (MJ/m^2 day)	FGI (MJ/m^2 day)	FKI	Latitude
Gaziantep	14.3	7.79	2.13	37.05
Şanlıurfa	18.5	9.00	4.0	37.08

10.2.1.2 Daily diffuse solar radiation

Daily total diffuse solar radiation on horizontal surfaces can be obtained using the following equation [69]:

$$I_y = I_o(1-B)^2\left(1+3B^2\right) \tag{10.2}$$

where I_o is the out-of-atmosphere radiation and B is the transparency index.

10.2.1.3 Momentary total solar radiation

Momentary total solar radiation on horizontal surfaces can be obtained through the following equation [21,22]:

$$I_o = \frac{24}{\pi} I_s(\cos(e)\cos(d)\sin(w_s) + w_s\sin(e)\sin(d))f \tag{10.3}$$

where I_s (W/m^2) is the solar constant, e is the latitude angle, and w_s is the sunrise hour angle (hour angle is 0° at 12. One hour corresponds to 15° longitudes. Hour angle has negative value before the noon and positive value after the noon), f is the solar constant correction factor. Declination angle is the angular distance between the locations of solar rays on north and south hemispheres and equator plane. This angle can be determined through the angle between a line drawn from the center of Sun to the center of the Earth and the projection of this line on the equator plane. Declination angle varies between −23.5° and 23.5° throughout the year. Variation of the declination angle is less than 0.5° during the 24 h. Thus, the declination angle is treated as constant (see Figure 10.4), d is the declination angle can be calculated using the related tables and equations. Latitude e is the angular distance of point P from the equator. This term is the angle between the projection of 0P line and 0P line on the equator plane. Northern latitudes are positive while southern latitudes are negative ($-90° \leq e \leq 90°$) (see Figure 10.4) [68].

Out-of-atmosphere radiation can be calculated using the following equation [70]:

$$I_{ts} = A_{ts}\cos\left[\frac{\pi}{t_{gi}}(t-12)\right] \tag{10.4}$$

where A_{ts} is the solar radiation and t_{gi} is the imaginary day length.

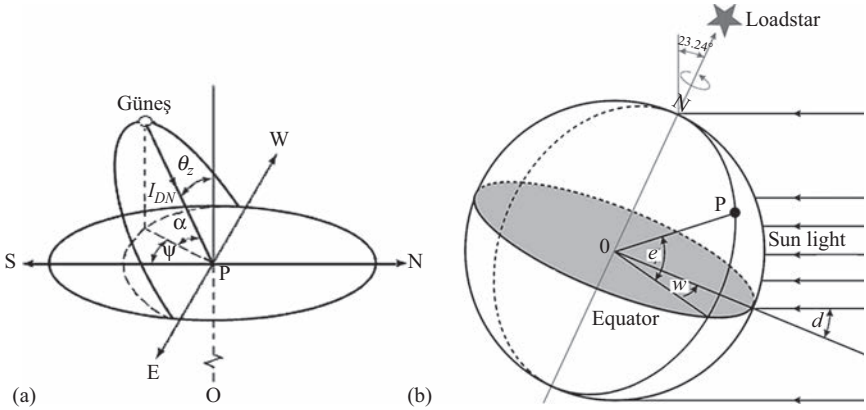

Figure 10.4 Basic (a) and derived (b) solar angles [68]

10.2.1.4 Momentary diffuse and direct solar radiation

Amount of momentary diffuse and direct solar radiation on horizontal surfaces can be obtained using (10.5) and (10.6) [71,72] where A_{ys} is function frequency:

$$I_{ys} = A_{ys} \cos\left[\frac{\pi}{t_g}(t - 12)\right] \tag{10.5}$$

$$I_{ds} = I_{ts} - I_{ys} \tag{10.6}$$

10.2.2 Calculating solar radiation intensity on inclined surface

10.2.2.1 Momentary direct solar radiation

Momentary direct solar radiation on inclined surfaces (30°–60°–90° angles) can be calculated using the equation below [72]:

$$I_{bc} = I_b R_b \tag{10.7}$$

where I_b is hourly direct radiation amount on horizontal surface (W/m^2) and R_b is direct radiation coefficient:

$$R_b = \frac{\cos\theta}{\cos\theta_z} \tag{10.8}$$

$$\cos\theta_z = \sin d \sin e + \cos d \cos e \cos w \tag{10.9}$$

where Solar Zenit angle θ_z is the angle of solar rays coming onto the P point (Figure 10.4) with horizontal surface. β is the slope angle:

$$\cos\theta = \sin d \sin(e - \beta) + \cos d \cos(e - \beta)\cos w \tag{10.10}$$

10.2.2.2 Momentary diffuse solar radiation

Value of momentary diffuse radiation on inclined surfaces can be obtained using the following equation [72]:

$$I_{ye} = R_y I_{ys} \tag{10.11}$$

Conversion factor R_y for diffuse radiation can be calculated using the following equation [22]:

$$R_y = \frac{1 + \cos(a)}{2} \tag{10.12}$$

Solar height angle, α, is the angle between solar rays and the projection of the solar rays on the horizontal surface ($\theta_z + \alpha = 90^\circ$) (see Figure 10.4).

R_y parameter provides the slope of the surface. For vertical surface ($a = 90^\circ$), R_y value is 0.5. This way, momentary values of diffuse radiation on inclined surfaces with 30°, 60°, 90° angles for 24-h time period can be calculated.

10.2.2.3 Reflecting momentary solar radiation

Reflecting radiation on inclined surfaces [72] can be calculated using the following equation:

$$I_{ya} = I_{ts} p \frac{1 + \cos(a)}{2} \tag{10.13}$$

Environment reflection rate is shown with ρ parameter and used with average value of $\rho = 0.2$ in calculations.

10.2.2.4 Total momentary solar radiation

Momentary total radiation on inclined surface [72] can be calculated using the following equation:

$$I_t = I_{de} + I_{ye} + I_{ya} \tag{10.14}$$

10.3 Methodology

Figure 10.5 provides the values of (i) change in annual momentary total solar radiation values for 24-h time period, (ii) change in annual momentary diffuse solar radiation values per hour and (iii) change in annual momentary direct solar radiation values for 24-h time period on horizontal surfaces.

Figure 10.6 provides the daily changes of (i) total solar radiation values per day, (ii) declination angle, (iii) hourly angle for sunrise, (iv) solar constant for correction factor, (v) solar radiation values out of atmosphere, (vi) graph of function frequency (A_{ys}), (vii) diffuse solar radiation (A_{ts}), (viii) transparency index (B) for a horizontal surface.

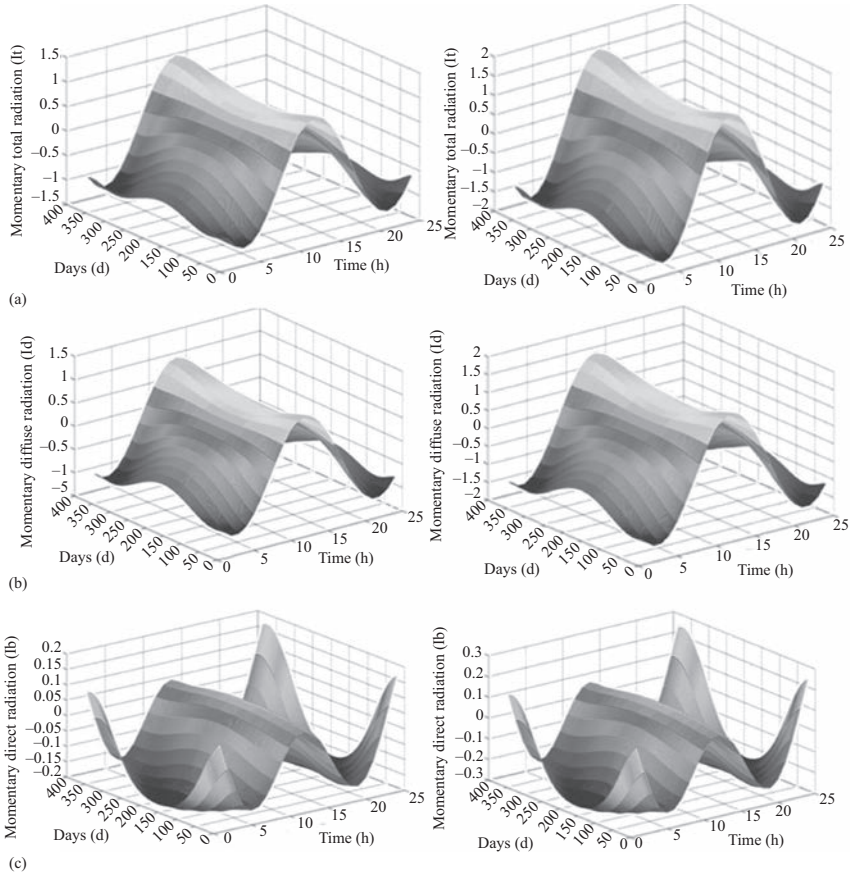

Figure 10.5 Change of annual solar radiation values for 24-h period on horizontal surface (Gaziantep vs. Şanlıurfa): (a) Change in annual momentary total solar radiation values, (b) change in annual momentary diffuse solar radiation values per hour and (c) change in annual momentary direct solar radiation values

Momentary direct radiation values with three different angles (30°, 60°, and 90°) for 24-h time period are provided in Figure 10.7. The highest values for all three angles are obtained on the 355th day at 12.00, while the lowest values are obtained on the same day at 15.00.

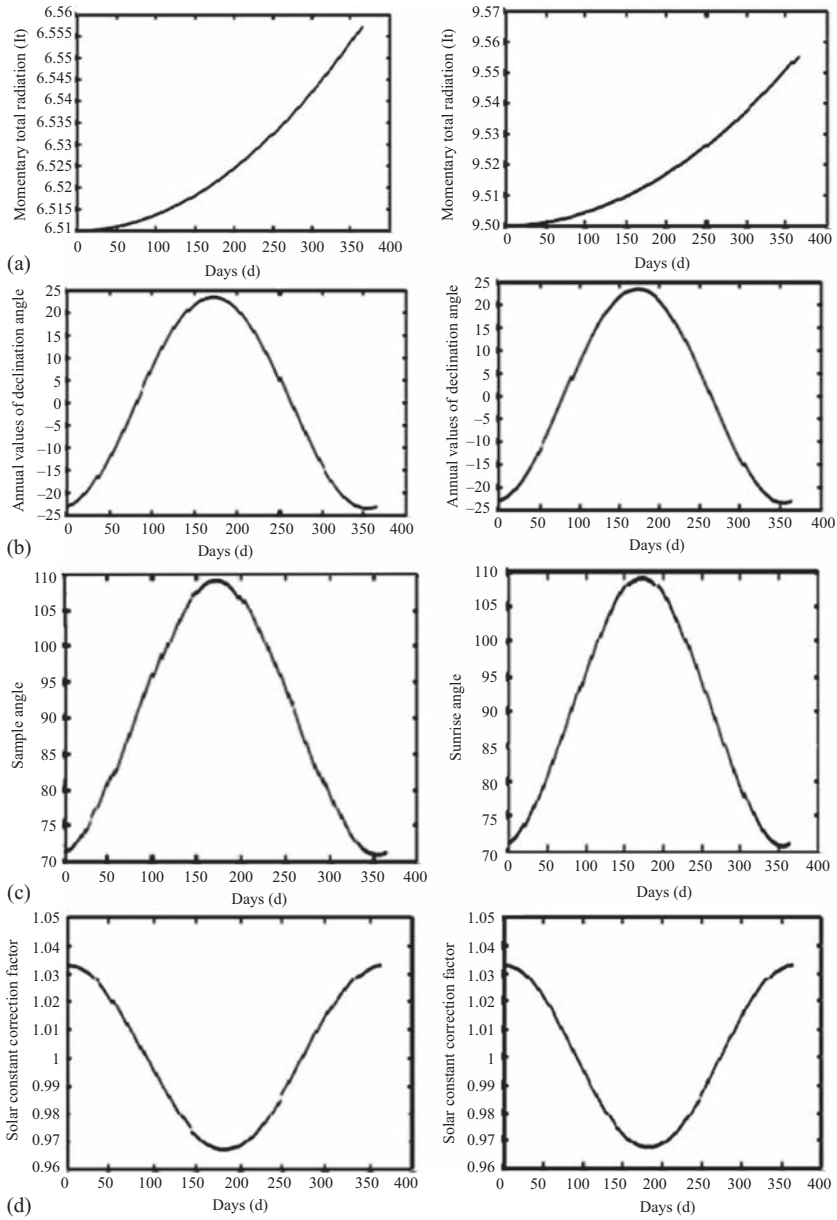

Figure 10.6 Radiation on horizontal surfaces (Gaziantep vs. Şanlıurfa): (a) total solar radiation values per day, (b) declination angle, (c) hourly angle for sunrise, (d) solar constant for correction factor, (e) solar radiation values out of atmosphere, (f) graph of function frequency, (g) diffuse solar radiation and (h) transparency index

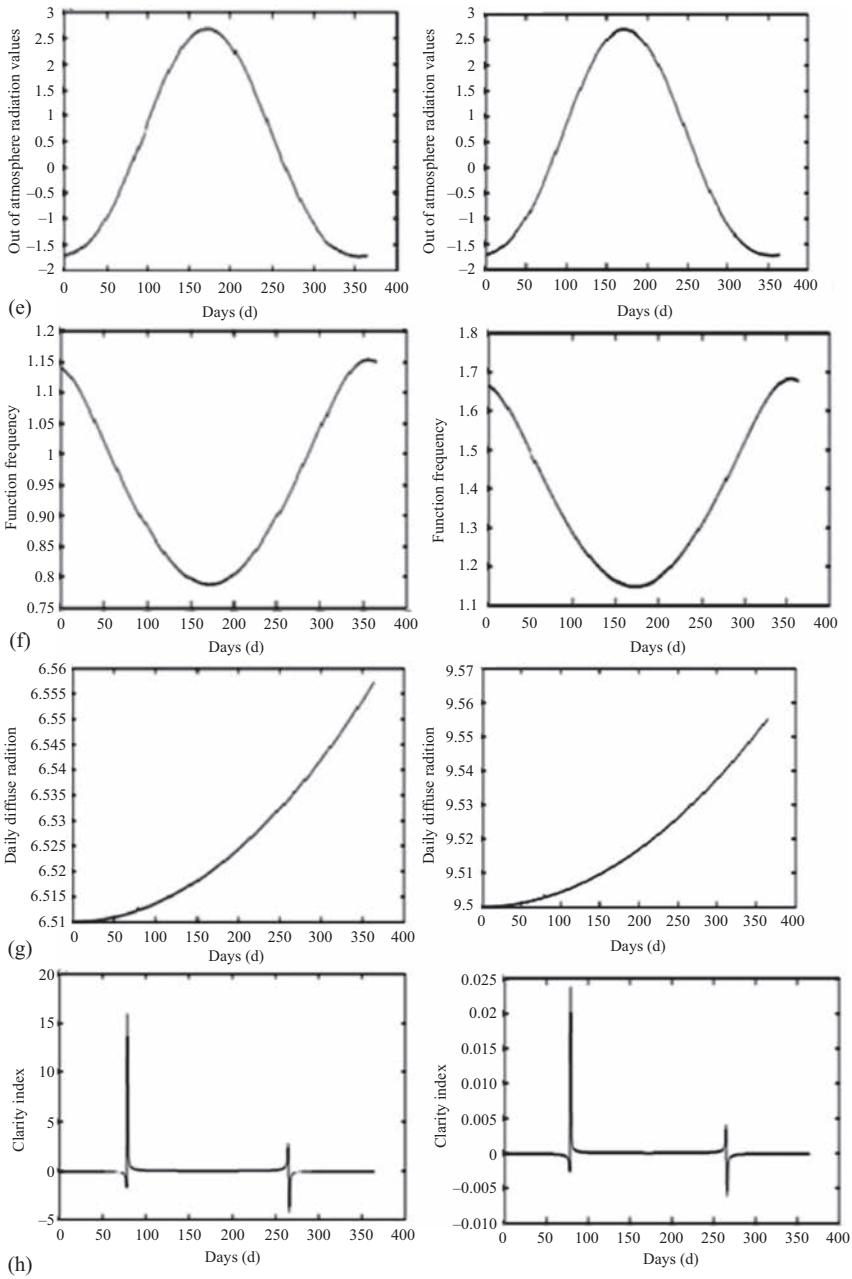

Figure 10.6 (*Continued*)

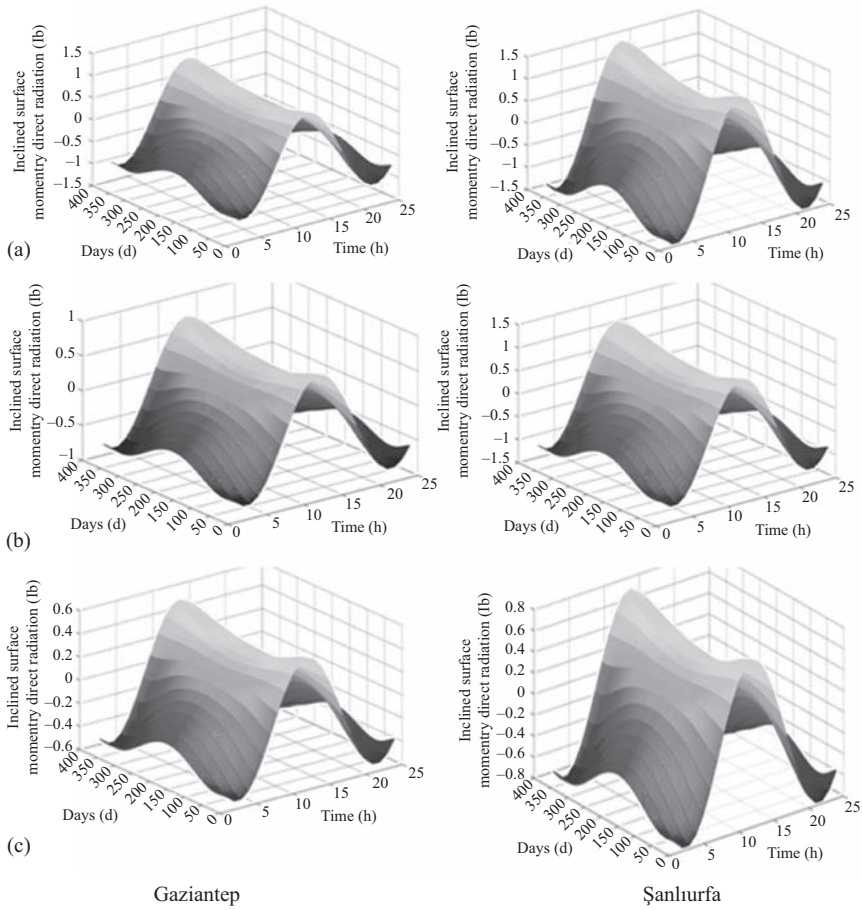

Figure 10.7 Annual momentary direct radiation values on inclined surface for 24-h period (Gaziantep vs. Şanlıurfa): (a) momentary direct radiation values on 30° inclined surface, (b) momentary direct radiation values on 60° inclined surface and (c) momentary direct radiation values on 90° inclined surface

Annual momentary diffuse radiation values for three angles (30°, 60°, and 90°) are provided in Figure 10.8. Annual values of total momentary solar radiation for 24-h periods are provided in Figure 10.9.

Total momentary solar radiation for annual angle and hours are provided in Figure 10.10.

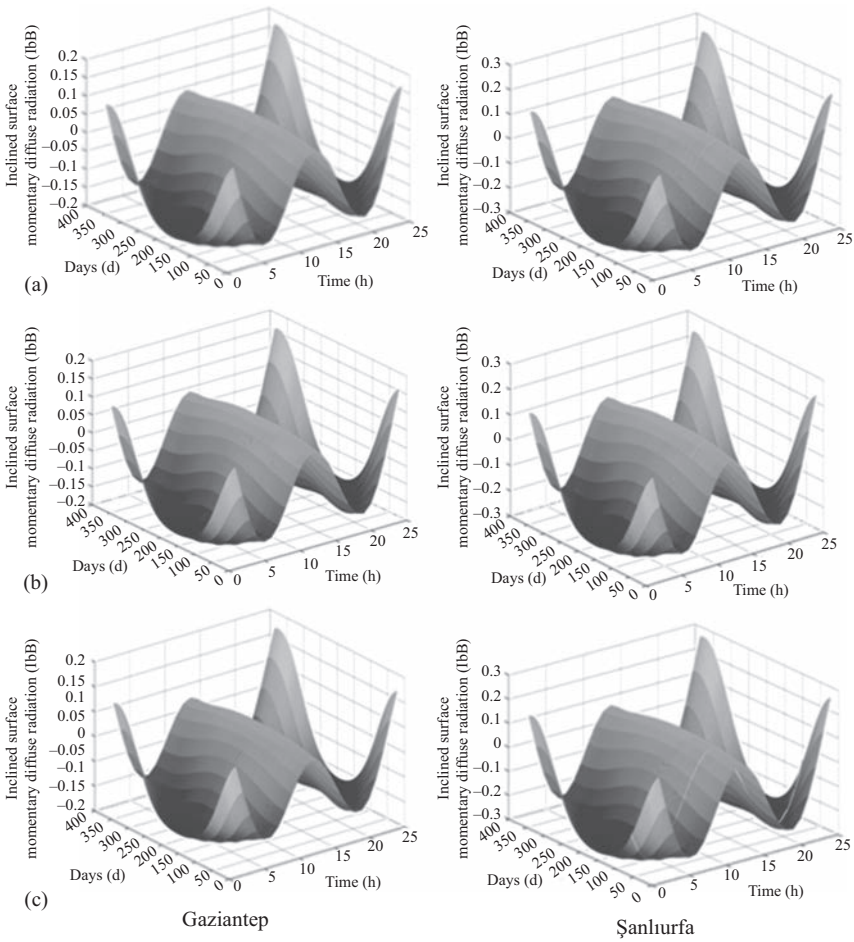

Figure 10.8 Annual momentary diffuse radiation values for inclined surfaces (Gaziantep vs. Şanlıurfa): (a) 30° momentary diffuse radiation, (b) 60° momentary diffuse radiation and (c) 90° momentary diffuse radiation

10.4 Findings and Results

Based on the above analysis, true potential of both cities can be evaluated through the solar characteristics calculations provided in Table 10.2.

Values of solar radiation on inclined and horizontal surfaces are calculated through MATLAB software. Based on the calculations, the values of the indicators show that potential for photovoltaic systems in both cities correspond to expected levels. Although both cities are classified in second region, total radiation value in Şanlıurfa (9.5574) is considerably higher than the one in Gaziantep (6.5584). An

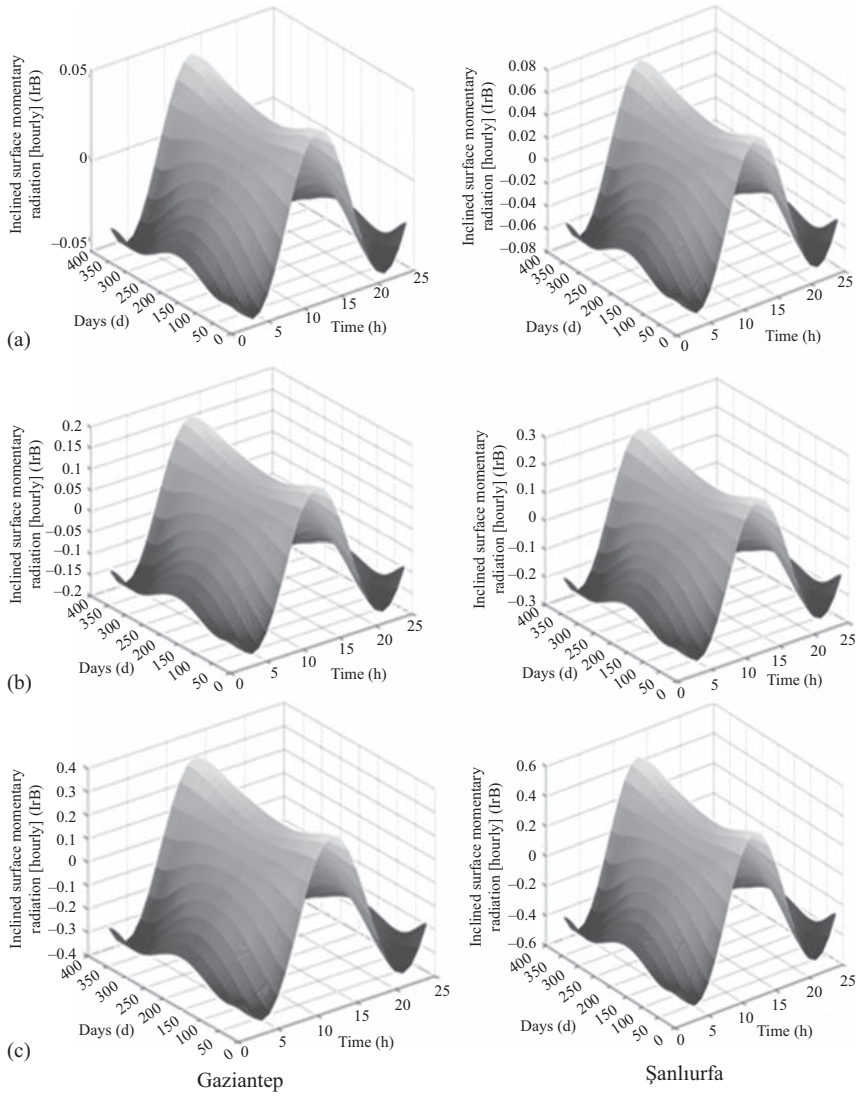

Figure 10.9 Annual total momentary radiation values for inclined surface (Gaziantep vs. Şanlıurfa): (a) 30° total momentary radiation values, (b) 60° total momentary radiation values and (c) 90° total momentary radiation values

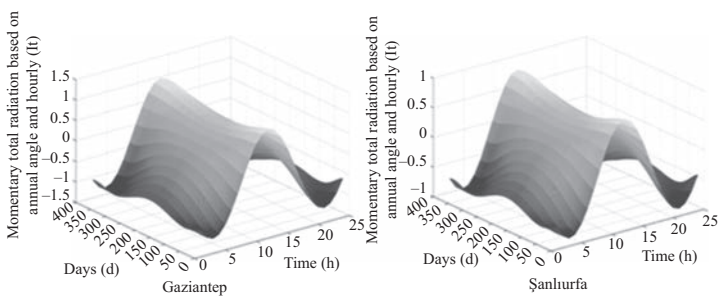

Figure 10.10 Total momentary radiation for annual angle and hours (Gaziantep vs. Şanlıurfa)

Table 10.2 Solar radiation attributes

Attributes		G. Antep	Şanlıurfa	Attributes		G. Antep	Şanlıurfa
Total radiation	I_{max} (W/m^2)	6.5584	9.5574	Momentary direct radiation	Idbmax(30°)	0.8299	1.4299
	I_{min} (W/m^2)	6.5100	9.5000		Idbmin(30°)	−1.3216	−1.4216
Declination angle	d_{max}	24.1498	23.5498		Idbmax(60°)	0.8346	1.0031
	d_{min}	−22.4478	−23.4445		Idbmin(60°)	−0.8346	−1.3624
Sunrise hour angle	w_{max}	108.9186	108.9986		Idbmax(90°)	0.5968	0.7136
	w_{min}	71.9815	72.8814		Idbmin(90°)	−0.5490	−0.8000
Out-of-atmosphere radiation	I_o(max) (W/m^2)	278,010	272,610	Momentary diffuse radiation	IbBmax(30°)	0.0513	0.0857
	I_o(min) (W/m^2)	−176,900	−179,800		IbBmin(30°)	−0.1762	−0.2595
Transparency index	B_{max}	0.1730	0.0278		IbBmax(60°)	0.0567	0.0101
	B_{min}	−0.5678	−0.0056		IbBmin(60°)	−0.1999	−0.2570
Total diffuse radiation	I_y(max) (W/m^2)	6.5589	9.5581		IbBmax(90°)	0.0497	0.0158
	I_y(min) (W/m^2)	6.5100	9.5000		IbBmin(90°)	−0.1876	−0.2545
Function frequency	A_{ts}(max)	1.1475	1.6875	Momentary reflecting radiation	IrBmax(30°)	0.0389	0.0606
	A_{ts}(min)	0.7804	1.1304		IrBmin(30°)	−0.0499	−0.0705
Momentary total radiation	It(max)	1.0075	1.5085		IrBmax(60°)	0.1578	0.2271
	It(min)	−1.4044	−1.6944		IrBmin(60°)	−0.1912	−0.2256
Momentary diffuse radiation	$(A_{ys})_{max}$	1.0784	1.5383		IrBmax(90°)	0.3567	0.5122
	$(A_{ys})_{min}$	0.7101	1.0928		IrBmin(90°)	−0.3867	−0.5513
	Id(max)	1.0253	1.4275				
	Id(min)	−1.4165	−1.7165				
Momentary direct radiation	Ib(max)	0.0463	0.0863				
	Ib(min)	−0.1551	−0.2851				

integral part of planning the photovoltaic systems is comparing the predicted values with the actual ones. The performance of the system depends on various parameters. Using realistic values of radiation has great importance for designing the optimum system. This study aims to establish a reference for choosing the most efficient solar panel by relying on the real solar radiation values obtained for the most efficient photovoltaic system design. The solar radiation values are evaluated to be at acceptable efficiency levels to design a photovoltaic system.

10.5 Conclusions

Solar technology is based on obtaining energy from an infinite source energy. The energy spread out by the Sun is the radiation energy coming out with the fusion process within the core of the Sun. Solar radiation intensity data are the main parameters required in the design of solar energy systems and evaluation of system performance. Thus, determining the amount of solar radiation on regions at various latitudes on the surface of Earth has great importance in many solar energy applications.

Considering the high installation expenses, the solar radiation data analysis for a specific city is quite significant when a sunlight-based photovoltaic energy system is considered to be established in that city.

First investment requirement needs economic sources' productive use and careful planning. The meteorically data is the most significant section of such in-depth research. Solar radiation data are of great significance to be able to estimate the solar energy systems' potential. On the other hand, solar radiation measurements are limited in global scale. Therefore, diverse models have been derived to meet the need for the missing values. These diverse models are dependent upon the region's specifics to be investigated.

For the most efficient photovoltaic power plant, the aim of this chapter is to detect a reference for choosing the most efficient solar panel by relying on the actual solar radiation data obtained. The solar radiation's values are commentated to be at appropriate performance levels to plan a photovoltaic power central.

In this chapter, for a photovoltaic power plant designed to be installed in Gaziantep and Şanlıurfa, sun irradiation data on inclined (900, 600, and 300) and horizontal solar panels are obtained by using MATLAB software, meteorological data, and the most practical–realistic solar models.

For 24-h time period, the change in yearly momentary direct sun irradiation values and the change in yearly momentary total sun irradiation values are researched for horizontal solar panels. In addition, the change in yearly momentary diffuse sun irradiation value per hour is investigated as well.

With solar radiation analysis model, declination angle, hourly angle for sunrise, diffuse sun irradiation function frequency, transparency index, sun irradiation values out of atmosphere, total sun irradiation function frequency, sun constant for correction factor, and total sun irradiation data per day values are determined for sun irradiation on horizontal surface.

The yearly momentary direct radiation values for 24-h period, the yearly momentary diffuse radiation values, the yearly total momentary irradiation values are obtained on inclined (900, 600, and 300) solar surfaces.

Based on solar radiation analysis, Gaziantep and Şanlıurfa cities' true potential can be assessed through the solar characteristics' calculations provided in Table 10.2.

The photovoltaic system's appropriateness is assessed by obtaining the best sun irradiation the dates and values where these values are determined.

In this case, the solar radiation's values are assessed to be at acceptable performance levels to plan a photovoltaic power central. Though data for a specific case is used here for the purpose of model verification, this chapter aims to develop a reference for selecting the most performance solar panel by relying on the sun irradiation values determined for the most performance photovoltaic power central.

References

[1] Kiehl JT, and Trenberth KE. Earth's annual global mean energy budget. Bulletin of the American Meteorological Society 1997; 78:197–208 https://www.e-education.psu.edu/earth103/node/1007.

[2] D. Bice. NASA CERES Satellite Report. March 2003 https://www.e-education.psu.edu/earth103/node/1007.

[3] Qazi A, Fayaz H, Wadi A, Raj RG, Rahim NA, and Khan WA. The artificial neural network for solar radiation prediction and designing solar systems: a systematic literature review. J Cleaner Prod 2015; 104:1–12.

[4] Piri J, and Kisi O. Modelling solar radiation reached to the Earth using ANFIS, NNARX, and empirical models (Case studies: Zahedan and Bojnurd stations). J Atmos Sol Terr Phys 2015; 123:39–47.

[5] Teke A, Yıldırım HB, and Celik O. Evaluation and performance comparison of different models for the estimation of solar radiation. Renew Sustain Energy Rev 2015; 50:1097–107.

[6] Teke A, Yıldırım HB, and Celik O. Evaluation and performance comparison of different models for the estimation of solar radiation. Renew Sustain Energy Rev 2015; 50:62.

[7] Park J-K, Das A, and Park J-H. A new approach to estimate the spatial distribution of solar radiation using topographic factor and sunshine duration in South Korea. Energy Convers Manage 2015; 101:30–9.

[8] Mefti A, Adane A, and Bouroubi MY. Satellite approach based on cloud cover classification: estimation of hourly global solar radiation from Meteosat images. Energy Convers Manage 2008; 49:652–9.

[9] Korachagaon I, and Bapat VN. General formula for the estimation of global solar radiation on earth's surface around the globe. Renew Energy 2012; 41:394–400.

[10] Behrang MA, Assareh E, Noghrehabadi AR, and Ghanbarzadeh A. New sunshine-based models for predicting global solar radiation using PSO (particle swarm optimization) technique. Energy 2011; 36:3036–49.

[11] Janjai S, Pankaew P, and Laksanaboonsong J. A model for calculating hourly global solar radiation from satellite data in the tropics. Appl Energy 2009; 86:1450–7.
[12] Behrang MA, Assareh E, Ghanbarzadeh A, and Noghrehabadi AR. The potential of different artificial neural network (ANN) techniques in daily global solar radiation modeling based on meteorological data. Sol Energy 2010; 84:1468–1480.
[13] Chelbi M, Gagnon Y, and Waewsak J. Solar radiation mapping using sunshine duration based models and interpolation techniques: application to Tunisia. Energy Convers Manage 2015; 101:203–15.
[14] Adaramola MS. Estimating global solar radiation using common meteorological data in Akure, Nigeria. Renew Energy 2012; 47:38–44.
[15] Jin Z, Yezheng W, and Gang Y. General Formula for estimation of monthly average daily global solar radiation in China. Energy Convers Manage 2005; 46:257–68.
[16] Bakirci K. Models of solar radiation with hours of bright sunshine: a review. Renew Sustain Energy Rev 2009; 13:2580–8.
[17] Shamim MA, Remesan R, Bray M, and Han D. An improved technique for global solar. Renew Sustain Energy Rev 2017; 70:314–29.
[18] Khorasanizadeh H, and Mohammadi K. Introducing the best model for predicting the monthly mean global solar radiation over six major cities of Iran. Energy 2013; 51:257–66.
[19] Khorasanizadeh H, and Mohammadi K. Introducing the best model for predicting the monthly mean global solar radiation over six major cities of Iran. Energy 2013; 51:41.
[20] Mohammadi K, Shamshirband S, Anisi MH, Alam KA, and Petković D. Support vector regression based prediction of global solar radiation on a horizontal surface. Energy Convers Manage 2015; 91:433–41.
[21] Almorox J, Hontoria C, and Benito M. Models for obtaining daily global solar radiation with measured air temperature data in Madrid (Spain). Appl Energy 2011; 88:1703–9.
[22] Dumas A, Andrisani A, Bonnici M, *et al*. A new correlation between global solar energy radiation and daily temperature variations. Sol Energy 2015; 116:117–24.
[23] Duzen H, and Aydin H. Sunshine-based estimation of global solar radiation on horizontal surface at Lake Van region (Turkey). Energy Convers Manage 2012; 58:35–46.
[24] Teke A, and Yıldırım HB. Estimating the monthly global solar radiation for Eastern Mediterranean Region. Energy Convers Manage 2014; 87:628–35.
[25] Ozgoren M, Bilgili M, and Sahin B. Estimation of global solar radiation using ANN over Turkey. Expert Syst Appl 2012; 39:5043–51.
[26] El-Sebaii AA, Al-Ghamdi AA, Al-Hazmi FS, and Faidah AS. Estimation of global solar radiation on horizontal surfaces in Jeddah, Saudi Arabia. Energy Policy 2009; 37:3645–9.

[27] El-Sebaii AA, Al-Hazmi FS, Al-Ghamdi AA, and Yaghmour SJ. Global, direct and diffuse solar radiation on horizontal and tilted surfaces in Jeddah, Saudi Arabia. Appl Energy 2010; 87:568–76.
[28] Li H, Ma W, Lian Y, and Wang X. Estimating daily global solar radiation by day of year in China. Appl Energy 2010; 87:3011–7.
[29] Katiyar AK, and Pandey CK. Simple correlation for estimating the global solar radiation on horizontal surfaces in India. Energy 2010; 35:5043–8.
[30] Wan Nik WB, Ibrahim MZ, Samo KB, and Muzathik AM. Monthly mean hourly global solar radiation estimation. Sol Energy 2012; 86:379–87.
[31] Yao W, Li Z, Wang Y, Jiang F, and Hu L. Evaluation of global solar radiation models for Shanghai, China. Energy Convers Manage 2014; 84:597–612.
[32] Yao W, Li Z, Wang Y, Jiang F, and Hu L. Evaluation of global solar radiation models for Shanghai, China. Energy Convers Manage 2014; 84:15.
[33] Manzano A, Martín ML, Valero F, and Armenta C. A single method to estimate the daily global solar radiation from monthly data. Atmos Res 2015; 166:70–82.
[34] Linares-Rodriguez A, Ruiz-Arias JA, Pozo-Vazquez D, and Tovar-Pescador J. An artificial neural network ensemble model for estimating global solar radiation from Meteosat satellite images. Energy 2013; 61:636–45.
[35] Besharat F, Dehghan AA, and Faghih AR. Empirical models for estimating global solar radiation: a review and case study. Renew Sustain Energy Rev 2013; 21:798–821.
[36] Khorasanizadeh H, and Mohammadi K. Prediction of daily global solar radiation by day of the year in four cities located in the sunny regions of Iran. Energy Convers Manage 2013; 76:385–92.
[37] Khorasanizadeh H, Mohammadi K, and Jalilvand M. A statistical comparative study to demonstrate the merit of day of the year-based models for estimation of horizontal global solar radiation. Energy Convers Manage 2014; 87:37–47.
[38] Besharat F, Dehghan AA, and Faghih AR. Empirical models for estimating global solar radiation: a review and case study. Renew Sustain Energy Rev 2013; 21:798–821.
[39] Besharat F, Dehghan AA, and Faghih AR. Empirical models for estimating global solar radiation: a review and case study. Renew Sustain Energy Rev 2013; 21:28.
[40] Zhao N, Zeng X, and Han S. Solar radiation estimation using sunshine hour and air pollution index in China. Energy Convers Manage 2013; 76:846–51.
[41] Zhao N, Zeng X, and Han S. Solar radiation estimation using sunshine hour and air pollution index in China. Energy Convers Manage 2013; 76:37.
[42] Wan KKW, Tang HL, Yang L, and Lam JC. An analysis of thermal and solar zone radiation models using an Angström–Prescott equation and artificial neural networks. Energy 2008; 33:1115–27.
[43] Şenkal O. Modeling of solar radiation using remote sensing and artificial neural network in Turkey. Energy 2010; 35:4795–801.

[44] Piri J, Shamshirband S, Petković D, and Tong CW. Rehman MHu. Prediction of the solar radiation on the earth using support vector regression technique. Infrared Phys Technol 2015; 68:179–85.
[45] Liu J, Liu J, Linderholm HW, *et al*. Observation and calculation of the solar radiation on the Tibetan Plateau. Energy Convers Manage 2012; 57:23–32.
[46] Mohandes MA. Modeling global solar radiation using particle swarm optimization (PSO). Sol Energy 2012; 86:3137–45.
[47] Şenkal O, and Kuleli T. Estimation of solar radiation over Turkey using artificial neural network and satellite data. Appl Energy 2009; 86:1222–8.
[48] Yadav AK, Malik H, and Chandel SS. Selection of most relevant input parameters using WEKA for artificial neural network based solar radiation prediction models. Renew Sustain Energy Rev 2014; 31:509–19.
[49] Yadav AK, Malik H, and Chandel SS. Application of rapid miner in ANN based prediction of solar radiation for assessment of solar energy resource potential of 76 sites in Northwestern India. Renew Sustain Energy Rev 2015; 52:1093–106.
[50] Yadav AK, and Chandel SS. Solar radiation prediction using Artificial Neural Network techniques: a review. Renew Sustain Energy Rev 2014; 33:772–81.
[51] Olatomiwa L, Mekhilef S, Shamshirband S, and Petković D. Adaptive neuro-fuzzy approach for solar radiation prediction in Nigeria. Renew Sustain Energy Rev 2015; 51:1784–91.
[52] Jiang H, Dong Y, Wang J, and Li Y. Intelligent optimization models based on hard-ridge penalty and RBF for forecasting global solar radiation. Energy Convers Manage 2015; 95:42–58.
[53] Zang H, Xu Q, and Bian H. Generation of typical solar radiation data for different climates of China. Energy 2012; 38:236–48.
[54] Li H, Ma W, Lian Y, and Wang X. Estimating daily global solar radiation by day of year in China. Appl Energy 2010; 87:3011–7.
[55] Janjai S, Pankaew P, Laksanaboonsong J, and Kitichantaropas P. Estimation of solar radiation over Cambodia from long-term satellite data. Renew Energy 2011; 36:1214–20.
[56] Janjai S, Pankaew P, Laksanaboonsong J, and Kitichantaropas P. Estimation of solar radiation over Cambodia from long-term satellite data. Renew Energy 2011; 36:55.
[57] Sun H, Yan D, Zhao N, and Zhou J. Empirical investigation on modeling solar radiation series with ARMA–GARCH models. Energy Convers Manage 2015; 92:385–95.
[58] Bakirci K. Correlations for estimation of daily global solar radiation with hours of bright sunshine in Turkey. Energy 2009; 34:485–501.
[59] Ayodele TR, and Ogunjuyigbe ASO. Prediction of monthly average global solar radiation based on statistical distribution of clearness index. Energy 2015; 90:1733–42.
[60] Park J-K, Das A, and Park J-H. A new approach to estimate the spatial distribution of solar radiation using topographic factor and sunshine duration in South Korea. Energy Convers Manage 2015; 101:30–9.

[61] Chen RS, Lu SH, Kang ES, *et al*. Estimating daily global radiation using two types of revised models in China. Energy Convers Manage 2006; 47:865–78.
[62] Yorukoglu M, and Celik AN. A critical review on the estimation of daily global solar radiation from sunshine duration. Energy Convers Manage 2006; 47:2441–50.
[63] Almorox J, and Hontoria C. Global radiation estimation using sunshine duration in Spain. Energy Convers Manage 2004; 45:1529–35.
[64] Angström A. Solar and Terrestrial radiation. Q J R Meteorolog Soc 1924; 50:121–5.
[65] Glover J, and McCulloch JDG. The empirical relation between solar radiation and hours of sunshine. Q J R Meteorolog Soc 1958; 84(360):172–5.
[66] Rietveld M. A new method for estimating the regression coefficient in the formula relating solar radiation to sunshine. Agric Meteorol 1978; 19(2):243–52.
[67] Newland FJ. A study of solar radiation models for the coastal region of South China. Solar Energy 1988; 31:227–35.
[68] Derse MS. (2014). Batman'ın İklim Koşullarında Eğimli Düzleme Gelen Güneş Işınımının Farklı Açılardan Belirlenmesi. Sayfa 37–47 Batman.
[69] Miguel AD, Bilbao J, Aguiar R, Kambezidis H, and Negro E. Diffuse solar irradiation model evaluation in the North Mediterranean belt area. Sol Energy 2001; 70:143–53.
[70] Mercan O. (2013). Marketing Photovoltaic Solutions in Turkey, Masters Thesis, Istanbul Bilgi University, Istanbul.
[71] Notton G, Poggi P, and Cristofari C. Predicting hourly solar irradiations on inclined surfaces based on the horizontal measurements: performances of the association of well-known mathematical models. Energy Convers Manage 2006; 47:1816–29.
[72] Erbs DG, Klein SA, and Duffie JA. Estimation of the diffuse radiation fraction for hourly, daily and monthly-average global radiation. Sol Energy 1982; 28(4):293–302.

Chapter 11

Nature-based building solutions: circular utilization of photosynthetic organisms

Onur Kırdök[1] and Ayça Tokuç[2]

Rapidly growing urban population and urbanization are exacerbating the problems of air, noise and water pollution while increasing the use of resources and decreasing natural lands. In this context, the environmental effects of urban areas are undeniable; however, today more than half of the world's population is living in cities, and this amount is continuing to increase, thus a rethinking of cities is necessary. Energy efficiency and decreasing the amount of energy per service for people are common solution strategies; yet they are not enough to reach a balance between nature and cities. In this context, the utilization of nature-based solutions is proposed and the most common solution is increasing the use of green spaces. More recently nature-based elements are used to attain psychological benefits, to decrease CO_2 concentration, heat island phenomena, and mitigate climate change effects.

This chapter proposes a circular agricultural system for integration of nature-based solutions, mainly photosynthetic elements into buildings and cities and evaluates its potential for utilization. The proposed system consists of the integration of three main nature-based solutions into a building: green roofs that filter water, photobioreactors (PBRs) that cultivate microalgae inside and aquaponics that grow both fish and vegetables. The system is powered by solar energy and its main purpose is to grow food in the urban context. Although there have been some studies about the energy and environmental effects of integrating nature-based systems in buildings, they are usually utilized for different purposes, yet the present chapter proposes and assesses one of the first examples, where three systems are combined together.

11.1 Nature-based solutions

The urban environment occupies only 2% of the Earth's land, yet it is associated with more than 50% of human occupancy [1], 80% of gross world products [2], 80% [3] of resource consumption and 75% of the global CO_2 emissions.

[1]Department of Architect, Begonya Mimarlık, Turkey
[2]Department of Architecture, Dokuz Eylul University, Turkey

Meanwhile environmental, social and economic challenges to the cities worldwide, including climate change, degradation of ecosystems and resource depletion are getting worse. Some innovative solutions in these areas were learned from watching and designing with nature in our minds. Nature-based solutions are strategies to transform our cities into sustainable systems using a holistic approach that are 'inspired by, supported by or copied from nature' [4]. Their principal goals are 'enhancing sustainable urbanization', 'restoring degraded ecosystems', 'developing climate change adaptation and mitigation' and 'improving risk-management and resilience' [4]. However, most of the nature-based solutions serve only one purpose such as flood prevention, water treatment, food provision, resource recovery or urban heat islands. Their combination in a synergistic way has the potential to show better performance than conventional systems and lead the way to a more resilient, sustainable and healthy urban environment [5].

Nature-based solutions are a priority area for investment under the European Union's Horizon 2020 research and innovation programme, and perhaps the most comprehensive evaluation framework to evaluate nature-based systems to date is the preliminary framework provided by their EKLIPSE Expert Working Group on Nature-based Solutions to Promote Climate Resilience in Urban Areas [6]. EKLIPSE is a mechanism that brings scientists, policy-makers and other stakeholders in the society together, to have a say in making decisions that affect the environment [7]. The aforementioned framework evaluates nature-based solutions according to their relationship with the following ten main challenges in mesoscale (region, metropolitan, urban) and microscale (street, building) [6].

Contribution of nature-based solutions to climate resilience: Macroscale; mitigation by enhancing carbon storage and sequestration, meso and microscale; adaptation through planting vegetation to improve the microclimate.

Water management: Relevant to the impacts of water run-off, flood risk, water quantity and water quality.

Coastal resilience: Maintenance, restoration, development and conservation of ecosystems, biodiversity and services especially against coastal storms and sea level rises.

Green space management: Making inventories, setting clear requirements, utilizing innovative, interdisciplinary methods and improving green and blue spaces and infrastructure.

Air/ambient quality: Planting trees, building green roofs, maintaining existing green infrastructure.

Urban regeneration: Enforcing interactions and ecological connectivity with community engagement, supporting energy and resource efficiency in buildings, converting brownfields to green areas and providing the urban brand with a narrative.

Participatory planning and governance: Creating spaces for dialogue, interaction and partnership in design, co-production and governance processes of different stakeholders about urban ecosystems.

Social justice and social cohesion: Distribute various types of nature-based solutions; support experiential learning and capacity building programs especially for excluded social groups.

Public health and well-being: Providing sufficient urban green space for positive health effects especially for children and elderly.

Potential for new economic opportunities and green jobs: Increasing knowledge, awareness and skills while restoring and encouraging nature-based solutions.

11.2 Nature-based building systems

There are lots of sustainable building system proposals in today's green building industry. This section discusses two of the most common and two innovative building-integrated nature-based building systems: green roofs, green walls, PBRs and aquaponics.

11.2.1 Green roofs

A 'green roof' or 'living roof' is a roof that is partially or completely covered with vegetation. It usually consists of a top vegetation layer, a substrate layer, filtering and drainage layers, insulation layers and a bottom structural layer (Figure 11.1).

Vegetation layer: The designer needs to consider the city's ecosystem for selection of the vegetation, since it will be a part of the city. The vegetation is associated with thermal performance, air quality and heat island mitigation.

Substrate layer: The substrate is usually not soil but a lighter material mixture that can provide both a structure for the roots of the vegetation and nutrients. The substrate and the plant roots in this layer not only detain water runoff but also provide thermal and acoustical benefits.

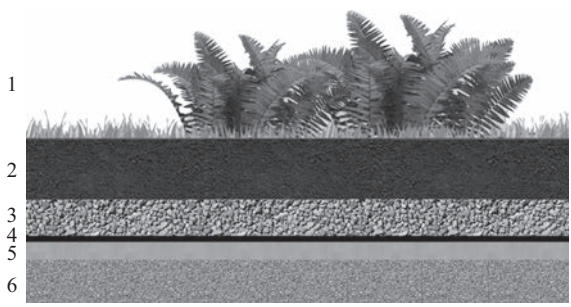

Figure 11.1 Green roof layers: (1) vegetation, (2) substrate, (3) filtering and drainage, (4) water insulation and root barrier, (5) thermal insulation and (6) structural

Filtering and drainage layers: On the one hand, these layers keep the soil particles and other harmful substances from reaching the roof membrane; on the other hand, they filter water and aerate it so that the filtered water can be used for other applications inside the building.

Water insulation and root barrier layer: Being waterproof is one of the primary duties of a roof, and being resistant to damage by roots is mandatory in any green roof. An additional thermal insulation layer may be sometimes necessary.

Structural layer: The structure of the building often carries the load from the roof, and it needs to be detailed accordingly.

The energy balance of a roof is dominated by the radiation gains from the sun and losses to the sky. In a green roof, the vegetation covers the roof and influences the heat transfer of the roof by causing shade, reflecting the solar radiation and evapotranspiration. Santamouris [8] found that applications of green roofs in city scale would decrease the ambient air temperature by 0.3 °C–3 °C. The plant height, leaf area index (LAI) – i.e. the green leaf area per unit ground surface area, fractional coverage, albedo and stomatal resistance are the most important parameters that influence the heat transfer in a green roof [9].

Since green roofs provide more thermal resistance and thermal mass than conventional roofs, they can be beneficial in reducing the heating and cooling demand of a building while stabilizing indoor temperatures and daily temperature swings. However, the influence of this effect depends on the climate and the characteristics of the buildings [10].

Niachou *et al.* [11] used EnergyPlus green roof module to investigate the impact of climate, LAI, and soil depth for four different climate conditions in the USA (Houston, Phoenix, Portland and New York). They found that green roofs are more effective in colder climates and benefit from increased soil depth, whereas increasing the LAI reduces the energy demand only for cooling-dominated climates. Berardi discusses the results of a green roof retrofit in Toronto, a heating dominated city. His simulations indicate that soil depth is more significant than LAI, and the adoption of a green roof accounted for only 0.4 °C of temperature reduction during the day. He found that a decrease of only 3% of energy demand and an improvement in the indoor comfort levels of the floor below the green roof was possible with the adoption of a green roof [9].

Jaffal *et al.* [12] mathematically modelled the addition of a green roof in a single family house in La Rochelle, France and showed that well-insulated buildings offer heating energy savings of 8%–9% and cooling energy savings of 0%, whereas older buildings with no insulation can have energy savings of up to 44%. Therefore, climate, the characteristics of the buildings and building physics parameters need to be carefully considered during the design process.

Li and Yeung [13] say that various benefits of environmental effects of green roofs were documented and give an overview of research on mainly the vegetation on the green roofs and its benefits towards the surrounding environments. They emphasize that vegetation is the key element in installing green roofs since it can

improve the urban environment by enriching the biodiversity, delaying the storm peak to the drainage system, diminishing the runoff quantity, purifying the air pollutants as well as the runoff quality. However, choosing suitable plants on rooftops is essential and factors including drought tolerance, solar radiation tolerance and LAI of plants should be considered. Both the growth substrate and the process of soil formation during the maturation of substrate played an important role in creating insect habitats and promoting urban biodiversity.

Carpenter *et al.* [14] document the response of a green roof to storm events. They experimentally examined an extensive green roof in Syracuse, New York, where the problem of combined sewer overflows to local surface waters needs to be solved. They examined the water quantity and quality response of a green roof discharge associated with precipitation events over a year. They found that regardless of the growth of vegetation, the water retention of the green roof was effective. Although the effectiveness decreased when the amount of precipitation increased, the mean per cent retention quantity for storm events was 96.8. Many similar green infrastructure studies and urban applications exist.

11.2.2 Green walls

Wood *et al.* define green walls as 'a system in which plants grow on a vertical surface, such as a building façade in a controlled fashion and with regular maintenance' [15]. Green walls have been utilized for the last two millennia [16]. A green wall is also called 'vertical greenery' or 'green façade', and similar terms include 'living wall' and 'bio wall'. A green wall usually consists of an outer vegetation layer, a substrate layer, insulation layers and a supporting structural layer (Figure 11.2).

Vegetation layer: Climbing plants or vegetation with low height is preferred; however, their selection affects the ecosystem, thermal response or the wall and air quality.

Substrate layer: Depending on the structural integration and the chosen vegetation, the geometry, thickness and type of the substrate layer changes. Pots or modular wall covering geometries can be utilized.

Insulation layers: The presence of a water insulation layer depends on the detailing of the wall and may not be necessary if there is a gap between the substrate and the wall. Thermal insulation is designed in accordance with the regulations and comfort considerations.

Structural layer: The green walls are classified according to their structures and relations to the building.

The most significant parameters that determine thermal comfort in buildings are the materials and systems used on the façades of a building, and the transparency ratio of the façade [17]. While vertical greenery is not the most suitable element to decrease the energy consumption of a single building, it usually creates multiple benefits upon implementation. Pérez *et al.* [18] have reviewed green walls as a passive tool for energy savings and specify four key aspects that may influence the

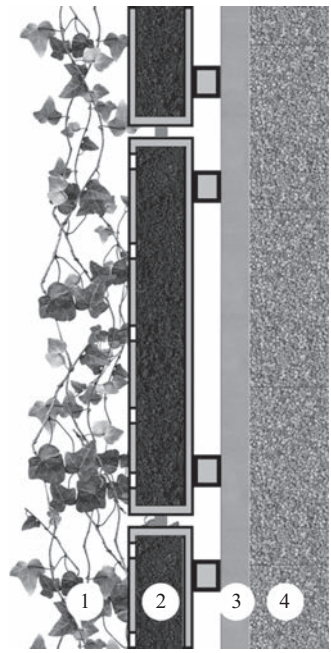

Figure 11.2 Green wall layers: (1) vegetation, (2) substrate, (3) insulation and (4) structural

operation of a vertical greenery system and should be considered accordingly: system classification, climate influence, plants species influence and operational methods (such as shade effect, cooling effect, insulation effect and wind barrier effect). Safikhani *et al.* [19] reviewed and discussed studies on the environmental, economic and social benefits of vertical greenery systems. They conclude that utilizing greenery is economical and easy, thus a suitable method to control environmental damage and decrease energy demand.

Green walls have numerous environmental and economic benefits, yet there is no agreement about the degree of these benefits. To gain more than social and aesthetic benefits, the selection of suitable plants, LAI properties and orientation and integration with other building systems are the main considerations in the design phase. Loh [20] lists the benefits of green walls as lowering energy consumption and greenhouse gas emissions, reduction of urban heat island effect, increasing the thermal performance of buildings (lowering energy costs), positive effects on hydrology and improving water-sensitive urban design, improvement of indoor air quality, reduction of noise pollution, increasing urban biodiversity and urban food production and improvement of health and well-being.

Manso and Castro-Gomes [21] review the characteristics of green wall systems especially in terms of construction and climatic restrictions. They conclude that the environmental impact of its components and associated costs during the entire

lifecycle of the building element should also be considered. Natarajan *et al.* [22] assessed the energy use, water use and greenhouse gas emissions from a vertical garden through its life cycle and have found that the use phase had the greatest impact in an assumed life of 20 years, thus attention to maintenance is crucial. During the implementation phase of vertical greenery integration with building systems, attention is necessary to the new ecological balance around green façades, additional loads to the structural system, detailing the growing medium, loading, planting and monitoring of the live plants.

11.2.3 Photobioreactors

PBRs are closed systems that can be utilized to grow algae inside. The integration of urban vertical farming and architecture with living algae facades is a relatively new concept with only three building scale applications and some conceptual studies [23]. Algae can only be cultivated in aquatic environments, and large areas are needed for the development of algae in open systems. Therefore, enclosed systems are easier to integrate with building systems. Other reasons to prefer closed systems include their smaller size, modular form, richness of available algal varieties, better control of production conditions and easy integration with buildings. A PBR usually consists of a middle cultivation layer, a surface layer and a control system (Figure 11.3).

Cultivation layer: The aquatic medium, in which the algae are cultivated, has to provide the necessary elements and adequate nutrients for optimum synthesis of the species. Sufficient mixing must be provided in order to allow the algae to utilize the necessary inputs within the closed system.

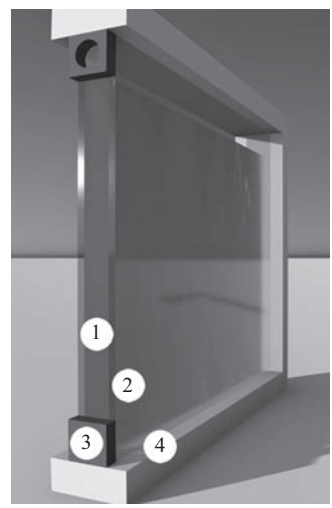

Figure 11.3 Elements of a photobioreactor (PBR): (1) cultivation layer, (2) surface layer, (3) control system and (4) structural frame

Surface layer: The most important condition for algae growth is access to light so that they can carry out photosynthesis in sufficient quantities. Enclosures should be made from a material with high light transmittance.

Control system: As the respiration of the algae increases at high temperatures, this prevents their reproduction; therefore, temperature needs to be controlled. It is also necessary to keep the level of gasses and nutrients inside this system so that the algae continue to thrive. Other conditions include salinity and pH value.

Structural frame: The structure should be able to carry all the dead weight of the system. In addition, details ensuring the durability and preventing leakage are necessary.

Algae have been on Earth for billions of years. They are photosynthetic organisms, which live in aquatic environments, and their place is essential on the ecosystems on earth. Their photosynthesis activities through millennia were the precursor to oxygen in the atmosphere, the creation of the ozone layer, and some scientists argue that plants evolved from one of the algae strains [24].

Algae serve as biofactories that take nutrients and CO_2, and change them into various valuable products and O_2 through photosynthesis and other cellular processes. They are currently responsible for nearly 50% of the oxygen production on Earth. In this context, they have the potential to help with mitigating global warming via biological carbon sequestration. They are also one of the basic food sources for many aquatic species and carry nutrients [25]. They grow faster than trees; some species can multiply to twice their size in 3.5 h under right conditions [26]. They can also provide nutrients for people [23]. The dying algae led to the creation of fossil fuels; in this context, there are various studies on using oil or other materials directly from algal bodies to produce biofuels [27]. Moreover, products of the photosynthesis process include lipids, biodiesel, carbohydrates, ethyl alcohol, hydrogen, proteins, fertilizers and resource materials for various energy-production technologies.

The type of PBR and the quality of the aquatic cultivation medium affect the productivity of the species. The light profile, temperature, mass transfer and biomass density inside the PBR and the equipment necessary to feed and harvest the PBR needs to be designed together with the technical equipment of the building. Major factors affecting final productivity are design, orientation, climate, date, geometry, direct and indirect solar radiation and scaling [28].

Algae can be fed with waste products from the buildings, while these living walls can be utilized to create more comfortable indoor environments, this would mimic the symbiotic relationship between some species in nature [29]. Visual comfort and thermal comfort are necessary in buildings. Solar control is essential for both visual and thermal comfort. PBR elements can also have a symbiotic relationship with other renewable energy sources. PBR as an architectural element can take on various colours; therefore, visible, green aesthetics and colour therapy are some interesting possibilities that make use of various species of available algae [30].

From rigid to flexible walls and from curtains to structural columns, the type of PBR system provides many possibilities. Although green walls make use of known facade systems, algae systems also need technical integration with the building; therefore, constructional considerations are mandatory. These include ease of installation, flexibility of design, modularity, size coordination and additional loads to the building. Building integration of PBRs is mostly experimental and expensive at the moment. Their costs are either neglected or the payback period is long. However, ongoing research is promising when the cost of carbon is also added to the system.

11.2.4 Aquaponics

Aquaponics is a method for producing food that combines recirculating aquaculture (raising fish in land-based tanks) with hydroponics (cultivating plants in water) [31]. A symbiotic cyclic system emerges with the integration of a tank and fish into plant production (Figure 11.4).

Fish tank: Fish produce nutrient-rich waste, which fertilizes the plants. The fish themselves is one of the end products of the system.

Plant beds: Plants filter the water from gases, acids and chemicals, such as ammonia, nitrates and phosphates for use in other elements of the system [32]. Production of plants is one of the requirements of the system.

Bacteria: Bacteria and worms play a role in breaking fish waste to utilizable elements for the plants.

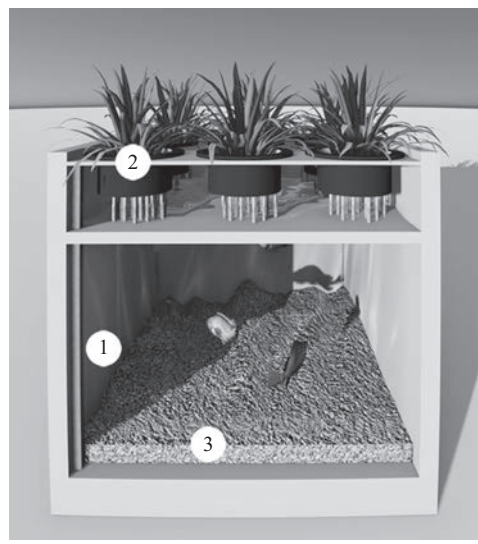

Figure 11.4 Elements of an aquaponic system: (1) fish tank, (2) plant beds and (3) bacteria

The whole system is connected through piping system to move water in a cycle. The water cycle provides the elements of the system with enough nutrients and water to be absorbed. It also brings air to the roots of the plants. When necessary, extra fish feed and ingredients can be added to the system to keep the balance.

The commercial applications in the field of aquaponics were researched till the 2000s, and they are now being practiced by farms, nonprofit organizations, community garden groups, schools and noncommercial gardeners. According to a survey of Love *et al.* [33], the motivating factors behind aquaponics gardening are growing their own food, improving the health of their community and helping with environmental sustainability. The benefits of the system include

- supporting locally grown food chains, while bringing fresh food into urban areas;
- nutrient-rich plant and fish growth through the whole year, even in cities;
- biological security, since the parasite and disease status of the fish and crops are known;
- production from day one, which is important for both food safety;
- more efficient use of ingredients and water compared to commercial farming methods;
- nearly no waste during production, since the whole cycle utilizes the other elements' waste;
- prevents the release of toxic chemicals into groundwater sources and
- reduction in chemical use such as pesticides since the system discourage pests and undesired vegetation.

Aquaponics gardens and soil-based gardens share similarities in size (~100 ft^2 or 9 m^2), location (at home) and the types of crops. Love *et al.* [33] found that aquaponics gardens contained more leafy greens than soil gardens, most likely because the nitrogen-rich water promotes leaf growth and because fruit trees and some rooting crops are not suited for aquaponics.

Rakocy *et al.* [34] indicate the environmental considerations that limit the system productivity are heat, pH, light and dissolved oxygen levels in the water, and they need to be controlled. Deviation from the optimum states would lower the yield and sometimes endanger the system to shut down; for example, sudden temperature changes can destroy the harvest. Another example would be that rising levels of ammonia or pH can wipe out the entire fish colony. Maintaining this controlled environment requires electricity, and without power, the cycle – therefore the whole system – would break down.

Suitable temperature for the plants is around 24 °C for many plant species. A pH level of 7 is also suitable to keep the nitrification process going on. The plants need light to thrive; therefore, their placement has to be organized according to the light the plants receive. The optimum amount of the dissolved oxygen level is around 6.2, and the movement of water helps to maintain the level of O_2 [35].

According to Al-Kodmany [32], a significant drawback of the system is the requirement of skilled or trained workers. While there are lots of low cost 'Do it yourself' projects on the internet and media to produce such a system, it still

requires some skills to operate and maintain. However, this drawback can be taken as an opportunity to facilitate the creation of local green jobs.

While there are many buildings that make use of nature-based solutions, they are usually piecemeal additions and not wholly integrated with the building systems. The following section shows the integration potential of nature-based solutions via a cyclic proposal for integration into a residential building.

11.3 Algaponic proposal

This proposal is a home-integrated agriculture and urban greenery project that creates a circular mechanism. Its design allows integration of different nature-based parts to generate a cycle of production to create a food chain. It can be installed as a balcony into a new building or as part of an independently supported renovation project. Modularity of the system makes it adjustable to many applications, from high rise to individual buildings. The system consists of a green roof that would collect and filter water on top, a water storage tank, a building-integrated PBR façade, a fish tank, plant beds, LED lighting to simulate sunlight and a photovoltaic (PV) installation on the roof to power the whole system (Figures 11.5–11.10).

Green roof: Green roofs are used to take water from the rain and filter it for utilization in the other parts of the system. The plants and substrate will be composed in accordance with the flora and fauna of the local ecosystem and are a part of the proposal for the purpose of water retention.

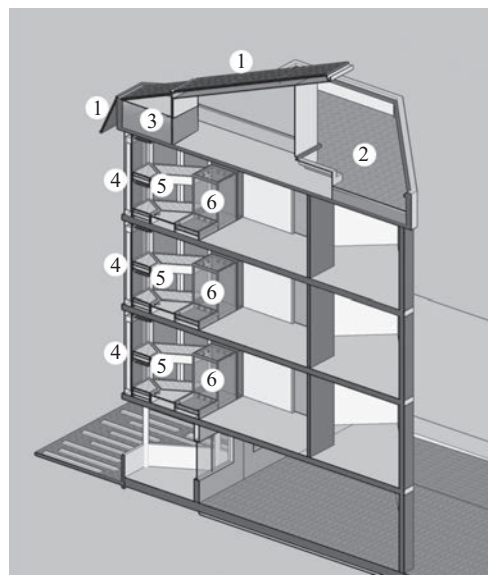

Figure 11.5 General section of algaponic system: (1) PV panels, (2) green roof, (3) water storage, (4) PBRs, (5) plant beds and (6) fish tanks

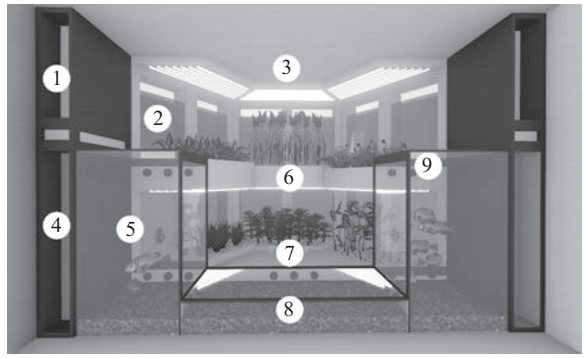

Figure 11.6 Algaponic unit: (1) PBR filter + controls, (2) PBRs, (3) LED grow lights, (4) fish tank filters + water pump, (5) fish tanks, (6) plant beds, (7) piping interlocks, intervention manifolds, (8) ammonium bacteria bed and (9) ultraviolet lamps

Figure 11.7 The algaponic application in a conceptual building I

Water storage: The water collected from the green roof is stored preferably in the roof. If there is not enough rainwater to circulate the system, filtered freshwater can be added as necessary. The stored water is pumped to the PBRs after being filtered by UV rays.

Photobioreactor: The PBRs are placed on the façade of the building, on the three edges of the balcony. Their size is determined according to other system parts.

Figure 11.8 The algaponic application in a conceptual building II

Figure 11.9 The algaponic application in a conceptual building III

Figure 11.10 The algaponic application in a conceptual building IV

Fish tank: The fish tank is made of two water tanks on the two sides of the balcony and a connecting piece at the bottom. Depending on the user requirements, the fish can range from small fishes like goldfish to big fish such as salmon. The fish can be harvested for food when grown. The water in the tanks will be cycled to provide nutrients to the plant beds.

Plant beds: These parts are used for the production of fresh vegetables or other desired plants. Its requirements limit the size of other parts as more square meter of growing medium would need more water and nutrients. Additional food supplements can be necessary to meet dietary requirements.

LED lighting: This part is used to maximize the production of both algae inside the PBR and the vegetables in the plant beds. It is powered by the PV system.

Photovoltaics: The PV system is placed on the building roof and oriented for maximum efficiency.

11.3.1 Green roof and water storage

The water treatment and storage system in the proposal will be installed onto the building's roof. The green roof will detain and filter rainwater. The collected water will be placed inside water-storage tanks on the roof. Filtered water will support the algaponics, house systems and watering the surrounding vegetation. If more water than can be stored is collected, the excessive amount will be directed through a drainage system. In case there is not enough rain to support the system, potable water will be filtered from lime and given to the green roof for further utilization in the system. A connection with a city wide rainwater collection matrix can be established in the future.

11.3.2 Photobioreactor

The PBR will supply the system with nutrient-rich algae, which uses solar power to perform photosynthesis. They will take in the released CO_2 of the building and give out O_2. In this context, algae can be inferred as a solar-powered mechanism. The PBR itself was designed to turn solar power into nutrients – energy for humans – and O_2.

Design of the PBR will fit in place of a floor height window with the placement dimensions of 3 m tall, 1 m wide and 0.3 m deep (Figure 11.7). Six panels with these dimensions are organized to form three faces of an octagon, where each face will consist of two panels. This way, the modular plant beds will have 135° angles between them to ease the water circulation. This will let the users to cut-off the circulation of broken or problematic parts or bypass them with ease when repairing or changing the parts are necessary.

The cultivation medium in one PBR module has dimensions of 2.8 m height, 1 m width, and 0.06 m depth to grow algae, which will be covered with 2 cm thick tempered glass. Water level in the PBRs will be around 80% to allow for gas movement and relieve pressure. The PBR will also take light from the LED systems above the plant beds in addition to the sun. This will keep the PBR active for more algae production during the night.

PBRs will be directly placed to the facade and will act like a water wall. PBR that look like window openings will be used to grow algae to feed the fish, which will be living at the aquaponic farm. The algae production has two stages; in the first stage, the central part is used to grow small algae, and the grown algae are taken to the sides. The grown algae and growing medium will be sent to the fish tank in time intervals. The deposit to the fish tanks will take place next to the control units, at the side of the modules. The algae specie in this proposal is *Spirulina* sp. The medium needs to be between 32 °C and 38 °C to optimize the living conditions of the algae. If there is a surplus of algae, i.e. more algae than the fishes need, it will be filtered for human consumption and support the residents' diet, since it could either be used as a food supplement or directly eaten, even as a crisp [36].

11.3.3 Fish tank

The fish tanks will consist of three elements. Two square-shaped aquariums with 1 m × 1 m × 1.7 m dimensions are located at the ends of PBRs and therefore located at the entrance of the algaponic system. These units will serve to grow the fishes. The top covers of these aquariums can be opened to intervene with the fish culture. The third element will connect these aquariums at the bottom and has dimensions of 1 m × 2.1 m × 0.3 m. This element will also serve as a platform for the users to step on and easily reach to both fish tanks and plant beds. The sizes of the water tanks were determined as 400 L/m^2 of growing medium in accordance with the average requirements of people using aquaponic systems in the USA [37].

Fish species inside the tank can change according to the size, nutrient needs of the plants, residents' decision, etc. However, ornamental fishes or fishes like

carp, that directly feed on algae, would perform better in accordance with this proposal. Taking their nutrients by directly feeding on the algae, *Spirulina* sp., will result in nutrient-rich waste production and contain ingredients that the plants need to grow.

The waste of fish and leftovers of the feed increase ammonia levels in the water and would eventually poison the fish. To prevent this, the connection unit will serve to culture bacteria and molluskas which will clean the water. The bacteria will hold onto gravel and a dense group of small rocks embedded on the ground level of the fish tanks. The bacteria will act like a biofilter and break down fish waste. In this breaking chain, first *Nitrosomonas* bacteria will break ammonia into nitrites. *Nitrospira* bacteria will be next in the chain of filtration; they will convert nitrites into nitrates. Thus, they can feed the plants without poisoning the fish. Cycling the water through a biofilter will result in another ingredient to feed the plants.

Connection pipes between fish tanks and plant beds will be located next to the connection element of the tanks. These pipes will filter the cycling water from fishes to plants. All of the piping connections in the system will be manually locked so that any part can be taken off for maintenance. This system can be automatized in the future.

11.3.4 Plant beds

The plant beds are placed in front of the PBRs in two levels. There are a total of six beds facing three directions on two levels with 30 cm bucket depth. Sleeve depth of the plant beds will be 80 cm so as to optimize the residents' reach. The lower level will start from 30 cm above the fish tank connection, each bed on a level will be placed 5 cm lower than the previous bed to facilitate water movement. The lower levels of the planting beds are for growing long day species – in other words summer species – of vegetation. The upper plant bed will be placed 100 cm above the lower beds with the same height increments of 5 cm and will provide free space to grow plants as high as 140 cm. This layer will be for growing short day species of vegetation – in other words for winter species – since they grow longer. This design makes both the upper and lower layers ergonomic for the planting and gathering processes.

The space between the planting beds will create an area of approximately 2 m $\times$ 2.1 m area to manoeuvre while working. This free space creates suitable conditions for two persons to work at the same time. The 30 cm platform placed to ease access to the higher shelf will hide the piping system underneath. Shut valves and disconnection joints will be located here for use when intervention or maintenance is needed. There will also be an additional exit to the main plumbing to ease discharging the water from the units.

Ammonia produced by fishes is generally a problem for aquaponic farmers. The nutrient film technique used in the aquaponic plant bed applications will reduce the percentage of ammonia within the water. This technique has a floating material on the surface of the water, which holds the body of the plants as a tray with suitable holes. The plants are supported in small pots that enable the roots to

constantly be in the encircling water with the help of a water pump. The pots will be made of cocopeat, a growing medium produced from the outer shell of the coconut. This material would not deposit any additional ingredients or minerals; therefore, the plant will only take what is inside the algaponic system. This way, there will be no accumulation of the unused minerals; therefore, roots of the plants will freely reach the ingredients and air. This system also allows the residents to set water levels depending on the root length or maturity stage of the plants [31]. As the roots mature, the water levels will be lowered to encourage root growth. Continuous cycling of the nutrient-rich water directly to the roots from fish waste lets plants to meet their nutrient and water needs. The drawback of this system is that it is susceptible to power outages and pump failures.

Estimation of the approximate yield of the system is difficult since there are many unknowns to consider in the system including the algae, fish and vegetable species and the climate. According to the research presented by Love *et al.* and the authors' estimates, a planting area of 8 m^2 within aquaponic farming would be enough to supply the daily nutrients necessary for the diet of two persons [33]. However, to reach such an outcome, the placement, configuration and species of the vegetation should be wisely chosen. Each bed in the proposal consists of 1.33 m^2 space, which results in a total of 8 m^2 planting beds. There is a UV light source box of 10 cm $\times$ 10 cm $\times$ 80 cm at both the entrances and the exits of the plant beds. The UV rays will dissipate in the water, therefore the residents will not be exposed to UV light directly. A timer attached to this UV light source will make it flash in sequences to ensure there will be no contamination.

11.3.5 Other elements of the system

A lighting system made of LEDs will be located over the plant beds to simulate sunlight so that the plants would grow, during both day and night, with enough amount of light to produce plants independent of the sun. A light sensor and a timer attached to the LED system will control the light conditions according to residents' demands. This way, the system will support the growth of a wide range of vegetation, from short day vegetation to long day vegetation. Cooling units integrated with the water system will increase the lifespan of the LEDs. The lighting system will also have a mechanism to change its height so that more direct light can be given to the plants during their early growth period by shortening the space between the light source and the plant.

The roots of the plants will filter the water inside the system from its nutrients and minerals. If the water contains many minerals after the plants are grown, when this water goes to the PBR to grow algae, the extra minerals can cause corrosion in the PBR surfaces. Therefore, a filter for minerals and possible thrash is installed to the water circuit before entering the PBRs. Through this process, fish population will also filter water after the PBR, thus providing better living conditions for the fish. This will allow maximizing the fish population to the limits of the carrying capacity of the system. During the process, the outgoing CO_2 of the fish and the bacteria will be changed to O_2 by photosynthesis, which is another important aspect of this project.

The energy requirements of this system are for the LED lighting and pumps. Four rectangular PV panels with 2 m × 2.5 m dimensions and three with 1.4 m × 2.5 m can be installed over the balcony annex that contains the algaponic system. Approximately 2 m^2 of PV installation is estimated to compensate for the energy demand of this proposal. In addition, solar tubes would heat the water storage before discharging it to PBRs.

The control panels of the system will be placed on the side units while connecting fish tank and PBRs. Also PBR filters, fish tank filters and water pump will be hidden inside the unit. Sliding shelves ease the maintenance of the filters. The data acquired from the sensors will be displayed on a board over the unit. A different filter will collect the *Spirulina* sp. between the feeding periods of the fish. Excess yield will be used to support the residents' dietary requirements. Future studies will focus on the optimization of pH levels, CO_2 levels, light levels, the placement, configuration and species of the vegetation and interface controlled full automation of the system to ease the manual operation and optimization of the process; therefore, an experimental study has to be conducted.

11.4 Impact evaluation

There are a number of studies that classify and research nature-based solutions in regional, metropolitan, urban and street levels; however, they are very limited in the building scale. This chapter proposes a cyclic system for the building that makes use of a number of nature-based building elements integrated into an algaponic system to mainly grow food. Yet this system would have a number of other environmental, social and economic impacts on the residents. These are assessed in accordance with the EKLIPSE challenges given in Section 11.1 [6]. Since this system has no context in regards to the city it is a part of, this proposal has no effect on 'coastal resilience'; therefore, this evaluation uses nine of the ten main headings. In this proposal, all of the elements of the system, bacteria, algae, fishes and plants, should be carefully chosen since all of these living elements require certain conditions to thrive. In addition, both PBR façade systems and aquaponics are still in the development stage; therefore, their assessments will be limited.

11.4.1 Contribution of nature-based solutions to climate resilience

Climate resilience is based on the concepts of adaptation and mitigation. This proposal contains mitigation impacts since it incorporates many elements such as vegetation, soil and algae that will capture and sequester carbon inside, while also improving air quality.

Moreover, the green elements, vegetation and algae, will help with climate adaptation. Green roof application on the top of the building and additional plant growth on the balcony and facades will improve the climate at the micro-scale. Wide spread application of this proposal in the future would result in both improved climate performance in cities in the macro-scale and increased climate adaptation impacts at building and street levels.

This proposal offers the building sector a new way of collaborating with the nature as new gardens of the future cities. The residents would grow their own food at home scale, therefore would decrease the carbon emissions released during food-production process. In addition, this would cut down the carbon emissions released during the transportation of the food.

Another important aspect of the algaponic system is the use of water through all of the system elements. Since the algae require a certain temperature range, the water wall effect would help with keeping the algae alive, the proposed PBRs on the facades are expected to act like a water wall and decrease heating energy requirements. In addition, the water tanks in the building will act as additional thermal mass. Since the proposal will be made of steel, which has extremely limited mass, the additional thermal mass would help to increase indoor thermal comfort and carbon savings while decreasing energy requirements of the building.

11.4.2 Water management

Global natural resources of clean water supply are decreasing. To overcome this danger, it is necessary to collect rainwater that would help to regreen the cities, which are generally covered with hard surfaces. This is a huge problem in cities; therefore, green roof application, which is one of the most popular and least expensive solutions, is both very popular and necessary. This proposal foresees that these algaponic elements will be interlinked with a network in the future, thus would decrease floods via changing the discharge path of the water during bad weather conditions while reducing the water run-off and flood risks.

This system has a green roof to collect water and a storage tank. In addition, the whole mechanism acts as water storage and sustains itself with the use of as much water as the vegetation production requires. Any filtered water not used by the system will be discharged to underground water supplies.

Increasing the quality of the water with various treatments will be another significant effect of the proposal. The water cycle of the system will be as follows: the PBRs will take the filtered and heated water from the water storage, PBRs will pass this water to the fish tanks, fish tanks will pass it through the biofilter layer, biofilter will send it to planting beds for vegetable production, water will go back to the PBR and restart the cycle. Cycling the water in this way will require 90%–95% less water than conventional farming. The water in the system will also be filtered via all the biological elements and mechanical filters during the process, which will increase the water quality.

11.4.3 Green space management

Although this proposal is only accessible by the residents, another important outcome of the project is the reclamation of the built land in a high rise for nature-based applications. For an average building with eight levels built on 100 m^2 of land would reclaim production area will correspond to 64 m^2 of production area and more than 100 m^2 of green land with planting beds, PBR and green roof, while PBR and fish tanks would correspond to 18.4 m^3 of blue space reclamation; thus, the more land than used will be reclaimed.

One of the main ideas behind the proposal is adopting an innovative use of aquaponics within the building scale; in this way, both building and aquaponics will form a symbiotic relationship rather than the usual expectations. Future potentials of the proposal include increased connection between the green areas and buildings and to collect rainwater to sustain the surrounding green spaces.

Biodiversity potential of the proposal is high because of two reasons: first is the creation of green spaces to support the natural biodiversity in the city, such as in the green roof. This will affect urban biodiversity by providing habitats for many species from birds to insects. The second reason is the proposal itself, which proposes to create a polyculture between microorganisms, aquaculture and plants.

11.4.4 Air/ambient quality

The proposal consists of biological elements; plants and algae as photosynthetic organisms that would produce O_2 while capturing CO_2 from the surrounding air and water. The CO_2 produced by the fishes and bacteria will be converted into O_2 by this process. Additionally, these elements will capture air pollutants through both conversion and deposition. At the micro-scale, the proposal will enhance the air quality inside the building. Moreover, the proposal will improve the green infrastructure of the city.

11.4.5 Urban regeneration

Most of the components of this algaponic proposal are commercially available. There are many green roof projects some on bigger scales, a number of research and development-oriented building-integrated PBR projects and lots of aquaponics applications in building and smaller scales. While the design can readily be used in a new building, it can also be installed as an addition to an existing building with an independent structural system. Algaponic applications can be used to revitalize and regenerate derelict buildings. If it cannot be applied because of site considerations or regulations, the system can be applied directly within a room in accordance with the building's conditions. The modularity and self-sustainability of the system allows for a variety of applications.

The proposal created many links between urban development, innovative building elements, urban green infrastructure, urban aesthetics, social involvement, urban ecology, energy and water use. Nearly all parts of the project require and utilize solar energy and photosynthesis to keep themselves alive. Use of solar power is one of the life's supports of the nature-based solutions. The energy demand of the algaponic proposal would be higher than conventional farming since the LED system and water pumps will be assigned to maintain the cycle. Yet it will require less water use and building energy. To meet with the energy demand of the algaponics, PV panels will be installed on the roof facing optimum orientation.

11.4.6 Participatory planning and governance

While the building scale is a micro-scale for governance, it can be ideal for participatory governance. Many rights need to be regulated by the building authorities

in the building scale such as the rights to produce own electricity, have own roof garden, use PBR on the façade, grow own food at home, have own share of a garden and have own aquaponic balcony. If there is no regulation for an algaponic system, then it can be next to impossible to build such a balcony. This proposal can be applied in different scales and broadened to the macro-scale while connecting the rainwater collection with a matrix of green roofs in the future.

The proposal offers 8 m^2 of planting area and six PBRs with nearly 1 m^3 algae growth capacity for each balcony module application to support healthy living for the inhabitants. If this system is applied to all new buildings as one of the main program elements like a kitchen or a balcony, this would cause a massive impact for sustainability of the community and the cities of the future. Knowledge sharing, dialogue and common interests of residents would improve participation in governance activities.

11.4.7 Social justice and social cohesion

Farming itself is a recreational activity with meditative properties that answer the needs of every person in the community from nearly all age, sex and accessibility ranges. Application of algaponics and green roofs will increase the social awareness through personal and community gardening. This will start cycles of plant trade while different species of plantation may occur in each level of the building.

In addition to providing fresh and healthy food, the World Bank research report on aquaponics in the Gaza Strip, Palestinian Territories show that aquaponics applications can answer the needs of different socio-economic communities; such as the poor, youth or immigrants [31]. Exchanging food, experiencing food and sharing information will cause people to gather, form bonds and tighten them. The people joining this movement would eventually build trust for further interactions. Thus, further social cohesion is expected to occur with the spread of the system.

11.4.8 Public health and well-being

The questions about food safety, hazardous chemicals in our food, freshness, etc. are gaining prominence for the health of the community. This proposal is about a home-scale agriculture project that can create a circular mechanism to grow fresh food to deal with these issues. An additional benefit will be that working and interacting with green spaces and nature-based solutions will provide the urban residents with an opportunity to relax and relieve stress [38].

One of the opportunities this proposal creates is food security. Since accessibility to land is decreasing very rapidly in the cities, this is becoming a big problem for flat owners in cities. Flats with no land to use as a ‘yard’ decrease the opportunity to grow one’s own food. Another concern is the negative effects of chemicals used in agriculture such as pesticides on the land and on the public health. With this project, growing your own food in an appropriate scale that can be installed as a balcony or room of your flat, which is a dream for many, can become the future of city farming.

Other issues include safe delivery of food and freshness. By growing their own food, the residents can also ensure the food's quality with the knowledge of what they put inside the production cycle. This also opens the path of medicinal herb planting at home scale. Medicinal herb gathering is another opportunity with the problem of freshness. Algaponics will be an optimum space to grow and collect fresh medicinal herbs.

11.4.9 Potential for new economic opportunities and green jobs

The production of the proposal and its elements have the potential to open and grow new green jobs and economic opportunities. The algaponic system consists of some complex mechanisms such as PBR and aquaponics. The operation and maintenance of these elements require relevant areas of expertise. In addition, the optimal design and selection of algae, fish and vegetation species will require help from professionals. Moreover, inspecting the quality of the food and educating people in farming methods will be necessary. In parallel to this context, the application of this system would open new areas of research in many professions. Consequently, many new experts will be needed within the cities to keep the green industry going.

The whole system can have higher operational costs than current agricultural techniques. However, in terms of production capacity, this system will yield ten times more produce on a yearly basis since it operates fully without many restrictions, such as day and night. In addition, the plants and animals are fed with rich nutrients and water. Local farming chains, where everyone can contribute and barter with their own surplus produce will be another output of this project. The productions can differ from one apartment to another.

11.5 Conclusions

Currently, researchers all over the world are searching for solutions to problems, such as air pollution, climate change and other environmental issues. An innovative approach in this search is the utilization of nature-based solutions. It is associated with many ecological, bioclimatic and energy efficiency benefits in the context of building design. This chapter proposes a modular building element – a balcony annex – that makes use of nature-based solutions mainly for food production in an apartment building. The system is a self-sufficient system and uses solar power to maintain a cycle of life and production; therefore, it helps to create more green and blue areas in micro-scale of the urban context.

The proposed system can be called algaponic, and the architectural integration carefully considers four main elements: a green roof for water collection, PBRs for algae production, fish tanks for fish production and plant beds for vegetable production. All of these elements are connected through a water cycle and provide the necessary conditions for the other elements to perform. Additional elements such as pumps and lighting need energy to ensure the continuity of the cycle. Therefore, PV panels located on the roof of the proposed system will supply power to these units.

The algaponic proposal will be installed as a balcony to grow food in our homes. Personal gardening and food-production elements were part of the building program in the old times yet have changed and were lost with rapid urbanization and especially the increasing demand for high-rise buildings; however, this proposal will bring these elements back to the architect's agenda.

Application of such a nature-based system has many facets and need to be comprehensively assessed; however there is no assessment framework for such a building application; therefore the framework of EKLIPSE Expert Working Group on Nature-based Solutions to Promote Climate Resilience in Urban Areas was applied in this chapter. This framework assesses nature-based solutions according to their relationship with ten main challenges. The green roof application within the proposal is a common technology; therefore, its impacts were embedded into the assessment framework, yet assessment of many other elements and the whole system did not totally correspond with the framework. Therefore the necessity of a framework for building integrated nature-based solutions became evident.

The impacts of common utilization of such a system will be especially beneficial to the carbon sequestration and air-purifying mechanism in nature and energy efficiency of the building. Since people who are in close touch with nature tend to respect nature the most, this proposal targets residents of an apartment in a personal basis. Planting and harvesting cycle has been the central piece of a human's interaction with nature for a long time, and this system would increase public awareness and encourage involvement and reconnection with nature. However the ecological, economic and social effects of the system are dependent on the location of the application. The ecological approach behind this proposal is starting the change from our homes. Locally grown food will affect the households and the local economy rapidly. In addition, improving the diets of the users will improve public health.

Since this is only a conceptual study, there are many points to research and refine before an actual application, such as optimal design of the four main elements of the system and their connections: selection of algae, fish and vegetation species. A multidisciplinary approach is necessary to ensure the working of the algaponic system with high efficiency. One of the main ecological risks of the current technologies and knowledge is dependent on certain species; therefore, increasing the polycultural property of the ecosystem has to become a main research interest to successfully utilize nature-based solutions in the future. Thus, this proposal is expected to boost the diversity of the species living in the city in harmony with the city's inhabitants and enhance the habitat in a controlled manner.

References

[1] UNEP. *Towards a green economy: pathways to sustainable development and poverty eradication*. 2011.

[2] Koop S.H., and van Leeuwen C.J. 'The challenges of water, waste and climate change in cities'. *Environment, Development and Sustainability*. 2017, vol. 19(2), pp. 385–418.

[3] UNEP-DTIE. *Cities and buildings, UNEP initiatives and projects*. Sustainable Consumption and Production Branch, 2012. Available from http://www.unep.org/SBCI/pdfs/Cities and Buildings-UNEP DTIE Initiatives and projects hd.pdf.

[4] EC-European Commission. *Towards an EU Research and Innovation policy agenda for nature-based solutions & renaturing cities: final report of the Horizon 2020 Expert Group on "Nature-Based Solutions and ReNaturing Cities"* (*Full Version*). Publications Office of the European Union, Luxembourg, 2015. Available from http://dx.publications.europa.eu/10.2777/765301 2015a.

[5] COST Association. *Memorandum of understanding for the implementation of the COST action implementing nature based solutions for creating a resourceful circular city (Circular City Re.Solution) CA17133*, 2018.

[6] Raymond C.M., Berry P., Breil M., *et al. An impact evaluation framework to support planning and evaluation of nature-based solutions projects*. EKLIPSE Expert Working Group on Nature-based Solutions to Promote Climate Resilience in Urban Areas Report. Centre for Ecology & Hydrology, UK, 2017.

[7] EKLIPSE. EKLIPSE: enabling a science-policy dialogue on the future of biodiversity at the CBD CoP-14 Science-Policy Forum [online]. 2018. Available from http://www.eklipse-mechanism.eu/news.

[8] Santamouris M. 'Cooling the cities – a review of reflective and green roof mitigation technologies to fight heat island and improve comfort in urban environments'. *Journal of Solar Energy*. 2014, vol. 103, pp. 682–703.

[9] Berardi U. 'The outdoor microclimate benefits and energy saving resulting from green roofs retrofits'. *Energy and Buildings*. 2016, vol. 121, pp. 217–229.

[10] Ascione F., Bianco N., de Rossi F., Turni G., and Vanoli G.P. 'Green roofs in European climates. Are effective solutions for the energy savings in air-conditioning'. *Applied Energy.* 2013, vol. 104, pp. 845–859.

[11] Niachou A., Papakonstantinou K., Santamouris M., Tsangrassoulis A., and Mihalakakou G. 'Analysis of the green roof thermal properties and investigation of its energy performance'. *Energy and Buildings*. 2001, vol. 33(7), pp. 719–729.

[12] Jaffal I., Ouldboukhitine S., and Belarbi R. 'A comprehensive study of the impact of green roofs on building energy performance'. *Renewable Energy.* 2012, vol. 43, pp. 157–164.

[13] Li W.C., and Yeung K.K.A. 'A comprehensive study of green roof performance from environmental perspective'. *International Journal of Sustainable Built Environment*. 2014, vol. 3(1), pp. 127–134.

[14] Carpenter C.M., Todorov D., Driscoll C.T., and Montesdeoca M. 'Water quantity and quality response of a green roof to storm events: Experimental and monitoring observations'. *Environmental Pollution.* 2016, vol. 218, pp. 664–672.

[15] Wood A., Bahrami P., and Safarik D. *Green walls in high-rise buildings: An output of the CTBUH sustainability working group*. Mulgrave, VIC: Images Publishing, 2014.

[16] Tokuç A., and Inan T. 'A green outlook to tall building facades via Milan's vertical forest'. *Proceedings of the 8th International Advanced Technologies Symposium (IATS'17)*, Oct 2017. pp. 89–94.
[17] Aydın D., and Mıhlayanlar E. 'Yüksek konut yapılarındaki iç ortam kalitesinin incelenmesi'. *Megaron*. 2017, vol. 12(2), pp. 213–227.
[18] Pérez G., Coma J., Martorell I., and Cabeza L.F. 'Vertical greenery systems (VGS) for energy saving in buildings: a review'. *Renewable and Sustainable Energy Reviews*. 2014, vol. 39, pp. 139–165.
[19] Safikhani T., Abdullah A.M., Ossen D.R., and Baharvand M. 'A review of energy characteristic of vertical greenery systems'. *Journal Renewable and Sustainable Energy Reviews*. 2014, vol. 40, pp. 450–462.
[20] Loh S. 'Living walls – a way to green the built environment'. *BEDP Environment Design Guide*. 2008, vol. 1(TEC 26), pp. 1–7.
[21] Manso M., and Castro-Gomes J. 'Green wall systems: a review of their characteristics'. *Renewable and Sustainable Energy Reviews*. 2015, vol. 41, pp. 863–871.
[22] Natarajan M., Rahimi M., Sen S., Mackenzie N., and Imanbayev Y. 'Living wall systems: evaluating life-cycle energy, water and carbon impacts'. *Journal Urban Ecosystems*. 2015, vol. 18(1), pp. 1–11.
[23] Tokuç A., Köktürk G., and Savaşır K. 'A design option to decrease building related carbon emissions: algaetecture'. *Proceedings of the 12th International Green Energy Conference*, Xi'an, Shaanxi, China, Jul 31–Aug 3 2017.
[24] Milne J.L., Cameron J.C., Page L.E., Benson S.M., and Pakrasi H.B. *Report from workshop on biological capture and utilization of CO_2*. Charles F Knight Center, Washington University in St. Louis, USA, Sep 2009.
[25] Chacón Lee T.L., and González Mariño G.E. 'Microalgae for "healthy" foods—possibilities and challenges'. *Journal Comprehensive Reviews in Food Science and Food Safety*. 2010, vol. 9(6), pp. 655–675.
[26] Singh U.B., and Ahluwalia A.S. 'Microalgae: a promising tool for carbon sequestration'. *Mitigation and Adaptation Strategies for Global Change*. 2013, vol. 18, pp. 73–95.
[27] Kose A., and Oncel S.S. 'Algae as a promising resource for biofuel industry: facts and challenges'. *International Journal of Energy Research*. 2016, vol. 41, pp. 924–951.
[28] Outhwaite A. 'The Characterization of a Building-Integrated Microalgae Photobioreactor'. Master's Thesis, Dalhousie University, 2015.
[29] Fernandes B.D., Mota A., Teixeira J.A., and Vicente A.A. 'Continuous cultivation of photosynthetic microorganisms: approaches, applications and future trends'. *Journal Biotechnology Advances*. 2015, vol. 33, pp. 1228–1245.
[30] Kim K.-H. 'A feasibility study of an algae façade system'. *SB13 Seoul Conference*, Seoul, Korea, Jul 7–10 2013.
[31] Verner D., Vellani S., Klausen A.L., and Tebaldi E. *Middle East and North Africa refugee and host communities & frontier agriculture: climate smart and water saving agriculture technologies for livelihoods*. The World BANK Report, Sep 2017.

[32] Al-Kodmany K. 'The vertical farm: a review of developments and implications for the vertical city'. *Journal Buildings*. 2018, vol. 8(2), pp. 8, 24.
[33] Love D.C., Genello L., Li X., Thompson R.E., and Fry J.P. 'Production and consumption of homegrown produce and fish by noncommercial aquaponics gardeners'. *Journal of Agriculture, Food Systems, and Community Development*. 2015, vol. 6(1), pp. 161–173.
[34] Rakocy J.E., Losordo T.M., and Masser M.P. *Recirculating aquaculture tank production systems: integrating fish and plant culture*. SRAC Publication, No. 454. Southern Region Aquaculture Center, Mississippi State University, Stoneville, Mississippi, USA, 1992.
[35] Özdemir N., Kocaman E.M., Çiltaş A., and Yanik T. 'Sürdürülebilir Bir Ekosistem: Akuaponik'. *XV. Ulusal Su Ürünleri Sempozyumu*, Rize, Jul 2009. Available from www.akuademi.net.
[36] Jordahn S. *Space10 pavilion imagines a future where buildings produce food for residents* [online]. 2017. Available from https://www.dezeen.com/2017/12/06/video-space10-microalgae-pavilion-algae-dome-buildings-movie/?li_source=LI&li_medium=recommended_movies_block.
[37] Bernstein S. *How to start an aquaponics system part 1* [online]. 2015. Available from https://www.maximumyield.com/starting-up-cycling-an-aquaponics-system-part-1/2/1115.
[38] Roe J.J., Ward Thompson C., Aspinall P.A., *et al.* 'Green space and stress: evidence from cortisol measures in deprived urban communities'. *International Journal of Environmental Research and Public Health*. 2013, vol. 10, pp. 4086–4103. doi:10.3390/ijerph10094086.

Index

Energy Generation and Efficiency Technologies for Green Residential Buildings

Residential buildings consume about a quarter of all energy (including electrical and thermal) in industrialized countries and emit around 20% of the carbon emissions there. Older and outdated heating and cooling technology causes high energy demand and, depending on building type, secondary causes can include ventilation and lighting. Technology is available to mitigate high energy consumption, and to enable the use of renewable or environmentally friendly energy, partly generated locally.

This book, written by international experts from academia as well as industry, compiles and describes several key technologies available to reduce a residential building's energy consumption. Key themes include local energy generation, such as the use of sunlight to reduce heating needs, and photovoltaics for electricity. Case studies are included in most chapters to provide real-world context for the technologies described.

About the Editors

David S-K Ting is a professor in Mechanical, Automotive and Materials Engineering and the founder of the Turbulence & Energy Laboratory at the University of Windsor, Canada. He has co/supervised over seventy graduate students primarily in the Energy and Turbulence areas and co-authored more than one hundred and twenty related journal paper.

Rupp Carriveau is a professor with the Turbulence & Energy Laboratory, University of Windsor, Canada. His research focuses on the smart optimization of energy systems. He collaborates with energy and water utilities, agricultural, and automotive industries. He serves on the boards of several related journals, and is Co-Chair of the IEEE Ocean Energy Technology Committee.

ISBN 978-1-78561-947-2

9 781785 619472 >

Energy Engineering

The Institution of Engineering and Technology • www.theiet.org
978-1-78561-947-2